



**HAL**  
open science

# The Mid-Variscan Allochthon: Keys from correlation, partial retrodeformation and plate-tectonic reconstruction to unlock the geometry of a non-cylindrical belt

José Martínez Catalán, Karel Schulmann, Jean-François Ghienne

## ► To cite this version:

José Martínez Catalán, Karel Schulmann, Jean-François Ghienne. The Mid-Variscan Allochthon: Keys from correlation, partial retrodeformation and plate-tectonic reconstruction to unlock the geometry of a non-cylindrical belt. *Earth-Science Reviews*, 2021, 220, pp.103700. 10.1016/j.earscirev.2021.103700 . hal-03407421

**HAL Id: hal-03407421**

**<https://hal.science/hal-03407421>**

Submitted on 28 Oct 2021

**HAL** is a multi-disciplinary open access archive for the deposit and dissemination of scientific research documents, whether they are published or not. The documents may come from teaching and research institutions in France or abroad, or from public or private research centers.

L'archive ouverte pluridisciplinaire **HAL**, est destinée au dépôt et à la diffusion de documents scientifiques de niveau recherche, publiés ou non, émanant des établissements d'enseignement et de recherche français ou étrangers, des laboratoires publics ou privés.

1                   **The Mid-Variscan Allochthon: Keys from correlation, partial**  
2                   **retrodeformation and plate-tectonic reconstruction to unlock the geometry**  
3                   **of a non-cylindrical belt**

4  
5  
6  
7  
8  
9                   José R. Martínez Catalán <sup>a,\*</sup>, Karel Schulmann <sup>b,c</sup>, Jean-François Ghienne <sup>c</sup>

10  
11                   <sup>a</sup> *Departamento de Geología, Universidad de Salamanca, 37008 Salamanca, Spain*

12  
13                   <sup>b</sup> *Center for Lithospheric Research, Czech Geological Survey, Klárov 3, 11821, Prague 1,*  
14                   *Czech Republic*

15  
16  
17                   <sup>c</sup> *Institut Terre et Environnement de Strasbourg, UMR 7063 Université de Strasbourg —*  
18                   *CNRS, 1 Rue Blessig, 67084 Strasbourg, Cedex, France*

19  
20  
21  
22  
23  
24                   \* Corresponding author. *E-mail address:* [jrmc@usal.es](mailto:jrmc@usal.es) (José R. Martínez Catalán)

25  
26  
27  
28                   **Abstract** The non-cylindrical character of the Variscan Belt is established via a description of  
29                   its most salient geological characteristics and correlations among the main and relatively  
30                   minor massifs from Bohemia to Morocco on the basis of a bibliographical synthesis. Using  
31                   the firmly established tectonostratigraphic domains, the continuity of Variscan zones is  
32                   discussed, as well as the western termination of the one that occupies most of the central part  
33                   of the belt. This zone is characterized by its allochthony, and breaks the continuity of the  
34                   zonation, that is, the cylindricity of the belt. A proposal is made to call this zone the Mid-  
35                   Variscan Allochthon and its wedge shape in map view is explained performing a step by step  
36                   restoration of late Variscan deformation. Once the geometry of the belt is interpreted by a  
37                   succession of regionally significant deformation events, a kinematic reconstruction is  
38                   proposed. It is based on recent developments on the knowledge of Paleozoic plate tectonics  
39                   and intended to show that the deformation model is compatible with current  
40                   paleogeographical developments.

41  
42  
43                   **Keywords:** Variscan Belt, Zone correlation, Mid-Variscan suture, Late Variscan restoration,  
44                   North Gondwana, Paleozoic

31	<b>Contents</b>
32	
33	1. Introduction
34	2. Geological map of the Variscan Belt
35	3. Iberian Peninsula
36	3.1. Cantabrian Zone (CZ)
37	3.2. West Asturian-Leonese Zone (WALZ)
38	3.3. Central Iberian Zone (CIZ)
39	3.3.1. Ollo de Sapo and Schist-Greywacke Domains (OSD, SGD)
40	3.3.2. Obejo-Valsequillo Domain (OVD)
41	3.4. Ossa-Morena Zone (OMZ)
42	3.4.1. Central Unit (CU)
43	3.4.2. Évora-Aracena Metamorphic Belt (EAMB)
44	3.4.3. Beja-Acebuches Unit (BAU)
45	3.5. South Portuguese Zone (SPZ)
46	3.6. Galicia-Trás-os-Montes Zone (GTMZ)
47	3.6.1. Parautochthon
48	3.6.2. Lower Allochthon
49	3.6.3. Middle Allochthon
50	3.6.4. Upper Allochthon
51	3.7. Variscan intrusive magmatism in the Iberian Massif
52	3.7.1. Synkinematic granitoids
53	3.7.2. Postkinematic granitoids
54	3.7.3. Granitoids of the Rhenohercynian arc
55	3.8. Other Variscan massifs of the Iberian Peninsula
56	3.8.1. La Demanda and Iberian Chains
57	3.8.2. Pyrenees and Catalonia Coast Ranges
58	4. French and related massifs
59	4.1. Armorican Massif
60	4.1.1. Central Armorican Domain (CAD)
61	4.1.2. North Armorican Domain (NAD)
62	4.1.3. South Armorican Domain (SAD)
63	4.2. French Massif Central (FMC)
64	4.3. Vosges and Schwarzwald Massifs (VM, SWM)

65	4.4. Massifs of the southern Variscan Belt (MTM, Corsica, Sardinia, EmA)
66	4.5. Variscan intrusive magmatism in France
67	4.5.1. Granitoids of the Armorican Massif
68	4.5.2. Granitoids of the French Massif Central
69	4.5.3. Granitoids of other French and related massifs
70	5. Bohemian and related massifs
71	5.1. Rhenohercynian Zone (RHZ)
72	5.2. Moravo-Silesian Zone (MSZ) and Brunovistulian block
73	5.3. Saxothuringian Zone (STZ)
74	5.3.1. Mid German Crystalline High (MGCH)
75	5.3.2. Saxothuringian Autochthon
76	5.3.3. Saxothuringian allochthons
77	5.4. Teplá-Barrandian and Moldanubian
78	5.4.1. Moldanubian Zone (MZ)
79	5.4.2. Teplá-Barrandian Zone (TBZ)
80	5.5. Variscan intrusive magmatism in the Bohemian Massif
81	6. Morocco
82	6.1. Rif Domain
83	6.2. Meseta Domain
84	6.3. Anti-Atlas
85	7. Correlation of the Variscan massifs
86	7.1. Correlations in the Autochthon
87	7.1.1. Links of Morocco with northern Variscan massifs (AA, EM, WM, CB,
88	SB, CZ, CIZ, OVD, OMZ, CAD, NAD)
89	7.1.2. Links among Iberian and French autochthons (CZ, CIZ, OVD, OMZ,
90	CAD, NAD, SAD, VM, SWM, MN, Sardinia)
91	7.1.3. Links among Bohemian and western Variscan autochthons (STZ, OMZ,
92	CIZ, RHZ, SPZ, MSZ)
93	7.2. Correlations in the Allochthon
94	7.2.1. Links among Iberian and French allochthons (GTMZ, CAD, SAD,
95	FMC, VM, SWM, MTM, Corsica, Sardinia)
96	7.2.2. Links among Bohemian and western Variscan allochthons (STZ, TBZ,
97	MZ, VM, SWM, FMC, SAD, GTMZ)
98	7.3. Mid-Variscan suture and Mid-Variscan Ocean

99	8. Restoring late Variscan deformation
100	8.1. Scope and revision of age data
101	8.2. Step by step restoration
102	9. Plate tectonics and Variscan evolution
103	9.1. Sources and approach
104	9.2. Reconstruction
105	9.2.1. Terrane individualization
106	9.2.2. Early Variscan convergence
107	9.2.3. Variscan collision
108	9.2.4. Late Variscan deformation
109	10. Conclusions
110	Acknowledgements
111	References
112	Abbreviations
113	

## 114 **1. Introduction**

115           The Variscan Belt is the basement which formed along the Devonian, Carboniferous  
116 and early Permian in central and western Europe. Its limits are the Tornquist line or  
117 Teisseyre-Tornquist fault zone in the NE, separating the belt from the East European Craton,  
118 and the southern part of the Iberian Peninsula. However, the Moroccan Meseta and the Anti-  
119 Atlas are usually considered also part of it, and are included here because they are important  
120 for our reconstruction. The name derives from Curiae Variscorum, the Latin name of Hof, in  
121 Bavaria, Germany, which Tacitus described as the court of the Varisci (or Narisci), and which  
122 roughly coincides with the Vogtland region in Saxony and part of the adjacent Bavaria.

123           The first attempt to extend local understanding about the Variscan Belt to the scale of  
124 several massifs dates from the late 19th century, when Eduard Suess (1888) compared the  
125 central European massifs of the Sudetes, Erzgebirge, Black Forest, Vosges and Massif  
126 Central. His work found a continuation during the first third of the 20th century with the work  
127 of his son, Franz Eduard Suess (1912, 1926) and of Franz Kossmat (1927), who have shown  
128 the allochthonous character of large parts of the Bohemian Massif and established the  
129 subdivision of the Variscides that is still in use today.

130 During the second half of the 20th century, the theory of Plate Tectonics prompted the  
131 understanding of building of mountain chains by offering an explanation for their formation  
132 mechanisms and evolution. The Variscan Belt was not an exception, and received outstanding  
133 attention. Large-scale correlations, kinematic and evolutionary models were proposed at the  
134 end of the 20th century and beginning of the 21st. These included the movements of large  
135 plates and their interactions with smaller plates, generally formed at least in part by  
136 continental crust, the so-called terranes. For the global understanding of the belt, significant  
137 contributions include those of Philippe Matte (1986, 1991, 2001, 2002), Wolfgang Franke  
138 (1989, 2000) and Gérard Stampfli and his collaborators (Stampfli et al., 2002, 2013; Stampfli  
139 and Kozur, 2006).

140 However, despite the efforts devoted to the study of the Variscan Belt, and the  
141 thousands of published works, the belt is reluctant to be understood as a whole. For instance,  
142 there is no agreement on how many oceans were involved, which is to say how many sutures  
143 exist. The number of oceans varies between one (Rheic) and five: Rheic, Saxothuringian,  
144 Moldanubian, Rhenohercynian and Paleotethys (other names have been used for some of  
145 these and eventually different ones). The same is true for the number of peri-Gondwanan  
146 terranes separated by these oceans and presently included in the Variscides, which varies  
147 between one (Kroner and Romer, 2013) and at least four, even nine if those grouped in  
148 superterrane are considered (Stampfli et al., 2013).

149 The present work aims at contributing to a better understanding of the Variscan Belt. It  
150 forms part of recent efforts for reconstructing the evolution of the Variscan Belt from the  
151 early Paleozoic until the end of Carboniferous, which have been fueled in part by the analysis  
152 and tracing of detrital zircon age populations (Franke and Dulce, 2017; Pérez-Cáceres et al.,  
153 2017; Casas and Murphy, 2018; Stephan et al., 2019).

154 The paper starts by introducing a synoptic map (Fig. 1) showing the proposed  
155 correlation of the tectonostratigraphic zones across the entire belt that will be used later for  
156 interpretation. After a first section explaining how the map was constructed, the following  
157 sections are devoted to a description of the Variscan massifs, avoiding as much as possible  
158 unit names and geographic locations. Abbreviations are limited in the text to important  
159 geological entities, while they are widely used in the figures. The Iberian Peninsula is  
160 described first because the Iberian Massif offers a good representation of the Paleozoic  
161 sedimentary record, the different styles of the Variscan structures and types of plutonism, and

162 serves as a bridge for correlation among the rest of European massifs and northern Africa. A  
163 section is devoted to tackle such a correlation.

164 The main target of the paper is however to clarify the role of the units related to the  
165 suture that occupies a central position in the Variscan Belt and can be followed from the NW  
166 Iberian Massif to the Bohemian Massif. After the regional-scale reviews, it will be shown  
167 how these units form part of a wider distinctive tectonic assemblage here referred to as the  
168 Mid-Variscan Allochthon, the surrounding zones being considered as its relative Autochthon.  
169 Then, a partial retrodeformation of the Allochthon and Autochthon is proposed in a section  
170 which explains their current geometry in map view.

171 There is another zone including one or more sutures, known as the Rhenohercynian  
172 Zone. Wrapping around the NW part of the belt, it is usually understood as the Rheic or the  
173 Rhenohercynian suture, which are two distinct entities that can however coexist in the same  
174 zone. Finally, all tectonostratigraphic zones will be integrated in a comprehensive plate-  
175 tectonics reconstruction. The latter is based on published models of Paleozoic kinematics as  
176 far as the global framework and main plates are concerned, and on our own interpretation of  
177 the Variscan evolution acknowledging the key role of the Mid-Variscan Allochthon.

178 The Variscan Belt is part of a much large collisional orogen that continued toward the  
179 west by NW Africa and the Appalachians in North America, and to the east by the Balkans,  
180 Carpathians and Caucasus, northern Africa and central southern Asia. The orogeny receives  
181 different names depending on the geographical setting, the most popular being Alleghanian in  
182 North America, and Variscan in Europe and Asia. These parts of the orogen fall outside what  
183 we consider the Variscan Belt in a strict sense, and are not described neither included in our  
184 model. The same occurs with the Variscan terranes in southern Europe and northern Africa  
185 that were affected by the Alpine orogeny and whose late Variscan position is uncertain,  
186 although some references to them are included in the text.

187

## 188 **2. Geological map of the Variscan Belt**

189 Among early maps sketching the geology of several Variscan massifs and correlating  
190 their zones, the one published by Kossmat (1927; an English translation is provided by  
191 Meinhold, 2017) deserves special mention. It followed original tectonic subdivision of the  
192 central European Variscides established by Suess (1926) and shows the tectonostratigraphic  
193 zonation of the central European Variscan Belt. Correlations with the Armorican and Iberian

194 massifs had been proposed by Suess (1888), Kossmat (1921) and Stille (1924), and where  
195 supported shortly after by Lotze (1929). The allochthonous character of several Variscan  
196 zones was first recognized by Suess (1912, 1926) and Kossmat (1927) in the Bohemian  
197 Massif. In the French Massif Central, Variscan nappes were first described by Demay  
198 (1942), although allochthonistic interpretations were only accepted since the seventies  
199 (Mattauer and Etchecopar, 1976; Briand, 1978). In Iberia, it was first proposed by Carlé  
200 (1945) and became progressively accepted following the work of Ries and Shackleton (1971).

201 A correlation of thrust faults and allochthonous nappes between the southern  
202 Armorican Massif and NW Iberia was proposed by Matte and Burg (1981), and a map  
203 correlating the allochthonous units of the Bohemian Massif with equivalents of the  
204 Schwarzwald and Vosges, French Massif Central, South Armorican Domain and the NW  
205 Iberian Allochthon was included in Tollmann (1982). Sketches showing the Variscan  
206 zonation in many papers bear close similarities and are probably based on Tollmann's map,  
207 which is the case of the one presented here, an improved version of maps previously  
208 published by the first author and co-workers (Martínez Catalán, 2011; Martínez Catalán et al.,  
209 2007, 2020, Ballèvre et al., 2014).

210 Surprisingly, few attempts have been made to explain the weird shape of the  
211 allochthonous nappes in these maps. This shape is that of a wedge whose western edge is  
212 rather narrow. A model explaining that geometry by a tongue-shaped allochthon derived from  
213 southern Baltica, possibly an island arc, emplaced obliquely on the northern margin of  
214 Gondwana and deformed by dextral wrench motion was proposed by Martínez Catalán  
215 (1990). In later reconstructions (Martínez Catalán et al., 2007; Martínez Catalán, 2011), the  
216 island arc hypothesis was abandoned, the original curvature of the allochthon was smoothed  
217 and the role of transcurrence was emphasized and put in relation with dextral transpression  
218 along a wide shear zone developed between Gondwana and Laurussia. An elaborated version  
219 of the latter model is discussed in this paper.

220 The reconstruction shown in Figure 1 represents the Variscan Belt at the early  
221 Permian. It postdates ductile and brittle transcurrence, essentially dextral, assumed to have  
222 ended by *c.* 290 Ma, and is inspired by the map of present distribution of terranes in Europe  
223 (Oczlon, 2006), but the paleoposition of the continental realms is largely based on the  
224 reconstruction of Stampfli and Kozur (2006) for 300 Ma (Gzhelian), with several  
225 modifications. Early Permian deformation has been accounted for if significant but neglected  
226 if subordinate. Ireland has been approached to Great Britain *c.* 40 km to suppress Mesozoic-



227 Cenozoic extension in the Celtic Sea (Dyment et al., 1990). Subsequently, the British Isles  
228 have been rotated 8° counterclockwise to compensate for crustal thinning, rifting, and basic  
229 igneous activity, probably related with development of oceanic crust in Permian times, and  
230 mostly identified in the western part of the English Channel (Smith and Curry, 1975). The  
231 position of Morocco in relation with Iberia has been taken from Matthews et al. (2016), and  
232 both are separated by a large dextral fault common in plate reconstructions (Le Pichon et al.,  
233 1977; Stampfli and Kozur, 2006) and called here the South Iberia Fault (SIF). It is parallel to  
234 other late-Variscan faults disrupting the Variscan zonation and previous structures, the more  
235 important of which are the South Meseta Fault (SMF), the North Pyrenean Fault (NPF), the  
236 Bray Fault (BrF) and the Elbe Fault Zone (EFZ).

237 The position of Iberia in relation to France is shown prior to the opening of the Bay of  
238 Biscay, approximately following Le Pichon et al. (1977), and implying a post-Triassic  
239 clockwise rotation of *c.* 35° of the Iberian microplate to account for differences in  
240 paleodeclination to both sides of the North Pyrenean Fault (NPF; Van der Voo, 1969; Schott,  
241 1981; Boillot et al., 1984). Rotation in the southern part of the fault allowed the opening of  
242 the Bay of Biscay (Choukroune et al., 1973a, b) while the northern, straight segment acted as  
243 a left-lateral fault with a translation of *c.* 400 km between 110 and 75 Ma (Albian-Campanian;  
244 Boillot et al., 1984). Modern reconstructions, as that of Nirrengarten et al. (2018), differ  
245 somewhat but not essentially from that used here. What matters for the purpose of this  
246 contribution is not the precise reconstruction after the latest Variscan movements, but the  
247 relative positions of Iberia and the Armorican massif before these movements, which can be  
248 constrained with stratigraphy, structures and magnetic anomalies at both sides of the Bay of  
249 Biscay.

250 In France, the Armorican, Central and Vosges massifs have been drawn respecting  
251 their present-day relative position. Correlation of domains and faults between the two first  
252 massifs is in part based on Baptiste (2016). For the Maures-Estérel-Corsica-Sardinia Block  
253 (MECS), Edel et al. (2014) calculated a 90° clockwise rotation during the late Carboniferous  
254 and early Permian (305-280 Ma). These authors favor a position of the MECS at low latitude  
255 in the southern hemisphere, with the Corsica-Sardinia Block oriented W-E in the latest  
256 Carboniferous. This was followed by a 90°-100° clockwise rotation in the early Permian,  
257 when the block acquired a N-S attitude, while additional 60° clockwise rotation would have  
258 occurred during the Triassic.

259 This reconstruction differs from the one which considers a NE-SW orientation for the  
1 260 Corsica-Sardinia Block and the absence of rotations prior to the anticlockwise rotation to its  
2 261 present N-S position in the Miocene (Dewey et al., 1989; Rosenbaum et al., 2002). The NE-  
3 262 SW orientation is contemplated by Rossi et al. (2009), who place this block close to the  
4 263 French Massif Central. But for them, the connection between the Massif Central and the  
5 264 MECS occurs via a tight orocline in the Bohemian Massif following an extensive Stephanian  
6 265 dextral shear zone represented by the external massifs of the Alps, a model based on Matte  
7 266 (2001), which is no longer supported by the reconstruction of Edel et al. (2014, 2018). Thus,  
8 267 we consider an orientation for the MECS as in Edel et al. (2014, 2018), but occupying a  
9 268 somewhat southern position to account for continuity of structures with those of the French  
10 269 Massif Central (Fig. 1).

20 270 The Bohemian Massif has not been modified from its present position in central  
21 271 Europe, and is maintained in its orientation relative to the French Massif Central and the  
22 272 Rhenish Massif.

26 273 More details for the reconstruction are given in the following sections. They describe  
27 274 the main outcrops of the Variscan basement in central and western Europe, the Variscan Belt  
28 275 in a strict sense, and in Morocco. The description is intended to highlight the aspects  
29 276 meaningful for correlation among the massifs and the evolution of the belt as a whole. The  
30 277 sections corresponding to the Iberian Peninsula, the French massifs, the Bohemian Massif and  
31 278 Morocco include description of the established tectonostratigraphic zonation and other details  
32 279 pertinent to the reconstruction of the Variscan Belt.

### 42 281 **3. Iberian Peninsula**

44 282 The largest outcrop of the Variscan basement is the Iberian Massif, occupying the  
45 283 western half of the peninsula. Other are the Pyrenean Axial Zone, Catalonia Coast Ranges,  
46 284 Basque massifs and occurrences in the Iberian Chain (Fig. 2a). For outcrops occurring in the  
47 285 Betic Range, establishing the boundary with the Mesozoic cover is not always possible, and it  
48 286 is difficult to correlate these outcrops with the zones established in the Iberian Massif. They  
49 287 are not included in the map, but are briefly described together with rocks of the Rif Domain in  
50 288 northern Morocco.

58 289 The Iberian Massif is divided into six zones (Lotze, 1945; Julivert et al., 1972, 1980;  
59 290 Ribeiro, 1974; Farias et al., 1987), of which five run parallel to each other delineating the

291 hinge and southern limb of the Ibero-Armorican Arc: Cantabrian, West Asturian-Leonese,  
292 Central Iberian, Ossa-Morena and South Portuguese zones (Fig. 2a). The sixth is the Galicia-  
293 Trás-os-Montes Zone, an allochthonous ensemble emplaced above the Central Iberian Zone  
294 during the Variscan collision, and shown with more detail in Figure 2b and c. The following  
295 sections describe their tectonostratigraphic patterns and the Variscan magmatism, and the  
296 same is done for the smaller Iberian inliers. Figure 3 sketches the structure of NW, central and  
297 SW parts of the Iberian Massif.

298 For a general review of the geology of Iberian Massif or the Iberian Peninsula, the  
299 reader is referred to the books edited by Dallmeyer and Martínez-García (1990), Gibbons and  
300 Moreno (2002), Vera (2004) and Quesada and Oliveira (2019).

### 302 *3.1. Cantabrian Zone (CZ)*

303 This zone is unique in the Variscan Belt, cropping out in northern Spain, at the core of  
304 the Ibero-Armorican Arc (IAA) and possibly in the Basque Massifs of the Pyrenees and the  
305 Balearic island of Menorca (Figs. 1 and 2a). It forms a non- or little metamorphic foreland  
306 thrust belt developed in the late stages of Variscan deformation. The CZ includes a rather  
307 complete Paleozoic preorogenic sequence representing a shallow-water stable continental  
308 platform resting unconformably above a thick terrigenous Ediacaran succession. It occupied a  
309 proximal segment of the northern passive margin of Gondwana, and recorded tholeiitic and  
310 alkaline magmatism related to Cambro-Ordovician rifting (Corretgé and Suárez, 1990).  
311 Moreover, it shows relatively ice-proximal Upper Ordovician glacigenics (Gutiérrez-Marco et  
312 al., 2010). The synorogenic sequences include terrigenous alternances, carbonates and coal  
313 (Truyols et al., 1990; Pérez-Estaún et al., 2004).

314 The CZ is an example of thin-skinned tectonics (Pérez-Estaún et al., 1988, 1994).  
315 Deformation occurred during the middle and upper Carboniferous (325-300 Ma), and  
316 consisted on east-directed thrusting (Bastida et al., 1984; Pérez-Estaún et al., 1988; Alonso et  
317 al., 2009). A subsequent event formed the Asturian Arc (the core of the IAA), an orocline that  
318 folded the thrust faults about a vertical axis (Gutiérrez-Alonso et al., 2004; Weil et al., 2012).  
319 The formation of the Asturian Arc occurred between the latest Carboniferous and the earliest  
320 Permian (310-295 Ma; Weil et al., 2010; Pastor-Galán et al., 2011). Thrusting took place  
321 under diagenetic conditions, but a late extensional episode, produced anchizonal and localized  
322 epizonal metamorphism at the core of the arc (García-López et al., 1999; Aller et al., 2005;

323 Valín et al., 2016; Blanco-Ferrera et al., 2017), and some small granitic bodies intruded in the  
324 metamorphic areas at 292 Ma (Valverde-Vaquero et al., 1999).

325

### 326 3.2. *West Asturian-Leonese Zone (WALZ)*

327 This zone is a slate belt derived from somewhat more distal parts of the Gondwana  
328 margin than the CZ, and is also represented only in Spain. Its stratigraphy is similar to that of  
329 the CZ, including a thick terrigenous Ediacaran and a complete, shallow marine Paleozoic  
330 succession, generally thick and continuous from the early Cambrian to the Lower Devonian  
331 (Pérez-Estaún et al., 1990).

332 The WALZ was affected by recumbent folding and thrusting (Matte, 1968; Bastida et  
333 al., 1986; Pérez-Estaún et al., 1991; Martínez Catalán et al., 2003) and by medium pressure  
334 Barrovian metamorphism. Crustal thickening was followed by a high-temperature (T) and  
335 low-pressure (P) event coeval with extensional collapse which also produced detachments and  
336 gneiss domes (Figs. 2a and 3a; Capdevila, 1969; Arenas and Martínez Catalán, 2003;  
337 Martínez Catalán et al., 2014).

338 Regional cleavage axial planar to recumbent folds is dated at *c.* 335 Ma to the east of  
339 the WALZ and *c.* 360 Ma in the adjacent and more internal Central Iberian Zone (Dallmeyer  
340 et al., 1997), indicating diachronism and propagation toward the external domain of the belt.  
341 The same can be deduced for thrusting, dated at *c.* 343 Ma in the basal thrust of the  
342 allochthonous Galicia-Trás-os-Montes Zone, and 321 Ma at the limit between the WALZ and  
343 the CZ. Extensional detachments and doming are late Carboniferous, dated around 315-300  
344 Ma.

345

### 346 3.3. *Central Iberian Zone (CIZ)*

347 Also a slate belt, the CIZ derived from more distal parts of the northern Gondwana  
348 platform than the WALZ. Its stratigraphy is similar to that of the CZ and WALZ, although  
349 differences in the Ediacaran succession, volcanic component and tectonic style allows defining  
350 three domains.

351

352 3.3.1. *Ollo de Sapo and Schist-Greywacke Domains (OSD, SGD)*

1  
2 353 The terrigenous Ediacaran succession of the CIZ is known as the Schist-Greywacke  
3  
4 354 Complex (Teixeira, 1955) or the Alcludian (Tamain, 1971). It reflects sedimentation in a  
5  
6 355 Cadomian retro-arc basin representing the transition from a Cadomian arc in the periphery of  
7  
8 356 the West African Craton to Cambrian rifting marking the start of peri-Gondwanan terrane  
9  
10 357 dispersion (Linnemann et al., 2008). An Ediacaran glaciation (*c.* 565 Ma) has been identified  
11 358 by glaciomarine deposits in the southern part of the CIZ (Linnemann et al., 2018).

12  
13 359 Late Cambrian-Lower Ordovician voluminous felsic magmatism characterizes most of  
14 360 the CIZ, including felsic volcanics dated at 490-475 Ma, and intrusive granitoids of 500-465  
15 361 Ma (Valverde-Vaquero and Dunning, 2000; Bea et al., 2006; Zeck et al., 2007a; Solá et al.,  
16 362 2008; Montero et al., 2009a; Díez Montes et al., 2010; Rubio Ordóñez et al., 2012; Talavera  
17 363 et al., 2013). Volcanic and subvolcanic rocks are particularly voluminous at the NE border of  
18 364 the CIZ, where the felsic Ollo de Sapo Fm. crops out at the core of the 570 km long Ollo de  
19 365 Sapo Antiform (Fig. 2a, b). The rocks in the antiform were deformed first by recumbent and  
20 366 then by upright folds. Due to the occurrence of the Ollo de Sapo Fm. and to deformation  
21 367 characteristics, this NE band has been described either as the Ollo de Sapo Domain (OSD;  
22 368 Martínez Catalán et al., 2004a) or the Domain of recumbent folds (DRF, Fig. 3a; Díez Balda  
23 369 et al., 1990). Most of the rest of the CIZ is described by the same authors respectively as the  
24 370 Schist-Greywacke Domain (SGD) and Domain of upright folds (DUF, Fig. 3b).

25  
26 371 The main difference between the CIZ and the CZ and WALZ is the presence of the  
27 372 Lower Ordovician Toledanian unconformity, responsible for the partial or total absence of  
28 373 Cambrian deposits. In the central and southern parts of the CIZ, the Ordovician starts with red  
29 374 beds including conglomerates, sandstones, silts and pelites, indicating transgression above a  
30 375 paleorelief or/and sedimentation in (half)grabens. Above, the Armorican Quartzite is almost  
31 376 always present, followed by more pelitic successions and culminating by a discontinuous  
32 377 level of limestone and Hirnantian diamictites, often missing due to a glacio-eustatic  
33 378 disconformity (Robardet, 1981; Martínez Poyatos et al., 2004; Gutiérrez-Marco et al., 2019).

34  
35 379 The synorogenic sequence, late Tournaisian to Westphalian, consists of paralic to  
36 380 flysch-like deposits, the more important of which is Los Pedroches Culm in the south of the  
37 381 SGD, up to 6000 m thick and occupying the core of a late-Variscan syncline which coincides  
38 382 with its depocentre (Martínez Poyatos, 2002).

383 The CIZ is structurally characterized by the overthrusting of the Galicia-Trás-os-  
384 Montes Zone (the Allochthon) on its NW part (Fig. 3a), and by two folding events, one  
385 preceding and the other following thrusting. The early folds are overturned or recumbent in  
386 the area adjacent to the WALZ in the NW, and in the relatively deep zones cropping out in the  
387 Central System (DRF) (Matte, 1968; Macaya et al., 1991; Díez Montes et al., 2010). Axial  
388 planar cleavage accompanies these folds. In the DUF, the early folds have an upright attitude  
389 (Fig. 3b), but they are not recognized in wide areas and may not develop cleavage. Where  
390 present, the early folds were either refolded or flattened by the late folds (Fig. 2a), but the  
391 style and size are quite similar for both fold systems. The interference is clear in the SE part  
392 of the DUF, and represents the southern part of the hinge zone of a curved structure (Aerden,  
393 2004) called here the Central Iberian Arc (CIA) after Martínez Catalán (2012) and Martínez  
394 Catalán et al. (2015). Although not fully accepted (*e.g.* Dias et al., 2016), the arc has been  
395 acknowledged in several old and recent publications (Staub, 1926, 1927; Llopis-Lladó, 1966;  
396 Shaw et al., 2012; Johnson et al., 2013; Simancas et al., 2013; Pastor-Galán et al., 2016).  
397 According to Martínez Catalán (2012), the CIA developed contemporaneously with the late  
398 folds, which are rather continuous and delineate the southern flank of the IAA (Fig. 2a).  
399 Interestingly, in the DRF the late folds are bent by the IAA, suggesting that both arcs are not  
400 coeval and the CIA predates the IAA. The first folds predate and the late folds deform early  
401 and middle Carboniferous synorogenic deposits, which often alternate with a bimodal  
402 volcanic suite linked to an extensional event that can also be identified in the whole SW part  
403 of the Iberian Massif (Martínez Poyatos, 2002; Martínez Poyatos et al., 2012).

404 The early folds were dated at 360-335 Ma in NW Iberia, where the emplacement of  
405 the Allochthon occurred there around 345-340 Ma. Subsequently, the thickened crust  
406 underwent extensional collapse starting at *c.* 335 Ma, whereas late folds are dated at 315-305  
407 Ma (Dallmeyer et al., 1997; Valle Aguado et al., 2005; Valverde-Vaquero et al. 2007a;  
408 Martínez Catalán et al., 2007, 2009; Rubio Pascual et al., 2013a). Ductile shear zones  
409 associated to the late folds have been dated at 310-305 Ma (Gutiérrez-Alonso et al., 2015).

410 Metamorphism is similar to that of the WALZ. Medium and high grade rocks are  
411 exposed surrounding the NW Iberian Allochthon and in the Alpine horst forming the Central  
412 System. A Barrovian event related with crustal thickening, dated around 350 Ma was  
413 followed by a low-P/high-T Buchan episode during subsequent extension at 335-325 Ma, late  
414 folding, and renewed extension between 315-300 Ma (Escuder Viruete et al., 1994; Díez  
415 Balda et al., 1995; Rubio Pascual et al., 2013a, 2016). Extensional detachments and gneiss

416 domes developed where crustal thickening had been large, in the area covered by the  
417 Allochthon and in the Central System (Fig. 2a).

418 No sutures occur among the CZ, WALZ and CIZ, which represent a preserved,  
419 coherent segment of the northern Gondwanan platform (Gutiérrez-Marco et al., 1999a;  
420 Robardet, 2002, 2003), some aspects being comparable to other outer segments that escaped  
421 the Variscan deformation (*e.g.* southern Turkey; Ghienne et al., 2010). The Hirnantian  
422 glaciation is identified in the CIZ and CZ (Martínez Catalán et al., 1992; Gutiérrez-Marco et  
423 al., 2010; Subias et al., 2015). The boundaries among these three zones are presently Variscan  
424 structures such as early folds and thrust or detachment faults (Fig. 3a), thought to represent  
425 inverted normal faults of the Gondwana platform which conditioned variations of thickness  
426 and facies in the preorogenic sequences (Pérez-Estaún et al., 1990; Martínez Catalán et al.,  
427 1992).

### 429 3.3.2. Obejo-Valsequillo Domain (OVD)

430 In the southern part of the CIZ, the Obejo-Valsequillo Domain (Apalategui et al.,  
431 1985) has a Paleozoic sequence comparable to that of the SGD while the underlying  
432 Ediacaran is the same as in the Ossa-Morena Zone. Arc-related intrusives in the Ediacaran  
433 have yielded 580-570 Ma (Bandrés et al., 2004; Talavera et al., 2008), and low-grade  
434 metamorphism was dated at *c.* 550 Ma (Blatrix and Burg, 1981).

435 Martín Parra et al. (2006) locate the northern limit of the OVD at an extensional shear  
436 zone to the north of the Pedroches Carboniferous Culm basin and the elongated Pedroches  
437 batholith, but the Paleozoic sequence immediately south of the batholith is rather similar to  
438 that of the SGD. The proposed boundary is the northernmost of a series of sinistral wrench  
439 faults south of the batholith (Fig. 2a), where the sequence changes and the Lower Devonian  
440 directly overlies the early Ordovician.

441 Structurally, the OVD is characterized by thrust faults, NW-SE upright late folds, and  
442 high-angle, left-lateral and reverse faults (Fig. 3b, c), all affecting synorogenic Culm and  
443 paralic deposits. These are late Variscan structures, but the southern part, the OVD includes  
444 an early Variscan large recumbent syncline-anticline pair with NE vergence, probably Upper  
445 Devonian in age, which predates the Culm (Azor et al., 1994; Martínez Poyatos, 2002;  
446 Martínez Poyatos et al., 1995, 1998, 2012). Thrusting took place during the middle  
447 Carboniferous and late folding and faulting, both related to sinistral wrenching, are

448 Westphalian in age (c. 315-300 Ma). Variscan metamorphism ranges between very low grade  
449 to lower greenschist facies (Martínez Poyatos et al., 2001).

450

### 451 *3.4. Ossa-Morena Zone (OMZ)*

452 The OMZ is a slate belt comparable to the CIZ, although with differences in the  
453 stratigraphy and structural evolution. At its NE and SW limits, three units depart from the  
454 general zone definition and show high-grade metamorphism or even are not metasedimentary.  
455 These units are described separately. Most of the OMZ was, as the CIZ, part of the northern  
456 Gondwanan platform, although with differences in the faunal content and facies of the  
457 Paleozoic, which are more distal in the OMZ (Robardet and Gutiérrez Marco, 1990). The  
458 Lower Ordovician shallow-water Armorican Quartzite is absent, but the Hirnantian glatiation  
459 is well represented. The Ediacaran is also different, and consists of a lower sequence, the  
460 Black Series, with terrigenous sediments, carbonates, black quartzites, cherts, felsic volcanics  
461 and amphibolites of possible arc derivation, and an upper unit with massive basic arc  
462 volcanism and detrital alternations.

463 The protolith of an amphibolite was dated at c. 611 Ma (Schäfer, 1990), and  
464 orthogneisses yielded 585 Ma (Schäfer et al., 1993a). These ages are comparable to those of  
465 the OVD in the CIZ and in the eastern part of the WALZ (600 Ma, Fernández-Suárez et al.,  
466 1998). Younger protolith ages vary between 560 and 500 Ma (Galindo et al., 1990; Ochsner,  
467 1993; Ordóñez Casado, 1998; Salman and Montero, 1999; Montero et al., 2000).  
468 Amphibolite-facies metamorphism is dated around 600 Ma in the Black Series while the  
469 overlying basic volcanic unit was metamorphic before the Cambrian (560-550 Ma; Dallmeyer  
470 and Quesada, 1992). The older ages chart the Cadomian arc while the upper Ediacaran ages  
471 correspond to shortening and thickening related to arc-continent collision. The Cambrian ages  
472 date the collapse of the Cadomian arc (Bandrés et al., 2004), and the transition to rifting  
473 inside the Gondwana margin (Sánchez-García et al., 2008, 2010, 2014), which continued  
474 during the Lower Ordovician with bimodal, sometimes alkaline magmatism (470-460 Ma;  
475 García Casquero et al., 1985; Galindo, 1989; Ochsner, 1993).

476 The Variscan structure of the central part of the OMZ includes a first event of  
477 recumbent folds with a NW-SE attitude and SW vergence followed by thrusting toward the  
478 SW, extension and late upright NW-SE folds (Expósito et al., 2002, 2003). Early folding was  
479 Devonian, and a synorogenic flysch rests unconformably above. Most is early Carboniferous



480 (Boogaard and Vázquez, 1981; Giese et al., 1994), but Lower Devonian fossils found at the  
481 base may be inherited or indicate an older age (Piçarra, 1997; Piçarra et al., 1998; Pereira et  
482 al., 1998).

483 The early folds were cut and displaced to the SSW by brittle-ductile thrust faults  
484 probably developed in continuation of folding. Later, during the early Carboniferous, an  
485 extensional episode produced normal faults and basins where detrital and carbonate rocks  
486 were deposited together with volcanics. The late folds are related to Namurian-Westphalian  
487 sinistral transpression, and were accompanied by reverse and left-lateral faults whose  
488 development continued until the Stephanian (Simancas et al., 2001; Expósito et al., 2002).  
489 Sinistral wrenching affected the whole OMZ (Expósito et al., 2002).

490 It has been proposed that the limit between the CIZ and OMZ represents a suture,  
491 although its age has been considered Cadomian, then reworked as a Variscan shear zone  
492 (Ribeiro et al., 1990; Quesada, 1991; Ábalos et al., 1991; López-Guijarro et al., 2008),  
493 Cambro-Ordovician (Palacios et al., 2010), or Variscan (Brun and Burg, 1982, Matte, 1986;  
494 Azor et al., 1994; Simancas et al., 2001, 2002). A difference of 15° in paleolatitude was  
495 reported by Perroud et al. (1985) for the Upper Devonian on opposite sides of the CIZ/OMZ  
496 boundary (Figs. 1 and 2a). Such a difference, with the OMZ occupying the southernmost  
497 position, was questioned by Robardet (2002) based on paleobiographical constraints. He  
498 considered the CIZ and OMZ as different paleogeographic domains and proposed a more  
499 distal (western) position of the OMZ off NW Africa, but did not interpret the limit as a suture.

500

### 501 *3.4.1. Central Unit (CU)*

502 Supporting the Variscan suture hypothesis is the occurrence of eclogites in the so-  
503 called Central Unit (Azor Pérez, 1997; Azor et al. 1994), a confusing name for a unit used to  
504 define the northern boundary of the OMZ. This unit is a narrow band consisting on migmatitic  
505 paragneisses, schists, Lower Ordovician orthogneisses and amphibolites with occasional  
506 eclogitic relics. High-P metamorphism (1.45-1.9 GPa, 550 °C (Ábalos et al., 1991; López  
507 Sánchez-Vizcaíno et al., 2003; Pereira et al., 2010), is dated at 377±19 Ma (Abati et al.,  
508 2018). An oceanic signature has been inferred from some of the basic rocks (Gómez Pugnaire  
509 et al., 2003), but the absence of ophiolites casts doubt on the suture, which in any case would  
510 be cryptic, hidden by the strong left-lateral imprint of the Badajoz-Córdoba Shear Zone  
511 (BCSZ) at the CIZ/OMZ boundary.

512 The structural significance of the CU is hindered by its coincidence with the BCSZ  
1 513 and the fact that it is bounded by two faults (Fig. 3b, c), a normal detachment with left-lateral  
2 514 component at its northern limit and a sinistral structure probably hiding an older thrust fault  
3 515 responsible for the exhumation of the high-P rocks to the south (Azor et al., 1994; Simancas  
4 516 et al., 2001). The seismic profile IBERSEIS (Fig. 3c), crossing the OMZ and the OVD, shows  
5 517 NE-dipping reflections that coincide with these two faults (Simancas et al., 2003). The  
6 518 seismic profile ALCUDIA, traversing the southern part of the CIZ (Fig. 3b), also images a  
7 519 NE-dipping reflection coincident with the northern fault (Martínez Poyatos et al., 2012).

14 520 The CU generally shows the foliation dipping to the NE or subvertical, which  
15 521 reinforced by the NE-dipping seismic reflections led to interpret a subduction of the OMZ  
16 522 under the CIZ (Simancas et al., 2001, 2003). However, some geological transects across the  
17 523 middle part of the CU unveil an antiformal structure (Apalategui Isasa and Higuera, 1980;  
18 524 Arriola et al., 1981; Gonçalves, 1971). Ultramylonites at the hinge zone of the antiform show  
19 525 a stretching lineation trending NW-SE to N-S, with top to the north kinematics, and  
20 526 migmatitic paragneisses are quickly replaced upward or northward by schists. This points to a  
21 527 N-dipping ductile extensional detachment related with the ascent of a gneiss dome that could  
22 528 explain the exhumation of the high-P rocks. The dome was later stretched by left-lateral  
23 529 shearing along the BCSZ, being presently very narrow (Fig. 2a).

### 34 530

#### 35 531 3.4.2. Évora-Aracena Metamorphic Belt (EAMB)

36 532 The southern boundary of the OMZ is interpreted as a suture, partly occurring at the  
37 533 EAMB, a low-P/high-T domain with a high-P ensemble located tectonically above, the  
38 534 Cubito-Moura Unit (Rubio Pascual et al., 2013b). The Évora Massif in Portugal is wide (Fig.  
39 535 2a), and has been interpreted as a gneiss dome where a ductile detachment with top to SE  
40 536 kinematics separates gneisses and schists, below, from the overlying Cubito-Moura Unit, a  
41 537 phyllonitic mélange including lenses of eclogite and blueschists (Araújo and Ribeiro, 1996;  
42 538 Dias da Silva et al., 2018) which attest for a high-P metamorphic event dated at 370-360 Ma  
43 539 (Moita et al., 2005). The high-P rocks are tectonic imbrications mixed with ophiolitic  
44 540 fragments and emplaced toward the N-NE before early Variscan recumbent folding with west  
45 541 and SW vergence occurred (Araújo and Ribeiro, 1996; Simancas et al., 2003). The fragments  
46 542 include MORB-type, c. 480 Ma old metabasites in greenschist and amphibolite facies and  
47 543 ultramafics, interpreted as remnants of the Rheic Ocean (Fonseca et al., 1999; Pedro et al.,  
48  
49  
50  
51  
52  
53  
54  
55  
56  
57  
58  
59  
60  
61  
62  
63  
64  
65

544 2010). Low-P/high-T granulite-facies metamorphism of the EAMB took place at 343-330 Ma  
545 (Dallmeyer et al., 1993; Castro et al., 1999), while magmatism associated to dome  
546 development is dated at 343-319 Ma (Dias da Silva et al., 2018). Late upright folding  
547 occurred in a left-lateral shearing environment bounded by the Southern Iberian Shear Zone  
548 (SISZ) which separates the OMZ from the SPZ (Crespo-Blanc and Orozco, 1988, 1991).

549 In Spain, the Aracena Belt is a narrow, strongly sheared band, the upper part of which  
550 includes high-P rocks in the Cubito-Moura Unit and also in the underlying Fuenteheredos  
551 Group. Both form part of a NE-verging orogenic wedge with pieces of subducted continental  
552 and oceanic crust, later emplaced on top of the OMZ (Rubio Pascual et al., 2013b). Part of  
553 this wedge is preserved also in the South Portuguese Zone.

### 554 3.4.3. Beja-Acebuches Unit (BAU)

555 The BAU is a narrow mafic and ultramafic unit separating the OMZ and the SPZ,  
556 where diorite and granodiorite were dated at 352 Ma (Pin et al., 2008; Pin and Rodríguez,  
557 2009) and metabasites at 345-330 Ma (Azor et al., 2008, 2009). It has been interpreted as i) an  
558 ophiolite (Andrade, 1985; Crespo-Blanc and Orozco, 1991), ii) linked to an arc related with  
559 northward oceanic subduction (Santos et al., 1990; Quesada et al., 1994), iii) the product of  
560 ocean ridge subduction (Castro et al., 1996a, 1996b), iv) reflecting slab break-off following  
561 subduction and collision (Pin et al., 2008), and v) an ephemeral oceanic realm opened after  
562 consumption of the Rheic lithosphere and possibly related to a mantle plume (Azor et al.,  
563 2008).

564 According to its age, the BAU can be related to the extensional event affecting the  
565 southern part of the CIZ, the OMZ and the SPZ between the uppermost Devonian and the  
566 Viséan, which produced abundant magmatism and an elevated thermal gradient in the upper  
567 crust. This magmatism is linked to the emplacement of the Iberian Reflective Body (IRB),  
568 identified in the IBERSEIS seismic profile (Simancas et al., 2003), and was responsible for  
569 the middle Carboniferous low-P/high-T metamorphism undergone by the EAMB (Rubio  
570 Pascual et al., 2013b). The IRB intruded along a detachment rooted in the middle crust (Fig.  
571 3c), and a possible link with local oceanization or a mantle plume has been suggested by  
572 Simancas et al. (2006) and Azor et al. (2008). The latter was questioned by Pin et al. (2008)  
573 based on the geochemical signature of the Beja igneous complex.  
574

575 The BAU was affected by the middle Carboniferous, low-P granulite-facies  
1 576 metamorphism of the EAMB, and is strongly sheared by the SISZ. High-T mylonites  
2 577 developed in a context of ductile thrusting, and greenschist-facies mylonites developed later  
3 578 related with sinistral wrenching (Díaz Azpiroz and Fernández, 2005; Díaz Azpiroz et al.,  
4 579 2006; Pérez-Cáceres et al., 2016). Actually, the whole OMZ, together with the OVD of the  
5 580 CIZ and the northern part of the South Portuguese Zone can be considered a wide and  
6 581 heterogeneous shear zone, with two main zones where deformation concentrated, the BCSZ in  
7 582 the NE and the SISZ in the SW.

### 17 584 *3.5. South Portuguese Zone (SPZ)*

19 585 This zone represents a Variscan foredeep basin characterized by thin-skinned thrust  
20 586 tectonics, and is usually correlated with the Rhenohercynian Zone of Kossmat (1927) in the  
21 587 Bohemian Massif (Fig. 1). It is separated from the OMZ by an accretionary prism, the Pulo do  
22 588 Lobo Unit, and by the BAU (Figs. 2a and 3c; Silva et al., 1990; Onézime et al., 2002;  
23 589 Nysaether et al., 2002; Simancas et al., 2003; Nance and Linnemann, 2008). The Pulo do  
24 590 Lobo and the ofiolitic relicts of the Cubito-Moura Unit in the OMZ represent the Rheic  
25 591 suture, as the age of the latter (480 Ma) is that of the opening of the Rheic Ocean (Franke et  
26 592 al., 2017). So, the basement beneath the SPZ thrust belt should be that of Avalonia, which is  
27 593 supported by zircon age populations (de la Rosa et al., 2002; Braid et al., 2011; Pereira et al.,  
28 594 2014; Rodriguez et al., 2015; Pérez-Cáceres et al., 2016, 2020).

30 595 According to Rubio Pascual et al. (2013b), at *c.* 400 Ma the ocean was closed after  
31 596 subduction toward the SW (in present coordinates). Previously, an arc was built above, and is  
32 597 preserved in La Minilla, a unit of the SPZ with evidences of high-P metamorphism. The  
33 598 Lower to Middle Devonian Pulo do Lobo Unit was probably, deposited in the back-arc, and  
34 599 later subducted, as indicated by lawsonite pseudomorphs. These two units represent a NE-  
35 600 verging accretionary wedge partly preserved in the SPZ (Onézime et al., 2002; Rubio Pascual  
36 601 et al., 2013b) and partly in the Cubito-Moura Unit and the Fuenteheridos Group of the  
37 602 EAMB. They derive from the SW margin of the OMZ and were thrust above it after  
38 603 subduction.

39 604 Building and exhumation of the accretionary wedge occurred at the Lower-Middle  
40 605 Devonian (Silva et al., 1990; Eden and Andrews, 1990), and Upper Devonian to early  
41 606 Carboniferous synorogenic formations were deposited on top of high-P rocks. Terrigenous

607 formations were laid down and during the uppermost Devonian and Visean alternate with  
608 submarine, mostly siliceous volcanics, including massive sulfide deposits forming the  
609 Volcano-Sedimentary Complex during an extensional episode (Dunning et al., 2002; Rosa et  
610 al., 2009). Extension and magmatism affected the SPZ and OMZ, indicating that the two  
611 zones were accreted by the Upper Devonian (Simancas et al, 2003, 2005; Pereira et al., 2007a;  
612 Pereira et al., 2006b, 2007b; Pin et al., 2008). If early Carboniferous extension created a  
613 narrow ocean, this was the Rhenohercynian, its suture being represented by the BAU.

614 Renewed shortening during the Visean was recorded by the Culm, representing in the  
615 SPZ a foredeep basin with sedimentation propagating toward the SW while a thin-skinned  
616 thrust belt developed from the late Visean until the Moscovian (*c.* 330-310 Ma; Simancas et  
617 al., 2004). Synkinematic low-P metamorphism affecting the Upper Devonian and  
618 Carboniferous rocks increases to the north from diagenesis to anchimetamorphic and  
619 greenschist facies, reaching andalusite, cordierite and sillimanite zones in the east, around the  
620 northern Sierra de Sevilla batholith (Abad et al., 2001, 2004).

### 622 *3.6. Galicia-Trás-os-Montes Zone (GTMZ)*

623 This zone represents the NW Iberian Allochthon (Fig. 2a), a nappe pile preserved in  
624 five large complexes and consisting in three groups of stacked allochthonous units and an  
625 underlying Parautochthon (Martínez Catalán et al., 2009; Ballèvre et al., 2014; Arenas et al.,  
626 2016). The Upper Allochthon is a peri-Gondwanan terrane rifted at *c.* 500 Ma leaving behind  
627 an oceanic domain, the Galicia-Brittany-Massif Central Ocean (Matte, 2001, 2007). The  
628 Middle Allochthon includes units derived from this Cambro-Ordovician ocean which  
629 recorded renewed activity during the Lower Devonian. The Lower Allochthon derives from  
630 the outermost margin of north or NW Gondwana and the Parautochthon represents a more  
631 proximal region of the same margin. The Allochthon was progressively assembled in an  
632 accretionary prism during early Variscan convergence, their units being stacked during  
633 subduction or underthrusting between 400-395 Ma (Upper Allochthon) and 375-365 Ma  
634 (Lower Allochthon), before being thrust above the CIZ at *c.* 340 Ma having incorporated  
635 the Parautochthon to its base.

636 Three of the allochthonous complexes occur in Galicia (NW Spain): Cabo Ortegal,  
637 Órdenes and Malpica-Tui (Figs. 2b and 3a), and two in Trás-os-Montes (northern Portugal):  
638 Bragança and Morais (Fig. 2c). They are circular, elliptical or elongated klippen preserved in

639 synforms and structural basins developed among gneiss domes, and more or less flattened  
640 subsequently by the late set of upright folds. The following sections describe the  
641 allochthonous groups from bottom to top of the nappe stack.

642

### 643 *3.6.1. Parautochthon*

644 This ensemble consists of early Carboniferous synorogenic deposits forming a rather  
645 continuous carpet at the base of the Allochthon, tectonically overlain by lower Paleozoic  
646 sediments and metavolcanics. Both are internally imbricated and the whole package is limited  
647 by a basal detachment developed along a weak level of Silurian black shales. Deformation is  
648 pervasive in both ensembles, and metamorphism is of the greenschist facies, but the  
649 synorogenic sediments are characterized by lower temperature.

650 The synorogenic deposits include flysch-type, turbiditic deposits with detrital zircons  
651 indicating an early Carboniferous maximum depositional age and derivation essentially from  
652 the Allochthon (Dias da Silva et al. 2014a; Martínez Catalán et al., 2008, 2016). A different  
653 type comprises alternations of slate with sandstone or limestone and include small to large  
654 olistoliths of the preorogenic sequence (Dias da Silva et al. 2014b; González Clavijo et al.,  
655 2016, 2021). The synorogenics were deposited in flexural basins in front of the allochthonous  
656 orogenic wedge, being later incorporated into thrust sheets (Martínez Catalán et al., 2016;  
657 Farias and Marcos, 2019).

658 The preorogenic sequence is comparable to that of the CIZ although more distal.  
659 Greenish and purple (lie-de-vin) schists are common (Ribeiro, 1974), as well as  
660 metavolcanics, bimodal but dominantly felsic interbedded with the upper Cambrian and  
661 Ordovician sediments comparable to the Cambro-Ordovician of the Autochthon. The  
662 youngest zircon population found in Galicia has 560 Ma (Díez Fernández et al., 2012a). In  
663 Portugal, basic rocks are dated at 494 Ma, and felsic volcanics identical to the Ollo de Sapo  
664 Fm. of the CIZ yield also the same age, 485 Ma (Dias da Silva et al., 2014c). A metaquartzite  
665 provided a few *c.* 486 Ma detrital zircons (Dias da Silva et al., 2014a). Younger Ordovician to  
666 Silurian volcanism includes alkaline felsic rocks dated between 475-440 Ma (Valverde-  
667 Vaquero et al., 2005, 2007b), as well as basic tuffs, metabasalts and diabase sills (Ferragne,  
668 1972; Gallastegui et al., 1988; Ancochea et al., 1988; Meireles, 2013).

669

670 *3.6.2. Lower Allochthon*

1  
2 671 This group of units consists of a thick sequence with paragneisses (metagreywackes),  
3  
4 672 schists, phyllites, carbonaceous schists, calc-silicate rocks and meta-quartzites intruded by  
5  
6 673 late Cambrian-Early Ordovician igneous rocks. The youngest zircon population in Galicia has  
7  
8 674 566 Ma, suggesting an Ediacaran age of the sequence. Age spectra indicate a paleoposition to  
9  
10 675 the NE of the West African craton (Díez Fernández et al., 2010). In Portugal, the sequence  
11  
12 676 includes early Paleozoic metasediments and a bimodal volcanic suite dated at 455 Ma (Dias  
13  
14 677 da Silva et al., 2016).

15 678 Intrusive rocks consist of a granitic calc-alkaline suite formed by high-K granites,  
16  
17 679 granodiorites, tonalites, an alkaline to peralkaline suite, and basic rocks (Floor, 1966;  
18  
19 680 Rodríguez Aller, 2005; Montero et al., 2009b; Abati et al., 2010; Díez Fernández et al.,  
20  
21 681 2012b). Rb-SR and U-Pb dating shows magmatic pulses at *c.* 490 Ma for granodiorites, 475  
22  
23 682 Ma for granites, and 475-470 Ma for alkaline/peralkaline intrusions (Van Calsteren et al.,  
24  
25 683 1979; García Garzón et al., 1981; Santos Zalduegui et al., 1995; Díez Fernández et al.,  
26  
27 684 2012b). Geochemical data point to a geodynamic setting in a back-arc or retro-arc  
28  
29 685 environment (Fuenlabrada et al., 2012).

30 686 Metamorphism records an early Variscan high-P/low- to medium-T metamorphism  
31  
32 687 identified by eclogites, jadeite-bearing orthogneisses and blueschists, and interpreted as the  
33  
34 688 product of continental subduction (Munhá et al., 1984; Schermerhorn and Kotsch, 1984;  
35  
36 689 Ribeiro, 1991; Gil Ibarra and Dallmeyer, 1991; Arenas et al., 1995). According to Ar-Ar  
37  
38 690 and U-Pb data, subduction may have started before 370 Ma and ended at *c.* 365 Ma (Van  
39  
40 691 Calsteren et al., 1979; Santos Zalduegui et al., 1995; Rodríguez et al., 2003; Abati et al.,  
41  
42 692 2010). Emplacement by thrusting occurred after 346 Ma, as shown by U-Pb age of monazite  
43  
44 693 in migmatites developed during exhumation (Abati and Dunning, 2002).

45  
46 694

47  
48 695 *3.6.3. Middle Allochthon*

49  
50 696 This group includes true oceanic units and others interpreted as transitional between  
51  
52 697 the extended continental margin of northern Gondwana and the Rheic oceanic crust. Ages of  
53  
54 698 igneous protoliths are either Cambro-Ordovician or Lower Devonian, which leads to a  
55  
56 699 subdivision in two groups, Cambro-Ordovician ophiolites and oceanic supracrustals, and  
57  
58 700 Lower Devonian ophiolites. When both groups occur together, the older occupies a lower  
59  
60  
61  
62  
63  
64  
65

701 structural position, just above the Lower Allochthon, implying that it was located closer to the  
1 702 extended margin of Gondwana (Martínez Catalán et al., 1996, 2002).

3  
4 703 The Cambro-Ordovician group includes three types of units: i) with a clear oceanic  
5 704 affinity, ii) continental-oceanic transitional units and iii) the ophiolitic part of a tectonic  
6 705 mélange. The first type is well represented by an unit consisting on metagabbroic  
7 706 amphibolites, gabbros, pegmatoid gabbros, pyroxenites, ultramafic rocks and minor tonalites  
8 707 and leucogabbros (Martínez et al., 2012; Arenas and Sánchez Martínez, 2015). Their  
9 708 geochemistry is that of island-arc tholeiites, N-MORB and within-plate basalts, with trace  
10 709 elements similar to those generated in plume-ridge interactions. Isotopic composition of  
11 710 zircons points to a juvenile mafic protolith without interaction with crustal components. U-Pb  
12 711 zircon ages yield two populations of 495 and 475 Ma dating respectively the gabbroic  
13 712 protolith and granulite facies metamorphism transitional between low- and medium-P types,  
14 713 possibly related to mid ocean ridge subduction. Other units of the first type are strongly  
15 714 deformed and consists of a tectonically repeated succession of metabasites, metapelitic  
16 715 phyllites, metagabbros and serpentinites with some layers of granitic orthogneisses and  
17 716 metacherts. Basic rocks plot in the fields of island-arc tholeiites, supra-subduction zone  
18 717 basalts or destructive plate-margin basalts. An orthogneiss yielded  $497\pm 4$  Ma, and their  
19 718 immobile trace elements point to a volcanic arc or a supra-subduction zone granitoid (Arenas  
20 719 et al., 2007a, b; Arenas and Sánchez Martínez, 2015). These units underwent a high-P event  
21 720 followed by a mylonitic greenschist-facies foliation, axial planar to tight recumbent folds and  
22 721 dated at 363-367 Ma (Dallmeyer et al., 1997).

23  
24  
25  
26  
27  
28  
29  
30  
31  
32  
33  
34  
35  
36  
37  
38  
39 722 The second type of Cambro-Ordovician units is interpreted as the upper part of a  
40 723 transitional crust between the attenuated Gondwana margin and an oceanic domain. They  
41 724 consist of phyllites, schists, mafic igneous rocks with N-MORB affinity and alkaline  
42 725 metavolcanics. Detrital zircons in metasediments yield a maximum depositional age of 512  
43 726 Ma and suggest a position relatively distal in relation to a late Cambrian source (Díez  
44 727 Fernández et al., 2010). These units were affected by blueschist-facies metamorphism, dated  
45 728 at  $363\pm 2$  Ma, followed by amphibolite to greenschist facies during exhumation by thrusting  
46 729 followed by extensional collapse dated at  $337\pm 3$  Ma (Pereira et al., 2003; Rodríguez Aller,  
47 730 2005; López-Carmona et al., 2010, 2013, 2014).

48  
49  
50  
51  
52  
53  
54  
55  
56 731 The third type occurs in the eastern of the Cabo Ortegal Complex, and is formed by an  
57 732 ophiolitic mélange in the upper part and a mixture of ophiolitic and metasedimentary slices  
58 733 (Arenas et al., 2009). The ophiolitic part includes two igneous series, one with calc-alkaline



734 affinity and the other with tholeiitic island-arc affinity. Both were generated in a mature  
735 volcanic arc in the periphery of Gondwana between 527 and 485 Ma (protolith ages of  
736 amphibolites and orthogneisses). The metasediments include phyllites, phyllonites, marbles,  
737 quartzites and a conglomerate whose detrital zircons yielded a population of 630-464 Ma  
738 constraining the end of magmatic arc activity to the Lower Ordovician. The mélange was  
739 formed during the Upper Devonian in a Variscan subduction zone.

740 The Lower Devonian ophiolites are well represented in the Órdenes and Morais  
741 Complexes. They include metaperidotites (harzburgites) overlain by metagabbros and diabase  
742 to pegmatoid dikes (Díaz García et al., 1999a; Pin et al., 2002, 2006). The chemistry of the  
743 basic rocks is that of island arc tholeiites or transitional between N-MORB and island-arc  
744 tholeiites. A negative Nb anomaly suggests a supra-subduction zone setting (Sánchez  
745 Martínez et al., 2007a). The protoliths are dated at 405-395 Ma, and initial highly positive  
746  $\epsilon\text{Nd}$  values point to magmas being juvenile (Díaz García et al., 1999a; Pin et al., 2002, 2006).

747 More deformed, often mylonitic representatives consist of foliated amphibolites  
748 derived from gabbroic protoliths and mylonitic greenstones alternating with pelitic schists and  
749 inclusions of metagabbros and serpentinites (Ribeiro, 1974; Marques et al., 1991-1992;  
750 Sánchez Martínez et al. 2007b; Arenas et al., 2014). The amphibolites derive from island-arc  
751 tholeiites and may represent the plutonic section of an arc-related ophiolite. Its age is 400-395  
752 Ma (Sánchez Martínez et al., 2007b, 2011; Arenas et al., 2014) but the age spectra include a  
753 zircon population of  $1155 \pm 14$  Ma, interpreted as extracted from the mantle during partial  
754 melting or from a Mesoproterozoic basement. The mylonitic greenschists are transitional  
755 between island-arc tholeiites and N-MORB, with a small negative Nb anomaly.

756 P-T conditions recorded by garnet amphibolites in a metamorphic sole of an  
757 amphibolite-facies unit of the Órdenes Complex yielded 650 °C and 1.15 GPa, pointing to a  
758 relatively hot subduction environment for ophiolite imbrication (Díaz García et al., 1999a).  
759 The prograde foliation was dated at 390-380 Ma (Peucat et al., 1990; Dallmeyer et al., 1991,  
760 1997), and greenschist-facies mylonitic fabric at 364 Ma (Dallmeyer et al., 1997).

#### 761 762 *3.6.4. Upper Allochthon*

763 This ensemble includes two groups separated by a subtractive, low-dipping  
764 detachment. They have a comparable lithological association but differ in the metamorphic  
765 evolution: the structurally lower group underwent early Variscan high-T and high-P

766 metamorphism reaching eclogite facies. In the overlying group, the early Variscan event was  
767 Barrovian but recorded a Cambro-Ordovician, granulite-facies intermediate-P event . Both  
768 groups consist of a thick terrigenous sequence intruded by Cambro-Ordovician gabbros,  
769 granitoids and diabase dikes. Ultramafics occur only in the lower group, where serpentized  
770 ultrabasic rocks of one unit contribute, together with similar rocks of a Lower Devonian  
771 ophiolite, to the magnetic anomaly of the eastern Órdenes Complex (Martínez Catalán et al.,  
772 2012), used for correlation with the Armorican Massif (Fig. 1).

773 The metasediments of the lower group are high-grade paragneisses whose maximum  
774 depositional age is *c.* 510 Ma (Albert et al., 2015). Low grade units occurring on top of the  
775 upper group include metapelites and scarce quartzites and conglomerates. There, the youngest  
776 detrital zircon age population (530-500 Ma), and a diabase dike (510 Ma) indicate a middle  
777 Cambrian maximum depositional age (Fernández-Suárez et al., 2003; Díaz García et al.,  
778 2010; Castiñeiras et al., 2010; Fuenlabrada et al., 2010). The intrusives are dated at 520-490  
779 Ma in both groups (Dallmeyer and Tucker, 1993; Abati et al., 1999; Ordóñez Casado et al.,  
780 2001; Fernández-Suárez et al., 2002, 2007). In the lower group, basic rocks are tholeiitic,  
781 related to continental rifting (Gil Ibarguchi et al., 1990; Galán and Marcos, 1997), while in the  
782 upper group they are tholeiites generated in an ensialic magmatic arc (Andonaegui et al.,  
783 2002, 2016), which is confirmed by the chemistry of granitoids (Andonaegui et al., 2012).

784 Ultramafic rocks are spinel-bearing harzburgites, dunites and pyroxenites of oceanic  
785 affinity (Girardeau and Gil Ibarguchi, 1991) or representing the mantle root of a magmatic  
786 arc. Sm-Nd dating yielded a protolith age of *c.* 500 Ma, whereas growth of garnet in  
787 pyroxenite dated at 390 Ma reflects high-P/high-T, early Variscan metamorphism (Moreno et  
788 al., 2001; Santos et al., 2002). In the intrusives and metasediments of the lower group, this  
789 event reached high-P granulite and eclogite facies (Vogel, 1967; Hubregtse, 1973; Arenas and  
790 Martínez Catalán, 2002) dated at *c.* 400 Ma (Schäfer et al., 1993b; Santos Zalduegui et al.,  
791 1996; Ordóñez Casado et al., 2001; Fernández-Suárez et al., 2002, 2007). Subsequent  
792 exhumation produced migmatization dated at 395-385 Ma (Fernández-Suárez et al., 2002),  
793 and continued by amphibolite-facies mylonitization at 390-380 Ma (Dallmeyer et al., 1991,  
794 1997; Valverde Vaquero and Fernández, 1996; Gómez Barreiro et al., 2006) and Variscan  
795 recumbent folding and thrusting under amphibolite and mainly greenschist facies conditions.

796 In the upper group, the intermediate-P metamorphism is dated at 495-482 Ma, an age  
797 slightly younger than that of the large igneous granodioritic and gabbroic protoliths, close to  
798 which granulite facies was attained. Metamorphism is attributed to crustal thickening nearly

799 coeval to magmatic underplating in the ensialic arc (Abati et al., 1999, 2003, 2007;  
1 800 Andonaegui et al., 2002). Rutile of 390-380 Ma (Abati, 1999) and Ar-Ar ages of  
2 801 amphibolites and metasediments (400-370 Ma; Dallmeyer et al., 1997; Gómez Barreiro et al.,  
3 802 2006) date an early Variscan Barrovian metamorphic overprint associated to recumbent folds  
4 and thrusts.  
5  
6  
7

8  
9 804 In the Upper Allochthon, changes in metamorphic grade are abrupt and occur along  
10 extensional detachments (Díaz García et al., 1999b; Álvarez Valero et al., 2014). Even if their  
11 805 metamorphic histories differ, the lower and upper groups are considered parts of the same  
12 806 terrane because no suture has been found between them. Actually, relics of the Cambro-  
13 807 Ordovician high-T metamorphic event characteristic of the upper group has also been  
14 808 identified in the lower group (Fernández-Suárez et al., 2002).  
15  
16  
17  
18  
19

20  
21 810

### 22 23 811 *3.7. Variscan intrusive magmatism in the Iberian Massif*

24  
25 812 The Variscan Belt is characterized by high-T metamorphism and the abundance of  
26 813 granitoids. It is a hot orogen whose causes, according to Rey et al. (1997) include i) large  
27 814 crustal thickening resulting from collision, ii) the fact that later extension was caused by  
28 815 gravitational collapse instead of plate dynamics, and iii) perhaps high initial geothermal  
29 816 gradients and mantle involvement. In the Iberian Massif, granitoids are abundant in the NW,  
30 817 beneath and around the GTMZ Allochthon, in the Central System and in the SW at both sides  
31 818 of the OMZ/SPZ boundary. Their types and the origin of such a distribution are discussed in  
32 819 the next sections.  
33  
34  
35  
36  
37  
38  
39

40  
41 820

#### 42 43 821 *3.7.1. Synkinematic granitoids*

44  
45 822 In NW Iberia, Capdevila (1969) and Capdevila and Floor (1970) identified three  
46 823 groups of Variscan granitoids, which were recognized in other parts of the Iberian Massif  
47 824 (Fig. 2a). The first and oldest group includes per- and metaluminous, biotite-rich  
48 825 synkinematic granodiorites, often with tonalitic facies, representing magmas with poor fluid  
49 826 content. They are allochthonous in relation to their country rocks and derived from partial  
50 827 melting of the lower crust with some contribution from the mantle (Galán et al., 1996).  
51 828 Vaugnerites (durbachites) have been found associated to these rocks in NW Iberia (Gil  
52 829 Ibarra, 1981; López-Moro and López-Plaza, 2004; Gallastegui, 2005). The age of this  
53  
54  
55  
56  
57  
58  
59  
60  
61  
62  
63  
64  
65

830 group was established at 345-320 Ma (Serrano-Pinto et al., 1987; Fernández-Suárez et al.,  
1 831 2000; Gallastegui, 2005; Gloaguen, 2006; Gloaguen et al., 2006; López-Moro et al., 2017).

832 Early Carboniferous plutons, dated at 347-337 Ma, intruded in or close to the  
5 Parautochthon and Lower Allochthon of the GTMZ (Gutiérrez-Alonso et al., 2018). The age  
6 833 of thrusting of the GTMZ upon the CIZ is 345-340 Ma (Dallmeyer et al., 1997; Abati and  
7 834 Dunning, 2002), and none of the plutons piercing the GTMZ is older than 345 Ma, while  
9 835 several of them intruded along faults that cut across thrust faults related to the emplacement  
10 836 of that allochthonous zone. The transition from building the allochthonous accretionary  
11 837 wedge to the establishment of a collisional regime took place at 360 Ma (Martínez Catalán et  
12 838 al., 2007, 2009), and crustal thickening of the orogenic crust started then. Deep-generated  
13 839 magmas reached upper crustal levels 15-25 m.y. later, when the Allochthon had been  
14 840 emplaced yet. Intrusion of the younger plutons of the granodiorite suite at 325-320 Ma is  
15 841 coeval with an extensional event which followed 15-25 m.y. of thermal relaxation after  
16 842 thrusting of the GTMZ at 345-340 Ma (Martínez Catalán et al., 2014; Alcock et al., 2015).  
17 843 Partial melting of the lower crust and upper mantle probably resulted from radiogenic heating  
18 844 aided by decompression and by water supplied through crustal-scale shear zones.  
19 845

20 846 The second group of granitoids consists of peraluminous two-mica synkinematic  
21 847 granites and adamellites, rich in fluid phases and metasedimentary enclaves. They derive from  
22 848 metasediments and orthogneisses of the middle crust, and are subautochthonous to  
23 849 allochthonous. Their ages fall within the 322-305 Ma time range, with a maximum between  
24 850 310-305 Ma. At that time, the middle crust had reached the temperature necessary to generate  
25 851 melts of monzogranitic composition. These granitoids are concentrated in the GTMZ and  
26 852 around it in the CIZ, suggesting a relationship with crustal thickening and subsequent  
27 853 collapse, as in the case of the younger synkinematic granodiorites. 1-D and 2-D numerical  
28 854 thermal models (Alcock et al., 2009, 2015) show that thickening induced by recumbent  
29 855 folding and thrusting in the GTMZ, CIZ and WALZ may explain the low-P/high-T late-  
30 856 Variscan metamorphic event and also granite production.

31 857 Granitoids of the two synkinematic groups were deformed during emplacement along  
32 858 the extensional event, and by strike-slip ductile shear zones clustering around 310-305 Ma  
33 859 (Gutiérrez-Alonso et al., 2015) associated to which late folds developed (Iglesias Ponce de  
34 860 León and Choukroune, 1980).

35 861

### 862 3.7.2. *Postkinematic granitoids*

1  
2 863 The third group of granitoids (Capdevila, 1969; Capdevila and Floor, 1970) includes a  
3  
4 864 wide range of compositions from gabbro (scarce) to granodiorite and monzogranite, which  
5  
6 865 have the common characteristic of being post-kinematic and allochthonous in relation to the  
7  
8 866 country rocks. They are abundant in the CIZ surrounding the GTMZ, in the Central System  
9  
10 867 and to the south until the limit with the OMZ (Fig. 2a). Late- to post-kinematic granitoids  
11 868 have been dated at 310-285 Ma (Gutiérrez-Alonso et al., 2011 and references therein).

12  
13 869 For those surrounding the GTMZ, thermal modeling by Alcock et al. (2015) explains  
14  
15 870 the voluminous granitic magmatism by crustal thickening followed by thermal relaxation and  
16  
17 871 collapse. They show that the lithospheric mantle gets thinner, facilitating a contribution of the  
18  
19 872 asthenosphere to the heat budget needed for the voluminous magmatism in the internal zones  
20  
21 873 of NW and Central Iberia.

22  
23 874 South of the GTMZ, and in the western part of the Central System batholith, most  
24  
25 875 massifs are postkinematic (Fig. 2a), but some older massifs exist (322-310 Ma), and a smooth  
26  
27 876 transition from the Barrovian event to low-P/high-T conditions and granite intrusion is  
28  
29 877 observed (Valle Aguado et al., 2005, 2017; Díaz-Alvarado et al., 2013; Pereira et al., 2018).  
30  
31 878 In the eastern part of the Central System batholith, all granitoids are postkinematic (308-298  
32  
33 879 Ma), result from partial melting of the lower crust, and their high-grade country rocks were  
34  
35 880 cold at the time of intrusion (Orejana et al., 2012; Villaseca et al., 2017). In anatectic areas of  
36  
37 881 central Iberia, Castiñeiras et al. (2008) found that the later generation of granitoids was  
38  
39 882 unrelated with mid-crustal anatectic processes and had a deeper crustal derivation, so that the  
40  
41 883 mechanisms for granite production there was different, with a stronger mantelic heat input  
42  
43 884 and little contribution of crustal thickening. Several small stocks of postkinematic gabbros  
44  
45 885 and diorites support this interpretation (Zeck et al., 2007b; Orejana et al., 2009).

46 886 An alternative model put forward by Pereira et al. (2015a) defends that the late  
47  
48 887 Carboniferous and early Permian batholiths (315-280 Ma) are calc-alkaline, related with the  
49  
50 888 subduction of Paleotethys oceanic lithosphere and the formation of the Iberian orocline  
51  
52 889 (IAA). Their model is that of plume-assisted relamination, related to a Paleotethyan magmatic  
53  
54 890 arc and unrelated with the Variscan collision.

55 891 In the southern part of the CIZ, two large postkinematic elongated plutons occur  
56  
57 892 parallel to the NW-SE CIZ/OMZ boundary. In the NW, the Nisa-Albuquerque pluton, dated  
58  
59 893 at 310-305 Ma, straddles the Portugal/Spain border (Fig. 2a) and consists of S-type  
60  
61

894 monzogranite to syenogranite, with a core of I-type tonalite-granodiorite (Solá et al., 2009). In  
1 895 the SE, Los Pedroches is a long batholith (Figs. 2a and 3b) dated at 314-304 Ma, whose  
2  
3 896 composition varies from granodioritic to granitic, and that hosts a bimodal dike complex also  
4  
5 897 striking NW-SE (Carracedo et al., 2009). The ensemble occupies the core of the late syncline  
6  
7 898 where the Pedroches Culm is preserved (Fig. 3b). The pluton intruded along a previous crustal  
8  
9 899 to lithospheric-scale fracture (Ábalos and Díaz Cusí, 1995) during an extensional episode  
10  
11 900 responsible for a S-dipping extensional shear zone and faults at the northern limit of the Culm  
12  
13 901 (Martín Parra et al., 2006). In this case, no previous crustal thickening may justify crustal  
14  
15 902 melting, while mantle input (basaltic underplating?) and extension seems the main causes of  
16  
17 903 postkinematic magmatism.

18 904

### 21 905 *3.7.3. Granitoids of the Rhenohercynian arc*

23 906 A magmatic complex straddles the OMZ/SPZ boundary. It occurs at the SW of the  
24  
25 907 OMZ, mostly intruded in the EAMB (Fig. 2a), where it is known as the Beja Igneous  
26  
27 908 Complex. In the east of the SPZ, it is known as the Northern Sierra de Sevilla Batholith. The  
28  
29 909 complex is an association of ultramafic to felsic intrusions dated at 355-335 Ma, the same age  
30  
31 910 as the BAU and partially coeval with the Volcano-Sedimentary Complex formed during the  
32  
33 911 uppermost Devonian to Viséan extensional episode in the SPZ. The left-lateral Southern  
34  
35 912 Iberian Shear Zone (SISZ) displaced the northern part to the west relative to the southern part,  
36  
37 913 and the BAU is essentially a stripe of the Beja gabbro (342 or 352 Ma; Jesus et al., 2007; Pin  
38  
39 914 et al., 2008) strongly sheared by the SISZ.

40 915 The rocks belong to two magmatic suites, tholeiitic-calc-alkaline (basic intrusives and  
41  
42 916 ultrabasic cumulates) and calc-alkaline (monzogranites, subvolcanic granitoids and  
43  
44 917 intermediate rocks; de la Rosa et al., 1992; de la Rosa and Castro, 2004). Basic rocks  
45  
46 918 originated from a basaltic magma and produced some crustal assimilation, generating the  
47  
48 919 intermediate and felsic rocks. The abundance of Mesoproterozoic zircons in a composite  
49  
50 920 pluton (gabbro to granite) adjacent to the BAU suggests that the rocks pierced the SPZ crust,  
51  
52 921 as zircons of that age are uncommon in the OMZ (Gladney et al., 2014), which supports the  
53  
54 922 contention that the SPZ basement is of Avalonian type (Fig. 3c).

55 923 Given the calc-alkaline character of magmatism, genetic models implying subduction  
56  
57 924 are the more reasonable. These include a suprasubduction setting (Quesada et al., 1994)  
58  
59 925 perhaps including slab break-off (Pin et al., 2008) or ridge subduction (Castro et al., 1996a,

926 1996b). Because of its age, subduction cannot be that of the Rheic lithosphere, but that of the  
927 Rhenohercynian Ocean, the closure of which formed the Rhenohercynian arc identified in the  
928 NW of the Bohemian Massif and active between 360-325 Ma (Zeh and Will, 2010).

929 A group of granitoids in the central and eastern parts of the OMZ are also related with  
930 the Rhenohercynian arc (Fig. 2a). Their composition includes ultramafics, gabbro, tonalite,  
931 granodiorite, and minor bodies of granite and leucogranite. Intermediate rocks are the most  
932 abundant. They are metaluminous, show a calc-alkaline character and are dated at 355-330  
933 Ma (Casquet and Galindo, 2004).

### 934 3.8. Other Variscan massifs of the Iberian Peninsula

#### 935 3.8.1. La Demanda and Iberian Chains

936 The basement outcrops of La Demanda and the Iberian Chain are considered the  
937 continuation of the WALZ (Fig. 2a). Both share a similar Neoproterozoic and Paleozoic  
938 sequence (Gutiérrez-Marco, 2004a; Gutiérrez-Marco et al., 2002, 2004; Liñán et al., 2002,  
939 2004) with the difference of a thick Devonian sequence of siliciclastics and carbonates in the  
940 Iberian Chain (Carls et al., 2004), missing in the WALZ due to erosion. The Variscan  
941 structure in these Alpine basement uplifts includes steep to overturned early folds (pre-  
942 Westphalian), some thrust faults in La Demanda and only upright early folds in most of the  
943 Iberian Chain. Shortening and crustal thickening was less important than in the WALZ.  
944 Metamorphism is of low-T greenschist facies and a slaty cleavage accompanies the folds,  
945 which delineate the northern limb and part of the hinge zone of the CIA (Fig. 2a).

#### 946 3.8.2. Pyrenees and Catalonia Coast Ranges

947 The massifs occurring at the northern limb of the IAA include the central and eastern  
948 Pyrenees and the Catalonia Coast Ranges. They can be correlated with the WALZ and CIZ of  
949 the Iberian Massif, but two main differences exist. One is the age of the Ordovician  
950 voluminous felsic magmatism, which is younger in the Pyrenees (477-446 Ma; Casas et al.,  
951 2017; Casas and Murphy, 2018; Clariana et al., 2017), than in the CIZ (500-465 Ma; Solá et  
952 al., 2008; Montero et al., 2009a; Díez Montes et al., 2010; Talavera et al., 2013). The other is  
953 the Sardinian unconformity, found elsewhere in the Mediterranean province (Álvaro et al., 2017;  
954 Casas, 2010) but not found in the CIZ (González-Clavijo et al., 2017). In western Pyrenees,  
955

957 the Basque Massifs (Fig. 2a) differ from the rest of the chain because the Lower Ordovician  
958 includes shallower water successions and the Sardinic unconformity is absent (Gutiérrez-  
959 Marco, 2004b). This, and the absence or very low grade metamorphism rather suggest a  
960 correlation with the CZ. Moreover, a similar late Carboniferous conodont fauna has been  
961 found in the CZ and the Basque Quinto Real Massif (Sanz-López and Blanco Ferrera, 2012,  
962 2013; Rodríguez-Cañero et al., 2018).

963 In the central and eastern Pyrenees (Axial Zone), an early Carboniferous Barrovian  
964 event was followed by a low-P/high-T event (Guitard et al., 1995; de Hoym de Marien et al.,  
965 2019). A detachment separates an upper, low-T crust (superstructure) from a middle crust  
966 with numerous gneiss domes and postkinematic granitoids (infrastructure). Partitioning of  
967 deformation occurred at 310-290 Ma in a context of dextral transpression (Carreras and  
968 Druguet, 2014; Cochelin et al., 2017): while the middle crust recorded E-W lateral flow and  
969 dome emplacement, the upper crust was thickened developing E-W folds and a steep, low-  
970 grade axial planar cleavage. Late growth of kyanite occurred locally, caused by isobaric or  
971 slightly compressional cooling during dextral transpression (Guitard et al., 1995).

972 Folds previous and oblique to the E-W system, are recognized in the Basque Massifs.  
973 They are overturned toward the west or SW and often cut across by thrust faults, which is  
974 coherent with a continuation of the northern limb of the IAA. These early structures affect the  
975 synorogenic Namurian flysch, which supports correlation with the CZ.

976 The Catalonia Coast Ranges show stratigraphic affinities with the Variscan  
977 Mediterranean province and can be correlated with the Pyrenean and Sardinian successions  
978 (Gutiérrez-Marco, 2004a). No differences exist between the NE and SW massifs (Gutiérrez-  
979 Marco et al., 2004), which leaves little room for the continuation of the CZ to the south. A  
980 right-lateral fault trending NW-SE (Malod, 1982; Boillot et al., 1984) may have contributed to  
981 hide part of the eastern prolongation of the CZ acting as reverse during the late stages of arc  
982 closure. The CZ may however continue in the island of Menorca, where pre-orogenic  
983 Devonian and synorogenic Carboniferous sequences occur (Obrador et al., 2004).

984 North of the North Pyrenean Fault (NPF), the basement of the Aquitaine Basin is  
985 known from boreholes. According to Paris and Le Pochat (1994), lithologic and faunal  
986 evidences suggest affinity with the Pyrenees, the Montagne Noire and the Cantabrian  
987 Mountains. The existence in Aquitaine of recumbent folds, cleavage and low grade  
988 metamorphism suggests correlation with either the WALZ or CIZ. As there are no criteria to



989 distinguish between CIZ and WALZ in the northern branch of the IAA, both zones have been  
1 990 merged as the continuation of the CIZ because it is wider, Ordovician orthogneisses are  
2 991 common in the CIZ and the Axial Zone and absent in the WALZ, and tectonometamorphic  
3 992 evolution of the Pyrenean Axial Zone can be compared with that of the CIZ.  
4  
5  
6

7 993 A dextral displacement of 300 km along the NPF balances the appearance of the CZ in  
8 994 the Cinco Villas Basque Massif, north of the NPF (Fig. 1). Its Permian cover yielded  
9 995 paleodeclinations with a European orientation (NNE-SSW; Van der Voo and Baessenkool,  
10 996 1973), while south of the NPF, paleodeclinations are NNW-SSE (Boillot et al., 1984). The  
11 997 NPF occurs south of the Cinco Villas Massif (Gil Peña and Barnolas, 2004), and may be  
12 998 continued north of the Quinto Real Massif (Fig. 2a), implying that the latter could have  
13 999 remained in the Iberian side, while the northern Basque massifs formed part of the northern  
14 1000 block. In Figure 1, the contour of the Basque Massifs is duplicated, but the darker color  
15 1001 suggests the position of the northern and southern massifs. The 300 km of late Variscan  
16 1002 dextral displacement nearly balances the 400 km of left lateral movement during the  
17 1003 Cretaceous (Boillot et al., 1984)), so that the northern and southern massifs would have been  
18 1004 relatively close during most of the Variscan deformation.  
19  
20  
21  
22  
23  
24  
25  
26  
27  
28  
29  
30  
31

#### 32 1006 **4. French and related massifs**

33 1007 The main Variscan outcrops in France occur in the Armorican Massif and the Massif  
34 1008 Central. Other massifs include the Axial Zone of the Pyrenees, Maures-Tanneron, Corse, the  
35 1009 Vosges, a small part of the Rhenish Massif, which continues in Belgium, Luxemburg and  
36 1010 Germany, and part of the External Massifs of the Alps, (Fig. 4). This section describes these  
37 1011 massifs, except the Pyrenees, which were described in the Iberian Peninsula section, and the  
38 1012 Rhenish Massif, essentially formed by the Rhenohercynian Zone and which will be described  
39 1013 together with the Bohemian Massif. In addition, the Sardinia and the Schwarzwald are  
40 1014 described here because of their close relation with Corse and the Vosges respectively. For a  
41 1015 comprehensive text describing the Variscan geology of France, see the book edited by Keppie  
42 1016 (1994). Compilations for the main massifs, mostly dealing with the Allochthon, can be found  
43 1017 in the volume edited by Schulmann et al. (2014a).  
44  
45  
46  
47  
48  
49  
50  
51  
52  
53  
54  
55  
56  
57  
58  
59  
60  
61  
62  
63  
64  
65

1019 *4.1. Armorican Massif*

1  
21020 The most salient characteristic of this massif is the transpressional type of tectonics.  
3  
41021 Strike-slip faults and shear zones, mostly right-lateral, cut across the Massif and the more  
5  
61022 important of them separate three domains named North, Central and South. Only the  
7  
81023 Autochthon exists in the North and Central domains, with the exception of a narrow band of  
9  
101024 Parautochthon in the latter, whereas the South Armorican Domain is largely occupied by the  
111025 Allochthon.  
12

13  
141026  
15  
161027 *4.1.1. Central Armorican Domain (CAD)*  
17

181028 This domain is bounded by the North Armorican Shear Zone, whereas its southern  
19  
201029 boundary is usually located at the Nort-sur-Erdre Fault (Fig. 4), as it represents the northern  
21  
221030 limit of the three groups forming most of the Allochthon in the South Armorican Domain  
23  
241031 (Ballèvre et al., 2014). So defined, the CAD is a WNW-ESE striking band 45-90 km wide.  
25

261032 To the north of the Nort-sur-Erdre Fault, the St. Georges-sur-Loire Unit includes  
27  
281033 Upper Ordovician to Middle Devonian metasediments (Lardeux and Cavet, 1994), whose  
29  
301034 prevailing lithologies are low-grade schists, often with greenish and purple colors. Also  
31  
321035 frequent are black cherts and volcanics (spilites, basic tuffs, quartz-porphyrries) which show  
33  
341036 little continuity. Cartier and Faure (2004) describe this unit as formed by two allochthonous  
351037 subunits. The southern subunit includes olistostromes and exotic blocks of black cherts,  
36  
371038 limestone, sandstone, acid and basic volcanics, of Silurian and Devonian ages, embedded in a  
38  
391039 pelitic or sandy matrix. The age of sedimentation is unknown, but must be more recent than  
40  
411040 the younger limestone blocks, which are Middle Devonian. Metamorphism is of greenschist  
42  
431041 facies, close to blueschist facies (Rolet et al., 1994). The northern subunit consists of  
44  
451042 sandstone and pelite alternation with a thick quartzitic level, and its age is probably  
461043 Ordovician. Thrusting of the unit upon the northern autochthonous CAD is established at 360-  
47  
481044 350 Ma (Rolet et al. 1994).  
49

501045 To the north of the St. Georges-sur-Loire Unit, the CAD is represented by  
51  
521046 Neoproterozoic (Brioverian) strata, representing a foreland where the effects of the Cadomian  
53  
541047 orogeny are limited to gentle folding (Trautmann et al., 1994), and by Paleozoic pre- and  
55  
561048 synorogenic sequences. No Cadomian or Cambrian intrusions, neither pre-Variscan  
57  
581049 deformation or metamorphism are recognized, and the sequence is thick and terrigenous,  
59  
601050 often bearing clasts of black cherts, and including some carbonates and volcanic alternations  
61

1051 (Chantraine et al., 1994a, b). The Brioverian is unconformably overlain by Lower Ordovician  
1052 detritals, starting with continental red beds and overlain by the Armorican Quartzite. The  
1053 Ordovician is complete and culminates with Hirnantian glaciation-related deposits (Vidal et  
1054 al., 2011; Dabard et al., 2021). A few Ordovician granitic plutons dated at 495-450 Ma occur  
1055 in this domain. The Silurian is also rather complete, and characterized by the abundance of  
1056 black shales, and the Devonian is marine, with abundant silts and quartzites, often  
1057 ferruginous, alternating with shales and limestones (Robardet et al., 1994).

1058         Synorogenic early-middle Carboniferous deposits lie unconformably upon the  
1059 Paleozoic sequence, although the latter is often fully preserved. Weak folding and erosion  
1060 preceded Carboniferous volcanism and deposition, which allowed Stille (1928) to define the  
1061 Bretonnic phase based in the maps of the central Brittany fold set (Paris et al., 1982). The  
1062 main carboniferous outcrop of the CAD occurs in the NW, at the core of the large E-W  
1063 Chateaulin Syncline. It is terrigenous with volcanic alternations and evidence of syntectonic  
1064 deposition highlighted by exotic blocks, Carboniferous platform carbonates olistoliths and  
1065 mudflows. Its age is Tournaisian to early Namurian (Pelhate, 1994).

1066         Variscan deformation is dominated by a set of late Variscan folds slightly oblique to  
1067 the limits of the domain, which are dextral strike-slip faults. Early pre-Carboniferous folds are  
1068 responsible for the Bretonnic unconformity, but they are open, scarce, and their geometry is  
1069 mostly unknown. Some NE- and NW-trending folds in the Crozon Peninsula, at the western  
1070 termination of the CAD may correspond to this phase. Also, the interference pattern shown by  
1071 the central Brittany fold set may result from superposition of roughly E-W late folds on a set  
1072 of previous, NNE-trending folds (Fig. 4).

1073         The main Variscan deformation in the CAD has been interpreted as resulting from  
1074 crustal-scale simple shear deformation (Gumiaux, 2003; Gumiaux et al., 2004). Shearing was  
1075 dextral (Figs. 4 and 5a), and generated the late Variscan “en échelon” folds subsequently  
1076 flattening and rotating them toward the flow plane of regional shearing. A statistical estimate  
1077 of cleavage orientation (N 95°-100° E) and its relation with the shear plane (N 125° E) yields a  
1078 mean angle of 26°, equivalent to a shear value  $\gamma = 1.5$ , equivalent to a shear angle of 56°  
1079 (Gumiaux et al., 2004). No significant vertical stretching occurred. Assuming that  
1080 deformation was only by simple shear, this implies 50 % shortening perpendicular to the  
1081 cleavage.

1082 Metamorphism is generally of low to very low grade, although P-T conditions increase  
1083 to the west, where the amphibolite facies is reached, and south of the CAD, close to the  
1084 northern branch of the South Armorican Shear Zone. The baric type is of low- to  
1085 intermediate-P type with kyanite occurrences in shear zones, and of high-T around granite  
1086 plutons, associated to which, migmatitic gneisses may occur (Rolet et al., 1994).

#### 4.1.2. North Armorican Domain (NAD)

1087 This domain, bounded by the North Armorican Shear Zone, is interesting for the  
1088 occurrence of an old, Paleoproterozoic basement, abundant evidences of the Cadomian  
1089 orogeny, and three main Paleozoic unconformities. The Icartian basement crops out at the  
1090 outermost coastal regions to both sides of the Saint-Malo Gulf and in the outer Channel  
1091 Islands. It includes granodioritic and monzogranitic orthogneisses often migmatitic, as well as  
1092 banded gneisses of sedimentary and volcanic origin. Their ages, ranging 1.8-2.2 Ga, point to a  
1093 Gondwanan provenance (Chantraine et al., 1994b).

1094 The sedimentary and volcanic succession is Neoproterozoic and collectively named  
1095 the Brioverian (Barrois, 1899). It is made of two groups, the lower of which bears bedded  
1096 black cherts whereas the upper group includes this lithology only as clasts. The lower  
1097 Brioverian is profusely intruded by Cadomian plutons dated at 670-580 Ma, and is interpreted  
1098 as developed in an active margin on which three SW-NE trending subdomains have been  
1099 recognized from NW to SE: a magmatic arc, a back-arc and a continental margin. The latter is  
1100 characterized by the abundance of bedded black cherts and tholeiitic volcanics (Bale and  
1101 Brun, 1983; Chantraine et al., 1994a, c), and its development was contemporaneous with arc  
1102 magmatism. The upper Brioverian was deposited at *c.* 580-540 Ma and intruded by  
1103 postorogenic 540-520 Ma plutons. Voluminous volcanism, mostly rhyolitic and ignimbritic,  
1104 characterizes the Proterozoic-Paleozoic boundary, and has been dated between 545-520 Ma.

1105 The main Cadomian orogenic phase occurred at 600-580 Ma, and zonation of the  
1106 deformation includes a large area with vertical cleavage and late-tectonic plutonism (540 Ma)  
1107 occupying a triangular zone between the Granville-Cancale Fault and the North Armorican  
1108 Shear Zone (Fig. 4). The SW-NE trending band to the north includes, from SE to NW, a zone  
1109 of high-T metamorphism with migmatites, another characterized by thrusting and sinistral  
1110 wrenching, with 615-585 Ma syntectonic plutonism, and inside the latter to the north, areas of  
1111 no cleavage with post-orogenic plutonism (Rabu et al., 1994).

1114 Thick terrigenous early Cambrian deposits unconformably overlay the Brioverian in  
1115 the NE, alternating with ignimbrites, rhyolites and scarce andesites, as well as carbonates.  
1116 These are in turn unconformably covered by Lower Ordovician red beds deposited in deltaic  
1117 environments and by the Armorican Quartzite, which may show a gradual transition from the  
1118 red beds or lay directly upon the Cambrian or the Brioverian (Robardet et al., 1994). No  
1119 Ordovician granitic plutons occur in the NAD. The rest of the preorogenic succession does  
1120 not differ significantly from that of the CAD, although ages of the detrital zircons in  
1121 Ordovician strata differ notably (Dabard et al., 2021). The third significant unconformity is  
1122 marked by the synorogenic Carboniferous deposits, characterized by an initial extensional  
1123 phase marked by rhyolites and ignimbrites, and by conglomerates, sandstones, mudstones,  
1124 coal beds and platform limestones, reflecting a paralic environment and reaching the early  
1125 Namurian (Pelhate, 1994).

1126 In the Pays de Léon, to the north of the westernmost Armorican Massif, high-P rocks  
1127 have been identified in what seems a different domain or zone. There, a lower unit of coarse-  
1128 grained augengneisses, probably Paleozoic, is the footwall to an upper unit of ortho- and  
1129 paragneisses, migmatized and with lenses of eclogite at its base. High-P metamorphism was  
1130 dated not very precisely around 440-415 Ma (Cabanis and Godard, 1987; Paquette et al.,  
1131 1987; Ballèvre et al., 1994). Later, pervasive migmatization gave rise to a gneiss dome (Rolet  
1132 et al., 1994). This unit has been interpreted as probably derived from the South Armorican  
1133 Domain, displaced at least 150 km to its present position by dextral transcurrent shear zones  
1134 (Balé and Brun, 1986), as representing the Saxothuringian Zone (Schulz et al., 2007), and as  
1135 an equivalent to the Mid German Crystalline High (Faure et al., 2010a).

1136 Except for the Léon, Variscan reworking was weak in the NAD. North of the Gravelle-  
1137 Cancale Fault, deformation started during the Upper Devonian by remobilization of Cambrian  
1138 faults, which produced WSW-ENE folds in the north and continued during the early  
1139 Carboniferous by NNE and SSW-verging thrusts and N 110° E folds. Folds in the north are  
1140 locally associated with a strong, greenschist facies cleavage (Rolet et al., 1994). The  
1141 triangular zone between the Gravelle-Cancale Fault and the North Armorican Shear Zone  
1142 (Fig. 4) is characterized by Cadomian late-tectonic plutonism and vertical cleavage. Variscan  
1143 deformation there is so weak that a N-trending dolerite dike swarm (Le Gall, 1999), early  
1144 Carboniferous and perpendicular to the late Variscan folds, is undeformed.

1146 *4.1.3. South Armorican Domain (SAD)*

1  
21147 Most of the Armorican Massif SW to the Nort-sur-Erdre Fault is occupied by  
3  
41148 allochthonous units which have been grouped in three ensembles that correlate with  
5  
61149 equivalents in NW Iberia (Ballèvre et al., 2014 and references therein). The Allochthon crops  
7  
81150 out in a triangular zone between the Nort-sur-Erdre Fault and the southern branch of the  
9  
91151 South Armorican Shear Zone, and also as klippen south of the latter (Fig. 4). The original  
10  
111152 contacts between units are interpreted as thrust faults, although in many cases, including the  
12  
131153 contact with the Autochthon, they were overprinted by extensional detachments.  
14

15  
161154 The Autochthon consists of Cambrian to Devonian metasediments and metavolcanics  
171155 in the SE and mostly schists, granitic orthogneisses and migmatites toward the NW. In the  
18  
191156 south (Vendée littorale), the sequence includes from bottom to top migmatites and high-grade  
20  
211157 gneisses, a thick succession of Cambro-Ordovician aluminous schists with rare carbonates,  
22  
231158 Lower Ordovician porphyroids, thin quartzite layers and monotonous grey slates. Above, and  
24  
251159 separated by a thrust fault, synorogenic deposits, low-grade schists, ampelites and black  
26  
271160 cherts probably represent the Parautochthon (Ballèvre et al., 2012). Lower Ordovician felsic  
281161 magmatism in the Autochthon and Parautochthon is interpreted by Pouclet et al. (2017) as  
29  
301162 related with a continental rift where magmatic underplating produced abundant crustal  
31  
321163 melting, and which can be followed from central and northern Iberia to southern France.  
33

341164 Above, a thrust sheet with Lower Ordovician porphyroids is still considered the  
35  
361165 Parautochthon, and occurs beneath the Lower Allochthon and the high-P Middle Allochthon  
37  
381166 represented by the Bois-de-Cené Unit (Figs. 4 and 5a). Migmatization of the lower parts of  
39  
401167 the Autochthon postdate emplacement of the allochthonous pile, and was overprinted by the  
41  
421168 southern branch of the South Armorican Shear Zone.  
43

441169 The Lower Allochthon is well represented in the Champtoceaux Complex, along the  
45  
461170 Vendée coastline to the south, and in poorly exposed klippen NW of the latter (Figs. 4 and  
47  
481171 5a). The better exposures occur at the core of the antiform where the Champtoceaux Complex  
49  
501172 crops out. It consists of a thick sequence of albite-bearing micaschists derived from late  
51  
521173 Neoproterozoic greywackes, fine-grained leucocratic gneisses with eclogite lenses, garnet  
531174 micaschists, and graphitic schists. Leucocratic orthogneisses of calc-alkaline and alkaline  
54  
551175 composition were dated at *c.* 495-475 Ma (Ballèvre et al., 1987, 1989, 2014). The eclogite  
56  
571176 protoliths are doleritic dikes intruding the Lower Ordovician granitoids and felsic volcanics  
58  
591177 (Godard, 1988).  
60  
61  
62  
63  
64  
65

1178 Early Variscan high-P metamorphism is recorded in eclogites, orthogneisses and felsic  
1179 gneisses. In the Champtoceaux Complex, an along-strike gradient shows increasing  
1180 metamorphic conditions toward the west (from 1.5-2 GPa to *c.* 2.5 GPa; Godard et al., 1981;  
1181 Ballèvre and Marchand, 1991; Bosse et al., 2000), indicating continental subduction toward  
1182 the NW in present coordinates. High-P metamorphism has been dated at *c.* 360 Ma in a  
1183 glaucophane-bearing eclogite by U-Pb and Sm-Nd methods (Paquette, 1987; Bosse et al.,  
1184 2000; Paquette et al., 2017). Ar-Ar data on phengite yielded *c.* 350-340 Ma (Bosse et al.,  
1185 2000; Maurel et al., 2003), probably reflecting decompression, which took place during  
1186 stacking of the units and thrusting onto the Autochthon. This stage was associated with  
1187 inverted metamorphism, followed by fast cooling at 340-330 Ma (Pitra et al., 2010).

1188 The Middle Allochthon includes a group of Cambro-Ordovician oceanic units and at  
1189 least an Upper Devonian unit. The older group is exposed in the Audierne Bay, Ile-de-Groix  
1190 and Vendée littorale (Bois-de-Cené Unit; Figs. 4 and 5a). In the Audierne Bay Complex, a  
1191 metaophiolite unit includes serpentized peridotites, metagabbros and greenschists that most  
1192 probably derive from basaltic flows and tuffs (Peucat, 1973; Peucat and Cogné, 1974;  
1193 Hanmer, 1977). The basic rocks belong to a tholeiitic suite with MORB compositions  
1194 (Bernard-Griffiths and Cornichet, 1985; Lucks et al., 2002). The unit has a distinct magnetic  
1195 signature that can be followed offshore to the SW for more than 100 km (BRGM, 1972; de  
1196 Poulpiquet, 1988). A plagioclase-rich metagabbro of the ophiolite was dated at 482 Ma  
1197 (Paquette et al., 2017). The rocks were intensely deformed under amphibolite facies  
1198 conditions.

1199 Other rocks of oceanic affinity include the blueschist-facies metabasites and  
1200 micaschists of Ile-de-Groix and Bois-de-Cené units. The latter unit lies above the Lower  
1201 Allochthon occupying the core of a synform, while the structural position of Ile-de-Groix is  
1202 unknown. The metabasites derive from basaltic lava flows or sills that underwent extensive  
1203 alteration by oceanic hydrothermalism, but E-MORB affinities can be recognized (Bernard-  
1204 Griffiths et al., 1986; El Korh et al., 2009). Oceanic sediments include cherts and  
1205 manganiferous nodules. The age of this sequence is constrained by rare layers of fine-grained  
1206 felsic gneisses which have provided a zircon age of 481 Ma (El Korh et al., 2012). The  
1207 metamorphic history is dominated by blueschist-facies metamorphism (Ballèvre et al., 2003;  
1208 El Korh et al., 2009). The metamorphic zonation in the Ile-de-Groix (Triboulet, 1974) has  
1209 been interpreted as due to the superposition of two units that slightly differ in their P-T paths  
1210 (Bosse et al., 2002; Ballèvre et al., 2003). Rb-Sr and Ar-Ar data indicate that the high-P event

1211 took place 370-360 Ma ago, while cooling was achieved in rocks overprinted by greenschist-  
1212 facies metamorphism at *c.* 350-340 Ma (Bosse et al., 2005). U-Pb data on titanite confirmed  
1213 the Late Devonian age of the high-P event (El Korh et al., 2012).

1214 A narrow belt of oceanic rocks occurs in Vendée east of the Bois-de-Cené Unit  
1215 (Ballèvre et al., 2009). Its composition ranges from amphibolites of basaltic composition to  
1216 rhyodacitic leucocratic banded gneisses. Geochemically, the suite follows a tholeiitic trend,  
1217 and has been interpreted as a volcanic sequence perhaps erupted in an island-arc or forearc  
1218 setting (Thiéblemont et al., 1987a). Metamorphism is characterized by the lack of eclogite-  
1219 facies relics and peak P-T conditions at *c.* 0.7 GPa at 470-550 °C (Thiéblemont et al., 1988).  
1220 The ages of the protoliths and their metamorphism have not been investigated, but they are  
1221 tentatively considered Early Ordovician in age (Ballèvre et al., 2014). Another possible  
1222 ophiolitic unit of unknown age is intercalated in the Lower Allochthon of the Champtoceaux  
1223 Complex (Figs. 4 and 5a).

1224 A Devonian ophiolitic unit bounds the Champtoceaux Complex, separating the Lower-  
1225 from the Upper Allochthon. In the east, it is made of serpentized peridotites and  
1226 metagabbros. Most metagabbros have been severely deformed under amphibolite facies  
1227 conditions, but some of them preserve magmatic textures and mineralogy. The metagabbros  
1228 show compositions of cumulates or of N-type MORB (Bernard-Griffiths and Cornichet, 1985;  
1229 Paquette, 1987), and one of them was dated as Upper Devonian (*c.* 380 Ma; Paquette, 1987;  
1230 Paquette et al., 2017). Toward the west, the unit changes into greenschists and micaschists  
1231 possibly representing the upper part of the oceanic crust.

1232 The Upper Allochthon in the SAD includes a lower group of units characterized by an  
1233 eclogite-facies event and an upper group of low-grade Cadomian basement unconformably  
1234 overlain by Cambrian to Carboniferous sediments. The best example of the high-P group is  
1235 the Essarts Unit, cropping out SW of the southern branch of the South Armorican Shear Zone  
1236 (Figs. 4 and 5a). This unit consists of eclogites, orthogneisses and migmatized paragneisses.  
1237 The eclogites derive from metagabbros forming a MORB-type tholeiitic suite (Godard, 1988,  
1238 2001) and interlayered banded gneisses derived from plagiogranites point to an oceanic crust  
1239 provenance (Montigny and Allègre, 1974; Godard, 1983, 1988; Bernard-Griffiths and  
1240 Cornichet, 1985). Magmatic zircons from an eclogite provided a protolith age around 490 Ma  
1241 (Paquette et al., 2017). The unit also contains orthogneisses, one of them dated at 483 Ma  
1242 (Lahondère et al., 2009). Moreover, polycyclic gneisses record a high-T metamorphism  
1243 predating the eclogite-facies event (Godard, 2001, 2009). The early high-temperature event is



1244 recorded by migmatitic, cordierite-bearing gneisses that also show evidences of cooling. A  
1245 first generation of monazite is associated with the high-T event and was dated at 460 Ma, no  
1246 far from protolith ages of gabbros and granitoids, to which it is possibly related. A younger  
1247 population gave 375 Ma, potentially dating the high-P event or later exhumation of the unit.

1248 An eclogitic unit also occurs in the Audierne Bay Complex, where a few tectonic  
1249 slices display garnet-diopside mafic granulites, eclogites and garnet-kyanite gneisses (Velde,  
1250 1972; Marchand, 1982; Lucks et al., 2002). They occur on top of the Cambro-Ordovician  
1251 oceanic unit and are separated from it by a strongly deformed orthogneiss which may occur at  
1252 a ductile extensional detachment (Ballèvre et al., 1994). All slices record a high-P/high-T  
1253 metamorphism (*c.* 1.8-2.0 GPa, 800-900 °C). U-Pb data on zircons (Peucat, 1983; Paquette et  
1254 al., 1985) suggest an Early Ordovician age for the granulite protoliths (485-480 Ma) and the  
1255 orthogneiss (480-470 Ma). The high-P event is constrained at 390-380 Ma.

1256 Another unit has been recognized in the Audierne Bay Complex, consisting of  
1257 metagreywackes and interbedded amphibolites. The age of the protoliths is unknown, and the  
1258 metamorphic grade is of the albite-epidote-amphibolite facies. The affinity of this unit is still  
1259 unclear, but due to its structural position above the ophiolite complexes, it can be tentatively  
1260 ascribed to the Upper Allochthon and correlated with the intermediate-P units of NW Iberia  
1261 (Ballèvre et al., 2014).

1262 The upper group of the Upper Allochthon in the SAD includes two low-grade units,  
1263 one overlying the Champtoceaux Complex (Mauges Unit) and the other above the Essarts  
1264 Unit (Roc-Cervelle). The former displays a Proterozoic basement made of low-grade schists  
1265 with a layer of black cherts associated with mafic volcanics. An increasing grade of  
1266 metamorphism is recorded towards the contact with the underlying Devonian ophiolitic unit,  
1267 where a sequence of mylonitized amphibolite-facies gneisses 1 km thick occurs.

1268 In the southern part of the Mauges Unit, the Paleozoic cover consists of Cambrian  
1269 conglomerates and schists (Cavet et al., 1966; Ducassou, 2010) overlain and partly intruded  
1270 by a complex of mafic to felsic volcanic rocks dated at *c.* 520 Ma (Thiéblemont et al., 1987b,  
1271 2001). Along the northern boundary, the Neoproterozoic basement is unconformably overlain  
1272 by Lower Ordovician reddish siltstones (Cavet et al., 1971). Cambrian volcanics (Perroud and  
1273 van der Voo, 1985) and Lower Ordovician siltstones (Perroud et al., 1986) have provided  
1274 paleomagnetic evidence of high southerly latitudes, consistent with a northern Gondwana  
1275 setting. Above lies unconformably a Lower-Middle Devonian formation starting with

1276 sandstone, following by reefal limestone and culminating with immature sandstones rich in  
1277 plant debris (Ducassou et al., 2009). A more distal sequence includes Upper Ordovician  
1278 sediments displaying a typical glaciomarine record covered by Silurian graptolite-rich cherts  
1279 (Piçarra et al., 2002, 2009), pelites and Emsian pelagic carbonates. Synorogenic sediments  
1280 exist in the north: early Carboniferous lacustrine and alluvial deposits laid down in a  
1281 transtensional basin (Ballèvre and Lardeux, 2005; Ducassou, 2010).

1282 Another Upper Allochthon low-grade unit (Roc-Cervelle) is located SE of the Essarts  
1283 Unit and consists of low-grade schists perhaps Cadomian (Bouton and Branger, 2007; Bouton  
1284 and Camuzard, 2012). A Devonian sequence cropping out nearby might have been deposited  
1285 on top of the schists. It includes from bottom to top Givetian fluvatile sandstones, shales and  
1286 reefal limestones (Le Maître, 1937), recording a marine transgression close to an emerged  
1287 land. The low-grade units of the Upper Allochthon in the SAD record the sedimentary  
1288 evolution at the beginning of the convergence. Because the sediments contain abundant  
1289 volcanic-derived material, it is possible that the Upper Allochthon were part of a continental  
1290 magmatic arc during late Lower-Middle Devonian (Ducassou et al., 2014).

#### 1291 4.2. *French Massif Central (FMC)*

1292 The FMC is essentially formed by allochthonous terranes, while the Autochthon crops  
1293 out only to the south, in the Montagne Noire region. Lardeux et al. (2014) correlate this  
1294 Massif with that of Bohemia and include its allochthonous part in the Moldanubian Zone. The  
1295 following description is based on their overview and that of Faure et al. (2009), and proceeds  
1296 describing the structural pile from bottom to top.

1297 A fold and thrust belt affecting Cambrian to early Carboniferous sediments and  
1298 igneous rocks developed in the Montagne Noire region, which is considered the continuation  
1299 of the Pyrenean Axial Zone. It consists of Cambrian to middle Carboniferous low-grade  
1300 metasediments representing a passive margin. Sediments are mostly terrigenous except for a  
1301 thick carbonate platform developed during the Middle Devonian to early Carboniferous. In  
1302 the north, the structure consists of large, south-vergent recumbent folds and thrust faults  
1303 deformed in the Axial Zone of the Montagne Noire by two large, adjacent flattened gneiss  
1304 domes whose emplacement is linked with a pull-apart structure created during dextral  
1305 transcurrence (Franke et al., 2011). The domes consist essentially of Cambro-Ordovician  
1306 orthogneisses pervasively migmatized. Protoliths have yielded ages between 550 and 450 Ma,  
1307

1308 and low-P/ high-T metamorphism is dated at 340-320 Ma (Cocherie et al., 2005; Faure et al.,  
1309 2010b, 2014). An earlier high-P event is represented by eclogites resulting from the  
1310 metamorphism of basic dikes. High-P metamorphism has been dated at *c.* 355-350 Ma, and  
1311 interpreted as the result of intracontinental subduction (Faure et al., 2014). Large recumbent  
1312 folds developed between 340-330 Ma in the Paleozoic series, and were later deformed by  
1313 doming and flattening related to transpression at 330-315 Ma. Migmatization in the Axial  
1314 Zone took place between 320-295 Ma (Poujol et al., 2017) or 315-303 Ma (Trap et al., 2017).

To the south, a synorogenic turbiditic basin developed during the Visean-Namurian  
and can be continued under the recent cover until the Pyrenees. The basin was affected by  
recumbent folds and thrust faults with a NE vergence contemporaneously with its  
sedimentation, and large olistoliths were emplaced in proximal turbidite facies during the  
deformation (Engel et al., 1980; Chardon et al., 2020).

Above the Autochthon, a thrust sheet of low-grade metasediments represents the  
Parautochthon. It crops out in the SE of the FMC, and in tectonic windows on its western and  
northern parts (Fig. 4). It consists of schists, quartzites, rare limestones and felsic and mafic  
metaigneous rocks (Lardeaux et al., 2014). Metamorphism is Carboniferous and generally of  
low grade (greenschist to epidote-amphibolite facies), although anatexis was locally reached  
in areas intruded by voluminous Variscan granites.

The Parautochthon is overlain by the Lower Gneiss Unit (LGU), whose lithology is  
similar to that of the underlying unit but it is metamorphosed mostly under amphibolite-facies  
conditions. Cambro-Ordovician magmatism is tholeiitic or alkaline, similar to that of the  
Parautochthon, and derived from the northern Gondwana passive continental margin (Briand  
and Santallier, 1994). Basic and ultrabasic rocks are rare except in the Limousin (NW Massif  
Central). Relics of high-P granulites and eclogites have been found in some units of the  
western part of the FMC (Ledru et al., 1994a). Barrovian metamorphism reaching the  
sillimanite zone is identified in several units and with different ages, related with the  
diachronous evolution of the nappe pile. It is 360-355 Ma old in the west and 340-325 Ma in  
the south (Costa, 1989; Costa et al., 1993; Ledru et al., 1994b), clearly corresponding to  
different pulses. Partial melting and anatexis affected large parts of this unit, and is dated at *c.*  
375-365 Ma in the west. There, it might have followed a high-P event, being in turn followed  
by the widely recognized Barrovian imprint.

1339 An ophiolitic unit has been identified above the LGU in the Limousin (Girardeau et  
1340 al., 1986, 1994). It consists of harzburgites, dunites, wehrlites, troctolites and layered gabbros  
1341 mostly undeformed, and metamorphosed under low-P (0.2-0.4 GPa) static conditions,  
1342 probably by oceanic hydrothermal metamorphism (Berger et al., 2005). The ophiolites occur  
1343 in dismembered massifs 1-5 km long and up to 1 km thick in a *mélange* on which chlorite-  
1344 rich mylonites can be identified. The authors interpret the occurrence as marking a suture  
1345 between upper and intermediate allochthonous units. Lack of pervasive deformation and of  
1346 high-P metamorphism allow excluding them from the Cambro-Ordovician oceanic group  
1347 while a Devonian age is considered possible.

1348 The Upper Gneiss Unit (UGU) includes at its base the Leptyno-Amphibolitic Complex  
1349 (Forestier, 1963; Santallier et al., 1988), an assemblage of spinel and garnet peridotites and  
1350 the metamorphic by-products of gabbros, basalts, granites, rhyolites, tuffs and sediments.  
1351 Igneous protoliths are Cambro-Ordovician and high-P granulite/eclogite-facies  
1352 metamorphism is Lower-Middle Devonian (415-380 Ma; Pin and Lancelot, 1982; Paquette et  
1353 al., 1995; Lotout et al., 2018). This was followed by decompressive partial melting at 385-370  
1354 Ma which ended under amphibolite-facies conditions (Mercier et al., 1991; Faure et al., 2008;  
1355 Lotout et al., 2018). The high-P rocks occur at the base of Leptyno-Amphibolitic Complex,  
1356 where dismembered peridotites appear at several places, often associated with ultrahigh-P  
1357 eclogites equilibrated at 2.5-3.0 GPa at 412 Ma (Berger et al., 2010).

1358 The Leptyno-Amphibolitic Complex has been interpreted as representing an oceanic  
1359 lithosphere, a subduction *mélange*, a back-arc basin and a transitional continent-ocean  
1360 lithosphere (Lotout et al., 2018 and references therein). Several of these hypotheses, if not all,  
1361 are possibly correct, as the complex may include units of different origins and evolutions.  
1362 Perhaps the 35 Ma age interval found for high-P metamorphism can be explained by these  
1363 differences. We will consider that at least some units of the complex form the base of the  
1364 Upper Gneiss Unit and represent a subducted and exhumed part of a Cambro-Ordovician  
1365 terrane with a transitional but essentially continental crust, which continues upward by an  
1366 assemblage of paragneisses and orthogneisses that underwent Middle-Upper Devonian  
1367 migmatization but apparently not the earlier high-P event.

1368 The uppermost part of the nappe pile includes several units in different parts of the  
1369 Massif Central (Fig. 5b, c). In the SW, the Thiviers-Payzac Unit is formed by low- to medium  
1370 grade Cambrian greywackes, quartzites and rhyolites. Surrounded by this unit, Saint Génis is  
1371 either an *in situ* small ophiolitic unit including greenschist-facies metabasalts, cherts and

1372 Middle Devonian limestones, or an early Carboniferous olistostrome reworking a Middle  
1373 Devonian ophiolite (Faure et al., 2009).

1374 In the NE, the uppermost units include Middle-Upper Devonian calc-alkaline  
1375 volcanics forming the Morvan Arc (Pin et al., 1982; Lardeaux et al., 2014), and to the south,  
1376 the Brévenne Unit, an Upper Devonian ophiolite metamorphosed under greenschist-facies  
1377 conditions representing its back-arc. The latter is dated at 370-360 Ma (Pin and Paquette,  
1378 1998), and was deformed between 350-340 Ma (Leloix et al., 1999). Even younger, the so-  
1379 called Tuffs Anthracifères are formed by late Visean terrigenous and coal sediments  
1380 alternating with rhyolites and dacites unconformable upon metamorphic and granitic rocks.  
1381 The calc-alkaline character of Late Devonian to early Carboniferous magmatism and its  
1382 arc/back-arc polarity reflects south-dipping subduction (Lardeaux et al., 2014).

1383 The tectonometamorphic evolution of the FMC includes an early Variscan episode of  
1384 subduction, Lower-Middle Devonian in age although not very precisely dated (415-380 Ma),  
1385 recognized in the UGU. The conditions reached 1.8-2 GPa at 650-750 °C, although a  
1386 minimum ultrahigh-P of 2.8 GPa was identified in the Lyonnais (Lardeaux et al., 2001). By  
1387 380-360 Ma this unit was exhumed to *c.* 30 km depth by underthrusting or subduction of the  
1388 LGU, and was followed by migmatization of the latter at *c.* 375-365 Ma, younger than in the  
1389 UGU (385-370 Ma). An ocean possibly separated both units, although ophiolitic relics are  
1390 very scarce in the FMC. The intrusives of the tonalitic line of Limousin, emplaced at 380-360  
1391 Ma, were probably generated during its closure, as they occur only in the UGU (Figs. 4 and  
1392 5b). The same accounts for the Morvan Arc and the Saint Génis and Brévenne ophiolitic  
1393 units.

1394 According to Faure et al. (2009), the next event was Upper Devonian?-early  
1395 Carboniferous metamorphism characterized by Barrovian-type conditions, indicating that a  
1396 collisional regime had replaced previous subduction-related convergence. Recumbent folds  
1397 and thrust sheets were emplaced between 360-345 Ma producing significant crustal  
1398 thickening. This event was succeeded by middle Carboniferous (Visean) synmetamorphic  
1399 deformation recognized in the southern part of the FMC, characterized by southward vergence  
1400 and dated at 340-335 Ma, which propagated to the south until 325 Ma. Subsequently, late  
1401 Carboniferous (Namurian-Westphalian) extension dated at 325-295 Ma allowed the intrusion  
1402 of large plutons with fabrics indicating NW-SE crustal stretching which was however coeval  
1403 with continued compression to the north of the FMC and in the Montagne Noire and  
1404 Pyrenees.

1405 Kinematic criteria indicate tectonic transport toward the west (NW to SW) for early  
1406 Variscan fabrics (older than 350 Ma), and toward the SW-SSW for younger fabrics (Ledru et  
1407 al., 1994b). The older were formed under amphibolite-facies conditions, and often represent  
1408 retrogressive foliations following high-P, subduction-related metamorphism, and considered  
1409 coeval with nappe emplacement. The younger SW-SSW kinematic criteria occur mostly in  
1410 the southern part of the FMC according to Ledru et al. (1994b), and are distributed along the  
1411 whole massif for Faure et al. (2008). They are also related to nappe emplacement, including  
1412 that of the Allochthon above the Parautochthon and Autochthon, and that of the thrust sheets  
1413 of the northern Montagne Noire.

1414 Transpression characterizes some of the deformation episodes and was partly coeval  
1415 with local extensional structures. Dextral shear zones, roughly striking WNW-ESE, occur in  
1416 continuation of those in the Armorican Massif. To the east their strike changes to SW-NE due  
1417 open oroclinal folding that formed the Massif Central Arc (MCA). A fold system associated  
1418 to these faults is dated at 345-335 Ma (Gay et al., 1981; Costa et al., 1993). To the east, the  
1419 Velay Dome witnesses a late-Variscan low-P/high-T event dated at 320-295 Ma (Ledru et al.,  
1420 2001; Lardeaux et al., 2001), while a ductile detachment bounding the dome in the north is  
1421 dated at 320 Ma (Malavieille et al., 1990). W-E sinistral strike-slip faults occurred also in the  
1422 northern part of the FMC between 320-300 Ma (Ledru et al., 1994b), either contemporaneous  
1423 with a long lasting dextral system or intercalated among two separate dextral events.

#### 4.3. *Vosges and Schwarzwald Massifs (VM, SWM)*

1424  
1425  
1426  
1427  
1428  
1429  
1430  
1431  
1432  
1433  
1434  
1435  
1436  
1437  
1438  
1439  
1440  
1441  
1442  
1443  
1444  
1445  
1446  
1447  
1448  
1449  
1450  
1451  
1452  
1453  
1454  
1455  
1456  
1457  
1458  
1459  
1460  
1461  
1462  
1463  
1464  
1465  
1466  
1467  
1468  
1469  
1470  
1471  
1472  
1473  
1474  
1475  
1476  
1477  
1478  
1479  
1480  
1481  
1482  
1483  
1484  
1485  
1486  
1487  
1488  
1489  
1490  
1491  
1492  
1493  
1494  
1495  
1496  
1497  
1498  
1499  
1500  
1501  
1502  
1503  
1504  
1505  
1506  
1507  
1508  
1509  
1510  
1511  
1512  
1513  
1514  
1515  
1516  
1517  
1518  
1519  
1520  
1521  
1522  
1523  
1524  
1525  
1526  
1527  
1528  
1529  
1530  
1531  
1532  
1533  
1534  
1535  
1536  
1537  
1538  
1539  
1540  
1541  
1542  
1543  
1544  
1545  
1546  
1547  
1548  
1549  
1550  
1551  
1552  
1553  
1554  
1555  
1556  
1557  
1558  
1559  
1560  
1561  
1562  
1563  
1564  
1565  
1566  
1567  
1568  
1569  
1570  
1571  
1572  
1573  
1574  
1575  
1576  
1577  
1578  
1579  
1580  
1581  
1582  
1583  
1584  
1585  
1586  
1587  
1588  
1589  
1590  
1591  
1592  
1593  
1594  
1595  
1596  
1597  
1598  
1599  
1600  
1601  
1602  
1603  
1604  
1605  
1606  
1607  
1608  
1609  
1610  
1611  
1612  
1613  
1614  
1615  
1616  
1617  
1618  
1619  
1620  
1621  
1622  
1623  
1624  
1625  
1626  
1627  
1628  
1629  
1630  
1631  
1632  
1633  
1634  
1635  
1636  
1637  
1638  
1639  
1640  
1641  
1642  
1643  
1644  
1645  
1646  
1647  
1648  
1649  
1650  
1651  
1652  
1653  
1654  
1655  
1656  
1657  
1658  
1659  
1660  
1661  
1662  
1663  
1664  
1665  
1666  
1667  
1668  
1669  
1670  
1671  
1672  
1673  
1674  
1675  
1676  
1677  
1678  
1679  
1680  
1681  
1682  
1683  
1684  
1685  
1686  
1687  
1688  
1689  
1690  
1691  
1692  
1693  
1694  
1695  
1696  
1697  
1698  
1699  
1700  
1701  
1702  
1703  
1704  
1705  
1706  
1707  
1708  
1709  
1710  
1711  
1712  
1713  
1714  
1715  
1716  
1717  
1718  
1719  
1720  
1721  
1722  
1723  
1724  
1725  
1726  
1727  
1728  
1729  
1730  
1731  
1732  
1733  
1734  
1735  
1736  
1737  
1738  
1739  
1740  
1741  
1742  
1743  
1744  
1745  
1746  
1747  
1748  
1749  
1750  
1751  
1752  
1753  
1754  
1755  
1756  
1757  
1758  
1759  
1760  
1761  
1762  
1763  
1764  
1765  
1766  
1767  
1768  
1769  
1770  
1771  
1772  
1773  
1774  
1775  
1776  
1777  
1778  
1779  
1780  
1781  
1782  
1783  
1784  
1785  
1786  
1787  
1788  
1789  
1790  
1791  
1792  
1793  
1794  
1795  
1796  
1797  
1798  
1799  
1800  
1801  
1802  
1803  
1804  
1805  
1806  
1807  
1808  
1809  
1810  
1811  
1812  
1813  
1814  
1815  
1816  
1817  
1818  
1819  
1820  
1821  
1822  
1823  
1824  
1825  
1826  
1827  
1828  
1829  
1830  
1831  
1832  
1833  
1834  
1835  
1836  
1837  
1838  
1839  
1840  
1841  
1842  
1843  
1844  
1845  
1846  
1847  
1848  
1849  
1850  
1851  
1852  
1853  
1854  
1855  
1856  
1857  
1858  
1859  
1860  
1861  
1862  
1863  
1864  
1865  
1866  
1867  
1868  
1869  
1870  
1871  
1872  
1873  
1874  
1875  
1876  
1877  
1878  
1879  
1880  
1881  
1882  
1883  
1884  
1885  
1886  
1887  
1888  
1889  
1890  
1891  
1892  
1893  
1894  
1895  
1896  
1897  
1898  
1899  
1900  
1901  
1902  
1903  
1904  
1905  
1906  
1907  
1908  
1909  
1910  
1911  
1912  
1913  
1914  
1915  
1916  
1917  
1918  
1919  
1920  
1921  
1922  
1923  
1924  
1925  
1926  
1927  
1928  
1929  
1930  
1931  
1932  
1933  
1934  
1935  
1936  
1937  
1938  
1939  
1940  
1941  
1942  
1943  
1944  
1945  
1946  
1947  
1948  
1949  
1950  
1951  
1952  
1953  
1954  
1955  
1956  
1957  
1958  
1959  
1960  
1961  
1962  
1963  
1964  
1965  
1966  
1967  
1968  
1969  
1970  
1971  
1972  
1973  
1974  
1975  
1976  
1977  
1978  
1979  
1980  
1981  
1982  
1983  
1984  
1985  
1986  
1987  
1988  
1989  
1990  
1991  
1992  
1993  
1994  
1995  
1996  
1997  
1998  
1999  
2000  
2001  
2002  
2003  
2004  
2005  
2006  
2007  
2008  
2009  
2010  
2011  
2012  
2013  
2014  
2015  
2016  
2017  
2018  
2019  
2020  
2021  
2022  
2023  
2024  
2025  
2026  
2027  
2028  
2029  
2030  
2031  
2032  
2033  
2034  
2035  
2036  
2037  
2038  
2039  
2040  
2041  
2042  
2043  
2044  
2045  
2046  
2047  
2048  
2049  
2050  
2051  
2052  
2053  
2054  
2055  
2056  
2057  
2058  
2059  
2060  
2061  
2062  
2063  
2064  
2065  
2066  
2067  
2068  
2069  
2070  
2071  
2072  
2073  
2074  
2075  
2076  
2077  
2078  
2079  
2080  
2081  
2082  
2083  
2084  
2085  
2086  
2087  
2088  
2089  
2090  
2091  
2092  
2093  
2094  
2095  
2096  
2097  
2098  
2099  
2100  
2101  
2102  
2103  
2104  
2105  
2106  
2107  
2108  
2109  
2110  
2111  
2112  
2113  
2114  
2115  
2116  
2117  
2118  
2119  
2120  
2121  
2122  
2123  
2124  
2125  
2126  
2127  
2128  
2129  
2130  
2131  
2132  
2133  
2134  
2135  
2136  
2137  
2138  
2139  
2140  
2141  
2142  
2143  
2144  
2145  
2146  
2147  
2148  
2149  
2150  
2151  
2152  
2153  
2154  
2155  
2156  
2157  
2158  
2159  
2160  
2161  
2162  
2163  
2164  
2165  
2166  
2167  
2168  
2169  
2170  
2171  
2172  
2173  
2174  
2175  
2176  
2177  
2178  
2179  
2180  
2181  
2182  
2183  
2184  
2185  
2186  
2187  
2188  
2189  
2190  
2191  
2192  
2193  
2194  
2195  
2196  
2197  
2198  
2199  
2200  
2201  
2202  
2203  
2204  
2205  
2206  
2207  
2208  
2209  
2210  
2211  
2212  
2213  
2214  
2215  
2216  
2217  
2218  
2219  
2220  
2221  
2222  
2223  
2224  
2225  
2226  
2227  
2228  
2229  
2230  
2231  
2232  
2233  
2234  
2235  
2236  
2237  
2238  
2239  
2240  
2241  
2242  
2243  
2244  
2245  
2246  
2247  
2248  
2249  
2250  
2251  
2252  
2253  
2254  
2255  
2256  
2257  
2258  
2259  
2260  
2261  
2262  
2263  
2264  
2265  
2266  
2267  
2268  
2269  
2270  
2271  
2272  
2273  
2274  
2275  
2276  
2277  
2278  
2279  
2280  
2281  
2282  
2283  
2284  
2285  
2286  
2287  
2288  
2289  
2290  
2291  
2292  
2293  
2294  
2295  
2296  
2297  
2298  
2299  
2300  
2301  
2302  
2303  
2304  
2305  
2306  
2307  
2308  
2309  
2310  
2311  
2312  
2313  
2314  
2315  
2316  
2317  
2318  
2319  
2320  
2321  
2322  
2323  
2324  
2325  
2326  
2327  
2328  
2329  
2330  
2331  
2332  
2333  
2334  
2335  
2336  
2337  
2338  
2339  
2340  
2341  
2342  
2343  
2344  
2345  
2346  
2347  
2348  
2349  
2350  
2351  
2352  
2353  
2354  
2355  
2356  
2357  
2358  
2359  
2360  
2361  
2362  
2363  
2364  
2365  
2366  
2367  
2368  
2369  
2370  
2371  
2372  
2373  
2374  
2375  
2376  
2377  
2378  
2379  
2380  
2381  
2382  
2383  
2384  
2385  
2386  
2387  
2388  
2389  
2390  
2391  
2392  
2393  
2394  
2395  
2396  
2397  
2398  
2399  
2400  
2401  
2402  
2403  
2404  
2405  
2406  
2407  
2408  
2409  
2410  
2411  
2412  
2413  
2414  
2415  
2416  
2417  
2418  
2419  
2420  
2421  
2422  
2423  
2424  
2425  
2426  
2427  
2428  
2429  
2430  
2431  
2432  
2433  
2434  
2435  
2436  
2437  
2438  
2439  
2440  
2441  
2442  
2443  
2444  
2445  
2446  
2447  
2448  
2449  
2450  
2451  
2452  
2453  
2454  
2455  
2456  
2457  
2458  
2459  
2460  
2461  
2462  
2463  
2464  
2465  
2466  
2467  
2468  
2469  
2470  
2471  
2472  
2473  
2474  
2475  
2476  
2477  
2478  
2479  
2480  
2481  
2482  
2483  
2484  
2485  
2486  
2487  
2488  
2489  
2490  
2491  
2492  
2493  
2494  
2495  
2496  
2497  
2498  
2499  
2500  
2501  
2502  
2503  
2504  
2505  
2506  
2507  
2508  
2509  
2510  
2511  
2512  
2513  
2514  
2515  
2516  
2517  
2518  
2519  
2520  
2521  
2522  
2523  
2524  
2525  
2526  
2527  
2528  
2529  
2530  
2531  
2532  
2533  
2534  
2535  
2536  
2537  
2538  
2539  
2540  
2541  
2542  
2543  
2544  
2545  
2546  
2547  
2548  
2549  
2550  
2551  
2552  
2553  
2554  
2555  
2556  
2557  
2558  
2559  
2560  
2561  
2562  
2563  
2564  
2565  
2566  
2567  
2568  
2569  
2570  
2571  
2572  
2573  
2574  
2575  
2576  
2577  
2578  
2579  
2580  
2581  
2582  
2583  
2584  
2585  
2586  
2587  
2588  
2589  
2590  
2591  
2592  
2593  
2594  
2595  
2596  
2597  
2598  
2599  
2600  
2601  
2602  
2603  
2604  
2605  
2606  
2607  
2608  
2609  
2610  
2611  
2612  
2613  
2614  
2615  
2616  
2617  
2618  
2619  
2620  
2621  
2622  
2623  
2624  
2625  
2626  
2627  
2628  
2629  
2630  
2631  
2632  
2633  
2634  
2635  
2636  
2637  
2638  
2639  
2640  
2641  
2642  
2643  
2644  
2645  
2646  
2647  
2648  
2649  
2650  
2651  
2652  
2653  
2654  
2655  
2656  
2657  
2658  
2659  
2660  
2661  
2662  
2663  
2664  
2665  
2666  
2667  
2668  
2669  
2670  
2671  
2672  
2673  
2674  
2675  
2676  
2677  
2678  
2679  
2680  
2681  
2682  
2683  
2684  
2685  
2686  
2687  
2688  
2689  
2690  
2691  
2692  
2693  
2694  
2695  
2696  
2697  
2698  
2699  
2700  
2701  
2702  
2703  
2704  
2705  
2706  
2707  
2708  
2709  
2710  
2711  
2712  
2713  
2714  
2715  
2716  
2717  
2718  
2719  
2720  
2721  
2722  
2723  
2724  
2725  
2726  
2727  
2728  
2729  
2730  
2731  
2732  
2733  
2734  
2735  
2736  
2737  
2738  
2739  
2740  
2741  
2742  
2743  
2744  
2745  
2746  
2747  
2748  
2749  
2750  
2751  
2752  
2753  
2754  
2755  
2756  
2757  
2758  
2759  
2760  
2761  
2762  
2763  
2764  
2765  
2766  
2767  
2768  
2769  
2770  
2771  
2772  
2773  
2774  
2775  
2776  
2777  
2778  
2779  
2780  
2781  
2782  
2783  
2784  
2785  
2786  
2787  
2788  
2789  
2790  
2791  
2792  
2793  
2794  
2795  
2796  
2797  
2798  
2799  
2800  
2801  
2802  
2803  
2804  
2805  
2806  
2807  
2808  
2809  
2810  
2811  
2812  
2813  
2814  
2815  
2816  
2817  
2818  
2819  
2820  
2821  
2822  
2823  
2824  
2825  
2826  
2827  
2828  
2829  
2830  
2831  
2832  
2833  
2834  
2835  
2836  
2837  
2838  
2839  
2840  
2841  
2842  
2843  
2844  
2845  
2846  
2847  
2848  
2849  
2850  
2851  
2852  
2853  
2854  
2855  
2856  
2857  
2858  
2859  
2860  
2861  
2862  
2863  
2864  
2865  
2866  
2867  
2868  
2869  
2870  
2871  
2872  
2873  
2874  
2875  
2876  
2877  
2878  
2879  
2880  
2881  
2882  
2883  
2884  
2885  
2886  
2887  
2888  
2889  
2890  
2891  
2892  
2893  
2894  
2895  
2896  
2897  
2898  
2899  
2900  
2901  
2902  
2903  
2904  
2905  
2906  
2907  
2908  
2909  
2910  
2911  
2912  
2913  
2914  
2915  
2916  
2917  
2918  
2919  
2920  
2921  
2922  
2923  
2924  
2925  
2926  
2927  
2928  
2929  
2930  
2931  
2932  
2933  
2934  
2935  
2936  
2937  
2938  
2939  
2940  
2941  
2942  
2943  
2944  
2945  
2946  
2947  
2948  
2949  
2950  
2951  
2952  
2953  
2954  
2955  
2956  
2957  
2958  
2959  
2960  
2961  
2962  
2963  
2964  
2965  
2966  
2967  
2968  
2969  
2970  
2971  
2972  
2973  
2974  
2975  
2976  
2977  
2978  
2979  
2980  
2981  
2982  
2983  
2984  
2985  
2986  
2987  
2988  
2989  
2990  
2991  
2992  
2993  
2994  
2995  
2996  
2997  
2998  
2999  
3000

1437 migmatitic paragneisses and includes amphibolite and marble intercalations, while the  
1438 Granulite Unit derives from a *c.* 500 Ma igneous protolith. In the two latter, initial  
1439 metamorphism was of high-P/high-T type, and all units evolved later to low-P/high-T  
1440 conditions. The three units include lenses of peridotite, while amphibolites possibly  
1441 retrograded after granulites alternate with felsic rocks at the boundary between the Varied and  
1442 Granulite units, which together may be equivalent to the Leptyno-Amphibolitic Complex of  
1443 the FMC. The high-T rocks have been interpreted as vertical extrusions at mid-crustal levels,  
1444 contemporaneous with ultra-potassic magmatism (Schulmann et al., 2002; Skrzypek et al.,  
1445 2014).

1446 The Southern Vosges include a relative autochthon with Upper Devonian limestone  
1447 overlain by early Carboniferous flysch and continental sediments and volcanics intruded by  
1448 ultra-potassic rocks dated at 345-335 Ma (Tabaud et al., 2015). Above, an allochthonous unit  
1449 consists of an Upper Devonian ophiolite covered by thick Viséan flysch deposits. The  
1450 ophiolites, known as the Ligne des Klippes (Schneider et al., 1990), and dated at *c.* 372 Ma,  
1451 are equivalent to the Brévenne Unit of the FMC, and represent the opening of a small ocean,  
1452 probably a back-arc basin (Skrzypek et al., 2012).

1453 In the Schwarzwald, the dextral Baden-Baden Shear Zone, the eastward continuation  
1454 of the Lalaye-Lubine Shear Zone in the Vosges, separates the Moldanubian Zone from a  
1455 narrow belt of Cambro-Ordovician metasediments and metaigneous rocks in greenschist to  
1456 amphibolite facies representing the Saxothuringian Zone. The Moldanubian Zone includes the  
1457 Central and Southern Schwarzwald Gneiss complexes separated by a belt of Lower Paleozoic  
1458 to Carboniferous deposits. The Central Schwarzwald Gneiss Complex is formed by the same  
1459 three units described in the Central Vosges, although some differences exist: the Monotonous  
1460 Unit here includes eclogitic relicts indicating a high-P event previous to the low-P/high-T  
1461 conditions displayed by the migmatitic paragneisses, dated at *c.* 330 Ma. Conversely, no high-  
1462 P relics are preserved in the Varied Unit. The Granulite Unit reflects an igneous event of  
1463 Cambrian-Lower Ordovician age, and includes metasediments of probable Silurian-Devonian  
1464 age. The age of high-P metamorphism is estimated around 340 Ma (Kalt et al., 1994;  
1465 Marschall et al., 2003).

1466 The metasedimentary belt separating the two gneiss complexes consists of Ordovician-  
1467 Silurian metasediments, metavolcanics and deformed granitoids, but no metamorphic Lower  
1468 Devonian to Upper Carboniferous sediments and volcanics. The latter are correlated with  
1469 coeval rocks of the Southern Vosges. The Southern Schwarzwald Gneiss Complex is made of

1470 gneisses, high-P granulites and migmatites similar to those of the Varied Unit, overridden by  
1471 a thrust sheet with migmatitic gneisses, amphibolite and gabbro boudins with protolith ages of  
1472 350 Ma.

1473 The Variscan history of the VM and SWM is marked by the opening during the Upper  
1474 Devonian of a narrow back-arc, its inversion during the early Carboniferous, high-P/high-T  
1475 metamorphism and low-P/high-T overprint (Lardeaux et al., 2014). Although complex, this  
1476 evolution reflects Devonian-Carboniferous subduction toward the SE below the Moldanubian  
1477 crust (Edel and Schulmann, 2009; Skrzypek et al., 2014). According to the age of high-P  
1478 metamorphism and that of the Ligne des Klippes ophiolite, the subducted ocean was the  
1479 Saxothuringian, defined by Franke (2000) between the Saxothuringian Zone and Bohemia.

#### 1480 1481 *4.4. Massifs of the southern Variscan Belt (MTM, Corsica, Sardinia, EmA)*

1482 The southern European Variscan belt includes several relatively small crystalline  
1483 massifs whose tectonometamorphic and magmatic evolution is similar among them, and also  
1484 to that of the large massifs (Corsini and Rolland, 2009). These are the Maures-Tanneron  
1485 Massif (MTM), Corsica, Sardinia and the External Massifs of the western Alps (EmA).

1486 The MTM crops out along the Mediterranean coast south of the FMC, and consists of  
1487 a nappe stack with N-S structures that define three domains. The following description is  
1488 based on Corsini and Rolland (2009), and Schneider et al. (2014). In the Western Domain, the  
1489 thrust sheets dip to the NW and from west to east include Silurian metapelites, sandstones,  
1490 quartzite and limestone, a Cambrian volcano-sedimentary rift-related succession with alkaline  
1491 rocks, and a Precambrian basement with orthogneisses and metasediments. The whole  
1492 sequence is inverted by late Variscan back-thrusts, as demonstrated by sedimentary structures  
1493 in an early Carboniferous synorogenic flysch (Bronner and Bellot, 2000). Metamorphism in  
1494 this domain is of low- to medium grade, with temperature increasing toward the SE and  
1495 reaching the sillimanite zone.

1496 The Central Domain, described as the Leptyno-Amphibolitic Complex by Schneider et  
1497 al. (2014), comprises metapelites, quartzites and calc-schists, a bimodal magmatic suite with  
1498 alkaline and tholeiitic affinities, and peridotites with high-P relicts. Metamorphic grade is  
1499 higher than in the previous domain and partial melting is widespread. The structure is  
1500 antiformal, a flattened gneiss dome with migmatites surrounding a syntectonic Variscan  
1501 granite. The Eastern Domain consists of high-grade metasediments, metavolcanics and



1502 orthogneisses ranging in age from Neoproterozoic to Silurian, as well as abundant syntectonic  
1503 Variscan granitoids. Some ultrabasics also occur, as well as Cambro-Ordovician tholeiitic  
1504 metabasalts and metagabbro that Schneider et al. (2014) interpreted as a possible  
1505 dismembered suture. Relicts in metabasic rocks record an early high-P metamorphic event.

1506 The structural evolution includes a high-P event poorly dated but probably Devonian,  
1507 and whose P-T conditions have not been precisely established. It is identified in  
1508 metaperidotites and retroeclogites of the Central and Eastern domains, and reflects eastward  
1509 subduction in the internal zones. Barrovian metamorphism characterizes the Western Domain,  
1510 where early Carboniferous recumbent folds and thrust sheets with NW vergence were  
1511 overprinted by E-verging back-thrusts during the middle Carboniferous (Schneider et al.,  
1512 2014). Some of these were reactivated as normal faults during the late Carboniferous, which  
1513 is also characterized by granite intrusions and the formation of gneiss domes and late  
1514 Carboniferous intramontane basins, all related with the Variscan orogenic collapse. Coeval  
1515 with this stage, wrench structures more or less parallel to the trend of earlier ones developed.  
1516 In the MTM, these are roughly N-S shear zones and faults with dextral motion which had first  
1517 recorded a sinistral kinematics (Bellot et al., 2002).

1518 In Corsica, the pre-Alpine basement is mostly occupied by Variscan granites, but the  
1519 metamorphic rocks represent the Allochthon (Fig. 4). In Sardinia, the Allochthon occupies the  
1520 northern and central parts, while an Autochthon comparable to the Mediterranean peri-  
1521 Gondwanan province is exposed in the south (Fig. 1). The Allochthon is divided in two zones.  
1522 The Nappe Zone, in the centre, occupies most than half of the island surface, and is equivalent  
1523 to the Western Domain of the MTM while the Axial or Internal Zone, in the north, is  
1524 continuation of the Central and Eastern domains (Rossi et al., 2009; Schneider et al., 2014).  
1525 Both zones are separated by the Posada-Asinara Shear Zone, trending NW-SE and interpreted  
1526 as a dextral shear zone cutting across the thrust belt separating the Allochthon and the  
1527 Parautochthon (Fig. 1). What follows is a short description of zones and units from bottom to  
1528 top, based on Rossi et al. (2009) and Cocco et al. (2018).

1529 The Autochthon of SW Sardinia (Iglesiente) consists at its base of a terrigenous  
1530 Cambrian to Lower Ordovician sequence including a thick Lower Cambrian carbonate unit,  
1531 which is truncated by the Sardic unconformity. The ensemble is overlain by partially  
1532 syntectonic Upper Ordovician clastics and followed by shallow-marine glaciation-related  
1533 deposits including alkaline volcanics, overlain in turn by Silurian-Devonian black shales,  
1534 limestones and Culm deposits. Paleozoic deposits are at most anchimetamorphic. The original

1535 position of the Iglesias in the Variscan puzzle is poorly constrained. It might be derived  
1536 from a relatively remote domain significantly distinct from the Nappe Zone (Cocco et al.,  
1537 2018).

1538 Overlying the Autochthon, the Nappe Zone is divided into external and internal parts.  
1539 The External Nappes are a stack of units transported to the SW which include Cambrian to  
1540 Lower Ordovician sandstones and acid volcanites dated at 490 Ma, unconformably overlain  
1541 by thin conglomerates and a thick calc-alkaline volcanic sequence related to an Ordovician  
1542 arc (460-450 Ma). The conglomerates lie above the Sardinian unconformity, and an Upper  
1543 Ordovician transgression is marked by shallow-marine sandstones which continued by a  
1544 typical Silurian succession with black shales, marls and limestones representing the whole  
1545 Devonian and the lowermost Carboniferous. All rocks are metamorphic, with the grade  
1546 increasing northward and upward, from the lower greenschist to the amphibolite facies. A  
1547 klippe of the External Nappes has been reported lying above the Autochthon by Pavanetto et  
1548 al. (2012).

1549 The Internal Nappes, to the north, are a relatively narrow band 15-30 km wide mostly  
1550 characterized by amphibolite-facies rocks (Giacomini et al., 2006). At the contact with the  
1551 overlying Internal Zone, a strongly deformed metasedimentary belt with an inverted  
1552 Barrovian sequence includes retrogressed eclogites derived from MORB-type protoliths.  
1553 Conditions of the eclogitic event are estimated at *c.* 1.5 GPa and 600-700 °C (Cortesogno et  
1554 al., 2004), and the rocks did not record a high-T granulitic stage. This belt represents the  
1555 thrust contact between the Nappe and Internal zones, and indicates a southward emplacement  
1556 of the latter (Cappelli et al., 1992). The Posada-Asinara late Variscan dextral shear zone,  
1557 dated at *c.* 325-300 Ma (Carosi et al., 2020), generated a green-schist-facies phyllonite.

1558 The Internal Zone in Corsica is similar to the Leptyno-Amphibolitic Complex of the  
1559 FMC, and consists of early Paleozoic metasediments and orthogneisses with eclogite boudins  
1560 but also high-P/high-T basic granulites and ultrabasics. Peak conditions of high-P  
1561 metamorphism are estimated at 1.4-1.8 GPa and 900-1000 °C and dated at *c.* 360 Ma  
1562 (Giacomini et al., 2008) or *c.* 420-400 Ma (Rossi et al., 2009). In northern Sardinia and  
1563 Asinara Island, the Leptyno-Amphibolitic Complex includes orthogneisses dated at *c.* 460 Ma.  
1564 Magmatic affinity is alkaline in Asinara and calc-alkaline in northern Sardinia. An eclogitic  
1565 stage *c.* 400 Ma old was followed by a granulitic event and then by pervasive migmatization.

1566 What appears to be the uppermost allochthonous unit crops out in northern Corsica,  
1567 where quartzites and greywackes with interbedded metabasalts represent the Neoproterozoic.  
1568 A well-preserved Cambrian to Silurian detrital sequence includes Upper Ordovician  
1569 glaciomarine diamictites and Silurian radiolarites. An Upper Devonian Culm deposit appears  
1570 in faulted contact with the Paleozoic succession. Regional metamorphism was at most of  
1571 lower greenschist facies, but many occurrences are roof pendants of the late Variscan Corsica-  
1572 Sardinia batholith and were transformed into hornfelses.

Rossi et al. (2009) compare the low-grade Paleozoic succession of northern Corsica  
with that of SW Sardinia, finding significant differences. They conclude that northern Corsica  
was a different sedimentary area than SW Sardinia, the Maures or the Montagne Noire, and  
interpret it as deposited in a microcontinent separated from Gondwana during the Ordovician.  
Actually, this succession is quite similar in facies and thickness to that of the Mauges, in the  
SAD.

The External Massifs of the Alps (EmA) have not been included in the map of Figure  
1 because their position in the late Carboniferous is imprecise, even if generally considered  
part of the Allochthon because some of their units are polymetamorphic and include eclogites  
and high-P granulites. The EmA are shown on their present position in Figure 4. A good  
synopsis of their geology is offered by von Raumer et al. (1993). In the Belledonne and Mont  
Blanc massifs (Fig. 4), Ballèvre et al. (2018) separate three domains. The first is the western  
Belledonne domain, which consists of medium-grade schists derived from a monotonous  
terrigenous sequence of unknown age. The second domain occurs in southern Belledonne,  
where a Variscan nappe stack includes the Cambro-Ordovician Chamrousse Ophiolite, and  
ultramafic and gabbro complex with protoliths dated at *c.* 500 Ma (Pin and Carme, 1987;  
Ménot et al., 1988). Still forming part of the second domain as the relative autochthon of the  
ophiolite, a Devono-Carboniferous bimodal suite of leptynites and amphibolites occurs, in  
what may represent an active margin or be related with rifting (von Raumer et al., 1993).  
Moreover, a low-grade detrital and volcanic sequence of argilites, sandstones, conglomerates,  
spilites and keratophyre, probably Viséan, represent an intracontinental pull-apart basin  
(Ménot, 1988). The third domain is widely represented in the External Massifs and  
characterized by a polymetamorphic evolution. The age of eclogite or high-P granulite facies  
metamorphism is uncertain. Although largely taken as Ordovician, Silurian and Early  
Devonian ages have been reported (Paquette, 1987; Paquette et al., 1989), and more recent

1598 data point to a Carboniferous age (c. 330 Ma; Rubatto et al., 2010). It was overprinted by an  
1599 amphibolite-facies event culminating in partial melting.

1600 The internal zones of the Alps share also a Variscan basement and a Gondwanan  
1601 derivation, but their original position relative to the external zones and the Variscan Belt is  
1602 difficult to establish because they are separated from the EmA by the Zone Houillère,  
1603 interpreted by Ballèvre et al. (2018) as a transtensional basin developed along a late Variscan  
1604 dextral shear zone. According to von Raumer and Neubauer (1993), the Alpine basement may  
1605 include pieces detached from the north African margin after the Variscan orogeny, which may  
1606 be monometamorphic or polymetamorphic. The first can be ascribed to the Autochthon, while  
1607 the second, generally characterized by early high-P conditions, are possibly related with the  
1608 Allochthon, but could also represent different terranes. Due to this uncertainty, no further  
1609 discussion on the internal zones will be included. The same accounts for other basement  
1610 outcrops in Italy described by Molli et al. (2020), who propose a Permian paleoposition SW  
1611 to the Alps. For a discussion on linkages between the Alpine basement and other more or less  
1612 Alpinized Mediterranean Variscides see Neubauer and von Raumer (1993).

#### 4.5. *Variscan intrusive magmatism in France*

1615 Variscan plutonism is abundant in the two main French massifs, being more  
1616 voluminous in the Massif Central, probably because this was the area where crustal  
1617 thickening reached its maximum. Variscan magmatism is related to crustal thickening and  
1618 resulting crust/mantle interaction. In the Armorican Massif, a link with crustal-scale wrench  
1619 tectonics has been established. Devonian-early Carboniferous magmatism is also important,  
1620 as it reflects subduction processes and can be related with plate convergence. Variscan  
1621 magmatism is also voluminous in other French and related massifs: Vosges, Schwarzwald,  
1622 Corsica, Sardinia and the External Massifs of the Alps.

##### 4.5.1. *Granitoids of the Armorican Massif*

1625 In the Armorican Massif, Variscan granitoids occur mostly to the west in the CAD and  
1626 NAD, and also along the whole SAD (Fig. 4). According to their regional distribution, three  
1627 groups are distinguished: the red granite belt along the northern shore of Brittany, the Middle  
1628 Armorican Batholith with large elliptic plutons, and the leucogranite belt, with elongated

1629 plutons emplaced during the activity of the South Armorican Shear Zone (Carron et al.,  
1630 1994).

1631 The red granites of the northern belt are late Variscan granodiorites and syenogranites  
1632 of the I-type, emplaced at *c.* 300 Ma. These subalkaline granitoids probably derive from  
1633 fractional crystallization of basaltic magmas plus an important crustal contribution. The  
1634 middle Armorican plutons are mostly grey, porphyritic monzogranites, often with concentric  
1635 zoning and associated with both peraluminous and mafic bodies. Two series have been  
1636 distinguished depending on the presence or absence of cordierite. They were emplaced  
1637 between 340-290 Ma. Some are subalkaline, but even the cordierite-bearing plutons, which  
1638 have an important crustal component, may be related to mafic magmas. The plutons of the  
1639 leucogranite belt are progressively younger from the north and NE to the south and SW. They  
1640 are mostly of the S-type, derived from partial melting of the continental crust, and were  
1641 strongly deformed in the two branches of the South Armorican Shear Zone. Their  
1642 emplacement took place around 340-330 Ma in the N-NE, 330-310 Ma in the central band,  
1643 and 310-290 Ma in the S-SW (Carron et al., 1994; Edel et al., 2018).

1644 In addition to the Variscan granites, a few migmatitic orthogneisses in the Léon are  
1645 Lower-Middle Devonian (390 Ma) porphyritic granitoids (Marcoux et al., 2009). By their  
1646 position in the Variscan belt and age, they can be related with the Rheic suture of the model  
1647 of Zeh and Will (2010) for the Mid German Crystalline High.

1648 A younger early Variscan intrusion of gabbro-diorite with calc-alkaline affinity occurs  
1649 in the Upper Allochthon south of the Mauges Unit and north of the Chantonay Syncline (Fig.  
1650 4). It is dated at *c.* 373 Ma (Cuney et al., 1993), and could be related with a poorly dated  
1651 Devonian back-arc basin represented by mafic volcanics in the Chantonay syncline (Wyns et  
1652 al., 1989), and also with extensive felsic volcanism with massive sulphides developed during  
1653 the Famennian-Viséan in the eastern Massif Central (Delfour, 1989) and Vosges (Lefèvre et  
1654 al., 1994; Krecher et al., 2007). It is also interpreted as the westernmost representative of a  
1655 series of intrusives exposed in the western Massif Central, aged 380-360 Ma and collectively  
1656 known as forming the tonalitic line of Limousin (Bernard-Griffiths et al., 1985a; Bertrand et  
1657 al., 2001). It

1658

1659 4.5.2. *Granitoids of the French Massif Central*

1  
21660 Upper Paleozoic granitoids occupy *c.* 50 % of the outcropping surface in the FMC,  
3  
41661 with ages ranging 380-280 Ma. They include a calc-alkaline association with tonalites,  
5  
61662 granodiorites and monzogranites, and potassic subalkaline metaluminous and peraluminous  
7  
81663 associations with monzogranites, muscovite and cordierite granitoids, and two-mica  
9  
101664 leucogranites. The large massifs are igneous complexes composed of multiple phases  
11  
121665 spanning in time 40 Ma.

13  
141666 Early Variscan magmatism was widely developed in the FMC linked with plate  
15  
161667 convergence. It started with pervasive migmatization in the Upper Gneiss Unit (385-370 Ma),  
17  
181668 closely followed by that of the Lower Gneiss Unit (375-365 Ma), related in both cases to  
19  
201669 exhumation following subduction (Santallier et al., 1994; Faure et al., 2008), which induced  
21  
221670 the formation of migmatitic domes (Ledru et al., 1994b). The Upper Devonian plutons  
23  
241671 forming the tonalitic line of Limousin (380-360 Ma) occur only in the Upper Gneiss Unit,  
25  
261672 equivalent to the Iberian and Armorican Upper Allochthon. They are related to oceanic  
27  
281673 subduction previous to that of continental Lower Gneiss Unit. Contemporaneous rocks of the  
29  
301674 Morvan Arc and ophiolitic Brévenne Unit may be shallow manifestations of the same  
31  
321675 phenomenon, the closure of the ocean separating the Upper Allochthon from the rifted margin  
33  
341676 of northern Gondwana (Lower Allochthon). Conversely, the calc-alkaline volcanism of the  
35  
361677 Tuffs Anthracifères witnesses younger (350-330 Ma) back-arc magmatism (Lardeaux et al.,  
37  
381678 2014), and probably results from subduction of the Rhenohercynian Ocean.

39  
401680 Ages and magma types do not show a clear polarity, although they depict some  
41  
421681 zonation (Ploquin and Stussi, 1994; Ledru et al., 1994b). Most granitoids older than 330 Ma  
43  
441682 are distributed in the central part of the FMC, and are surrounded by younger intrusives. This  
45  
461683 central region is characterized by diachronous alumino-potassic granitoids, and includes the  
47  
481684 Velay Dome (Fig. 4), a large anatectic complex composed of a number of intrusions of  
49  
501685 varying composition, but essentially peraluminous although with spatially but not genetically  
51  
521686 related vaugnerites (Ploquin and Stussi, 1994). A calc-alkaline province with granodiorites  
53  
541687 and granites (325-315 Ma) occur in the Limousin cross-cutting the older plutons of the  
55  
561688 tonalitic line (Fig. 4), and also in the NE, where alumino-potassic, subalkaline and calc-  
57  
581689 alkaline granitoids intruded between 345 and 280 Ma, partially coeval with the formation of  
59  
601690 the Tuffs Anthracifères. In the southern region (Cévennes and Montagne Noire), plutons are  
61  
62  
63  
64  
65

1691 With the exception of the early Variscan calc-alkaline rocks of the Limousin and  
1692 Morvan, and those of the Tuffs Anthracifères, no relation with a subductive environment may  
1693 be established. Although a mantle contribution is not excluded, most Variscan granitoids  
1694 derive from a late Proterozoic crustal source including peraluminous metasediments,  
1695 orthogneisses and lower crustal granulites (Ploquin and Stussi, 1994; Chelle-Michou et al.,  
1696 2017). The large amount and long interval of granite generation implies maintained heat  
1697 production by radioactive decay, and points to significant crustal thickening. Amongst the  
1698 large Variscan Massifs, the FMC is the one where it can be granted that the Variscan  
1699 Allochthon occupied a largest proportion of its present extent (more than 90 %, nearly 100%  
1700 if the eclogites of the Montagne Noire are related with overburden induced by the  
1701 Allochthon).

1702 According to thermal models by Alcock et al. (2015), crustal thickening induced by  
1703 the Allochthon and to a lesser extent by recumbent folding in the Autochthon in NW Iberia,  
1704 may have provided a very significant contribution to the heat budget necessary for generalized  
1705 crustal melting, induced gravitational collapse and crustal extension and thinning. It is  
1706 noteworthy that the eastern part of the FMC is characterized by the thinnest crust among the  
1707 large Variscan Massifs (Dezes and Ziegler, 2002; see Fig. 5c).

#### 1708 1709 *4.5.3. Granitoids of other French and related massifs*

1710 Variscan granitoids are abundant in the Vosges and Schwarzwald. In the small  
1711 occurrence of the Saxothuringian Zone in the northern Vosges, diorites, granodiorites,  
1712 monzogranites and granites intruded between 335 and 320 Ma associated with ignimbritic  
1713 volcanism, represent a magmatic arc related with the subduction of the Rhehercynian  
1714 Ocean (Edel and Schulmann, 2009; Edel et al., 2013; Lardeaux et al., 2014). In the Central  
1715 Vosges, ultra-potassic magmas including durbachites were emplaced at 345-332 Ma, while  
1716 younger granite bodies intruded at 335-325 Ma (Tabaud et al., 2015). Intrusion of the ultra-  
1717 potassic rocks was coeval with diapiric ascent of high-T rocks from lower crustal levels  
1718 (Schulmann et al., 2002; Skrzypek et al., 2014). Ultra-potassic rocks dated at 345-335 Ma  
1719 also occur in the Southern Vosges, intruding Devonian and Carboniferous sediments.

1720 In the Schwarzwald, layered basic rocks dated at 350 Ma are interpreted as intrusions  
1721 related to early Carboniferous convergence. Later Variscan granitoids are abundant:  
1722 muscovite or two-mica granites intruded at 330-325 Ma in the Central Gneiss Complex, while

1723 in the Southern Gneiss Complex, emplacement of biotite and two-mica granites is dated at  
1724 335-330 Ma.

1725 In the Maures-Tanneron Massif, several magmatic events are described by Corsini et  
1726 al. (2009). The older consists of granodioritic melts related to the early Variscan subduction.  
1727 Although dated as Silurian-Lower Devonian (440-410 Ma; Demoux et al., 2008), they are  
1728 probably products of the Middle-Upper Devonian (385-375 Ma) partial melting that followed  
1729 *c.* 415-380 Ma early Variscan subduction of the Upper Gneiss Unit in the FMC (Lardeaux et  
1730 al., 2014). Later, crustal thickening produced anatectic granitoids intruded at *c.* 340 Ma, and  
1731 were followed by late Variscan leucocratic granites (320-315 Ma) related to isothermal  
1732 decompression, and by late-kinematic granites linked to dextral shearing (*c.* 300 Ma; Corsini  
1733 et al., 2009).

1734 In Corsica, Mg-K granitoids intruded at 345-335 Ma in relation with collision related  
1735 with the early Variscan suture (Rossi et al., 2009). In northern Sardinia, peraluminous  
1736 intrusions (330-308 Ma) predate the metaluminous intrusions of the Corsica-Sardinia  
1737 batholith. The latter consists of late Carboniferous-early Permian granitoids (310-290 Ma)  
1738 contemporaneous with the activity of a dextral shear zone developed between Gondwana and  
1739 Laurussia. The more abundant intrusive rocks are granodiorites and monzogranites, but the  
1740 whole spectrum includes also ultrabasic and basic rocks, tonalites and leucocratic granites,  
1741 and all of them have their counterpart in coeval volcanic rocks (Rossi et al., 2009). These  
1742 authors interpret the batholith as resulting from a Carboniferous asthenospheric rise producing  
1743 mafic magmatic underplating and voluminous crustal melting.

1744 In the External Alps, several early Carboniferous granitoids occur in the Belledonne  
1745 Massif (350-320 Ma), where Mg-K granites were emplaced during nappe stacking and  
1746 sinistral transpression, which also occurred in the Mont Blanc Massif at 330 Ma (Corsini et  
1747 al., 2009; Ballèvre et al., 2018). Regional crustal melting started at *c.* 320 Ma and most  
1748 granitoids derived from crustal and mantle sources intruded at 310-300 Ma, in relation with  
1749 major dextral shear zones. Upper Carboniferous granites occur mainly in the External  
1750 Massifs, while Permian granitoids characterize the more internal massifs (Ballèvre et al.,  
1751 2018). On the other side, Carboniferous sedimentation differs in age and nature at both sides  
1752 of the boundary between the EmA and more internal massifs, being Namurian-Westphalian  
1753 and shallow marine in the internal Zone Houillère and Stephanian and lacustrine in the EmA.  
1754 These differences drove these authors to interpret this zone as a transtensional basin opened  
1755 along a major dextral shear zone whose movement took place at 320-310 Ma.



1756

1

## 21757 **5. Bohemian and related massifs**

3

4

51758 This massif represents the cradle of subdivision in zones of the Variscan Belt and of  
6 correlation among its massifs by the pioneering work of Suess (father and son; 1888 1912,  
71759 1926) and Kossmat (1927). The following description is based on many sources, among  
8 which the contributions by Franke (2000), Franke and Żelaźniewicz (2000, 2002) for the  
91760 whole massif and Mazur and Aleksandrowski (2001), Aleksandrowski and Mazur (2002), and  
101761 Linnemann and Romer (2010) for significant parts of it.  
11  
121762  
13  
141763

15

161764 The Bohemian Massif (Fig. 6) is flanked by the Rhenohercynian and Moravo-Silesian  
17 zones, which represent foreland thrust belts (Fig. 7). Its central part includes the  
181765 Saxothuringian, Teplá-Barrandian and Moldanubian zones, whose interpretation varies  
19 depending of the authors. The Saxothuringian Zone is mostly considered the Autochthon  
201766 although it was covered by an allochthonous nappe stack partially preserved in three klippen.  
21 The Teplá-Barrandian is now considered allochthonous and the root of the Saxothuringian  
221767 klippen, while the character of the Moldanubian Zone is discussed.  
23  
241768  
25  
261769  
271770  
28

29

301771

31

### 321772 *5.1. Rhenohercynian Zone (RHZ)*

33

341773 Most of this zone actually crops out in the Rhenish Massif (Figs. 1 and 4), but is  
35 included here because it crops out in the Harz Mountains and underlies the Saxothuringian  
361774 Zone. In the western part of the Rhenish Massif and to the north of it, in the Brabant Massif,  
37 an autochthonous Cadomian basement of Avalonian affinity, and a Cambrian to Silurian  
381775 cover are unconformably overlain by Lower Devonian clastics of Laurentia or Baltica  
39 provenance (Franke, 2000; Sintubin et al., 2009). A Lower Devonian rifting is documented by  
401776 abundant felsic volcanism which turned dominantly basic during the Middle Devonian to  
41 early Carboniferous.  
421777  
43  
441778  
451779  
46  
471780  
48

49

501781 At the limit of the RHZ with the STZ, a narrow belt named Northern Phyllite Zone  
511782 (Fig. 6) includes a mixture of metasediments of different provenances and metavolcanics  
52 which may represent a late Silurian-Lower Devonian arc. According to Franke (2000), the  
531783 zone may host the suture of the Rheic Ocean.  
54  
551784  
56

57

581785 A new ocean, the Rhenohercynian, opened in the Emsian (~405 Ma) and closed in the  
591786 early Frasnian (380 Ma; Franke, 2000) or early Carboniferous (~350 Ma; Zeh and Gerdes,  
60  
61  
62  
63  
64  
65

1787 2010). This was followed by early Carboniferous turbidites derived from an active margin to  
1788 the SE, the Mid German Crystalline High (MGCH), which marks the closure of the  
1789 Rhenohercynian basin.

1790 NW-directed thrusting developed at 335-325 Ma (Oncken et al., 2000). The Giessen  
1791 Nappe of the SE of the Rhenish Massif (Fig. 4) which continues to the central part of the Harz  
1792 Mountains (Fig. 1), carries at its bottom tectonics slices of a Lower Devonian oceanic crust  
1793 and a mélange of sedimentary rocks of Saxothuringian provenance (Franke, 2000). The root  
1794 of the nappe seems to occur between the Northern Phyllite Zone and the MGCH, and could  
1795 represent the suture of the Rhenohercynian Ocean (Franke, 2000).

## 1796 5.2. Moravo-Silesian Zone (MSZ) and Brunovistulian block

1798 The Moravo-Silesian zone represents a *c.* 50 km wide and 300 km long tectonic  
1799 boundary between the internal Moldanubian zone and the easterly Neoproterozoic  
1800 Brunovistulian continental block (Dudek, 1980). This microcontinental block was formed as  
1801 an Ediacarian intraoceanic (730 Ma) and later Japan-type continental arc (600 Ma) established  
1802 on Paleoproterozoic crust (Collett et al., 2021). In Upper Silesia, the Brunovistulian basement  
1803 is unconformably covered by a thick early to mid Cambrian siliciclastic sequence and  
1804 sporadic upper Ordovician deposits (Bula et al., 2015). Detrital zircon and white mica age  
1805 populations (Habryn et al., 2020), as well as early Paleozoic biogeographic data indicate  
1806 derivation from NW Gondwana during the Cambrian, similarities with Avalonia and docking  
1807 to Baltica between the Cambrian and Silurian (Belka et al., 2000). This zone formed part of  
1808 southern Laurussia during the Devonian. The Devonian to Carboniferous sedimentary cover  
1809 of the western margin of the Brunovistulian block is traditionally compared to the RHZ.

1810 Both RHZ and MSZ share rifting during the Middle Devonian, indicated by mafic  
1811 volcanism, and shallow carbonate deposition during the Middle Devonian, followed by early  
1812 Carboniferous, synorogenic detrital and carbonate sedimentation and late Carboniferous  
1813 molasse. Lower Devonian (Pragian) clastic sedimentation (Chlupáč, 1989) was followed in  
1814 Silesia by deposition of volcanosedimentary material associated with mafic to intermediate  
1815 arc volcanism dated at 374 Ma (Janoušek et al., 2014). The Devonian rifting cycle terminated  
1816 with development of a thick Givetian carbonate platform semi-continuously covering the  
1817 whole western margin of the Brunovistulian block. The early Carboniferous Culm facies,  
1818 Tournaisian to lower Namurian, reaches a thickness of 7 km forming a doubly-vergent

1819 accretionary wedge thrust to the SE and NW that is deeper toward the westerly internal MZ  
1820 in Silesia and becomes more shallow toward the southeastern Moravian branch (*e.g.* Tomek et  
1821 al., 2019).

1822 The structure of the MSZ is imbricated, involving the basement at its inner west part  
1823 and of thin-skinned type toward the E (Fig. 7a). The western part of the MSZ emerges  
1824 through a thick Moldanubian nappe in form of three tectonic semi-windows: the Svatka and  
1825 Thaya domes and the Silesian domain (Suess, 1912, 1926). In the latter, thick-skinned  
1826 tectonics involve three basement and cover thrust sheets folded in three large antiforms (Fig.  
1827 7a): the Velké-Vrbno, Keprník and Desná domes (Schulmann and Gayer, 2000). To the  
1828 central and southern Svatka and Thaya windows, they are formed by basement and Devonian  
1829 cover duplexes at the bottom and two thick crystalline nappes at the top (Schulmann et al.,  
1830 1991, 1994). Variscan Barrovian metamorphism is inverted, grading from the chlorite zone in  
1831 the east to the kyanite-sillimanite zone in the west at the top of the sequence (Štípská and  
1832 Schulman, 1995; Štípská et al., 2020). The highest part of the pile is formed by middle to late  
1833 Cambrian ophiolitic sequences (*e.g.* Soejono et al., 2010; Collett et al., 2021) associated with  
1834 eclogites (1.6 GPa, 650-700 °C), kyanite-staurolite micaschists and serpentized ultramafics  
1835 (Konopásek et al., 2002; Štípská et al., 2006). The age of HP metamorphism is estimated as  
1836 Upper Devonian based on geochronology of metamorphosed and deformed rocks of the Staré  
1837 Město ophiolitic sequence in Silesia interpreted as an oceanic suture (Jastrzebski et al., 2013).  
1838 Structurally above ophiolitic sequences in Silesia and Moravia occur migmatites, partially  
1839 molten orthogneisses and high-P granulites of the Moldanubian nappe. The contact between  
1840 the highest allochthonous Moravo-Silesian units and the Moldanubian is thus formed by  
1841 remnants of a Cambrian ophiolite called in Silesia the Nýznerov Thrust (Skácel, 1989), which  
1842 is an equivalent of Moldanubian thrust in the south, formed by micaschists of the kyanite-  
1843 sillimanite zone containing a *mélange* of dismembered ophiolitic fragments and eclogites.

1844 Polyphase tectonic evolution of the MSZ is characterized by a first subduction of  
1845 oceanic crust probably during Late Devonian (Jastrzebski et al., 2013) followed by early  
1846 Carboniferous (345-340 Ma) westward continental underthrusting of the Brunovistulian  
1847 margin beneath the Moldanubian hot fold nappe (Ráček et al., 2017; Štípská et al., 2015;  
1848 2020). During this event started deposition of earliest sediments in the easterly flexural Culm  
1849 basin (Ráček et al., 2017; Tomek et al., 2019). The margin of the underthrust  
1850 Brunovistulian block was later imbricated producing two thick crustal nappes that were  
1851 emplaced over the autochthonous basement together with the hot Moldanubian subduction

1852 channel flow region at around 340-335 Ma (Schulmann et al., 2008; Racek et al., 2017). This  
1853 stage was associated with maximum deposition of sediments in the Culm foreland basin  
1854 further east (Ktaková et al., 2007; Tomek et al., 2019). At this stage the western and oldest  
1855 part of Culm sediments was underthrust and metamorphosed beneath the Moravo-Silesian  
1856 nappe pile thereby forming a bivergent accretionary wedge (Tomek et al., 2019). The tectonic  
1857 evolution of the MSZ is terminated by dextral shearing that reactivated the Moldanubian-  
1858 Brunovistulian boundary at around 330-325 Ma (Schulmann et al., 1994; Racek et al., 2017).

### 1860 *5.3. Saxothuringian Zone (STZ)*

1861 There is abundant geological information about this zone, much of which is collected  
1862 in the contributions gathered in Linnemann and Romer (2010). Brief accounts are provided by  
1863 Franke (2000) and Franke and Żelaźniewicz (2002). Most of this zone represents the  
1864 Autochthon of the Bohemian Massif, but several allochthons occur in klippen in the internal  
1865 parts, the more important being the Münchberg klippe in the west, those surrounding the  
1866 Krkonoše Massif, and the Góry Sowie Massif in the east. Furthermore, a poorly outcropping  
1867 belt in the north known as the Mid German Crystalline High is often included as a domain of  
1868 the STZ (*e.g.* Linnemann et al., 2007) but also considered as a separate entity (Franke and  
1869 Żelaźniewicz, 2000, 2002). These domains are described separately in the following sections.

1870 The STZ has two branches that surround the more internal parts of the massif. The  
1871 western branch is oriented SW-NE, and although mostly covered, can be continued through  
1872 the Odenwald and northern Vosges to join the western Variscan massifs (Figs. 1, 4 and 6).  
1873 The eastern branch has a NW-SE attitude derived from dextral shearing of the Elbe zone, of  
1874 which the Elbe Fault Zone represents its southern limit (Fig. 6). This branch is known as the  
1875 Lausitz Block.

#### 1877 *5.3.1. Mid German Crystalline High (MGCH)*

1878 This domain crops out in a few inliers, the three more important of which are  
1879 Odenwald, Spessart and Ruhla (Figs. 4 and 6), but information is also supplied by numerous  
1880 drill holes. According to Franke (2000), it represents the SE active margin of the RHZ,  
1881 characterized by arc-related plutonism. The MGCH may have a Cadomian basement, and  
1882 includes i) a Cambro-Ordovician succession of paragneisses and metabasites, ii) Upper  
1883 Ordovician-early Silurian granitoids, iii) Silurian and Lower Devonian arc-related magmatism

1884 similar to that of the Northern Phyllite Zone, iv) Upper Devonian calc-alkaline plutons  
1885 probably from a Devonian-early Carboniferous magmatic arc, v) Middle Devonian to  
1886 Tournaisian unmetamorphized sediments, and vi) arc-related middle Carboniferous granitoids  
1887 (340-325 Ma; Franke, 2000; Zeh and Will, 2010). Zircon provenance studies show  
1888 sedimentary derivation from Gondwana and Baltica in different groups of the Ruhla inlier and  
1889 in other units, implying that the MGCH hosts the Rheic suture, according to Zeh and Will  
1890 (2010) and Zeh and Gerdes (2010).

1891 Metamorphism is dated as early as 370 Ma, and indications of high-P rocks are  
1892 generally absent, but eclogite lenses occur in the NE of Odenwald. A fault zone separating  
1893 western from eastern Odenwald and Spessart is considered part of the Rheic suture by Will et  
1894 al. (2017). Granulite facies metamorphism in western Odenwald is dated between 430 and  
1895 349 Ma, whereas eclogite facies in eastern Odenwald has a minimum age of 363-350 Ma  
1896 (Scherer et al., 2002), and amphibolite facies there and in central Spessart yielded *c.* 324-316  
1897 Ma (Will et al., 2017). According to Will and Schmädicke (2001, 2003), minimum pressure  
1898 of 1.6 GPa at 650-750 °C characterize the eclogites, while granulites in the west reached a  
1899 maximum P of 0.4 GPa at minimum T of 680 °C.

1900 The eclogites crop out in the core of an antiformal structure interpreted as a tectonic  
1901 window which continues with a SSW-NNE attitude to the Spessart (Will et al., 2017). An  
1902 antiformal structure exists also at Ruhla with a similar attitude, which is oblique to present  
1903 SW-NE zone limits, interpreted as late Variscan strike-slip faults truncating earlier structures  
1904 (Franke, 2000).

1905 According to Zeh and Gerdes (2010), the Silurian-Devonian arc (425-392 Ma) resulted  
1906 from NW-directed subduction of the Rheic lithosphere beneath Laurussia continental shelf.  
1907 That subduction created a back arc leading to the opening of the Rhenohercynian basin and  
1908 the Lizard-Giessen Ocean to the NW at the Lower-Middle Devonian. The Variscan evolution  
1909 (360-320 Ma) started by the oblique (sinistral) collision between the peri-Gondwanan STZ  
1910 and the Rhenohercynian domain. Different parts of the MGCH underwent different structural  
1911 and metamorphic evolutions. The still preserved parts of the Rheic Ocean subducted to the  
1912 south, starting to form a new arc in the STZ. Then the Silurian-Devonian arc became accreted  
1913 to the base of a new arc and the Rhenohercynian Ocean was in turn closed, culminating the  
1914 growth of the new, Rhenohercynian arc. Accretion started at 360-350 Ma, contemporaneous  
1915 with flysch sedimentation in the Rhenohercynian basin, and ceased at *c.* 310 Ma. Formation  
1916 of the Rhenohercynian arc started at 360 Ma and reached a peak at 340-330 Ma.

1917

1

21918 *5.3.2. Saxothuringian Autochthon*

3

41919

5

61920

7

81921

9

101922

11

121923

13

141924

15

161925

171926

18

191927

20

211928

22

231929

24

251930

26

271931

28

291932

30

311933

32

331934

34

351935

36

371936

38

391937

40

411938

42

431939

44

451940

46

471941

48

491942

50

511943

52

531944

54

551945

56

571946

58

59

60

61

62

63

64

65

The rocks forming this domain are mostly low-grade metasediments of Neoproterozoic and Paleozoic age deposited at the northern or northwestern margin of Gondwana. The Neoproterozoic and lowermost Cambrian include volcanosedimentary complexes and massive intrusions developed between 570-535 Ma. They reflect the Cadomian orogenic event and the transition between plate convergence responsible for the arc and subsequent rifting, which opened the Rheic Ocean and pulled apart the peri-Gondwanan Avalonia microcontinent. Rifting was renewed at the Cambro-Ordovician boundary, with intrusions dated at 500-480 Ma (Linnemann et al., 2007, 2008). Bounding the MGCH to the south, the Vesser Rift or Southern Phyllite Zone is a Late Cambrian bimodal magmatic belt affected by greenschist facies Variscan metamorphism.

In the Cadomian basement, Linnemann et al. (2008) differentiate a northern external domain with distal turbidites including black cherts and volcano-sedimentary complexes dated at 570-543 Ma, which would represent the back-arc. The southern internal domain includes Ediacaran sediments of passive margin and flysch types, which represent respectively the margin of the back-arc and a Cadomian retro-arc basin. A *c.* 565 Ma glaciation has been identified by Ediacaran glaciomarine deposits of the Elbe Zone in the south of the Lausitz Block (Linnemann et al., 2018). Plutons of granodiorite composition are abundant and voluminous here, dated at 540-530 Ma.

For the Paleozoic, preorogenic sequences are mostly terrigenous, with carbonates of early-middle Cambrian and Devonian age, Lower Ordovician quartzites and pelites, and Silurian graptolite slates. All these are typical of relatively inner parts of the Gondwanan continental shelf, and comparable to successions in the Armorican and Iberian Massifs. Cambrian faunas in eastern Germany, including trilobites and archaeocyatha are comparable to those of France, Iberia and Morocco (Elicki, 2007). Upper Ordovician glacigenics have been found in the SW of the STZ (Katzung, 1961; Linnemann et al., 2003; Hofmann and Linnemann, 2013). Detrital zircon age spectra also indicate correlation with the OMZ of SW Iberia (Linnemann et al. 2008). The synorogenic sedimentation includes Tournaisian to Viséan Carboniferous flysch, progressively younger toward the NW, and late Viséan molasses (Franke and Engel, 1986). Both pre- and synorogenic autochthonous sequences are

1948 described together as the Thuringian Facies, mostly of shallow platform facies for the  
1949 preorogenic sequence.

1950 Variscan deformation in the western branch of the STZ is dominated by upright SW-  
1951 NE wrench shear zones and folds with an axial planar, low-grade pervasive cleavage. These  
1952 are late folds, as one or more previous cleavages are identified at the NW and SW wrench and  
1953 thrust zones and in the core of the antiform between them (Kroner et al., 2010). The folds,  
1954 cleavage and metamorphism affect early Carboniferous synorogenic deposits. The authors  
1955 describe the previous deformation events as consisting of crustal stacking and continental  
1956 subduction followed by exhumation. Their SW-NE wrench and thrust zones refer to the bands  
1957 coinciding with the MGCH in the NW and the allochthonous domain in the SE. Although  
1958 they do not mention the kinematics of wrenching, Franke and Żelaźniewicz (2002) consider it  
1959 dextral.

1960 Later dextral shear zones and faults with a NW-SE attitude cut across the whole  
1961 Bohemian Massif, with the Elbe zone, in the north, as the most important (Fig. 6). This zone  
1962 affects the Lausitz block, where the age of dextral shearing has been estimated between 334  
1963 Ma and 327 Ma by U-Pb ages of a synkinematic and an undeformed granite respectively, both  
1964 occurring close to the Elbe Fault Zone (Hofmann et al., 2009). Ar-Ar dating of the Intra-  
1965 Sudetic Fault (Fig. 6) yielded a younger age interval of 325-320 Ma (Marheine et al., 2002).  
1966 Franke and Żelaźniewicz (2002) interpret that the SW-NE early dextral system (380-340 Ma)  
1967 was cut across by the NW-SE dextral system, which was in turn overprinted by the NNE-  
1968 SSW Moldanubian Thrust, even when the ages of the two later are similar.

1969 In contrast with the general low-grade metamorphic imprint of most of the  
1970 autochthonous STZ, several gneiss domes occur surrounding the inner part of the Bohemian  
1971 Massifs. The Granulitebirge and Erzgebirge domes were formed beneath the outer rim of the  
1972 Allochthon, and the same was probably the case of the Krkonoše and Orlica-Śnieżnik domes  
1973 (Figs. 6 and 7a). Together, they form a curved alignment delineating an open Bohemian Arc  
1974 that was yet drawn by Suess (1885-1909) and Kossmat (1927).

1975 The Saxonian Granulitebirge and the Erzgebirge (Fig. 6) include high-grade and high-  
1976 and ultrahigh-P rocks (Massone, 2001; Massone et al., 2007; Collett et al., 2017). Their domal  
1977 structure indicates a provenance from intracontinental subduction of the Saxothuringian crust  
1978 and emplacement as gneiss domes or extrusions along the subduction zone, aided perhaps by  
1979 hydraulic overpressure (Franke and Stein, 2000).

1980 The Saxonian Granulitebirge is described by Rötzler and Romer (2010). Its rocks crop  
1 out in a SW-NE elongated dome with metamorphism progressively increasing toward its core,  
2 1981 out in a SW-NE elongated dome with metamorphism progressively increasing toward its core,  
3 1982 which consists of granulite-facies Cambro-Ordovician mainly bimodal igneous protoliths of  
4 calc-alkaline and tholeiitic character. These are surrounded by a detachment zone with slivers  
5 1983 of dismembered high-grade metapelites and mafic and ultramafic rocks, and by a low-P schist  
6 cover of early Paleozoic to Upper Devonian age. The granulites recorded near isothermal  
7 1984 decompression from metamorphic peak at 2-2.5 GPa, and post-peak recrystallization at 1.1  
8 GPa. Peak T is dated at 341 Ma, whereas retrogradation in the base of the schist cover is dated  
9 1985 at 334 Ma. Average rates of exhumation and cooling of the granulites have been calculated in  
10 7-13 mm/year and 40-70 °C/Ma. Kinematic criteria indicate top to the SE sense of shear in the  
11 1986 detachment zone (Fig. 7a; Kroner, 1995; Franke and Stein, 2000).  
12  
13 1987  
14 1988  
15 1989  
16 1990  
17  
18 1990  
19

20 1991 The Erzgebirge forms the structurally deepest part of the Saxothuringian basement. It  
21 is formed by a complex stack of Cadomian basement and early Paleozoic sedimentary and  
22 1992 bimodal volcanics (500-460 Ma) reflecting a passive margin environment, equivalent to that  
23 of the Thuringian Facies. The lowermost Gneiss-Amphibolite Unit includes Neoproterozoic  
24 1993 greywackes intruded by Cadomian granitoids (570-530 Ma), and affected by medium-  
25 P/medium-T amphibolite facies metamorphism. Above, a pile of Paleozoic rocks starts with  
26 1994 an ultrahigh-P/high-T Gneiss-Eclogite Unit, and continues upward by a high-P/high-T  
27 Gneiss-Eclogite Unit, high-P/low-T Mica schist-Eclogite Unit, medium-P/low-T Garnet  
28 1995 Phyllite Unit and low-P/low-T Phyllite Unit (Rötzler and Plessen, 2010). Mylonitic shear  
29 zones separate the units and the ensemble from the overlying schist mantle. The Gneiss-  
30 1996 Eclogite units also include granulites and ultramafic rocks, and micro diamonds occur in the  
31 underlying ultrahigh-P unit, pointing to pressures equivalent to at least 150 km . Závada et al.  
32 (2018) shown that the ultrahigh-P granulites and high-P granofelses preserved at the SE flank  
33 1998 of the Erzgebirge testify a paleogradient of continental subduction originally dipping to the  
34 east, and where the deepest rocks were exhumed along a subduction channel to mid-crustal  
35 1999 depths.  
36  
37 2000  
38  
39 2001  
40  
41 2002  
42  
43 2003  
44 2004  
45  
46 2005  
47  
48 2006  
49

50 2007 The eclogites had been exhumed yet before stacking, and later, the entire stack became  
51 overprinted by amphibolite-facies metamorphism, and was exhumed in the dome. The thrust  
52 2008 faults responsible from the metamorphic inversion show a tectonic transport to the west or to  
53 the N-NNE (Schmädicke, 1994; Franke and Stein, 2000). The upper detachment shows a  
54 2009 westward component of motion for the hanging wall (Krohe, 1996, Krawczyk et al., 2000).  
55  
56 2010  
57  
58 2011  
59  
60  
61  
62  
63  
64  
65



2012 According to Franke and Stein (2000) and references therein, ages of high-P and  
1  
2013 ultrahigh-P metamorphism are somewhat scattered, starting at *c.* 370 Ma and cooling through  
2  
3014 *c.* 350 Ma until a significant event around 340 Ma. However, specific ages for eclogite-facies  
3  
4  
5015 metamorphism range 360-335 Ma (Schmädicke et al., 1995). The older ages come from Ar-  
6  
7016 Ar and Sm-Nd analyses, and are discussed by Rötzler and Plessen (2010), who prefer the age  
8  
9017 group clustering around 340 Ma as indicating peak of high-P metamorphism during  
10  
11018 intracontinental subduction. Modern petrochronology studies (Závada et al., 2021) show that  
12  
13019 the ultrahigh-P conditions for coesite-diamond bearing rocks were reached at 350 Ma, while  
14  
15020 the granulites formed at around 340 Ma. The whole system was exhumed at around 338 Ma.  
16  
17021 A later group of ages around 330 Ma date retrograde penetrative deformation during  
18  
19022 exhumation.

20  
21023 There are two other domes which also bear the imprint of intracontinental subduction  
22  
23024 and are overlain by units belonging to the Allochthon. One is the Krkonoše Massif, in the  
24  
25025 Lausitz Block, and the other the Orlica-Šnieżnik Dome in Central Sudetes.

26  
27026 The Krkonoše Massif (Figs. 6 and 7a) is a dome whose core is occupied by a late  
28  
29027 Carboniferous granitic pluton dated at 313 Ma (Marheine et al., 2002; Žák et al., 2013; Kryza  
30  
31028 et al., 2014). From bottom to top, four units have been described (Mazur and Aleksandrowski,  
32  
33029 2001; Žáčková et al., 2010; Jeřábek et al., 2016). The upper three units are interpreted as  
34  
35030 forming part of the Allochthon, and will be described in the next section. The lowermost of  
36  
37031 them is the Jizera-Kowary Unit, which may represent the STZ Autochthon. It consists of  
38  
39032 Cambro-Ordovician orthogneisses (*c.* 500 Ma) intruded in metasediments of probable  
40  
41033 Neoproterozoic age. To the west, the orthogneisses have intrusive contacts with Cadomian  
42  
43034 granitoids of the Lausitz Block, which supports that the Jizera-Kowary Unit forms part of the  
44  
45035 Autochthon.

46  
47036 This unit outcrops mostly to the north of the Variscan Krkonoše granite, where  
48  
49037 metamorphism ranges from greenschist to lower amphibolite facies. To the south and east of  
50  
51038 the Krkonoše granite, the unit includes albite-bearing micaschists, graphitic schists, quartzite,  
52  
53039 marble and calc-silicate rocks, amphibolite and granitic orthogneiss. An estimate of early  
54  
55040 metamorphic conditions in the south yielded 1.2-1.4 GPa at 460-520 °C, implying high-P  
56  
57041 conditions (Žáčková et al., 2010). On the other hand, the relatively young age of this  
58  
59042 metamorphism, *c.* 340 Ma (Konopásek et al., 2019) suggests a correlation with the  
60  
61043 Erzgebirge, instead of with the overlying units, where the high-P is Upper Devonian.

2044 The Orlica-Śnieżnik Dome represents the more oriental outcrop of the STZ  
1 2045 Autochthon and, as the Krkonoše Massif, it is overlain by the Allochthon, here represented by  
2 2046 the Moldanubian Zone (Figs. 6 and 7a). The Autochthon is dominated by amphibolite-grade  
3 2047 orthogneisses, locally containing lenses of high and ultrahigh-P eclogites and granulites,  
4 2048 alternating with bands of biotite- to staurolite-grade supracrustal rocks (Don et al., 1990;  
5 2049 Štípská et al., 2004; 2012). The orthogneisses have been dated at 520-490 Ma (Oliver et al.,  
6 2050 1993; Turniak et al., 2000; Kröner et al., 2001; Lange et al., 2005). The supracrustal  
7 2051 succession consists of a monotonous series of plagioclase-rich paragneisses and a variegated  
8 2052 formation consisting mostly of mica schists. A Saxothuringian affinity is revealed by zircon  
9 2053 provenance studies (Mazur et al., 2012, 2015). Occurrences of ultrahigh-P rocks provide a  
10 2054 record of continental subduction and subsequent melt-assisted extrusion of deeply subducted  
11 2055 rocks partly driven by buoyancy forces (Chopin et al., 2012) similar to that of the Erzgebirge.  
12 2056 The structure is interpreted as a large gneiss dome created by the expulsion of lower crustal  
13 2057 material at the rear of the Sudetic accretionary prism (Chopin et al., 2012; Štípská et al.,  
14 2058 2019). The dome comprises dismembered fragments of the Saxothuringian passive margin  
15 2059 that were subducted during the Variscan collision and then exhumed in front of the rigid  
16 2060 buttress of Brunovistulian block, according to Duretz et al. (2011) and Chopin et al. (2012).  
17  
18  
19  
20  
21  
22  
23  
24  
25  
26  
27  
28  
29  
30

### 31 2061 32 33 2062 *5.3.3. Saxothuringian allochthons*

34 2063 Figure 7b shows a section across the SW part of the Bohemian Massif perpendicular to  
35 2064 the western branch of the STZ. It shows the relationships between the Autochthon and the  
36 2065 allochthons of this zone, represented here by the Münchberg Klippe, and also with the also  
37 2066 allochthonous Teplá-Barrandian and Moldanubian. The Allochthon and Parautochthon in the  
38 2067 western branch of the STZ is represented by the Münchberg, Wildenfels and Frankenberg  
39 2068 klippen, whose units are separated by thrust faults (Fig. 6). Münchberg is the largest and  
40 2069 shows the most complete succession (Klemd, 2010), which is described from bottom to top.  
41  
42  
43  
44  
45  
46  
47  
48

49 2070 The lower part of the Parautochthon consists of early Carboniferous, mainly Viséan  
50 2071 proximal synorogenic flysch, often a wildflysch with blocks of probably Cambrian and also  
51 2072 Ordovician, Silurian and Devonian blocks and olistoliths (Franke, 1989; Linneman et al.,  
52 2073 2003; Klemd, 2010). The upper Parautochthon is represented by the distal and relatively deep  
53 2074 Bavarian facies, including Ordovician bimodal volcanism and clastic sediments, as well as  
54 2075 Silurian-Devonian volcanics, graphitic schists and cherts.  
55  
56  
57  
58  
59  
60  
61  
62  
63  
64  
65

2076 Above, a unit formed by phyllites and prasinites occurs, followed by another  
1  
2077 consisting of amphibolite represent the Middle Allochthon. They were formed around 400 Ma  
3  
2078 (Koglin et al., 2018), and metamorphosed at *c.* 365 Ma (Kreuzer et al., 1989).  
4

5  
62079 The two remaining units represent the Upper Allochthon. The first consists of  
7  
2080 metasediments, orthogneisses, metagabbros and serpentinites, while the culminating unit is  
8  
92081 made of banded hornblende gneisses, amphibolites and leucocratic gneisses, and includes  
10  
112082 eclogites at the base (Klemd, 2010). The igneous protoliths have ages of 525-480 Ma, and the  
12  
132083 eclogites point to equivalence with the high-P/high-T units, with peak pressure conditions  
14  
152084 roughly dated in Münchberg at 400 Ma and bearing a record of subsequent amphibolite-facies  
16  
172085 metamorphism at 380 Ma (Franke, 2000; Koglin et al., 2018).  
18

192086 The structural succession of the Frankenberg klippe consists of a low-grade  
20  
212087 volcanosedimentary complex that can be ascribed to the STZ autochthon. Above, a prasinite  
22  
232088 unit would be equivalent to the phyllite and prasinite unit of Münchberg, and represent an  
24  
252089 upper crustal piece of a Devonian oceanic crust. The klippe culminates with high-P  
26  
272090 amphibolite and gneiss units (Rötzler et al., 1999; Klemd, 2010) probably representing the  
28  
292091 Upper Allochthon. In Wildenfels, only the Upper Allochthon is represented by augengneisses,  
30  
302092 gneissic micaschists, amphibolitic gneisses and amphibolite units (Klemd, 2010).  
31

32  
332093 Kinematic criteria indicate final emplacement of the Münchberg klippe toward the  
34  
352094 NW, but previous kinematic criteria indicate top to the SW or WSW in augengneisses and  
36  
372095 mylonites of the Upper Allochthon (Blümel et al., 1990). Interestingly, a similar kinematics  
38  
392096 has been described in the Erbendorf-Vohenstrauß Unit, at the base of the Moldanubian Zone  
40  
412097 (Franke, 1990; Blümel et al., 1990).  
41

422098 In the eastern branch of the STZ, the Allochthon occurs in the west and central  
43  
442099 Sudetes, surrounding the Krkonoše Massif, and in the Góry Sowie Massif respectively. Figure  
45  
462100 7a shows a section partly oblique to the structure, but subparallel to it in the eastern branch of  
47  
482101 the STZ. It cuts across the Erzgebirge, Krkonoše and Orlica-Śnieżnik domes, which are  
49  
502102 equivalent (not successive) structures which delineate the Bohemian Arc. This part of the  
51  
522103 profile is intended to show the suggested mutual relationships among the different  
53  
542104 allochthons.  
54

55  
562105 South and SE of the Krkonoše Massif, three units have been described. The lowermost  
57  
582106 of them crops out in just a small area SW of the pluton. It consists of very low grade Devonian-  
59  
602107 Carboniferous sediments including Culm facies on top, and is considered the Parautochthon  
61  
62  
63  
64  
65

2108 by Mazur and Aleksandrowski (2001). Above, the South Krkonoše Unit crops out along the  
1 2109 southern flank of the dome. It is formed by garnet-free micaschists, phyllites and marbles with  
3 2110 a high proportion of metavolcanics, of which the metabasites show relics of blueschist facies  
5 2111 (1.2-1.5 GPa; Majka et al., 2016; Konopásek et al., 2019), dated around 365 Ma (Maluski and  
7 2112 Patočka, 1997; Konopásek et al., 2019).

9 2113 To the east of the Krkonoše Massif, another unit overlies the South Krkonoše Unit. It  
11 2114 consists of medium-P, MORB-type Cambro-Ordovician metabasites (Oliver et al., 1993;  
13 2115 Kryza et al. 1995; Winchester et al. 1995). It represents the older oceanic units of the Middle  
15 2116 Allochthon, and can be continued northward to the Kaczawa Complex (Figs. 6 and 7a).

17 2117 The Kaczawa Complex represents the Middle Allochthon, including its two oceanic  
19 2118 components (Martínez Catalán et al., 2020). Below, Cambro-Ordovician metasedimentary  
21 2119 and bimodal metavolcanics, with dominant alkaline basalts, represent the development of a  
23 2120 continental rift. Metamorphism in all these units reached blueschist facies, and was  
25 2121 overprinted by greenschist facies (Kryza et al., 1990, 2004, 2011). Above, a couple of Silurian  
27 2122 and Devonian units with thick, pillowed MORB-type basalts represent the evolved stages of a  
29 2123 rift and a deep-water environment, perhaps oceanic supracrustals (Furnes et al., 1994; Seston  
31 2124 et al., 2000). Another characteristic component is an Upper Devonian-early Carboniferous  
33 2125 flysch with chaotic assemblages and tectonic mélanges, always of very low metamorphic  
35 2126 grade (Kryza and Zalasiewicz, 2008). Some of these synorogenic deposits separate the lower  
37 2127 and upper units of the Kaczawa Complex. Moreover, a rather undeformed basaltic unit of  
39 2128 probable Upper Devonian age may represent an even younger ophiolite (Seston et al., 2000).

41 2129 The most oriental Allochthon of the STZ outcrops in and around the Góry Sowie  
43 2130 Massif (Figs. 6 and 7a). Although it is bounded by late Variscan faults, its lithological  
45 2131 association and tectonometamorphic evolution, together with the ophiolites surrounding a  
47 2132 catazonal unit favor an allochthonistic interpretation. These ophiolites are Lower Devonian  
49 2133 and collectively considered a dismembered ophiolite suite (*e.g.* Kryza et al., 2004). For  
51 2134 instance, the Ślęza ophiolite north of the massif consists of variably serpentinized  
53 2135 harzburgites and lherzolites, coarse grained gabbros and a roof assemblage of fine-grained  
55 2136 metagabbros, diabase and volcanics, including pillow lavas, and is dated at 400 Ma (Oliver et  
57 2137 al., 1993; Floyd et al. 2002; Dubińska et al., 2004).

59 2138 The Góry Sowie Massif consists of migmatitic paragneisses previously assumed to be  
61 2139 late Neoproterozoic to Cambrian based on microfossils (Gunia, 1999) and have been recently

2140 dated at 600-493 Ma using detrital zircons (Tabaud et al., 2021). There are also orthogneisses,  
1  
2 2141 dated at 490-480 Ma (Kröner and Hegner, 1998; Kryza and Fanning, 2007), and some  
3  
4 2142 coronitic metagabbros, amphibolites and ultramafics. A high-P/high-T granulite facies event  
5  
6 2143 is dated at 400-395 Ma, and an amphibolite-facies overprint occurred at 385-365 Ma (O'Brien  
7  
8 2144 et al., 1997; Bröcker et al., 1998; Kryza and Fanning, 2007; Tabaud et al., 2021). This  
9  
10 2145 tectono-thermal event was coeval with emplacement of Devonian ophiolitic rocks presently  
11  
12 2146 surrounding the Góry Sowie Massif.

#### 15 2148 *5.4. Teplá-Barrandian and Moldanubian*

17  
18 2149 The classical Moldanubian Zone (Kossmat, 1927) is considered a peri-Gondwanan  
19  
20 2150 coherent terrane bounded by sutures that separate it from the Saxothuringian Zone in the north  
21  
22 2151 and NW, and from the Moravo-Silesian Zone in the SE (Matte et al., 1990; Franke, 2000).  
23  
24 2152 Which are the oceans witnessed by these sutures is a matter of debate, as it is the correlation  
25  
26 2153 of the Moldanubian with other Variscan terranes or Zones. High-P basic and ultrabasic rocks  
27  
28 2154 occur in parts of this zone, and have been interpreted as klippen of a large thrust sheet, the  
29  
30 2155 Gföhl Nappe, emplaced to the N, E and ESE and having covered the whole zone (Tollmann,  
31  
32 2156 1982; Matte et al., 1990; Franke, 2000). This interpretation has been challenged by  
33  
34 2157 Schulmann et al. (2005, 2009, 2014b), who see the high-P units as exhumed pieces of the  
35  
36 2158 lower crust underlying the zone and being a consequence of continental relamination (Hacker  
37  
38 2159 et al., 2011).

39 2160 Two eclogitic units occur at the base of the Teplá-Barrandian and Moldanubian zones,  
40  
41 2161 Mariánské Lázně and Erbendorf-Vohenstrauß respectively (Figs. 6 and 7b). The Teplá-  
42  
43 2162 Barrandian Zone is considered either a separate terrane (Matte et al., 1990; Franke, 2014) or  
44  
45 2163 part of the Moldanubian terrane, occupying a relatively higher structural position, and  
46  
47 2164 separated from the Moldanubian Zone by large-scale normal and wrench faults (Pitra et al.,  
48  
49 2165 1999; Franke, 2000; Zulauf et al., 2002). It is possible that these faults hide the lateral  
50  
51 2166 transition between two parts of the same terrane with different characteristics (Schulmann et  
52  
53 2167 al. 2009; Lardeaux et al., 2014). In this case, the two zones would represent the upper  
54  
55 2168 ensemble of the Bohemian nappe pile, perhaps being equivalent to the Upper Allochthon of  
56  
57 2169 the French and Iberian massifs. Then, the two eclogitic units occurring at the base of the  
58  
59 2170 Teplá-Barrandian and Moldanubian zones (Mariánské Lázně and Erbendorf-Vohenstrauß  
60  
61 2171 respectively; Figs. 6 and 7b) would represent the suture of such a terrane. In the next sections

2172 the Moldanubian Zone is described first followed by the Teplá-Barrandian Zone, according to  
2173 the bottom to top mode followed in previous sections.

#### 2174 2175 5.4.1. Moldanubian Zone (MZ)

2176 This zone was divided by Fuchs (1976, 1986) into two major ensembles, Drosendorf  
2177 and Gföhl. The Drosendorf Unit includes a lower ensemble called the Monotonous Group,  
2178 consisting of migmatitic paragneisses, quartzites, amphibolites and numerous Paleo- to  
2179 Neoproterozoic gneiss fragments ranging from 1.3 to 0.56 Ga (Lindner and Finger, 2018;  
2180 Lindner et al., 2019) and gneissified early Paleozoic intrusions (*e.g.* Friedl et al., 2004). The  
2181 detrital zircon data suggest deposition of the Monotonous group sediments during Early  
2182 Paleozoic, most likely early Ordovician times (Košler et al., 2013). The higher ensemble  
2183 called the Varied Group comprises paragneisses, quartzites, marbles, amphibolites and  
2184 leptynites of Neoproterozoic and early Paleozoic age, interpreted as deposited in a back-arc  
2185 setting (Janoušek et al., 2008; Schulmann et al., 2009). The detrital zircon record points to  
2186 Early Paleozoic, possibly Silurian deposition (Košler et al., 2013). The Monotonous and  
2187 Varied groups underwent medium-P amphibolite facies (0.8-1 GPa, 600-700 °C) at *c.* 350-330  
2188 Ma, although eclogite boudins occur mainly at the contact between them (Schulmann et al.,  
2189 2005).

2190 The Gföhl Unit is viewed here as a collective name for several massifs, most of them  
2191 distributed in the north and SE of the MZ, but also occurring in the central part of the  
2192 Moldanubian (Kutna Hora and Blanský les units; Fig. 6), between the two main plutonic  
2193 belts. Rocks of the Gföhl Unit include felsic migmatites, felsic granulites, Ordovician  
2194 orthogneisses, retrograded eclogites of mantle and crustal origin, and mantle peridotites.  
2195 Mantle rocks attained P-T conditions of 6-3.3 GPa and 875-1150 °C, while crustal rocks  
2196 reached peak conditions above 3-4 GPa and 900-1000 °C at *c.* 350 Ma (Perraki and Faryad.,  
2197 2014; Nahodilová et al., 2020). This event was followed by major reequilibration of high-P  
2198 granulites at 1.8-2 GPa at 340 Ma (Štípská et al., 2016). Coeval potassic and ultra-potassic  
2199 intrusions (durbachites) occur spatially related to the granulites and include relics of high- and  
2200 ultrahigh-P basic and ultrabasic rocks (Janoušek and Holub, 2007; Janoušek et al.,  
2201 2020).

2202 The meaning of the Gföhl Unit and the role of the STZ subducted crust has been  
2203 discussed. Matte et al. (1990) and Franke and Żelaźniewicz (2000, 2002) interpreted the unit

2204 as a thrust sheet emplaced above the MZ, while Schulmann et al. (2005, 2009, 2014b)  
2205 describe the evolution of the MZ in terms of subduction of the STZ beneath a continental  
2206 terrane. The association of granulites and durbachites in the MZ has been interpreted as a  
2207 Visean product of relamination, as defined by Hacker et al. (2011) in subduction zones  
2208 bearing sediments or involving continental or arc crust. It implies emplacement of felsic  
2209 gneisses derived from lower plate and incorporated to the upper plate, mostly at the lower  
2210 crust. In the MZ, partially molten gneisses derived from the subducted continental lower crust  
2211 of the STZ may have penetrated horizontally from the subduction channel to the SE  
2212 relaminating the Moldanubian lower crust, part of which extruded later vertically reaching  
2213 upper crustal levels (Lexa et al., 2011; Kusbach et al., 2015).

2214 Chopin et al. (2012) have proposed flat subduction of the STZ continental crust  
2215 beneath the Teplá-Barrandian rocks and extrusion of ultrahigh-P to high-P rocks in the Orlica-  
2216 Šniežnik Dome. If true, the felsic granulites with high-P relics could derive directly from this  
2217 crust, and their occurrence can be explained by extrusion from the STZ crust and diapiric  
2218 intrusion close to the Moldanubian Thrust in the SE, and also in the central part of the MZ  
2219 (Fig. 7b; Lexa et al., 2011; Schulmann et al., 2014b; Kusbach et al., 2015).

#### 2220 2221 *5.4.2. Teplá-Barrandian Zone (TBZ)*

2222 Underlying the Mariánské Lázně and Erbendorf-Vohenstrauß units, an association of  
2223 low-grade metasediments, basic rocks, acid tuffs and serpentinites reaching at most epidote-  
2224 amphibolite facies occurs (Kladská unit of Kachlík, 1997). It overlies the Thuringian-facies  
2225 autochthonous Paleozoic and is similar to the unit with phyllites and prasinites of Münchberg.

2226 The Mariánské Lázně Unit consists of amphibolites, often migmatitic, with minor  
2227 alternations of felsic gneisses, and rare metasediments and pyroxenites. An eclogite-  
2228 amphibolite zone occurs between a basal layer of serpentinite and an overlying gabbro-  
2229 amphibolite zone (Collett et al., 2018). The protolith age of eclogites and amphibolites is *c.*  
2230 540 Ma old, while gabbros in the upper zone, often coronitic, have yielded 500 Ma  
2231 (Timmermann et al., 2004, 2006). Lu-Hf and Sm-Nd garnet-whole rock geochronology yield  
2232 *c.* 390 Ma for high-P metamorphism (*c.* 2.5 GPa, 650-750 °C) and 375 Ma for cooling after a  
2233 high-T overprint, in accordance with the previous age data (Collett et al., 2018 and references  
2234 therein). Calc-alkaline gabbros intruded the Mariánské Lázně eclogites during their  
2235 syncompressional and later extensional exhumation at *c.* 380 Ma (Deiller et al., submitted).

2236 Overlying the Mariánské Lázně Unit, the Teplá Crystalline Complex is a band 10 km  
1 2237 wide of Neoproterozoic metasediments and metabasalts where a Cambro-Ordovician low-  
2 2238 P/high-T metamorphic event (*c.* 485 Ma) was overprinted by a Late Devonian, Barrovian  
3 2239 event related with crustal thickening (*c.* 375 Ma), and then by low-P/high-T metamorphism  
4 2240 related to a giant detachment along which the Maránské Lázně complex was exhumed  
5 2241 (Peřestý et al., 2017).  
6  
7  
8  
9  
10

11 2242 The thick Neoproterozoic succession of the TBZ starts with Cadomian arc-related  
12 2243 magmatism at the east (Davle group) which characterizes the lower part of this zone (Hajná et  
13 2244 al., 2011), followed by late Ediacarian to Cambrian ocean floor stratigraphy and turbiditic  
14 2245 accretionary wedge sequences of the Štěchovice group (Hajná et al., 2018; Ackermann et al.,  
15 2246 2020). The uppermost unit is represented by a weakly metamorphosed Paleozoic section  
16 2247 preserved at the core of the Praha or Barrandian Syncline. Metamorphic grade decreases  
17 2248 upward from the basal Mariánské Lázně and Erbendorf-Vohenstrauß units through a thick  
18 2249 Neoproterozoic succession until the core of the Praha Syncline (Peřestý et al., 2017).  
19  
20  
21  
22  
23  
24  
25

26 2250 Above, a medium to low-grade Neoproterozoic succession is followed by the  
27 2251 Paleozoic of the Praha Syncline. This sedimentary pile starts with an Ordovician siliciclastic  
28 2252 succession (485-443 Ma) followed by early Silurian graptolitic shales which continuously  
29 2253 passes to late Silurian and Lower Devonian (Lochkovian and Pragian) limestones. The  
30 2254 sequence terminates with siliciclastic deposition of the Givetian Srbsko Formation, which  
31 2255 contains detrital zircons dated at 382 Ma (Vacek et al., 2019). Similarities between this  
32 2256 sequence and that of the Iberian Autochthon had been claimed based mostly in stratigraphic  
33 2257 and faunal correlations (Verneuil and Barrande, 1885; Delgado, 1908; Gutiérrez-Marco et al.,  
34 2258 1999b). However, a study of Ordovician trilobites carried out by Ballèvre (2016) shows that a  
35 2259 very limited number of species are common between the Barrandian and the Armorican and  
36 2260 Iberian Autochthon, which points to the TBZ as a terrane separated from mainland Gondwana  
37 2261 at the Cambro-Ordovician transition.  
38  
39  
40  
41  
42  
43  
44  
45  
46  
47  
48

49 2262 The first event affecting the TBZ produced upright folding and development of a NE-  
50 2263 SW trending vertical fabric associated to crustal thickening at around 380 Ma (Hajná et al.,  
51 2264 2012; Peřestý et al., 2017; 2020). The folding of the Praha syncline had to occur after the  
52 2265 Givetian hiatus. Its age can correlate with formation of strong vertical cleavage affecting the  
53 2266 eastern margin of the TBZ (Jílové Zone) which developed coeval with the syntectonic  
54 2267 intrusion of arc-derived magmas of the Central Bohemian Pluton (Žák et al., 2005). Therefore  
55  
56  
57  
58  
59  
60  
61  
62  
63  
64  
65



2268 the shortening of the eastern TBZ and folding of Praha synforms can be indirectly dated at  
2269 360-350 Ma (Hajná et al., 2012; Vacek and Žák, 2017).

### 2271 5.5. Variscan intrusive magmatism in the Bohemian Massif

2272 The main tectonic events have their counterpart in the granitic plutonism of the  
2273 Bohemian Massif. The earliest magmatic rocks are calc-alkaline gabbros and tonalites  
2274 intruding the eclogites of the Mariánské Lázně Unit at around 390-380 Ma (Deiller et al.,  
2275 submitted), c. 375 Ma granodiorite stocks (Čistá pluton, Venera et al., 2000), and gneissified  
2276 granitoids intruding the TBZ rocks further east (Mirovice and Sedlčany, Košler et al., 1993).  
2277 These magmatic rocks are interpreted as a manifestation of earliest Variscan arc magmatism  
2278 in the Bohemian Massif. However, large magmatic arc intrusions are dated at 354-337 Ma,  
2279 and mostly occur at the Central Bohemian Plutonic Complex (Žák et al., 2014). These calc-  
2280 alkaline magmas were generated during Upper Devonian to early Carboniferous subduction,  
2281 first of oceanic lithosphere and then of the continental Saxothuringian crust beneath the  
2282 Teplá-Barrandian Unit. For that reason, they are referred to as the Saxothuringian arc (Figs. 6  
2283 and 7b). The juvenile magmas intruded SE to the Praha Syncline at 355-340 Ma (Sázava  
2284 suite) while the magmatic pulse migrated eastward with magmas becoming progressively  
2285 richer in potassium (Janoušek et al., 2004; 2010; Žák et al., 2014). These rocks can be  
2286 compared with the intrusives of the tonalitic line of Limousin and the young ophiolites in the  
2287 French Massif Central (Peiffer, 1986; Pin and Paquette, 2002; Faure et al., 2009) and the  
2288 Vosges (Skrzypek et al., 2012).

2289 The next pulse of granitoid intrusions was that of the durbachites or Mg-K granitoids  
2290 (ultra-potassic and potassic melasyenites and melagranites), intruded in the MZ to the SE of  
2291 the Central Bohemian Plutonic Complex at 345-335 Ma (Janoušek and Holub, 2007; Žák et  
2292 al., 2014). These rocks are also found in NW Iberia (López-Moro and López-Plaza, 2004;  
2293 Gallastegui, 2005), the Vosges (Tabaud et al., 2015) and Corsica (Rossi et al., 2009). To the  
2294 scale of the Variscan belt, von Raumer et al. (2014) consider them melting products of  
2295 enriched subcontinental mantle related with the subduction of the Rheic slab into the mantle.  
2296 A similar view is sustained by Schulmann et al. (2009, 2014b) and Janoušek et al. (2007),  
2297 although for them, the durbachites may derive from the subducted crust of the STZ.

2298 Meanwhile, the northern margin of the Variscan Belt recorded intense activity. After  
2299 opening of the Rhenohercynian basin, the RHZ collided with the STZ, initiating the Variscan

2300 dynamics that lasted between 360-320 Ma. Initially, preserved parts of the Rheic lithosphere  
1  
22301 adjacent to the STZ were subducted to the south, followed by accretion of the Silurian-  
3  
42302 Devonian arc (Zeh and Will, 2010). This formed the Rhenohercynian arc, starting at 360 Ma,  
5  
62303 and whose activity lasted until *c.* 325 Ma with a magmatic peak at 340-330 Ma. Its rocks are  
7  
82304 very poorly exposed in the MGCH (Odenwald and Ruhla inliers; Figs. 4, 6 and 7b).  
9  
102305 Interestingly, their volcanic equivalents are widely exposed to the SW, represented by the  
11  
122306 abundant granitoids and ignimbritic volcanism in the Vosges (Tabaud et al., 2014), the  
13  
142307 layered basic intrusions and granitoids in the Schwarzwald, and the Tuffs Anthracifères in the  
15  
162308 northern Massif Central (Lardeaux et al., 2014).

172309 Post-collisional, mostly anatectic plutons characterize the last magmatic pulse. This  
18  
192310 event is associated with low-P/high-T metamorphism which followed a previous Barrovian  
20  
212311 event associated with crustal thickening (Gerdes et al., 2000). Its most voluminous occurrence  
22  
232312 is at the South Bohemian Batholith (335-300 Ma), which represents the SE limit of a ring of  
24  
252313 many plutons surrounding the core of the Bohemian Massif (Schulmann et al., 2009; Žák et  
26  
272314 al., 2014), of which the youngest are dated at *c.* 310-300 Ma.

28  
29

30  
312315

## 6. Morocco

32

332317  
34

352318  
36

372319  
38

392320  
40

412321  
42

432322  
44

452323  
46

472324  
48

492325  
50

512326  
52

532327  
54

552328  
56

572329  
58

592330  
60

612331  
62

63  
64  
65

60 bounding the High Atlas. The segments of the Variscan belt exposed in southernmost

2332 Morocco and the northwestern corner of Mauritania (Zemmour area; Souttoufides of  
1 2333 Villeneuve et al., 2015) and those defining the Mauritanides beyond the Reguibat Shield in  
2 2334 western Mauritania (Villeneuve, 2005) are not included in this description.  
3  
4

### 5 2335 6 7 8 2336 *6.1. Rif Domain* 9

10 2337 Pieces of the Variscan Belt are incorporated into the Alpine belt describing the  
11 2338 Alboran Arc, with the Betic Range in the north (Spain) and the Maghrebides (Rif in Morocco)  
12 2339 in the south (Do Couto et al., 2016). In the Betics, the sequences vary from little and no-  
13 2340 metamorphic Ordovician to early Carboniferous sediments in the Maláguide Complex  
14 2341 (Martín-Algarra et al., 2004) to metasediments difficult to separate from Mesozoic sediments  
15 2342 with Alpine metamorphic imprint in the Alpujarride and Nevado-Filábride complexes  
16 2343 (Alonso-Chaves et al., 2004; Puga et al., 2004). The deposition of the clastic protolith of the  
17 2344 latter complex was recently determined using detrital zircon ages ranging between 349-282  
18 2345 Ma (Santamaría-López and Sanz de Galdeano, 2018). Based on Carboniferous conodonts  
19 2346 found in the lowest Nevado-Filábride Unit, Rodríguez-Cañero et al. (2018) correlate that  
20 2347 Variscan basement with the Cantabrian Zone, while occurrences in the Alpujarride and  
21 2348 Maláguide complexes, integrated in the Alborán Domain, are placed in the northern margin of  
22 2349 a Paleotethys Ocean.  
23  
24

25 2350 High-grade Variscan metamorphic rocks are present in both Betic and Rif cordilleras  
26 2351 in southern Spain and Morocco. The metamorphic core of this previously thickened Cenozoic  
27 2352 orogen was dismembered during Neogene extension forming several discontinuous outcrops  
28 2353 along the Alboran Arc (Michard et al., 1997; Do Couto et al., 2016; Gimeno-Vives et al.,  
29 2354 2020). The polymetamorphic Variscan outcrops are found in the Internal Zone of the Alboran  
30 2355 Arc, namely in the Alpujarride-Sebtide complex, which form the metamorphic envelope of the  
31 2356 Ronda in the Betic Cordillera and the Ceuta and Beni Bousera peridotite massifs in the Rif  
32 2357 (*e.g.* Michard et al., 1997, Ruiz-Cruz and Sanz de Galdeano, 2013). The metamorphic pattern  
33 2358 of these complexes is characterized by downward increase of metamorphic gradient with  
34 2359 structurally deepest granulites, migmatites and higher gneisses and schists (Rossetti et al.,  
35 2360 2010, Acosta-Vigil et al., 2014). These units reveal a polymetamorphic record of both  
36 2361 Variscan and Alpine orogenic cycles for which the determination of age and pressure-  
37 2362 temperature conditions remains problematic (Michard et al., 1997; Massone, 2014). However,  
38 2363 it becomes increasingly evident that the granulite-migmatite unit of the Moroccan Sebtide  
39  
40  
41  
42  
43  
44  
45  
46  
47  
48  
49  
50  
51  
52  
53  
54  
55  
56  
57  
58  
59  
60  
61  
62  
63  
64  
65

2364 complex surrounding Beni Bousera peridotite preserves remnants of high-P/high-T late  
1  
2 2365 Carboniferous-Permian metamorphism reaching *c.* 1.6 GPa at 800 °C (Bouybaouene et al.,  
3  
4 2366 1998). These granulites and granite sills representing products of deep crustal anatexis were  
5  
6 2367 dated at 300-290 Ma using U-Pb zircon method (Rossetti et al., 2010, 2020). Similar peak  
7  
8 2368 pressure conditions of 1.2-1.4 GPa at 850 °C followed by reequilibration at 0.5-0.6 Gpa and  
9  
10 2369 800-850 °C were determined in the anatectic Jubrique envelope of the Ronda massifs (Barich  
11  
12 2370 et al., 2014). Here, the age of anatexis was determined by U-Pb zircon geochronology to 280-  
13  
14 2371 290 Ma (Acosta-Vigil et al., 2014) confirming EMP monazite age *c.* 287 Ma from the same  
15  
16 2372 unit (Massonne et al., 2014). These data corroborate the previously obtained metamorphic  
17  
18 2373 300 Ma ages from amphibolite facies schists (Zeck and Williams, 2000; Zeck and  
19  
20 2374 Whitehouse, 2002) and *c.* 283 Ma age of late Variscan pegmatite magmatism (Sánchez-Navas  
21  
22 2375 et al., 2014) from the metamorphic core of the central Betic Cordillera. Similar *c.* 281 Ma  
23  
24 2376 granite magmatism was also documented by U-Pb zircon geochronology of granite pebbles  
25  
26 2377 from a Tertiary conglomerate lying on a Ghomaride nappe of the eastern Rif (Olivier and  
27  
28 2378 Paquette, 2018).

29  
30 2379 Recently, ultrahigh-P conditions were discovered in diamond-bearing garnets  
31  
32 2380 preserved in the migmatitic Jubrique complex in Spain (Ruiz Cruz and Sanz de Galdeano,  
33  
34 2381 2014) and diamondiferous granulites of Ceuta inlier in Morocco (Ruiz Cruz and Sanz de  
35  
36 2382 Galdeano, 2013). Even if the precise age of ultrahigh-P conditions remains currently unknown  
37  
38 2383 the textural criteria indicate that it certainly preceded the main late Carboniferous-Permian  
39  
40 2384 Variscan high-T event and is considered older than 330 Ma (Ruiz Cruz and Sanz de  
41  
42 2385 Galdeano, 2014).

43  
44 2386 Altogether, the Variscan outcrops preserved in the Spanish and Morocco branches of  
45  
46 2387 Alboran arc show similar lithological and metamorphic evolution suggesting the existence of  
47  
48 2388 a high-P/high-T metamorphic belt before and during *ca* 300 Ma. Because of these similarities,  
49  
50 2389 this belt can be considered as a stitching zone between Iberian Variscides to the north and the  
51  
52 2390 Moroccan Meseta to the south. It coincides with the South Iberia Fault, which suggests that  
53  
54 2391 the latter was a plate boundary more complex than other subparallel wrench faults, and  
55  
56 2392 included convergence and probably extension during late Variscan evolution.  
57  
58  
59  
60  
61  
62  
63  
64  
65

2394 6.2. *Meseta Domain*

1  
22395 Although the main part of the Meseta is covered by Meso- and Cenozoic sediments,  
3  
42396 several massifs allow the separation of various domains (Fig. 8), namely the Eastern and  
5  
62397 Western Meseta, the later including the Coastal and Sehoul blocks (Piqué and Michard,  
7  
82398 1989). Except for the Coastal Block, these domains are characterized by a deformation  
9  
92399 stronger than in the Anti-Atlas, associated metamorphism, pre- and late orogenic magmatism  
10  
112400 and weakly deformed continental late Carboniferous and Permian deposits. The  
12  
132401 paleogeographic significance of these domains, limited by extensive shear zones (Michard et  
14  
152402 al., 2008; Accoto et al., 2020), however remains debatable, and only the Sehoul Block have a  
16  
172403 clearly distinctive signature (Tahiri et al., 2010; Pérez-Cáceres et al., 2017). The domain of  
18  
192404 strong Variscan deformation also includes most of the basement of the Atlas Mountains  
20  
212405 included within the South Meseta Zone, up to the South Meseta Front. It will be here  
222406 described collectively with the Meseta Domain, yet this domain has Anti-Atlas affinities.  
23

24  
252407 The preorogenic sequences can be compared with those of the Anti-Atlas. The lower  
26  
272408 Paleozoic is similar although the Cambrian carbonates are thinner and thick Cambrian clastics  
28  
292409 were deposited in graben structures fed by local sources and associated with tholeiitic  
30  
312410 volcanism, which accounts for early to late Cambrian extension (Pouclet et al., 2008; Letsch  
322411 et al., 2018). The graben system might have had a southward prolongation toward the Anti-  
33  
342412 Atlas (Piqué, 2003). The Ordovician is comparatively thinner, with a marked distalisation  
35  
362413 toward the NE across the Western Meseta (Baudin et al., 2003). Lower Ordovician red beds  
37  
382414 comparable to those of the Armorican Massif and southern CIZ are reported in Central  
39  
402415 Morocco and the Eastern Meseta, but are absent in the Anti-Atlas and nearly so in most of the  
412416 Coastal Block (Ouanaimi et al., 2016). The Hirnantian glacial episode is widely recorded  
42  
432417 throughout the Meseta, with the ice sheet having probably reached the Rehamna massif (Le  
44  
452418 Heron et al., 2007), and an ice-distal turbiditic succession being recognized in the Tazeka  
46  
472419 Massif (Ghienne et al., 2018). Extension continued during the early Paleozoic, marked by  
48  
492420 intraplate volcanism in the Lower Ordovician (El Hadi et al., 2014) and the Silurian (El  
502421 Kamel et al., 1998). Carbonate platforms developed in the Devonian. A more pronounced  
51  
522422 tectonic activity was recorded during the Lower-Middle Devonian around the Variscan  
53  
542423 Western Meseta Shear Zone (WMSZ; Fig. 8), where coarse continental conglomerates filled  
55  
562424 restricted fault-bounded basins (Michard et al., 2008).

57  
582425 Differences in the style and age of deformation occur among the different domains.  
59  
602426 The Eastern Meseta (EM) was affected by an early folding event, synmetamorphic, of early

2427 Carboniferous age. Detailed analysis of fold geometries at the scale of several massifs of the  
1 2428 Moroccan Meseta shows that these folds are recumbent, with variable vergence: W to SW  
2 2429 (Piqué, 2001; Michard et al., 2010a) and SE (Accotto et al., 2020). Axial traces delineate an  
3 2430 arc convex toward the west (Piqué, 2001; Michard et al., 2010a), called here Eastern Meseta  
4 2431 Arc (EMA). These recumbent folds and the associated subhorizontal schistosity have been  
5 2432 attributed to the Bretonnic phase (Piqué, 1988, 1989, 2001; Michard et al., 2008; Ouanaimi et  
6 2433 al., 2019), formed in a supra-subduction environment (Michard et al., 2008), or in a fore-arc  
7 2434 setting (Accotto et al., 2020). Metamorphism related to axial planar schistosity of the early  
8 2435 recumbent folds is of the greenschist facies, reaching amphibolite facies in the south. A  
9 2436 younger folding event produced upright folds trending ENE-WSW, dated at late Visean-early  
10 2437 Westphalian (*c.* 330-315 Ma), except in the west, where thrust sheets were emplaced  
11 2438 westward in the Nappe Zone (NZ; Fig. 8). There, thin-skinned tectonics was active and coeval  
12 2439 with synorogenic sedimentation during the same time interval, although early Variscan  
13 2440 structures are also recognized (Michard et al., 2008).

25 2441 The Western Meseta (WM; Michard et al., 2010a) is divided into a western, almost  
26 2442 undeformed part named the Coastal block, and an eastern part characterized by three principal  
27 2443 Variscan massifs (Central, Rehamna, and Jebilet). This domain is separated from the Eastern  
28 2444 Meseta by the Middle Meseta Fault Zone (MMFZ) and from the Coastal Block by the  
29 2445 Western Meseta Shear Zone (WMSZ). The structural and Raman spectroscopy thermometry  
30 2446 study of Lahfid et al. (2019) suggests that in the easternmost part of Western Meseta, the  
31 2447 latest Devonian to early Visean folding event, reminiscence of the above-described tectonic  
32 2448 evolution in the Eastern Meseta, was preceded by a high-T extensional Late Devonian event.  
33 2449 The late Variscan evolution of the Western Meseta is debated, but NW-verging, late  
34 2450 Carboniferous-Permian folds and thrust faults prevailed (Michard et al., 2010a). Chopin et al.  
35 2451 (2014) proposed that a south- to SSW-verging shortening event occurred in the latest  
36 2452 Carboniferous-earliest Permian, having no genetic connection with extensive Visean basins.  
37 2453 This event is bracketed by Delchini et al. (2018) between 325-310 Ma, while a second  
38 2454 deformation phase producing transpressional westward thrusting took place at 310-280 Ma in  
39 2455 relation with the WMSZ. This scenario is more compatible with the late Carboniferous nappe  
40 2456 tectonics recognized in the northern Anti-Atlas (Cerrina Feroni et al., 2010), as well as with  
41 2457 the Anti-Atlas tectonic evolution (Baïdder et al., 2016). Later, an Early Permian orthogonal  
42 2458 convergence occurred, and a post-tectonic pluton was emplaced at *c.* 275 Ma.

2459 The Coastal Block (CB), which includes the western parts of the Rehamna and Jebilet  
1 2460 massifs as well as parts of the Western High Atlas (Fig. 8), is weakly deformed except close  
2  
3 2461 to the WMSZ, a dextral shear zone where Cambrian to Lower Devonian sediments are  
4  
5 2462 strongly deformed. The Paleozoic overlies a Proterozoic basement including Paleoproterozoic  
6  
7 2463 relicts (El Houicha et al., 2018) but also Cadomian rocks: an orthogneiss has been dated a  
8  
9 2464 600-585 Ma (Baudin et al., 2003). Early-middle Cambrian recorded alkaline to tholeiitic  
10  
11 2465 volcanism as in the Anti-Atlas, and Lower Ordovician pillow lavas cropping out south of the  
12  
13 2466 Rabat-Tiflet Fault Zone were probably generated in an extensional environment (El Hadi et  
14  
15 2467 al., 2014). The Ordovician, coarser grained when compared to more eastern parts of the  
16  
17 2468 Western Meseta, can be correlated with that of the Anti-Atlas. Lower Ordovician red beds are  
18  
19 2469 scarce (Ouanaimi et al., 2016). Locally, a hiatus exists between the late Ordovician and the  
20  
21 2470 Silurian and Devonian formations (Michard et al., 2008, 2010a; Ouanaimi et al., 2016),  
22  
23 2471 whereas glaciogenics are still known laterally. At the WMSZ, Lower to Middle Devonian  
24  
25 2472 sandstones and conglomerates rest unconformably upon Cambrian and Ordovician  
26  
27 2473 formations, suggesting reactivation of pre-Variscan faults (Piqué and Michard, 1989).

28 2474 The Sehoul Block (SB; Fig. 8) is only represented in outcrops to the north but adjacent  
29  
30 2475 to the Rabat-Tiflet Fault Zone (RTFZ). It consists of thrustured Cambro-Ordovician  
31  
32 2476 metasediments which do not differ from other sequences of Morocco (Pérez-Cáceres et al.,  
33  
34 2477 2017), but was thought having been affected by pre-Silurian metamorphism, deformation and  
35  
36 2478 later granite intrusion, in consonance with old available isotopic dating (Piqué, 1989; Michard  
37  
38 2479 et al., 2008). More recent U-Pb dating of the calc-alkaline Rabat granite yielded *c.* 367 Ma  
39  
40 2480 (Tahiri et al., 2010), which together with the fact that the granite intruded previously folded  
41  
42 2481 Cambrian sediments, would imply an orogenic event previous to the early Variscan folding in  
43  
44 2482 the Eastern Meseta. It could be coeval with the early folds in the OMZ of SW Iberia.  
45  
46 2483 According to Ouanaimi et al. (2016), the SB forms probably part of the peri-Gondwanan  
47  
48 2484 realm in the continuation of the OMZ and SPZ of the Iberian Massif, and was displaced to its  
49  
50 2485 present position by the dextral RTFZ (Fig. 8).

51 2486 Thick Upper Devonian-early Carboniferous flysh-type sediments include volcanic  
52  
53 2487 rocks: tholeiitic to alkaline basalts in the Western Meseta and calc-alkaline in the Eastern  
54  
55 2488 Meseta (Kharbouch et al., 1985; Kharbouch, 1994; Simancas et al., 2005; Delchini et al.,  
56  
57 2489 2018). Recently, detrital zircon dating has evidenced a still unrecognized upper Devonian (*c.*  
58  
59 2490 376 Ma) magmatic source for the Upper Devonian turbidites of the Eastern Meseta (Accotto  
60  
61 2491 et al., 2020), which interestingly echoes the zircon record of SW Iberia (Pereira et al., 2017a;

2492 Pérez-Cáceres et al., 2017). Younger Variscan granitoids occur as small plutons sparsely  
1  
2493 distributed in all the Meseta domains, and generally postdate the early Variscan folding phase.  
3  
2494 Ages range 345-320 Ma (Oukemeni et al., 1995; Ajaji et al., 1998; Michard et al., 2008) and  
4  
52495 compositions include calc-alkaline and metaluminous type I granitoids derived from  
6  
72496 previously enriched mantle sources as well as type S with an important anatectic contribution.  
8  
92497 This distribution, together with the Upper Devonian-early Carboniferous bi-modal  
10  
112498 magmatism in the WM, was interpreted in terms of a SE-directed Upper Devonian-  
12  
132499 Carboniferous subduction context by Michard et al. (2008). Small postkinematic plutons  
14  
152500 occur mainly in the Western Meseta, dated at *c.* 305-280 Ma. (Michard et al., 2008).

### 16 172501 18 192502 *6.3. Anti-Atlas*

20  
21  
222503 This domain beyond the South Meseta Front (Fig. 8) is characterized by inliers of  
23  
242504 Precambrian basement, reworked during the Pan-African event, and a rather complete  
252505 preorogenic sequence from the late Neoproterozoic to the early Carboniferous. The  
26  
272506 sedimentary sequence, including late Ediacaran sediments, is 8-9 km thick in the west and 4-5  
28  
292507 km in the east. The Paleozoic was deposited in shallow marine environments, and reflects the  
30  
312508 latest Neoproterozoic-Cambrian-Lower Ordovician rift and post-rift sequence, with no major  
32  
332509 unconformity at the Ediacaran-Cambrian boundary. Carbonate horizons alternating with fine-  
34  
352510 grained detritals characterize the early Cambrian while thick sandstones and fine-grained units  
36  
372511 occur from the middle Cambrian to the Ordovician (Destombes et al., 1985). Rifting is  
382512 indicated by Cambrian basalts of tholeiitic and alkaline composition. The Hirnantian event is  
39  
402513 well represented by glaciogenic deposits, tunnel valleys and glacial pavements up to the High-  
41  
422514 Atlas, indicating that the end Ordovician ice sheet extended repeatedly across the Anti-Atlas  
43  
442515 (Le Heron et al., 2007; Ghienne et al., 2014). The Paleozoic continues dominated by shelfal  
45  
462516 shales with alternating sandstones and carbonates (Lubeseder, 2008), and extensional fault  
472517 activity was recorded in the Upper Devonian (Wendt, 1985; Toto et al., 2008; Frizon de  
48  
492518 Lamotte et al., 2013) leading to a so-called ‘disintegration’ of the Sahara platform. In the  
50  
512519 latest Devonian and during the early Carboniferous, clastic sedimentation renewed, including  
52  
532520 unconformable terrestrial deposits in places. Thick Viséan depocenters developed in the  
54  
552521 eastern Anti-Atlas, associated with synsedimentary extensional faults and flysch-type deposits  
56  
572522 including Ordovician to Tournaisian olistoliths, which are observed up to the adjacent Béchar  
582523 and Ben Zireg area in Algeria (Frizon Lamotte et al., 2013; Benyoucef et al., 2015).  
59  
602524 Sedimentation appears more or less continuous through the Viséan (Alvaro et al., 2014), with



2525 no clear intra-Visean unconformity in stark contrast with the Meseta. The generalization of  
1  
2526 carbonate mud mounds in the upper part of the Visean suggests a progressively decreasing  
3  
2527 tectonic activity and basin infill (Wendt et al., 2001, Alvaro et al., 2014), the youngest folded  
4  
52528 strata being late Visean in age. Unconformable, ‘molassic’, Upper Carboniferous deposits are  
6  
72529 preserved in Algeria (Fabre, 2005) above the folded sequence.

9  
2530 Structurally, the Anti-Atlas is a thick-skinned domain characterized by antiforms  
10  
112531 where the pre-Variscan basement crops out, and synforms occupied by the Paleozoic  
12  
132532 sequence (Burkhard et al., 2006; Baidder et al., 2016). The basement inliers are frequently  
14  
152533 bounded by strike-slip and reverse faults inherited from the early Paleozoic Gondwanan  
16  
172534 paleomargin that were reactivated (inverted) during the Variscan event. The Neoproterozoic  
18  
192535 basement was formed at the margin of the West African Craton (at *c.* 2 Ga), and both were  
20  
212536 affected by the Pan-African orogeny (Ennih and Liégeois, 2001; Hefferan et al., 2014;  
222537 Michard et al., 2017; Soulaïmani et al., 2018; Brahimî et al., 2018; Aït Lahna et al., 2020). In  
23  
242538 the western part, Variscan deformation appears stronger than in the east (Michard et al.,  
25  
262539 2010a). Metamorphism is absent in general but can be of very low-grade in the west, where  
27  
282540 axial planar cleavage developed locally. Fold interference patterns are common, with strikes  
29  
302541 varying around N-S, NE-SW, E-W and NW-SE, which are interpreted as related to the  
31  
322542 attitude of reactivated Panafrican to Cambrian faults (Robert-Charrue et Burkhard, 2008;  
332543 Baidder et al., 2008).

## 34 35 362544 37 382545 **7. Correlation of the Variscan massifs**

39  
40  
412546 Several of the zones described are represented or can be correlated with equivalents in  
42  
432547 the adjacent and even distant massifs, while others are limited to a single massif or their  
44  
452548 correlation is not straightforward. For instance, the Rhenohercynian Zone can be followed  
46  
472549 probably from the eastern Bohemian Massif through the Rhenish Massif and the southern of  
482550 the British Isles until SW Iberia. Conversely, the Cantabrian Zone has no equivalents in other  
49  
502551 massifs, except possibly in the western Pyrenees, and the Allochthon, with its several groups,  
51  
522552 is not represented in Morocco.

53  
542553 Figure 1 depicts the zone correlations in a late Variscan map reconstruction, and  
55  
562554 Figure 9 shows the correlation of zones, groups and units as well as that of early Variscan and  
57  
582555 Variscan orogenic magmatism for the main massifs. Figure 10 shows the timing of events in  
59  
602556 table format detailed by massifs, zones and units, and grouped by significant tectonic,

2557 metamorphic and magmatic events. This figure is intended to offer an outline of the age of  
1 2558 most significant events in the different massifs, with the time intervals corresponding to those  
2 2559 described in the text. It also serves for the purpose of age correlation of events among the  
3 2560 massifs. Note however that differences may be misleading due to scarcity of isotopic dating,  
4 2561 time of dating, methodological approach or difficulty to precisely date high-P events followed  
5 2562 by decompression at high-T.

10  
11 2563 The following sections highlight similarities among stratigraphy, pre-orogenic  
12 2564 magmatism, structural and metamorphic evolution of the massif described, analyzing  
13 2565 separately the groups and units forming the Allochthon from the underlying and surrounding  
14 2566 zones. The correlation of the Variscan orogenic magmatism is sketched in Figure 9 and has  
15 2567 been partly included in the description of the different massifs.

18  
19 2568 The particular similitude between the Iberian and Armorican massifs, explained by  
20 2569 their proximity, together with the fact that they occupy a central position in the Variscan Belt  
21 2570 determines here their use as elements of comparison for the other massifs. In this section, the  
22 2571 correlations are discussed separately for the Autochthon and Allochthon.

### 28 2572 29 2573 *7.1. Correlations in the Autochthon*

#### 30 2574 *7.1.1. Links of Morocco with northern Variscan massifs (AA, EM, WM, CB, SB, CZ, CIZ,* 31 2575 *OVD, OMZ, CAD, NAD)*

32 2576 A link between the Anti-Atlas and the Cantabrian Zone of the Iberian Massif was  
33 2577 suggested by Michard et al. (2010a). It can be established based on their common  
34 2578 interpretation as foreland belts and the general sedimentary and igneous evolution, although a  
35 2579 precise correlation of formations is not feasible. Both areas show a comparable ice-proximal  
36 2580 setting during the end-Ordovician, suggesting they belong to a same area relative to the ice  
37 2581 fronts, yet laterally distant. From a tectonic point of view they differ, being thin-skinned in the  
38 2582 whole CZ vs. thick-skinned in most of the central and eastern Anti-Atlas. May be, the reason  
39 2583 has to do with the existence of better detachment levels in the CZ, although they also  
40 2584 potentially exist in the Anti-Atlas at the Neoproterozoic-Cambrian transition. Other possible  
41 2585 explanations are the absence of faults related to the Cambrian-Ordovician rifting in the CZ,  
42 2586 that such faults were not reactivated due to the relative orientation of the stress field and the  
43 2587 faults, or to the different amount of Variscan shortening, 17-25 % in the western Anti-Atlas

2588 (Michard et al., 2008) and more than 50 % in the CZ (Álvarez-Marrón, 1995; Ayarza et al.,  
1 2589 1998).

3  
4 2590 Concerning the Meseta, Michard et al. (2008) argued against the possibility that it  
5  
6 2591 became separated from Gondwana and disconnected from the Anti-Atlas during the opening  
7  
8 2592 of the Paleotethys, as proposed by Stampfli and Borel (2002). Using stratigraphic, faunal and  
9  
10 2593 paleomagnetic data, they support restricted displacements relative to Africa, at least for the  
11 2594 main part of the Meseta.

12  
13  
14 2595 Based on the assumption that Morocco remained in Gondwana during the Paleozoic,  
15 2596 the similitude of the Carboniferous deposits with those of Iberia and the typology of Variscan  
16  
17 2597 granitoids, Simancas et al. (2009) proposed a continuation of the Iberian Massif by the  
18  
19 2598 Moroccan Meseta. More precisely, they correlate the WM with the CIZ and the EM with the  
20  
21 2599 WALZ and CZ, while the OMZ and SPZ would continue west of the present coast of  
22  
23 2600 Morocco except for the Sehoul block.

24  
25 2601 Michard et al. (2010a) consider zones of the Iberian Massif other than the CZ as  
26  
27 2602 equivalent to those of the Meseta, without proposing a detailed correlation among them  
28  
29 2603 except for the potential equivalence of the SPZ with the WM and CB. This last point is  
30  
31 2604 debatable, as it is based on similarities of the Carboniferous fauna and magmatism, including  
32  
33 2605 associated pyrrhotite-chalcopyrite ores. These can be explained by the important phase of  
34 2606 extension that also affected the SPZ, OMZ and the southern part of the CIZ during the early  
35  
36 2607 Carboniferous. It is possible that Carboniferous sedimentation and magmatism were partly  
37  
38 2608 controlled by subduction related with the closure of the Rheic or Rhenohercynian oceans. In  
39  
40 2609 this scheme, the suture would be submerged, but could occur close to the coast (Michard et  
41  
42 2610 al., 2010a).

43  
44 2611 Franke et al. (2020) proposed a correlation of the Moroccan Meseta and Coastal Block  
45  
46 2612 with the OMZ of SW Iberia, based on the possible continuation of the Badajoz-Cordoba  
47  
48 2613 Shear Zone by a suspect suture hidden under young deposits east of the Meseta.

49  
50 2614 A more reasonable correlation seems the one of Ouanaimi et al. (2016), based on the  
51  
52 2615 Paleozoic sequence and focused on the extent of Lower Ordovician red beds. They proposed a  
53  
54 2616 link of the Moroccan Meseta (EM and WM) with the Iberian CIZ and the Armorican CAD  
55  
56 2617 and NAD, while the WALZ and CZ of Iberia would better correlate with the Anti-Atlas.  
57 2618 Additional clues are provided by the zircon record, with abundant 1 Ga-old detrital zircons in  
58  
59 2619 the Lower-Middle Ordovician clastics of both the Tazekka massif (northern part of the WM-

2620 EM boundary, Fig. 8; Accotto et al., 2019) and coeval strata from the CIZ and the CAD but  
2621 not the NAD (Stephan et al., 2019 and references therein). The correlation between the EM  
2622 and the CIZ is also supported by a structural criterion: the common existence of early  
2623 Variscan folds which in both zones delineate an arc, the EMA and CIA respectively. In fact,  
2624 such an arc may be a key element for understanding the geometry of the Variscan Belt, as  
2625 shown in the essay of retrodeformation tackled in the next section.

2626 On the other hand, the Coastal Block shows links with the Anti-Atlas (Michard et al.,  
2627 2010a), but has also affinities with the OVD in southern Iberia and the NAD in France: i) the  
2628 relatively old (600-580 Ma) Cadomian basement, equivalent to the lower Brioverian,  
2629 cropping out in the three domains; ii) an Ordovician richer in terrigenous facies there than in  
2630 the CIZ, CAD and EM; iii) a zircon record with local sources and a virtual absence of 1 Ga  
2631 zircons, which echoes that of the NAD (Letsch et al., 2018; Dabard et al., 2021); iv) a  
2632 relatively weak Variscan deformation, except in the proximity of shear zones.

2633 The Sehouf Block could represent a fragment of Meguma for Michard et al. (2010a).  
2634 A similar although alternative correlation is supported by the Devonian zircon record from the  
2635 EM (Accotto et al., 2020), which suggest a sourcing from an Avalonian promontory which  
2636 also would explain similar zircon populations at the limit between the SPZ and OMZ in SW  
2637 Iberia (Pereira et al., 2012, 2017a; Pérez-Cáceres et al., 2017) and which might be represented  
2638 by the SB. However, the Cambrian deposits of the SB are similar to those of the Western  
2639 Meseta, suggesting paleogeographic proximity. And the early Variscan event represented by  
2640 the calc-alkaline Rabat granite can be related with the first orogenic event in the OMZ.

2641 Based on Ouanaïmi et al. (2016), and on the arguments given above, a correlation is  
2642 proposed for the Sehouf Block with the OMZ, the Coastal Block with the OVD and NAD, the  
2643 Meseta with the CIZ and the Anti-Atlas with the CZ (Figs.1 and 8).

2644 The possible suture envisaged by Michard et al. (2010a) offshore but close to the coast  
2645 could continue to the south in the northern Mauritanides, where a thrust belt with eastern  
2646 vergence includes basic rocks in eclogite facies dated at  $333 \pm 25$  Ma (Le Goff et al., 2001),  
2647 and in central and southern Mauritanides, marked by oceanic assemblages at the limit  
2648 between internal and external zones (Caby and Kienast, 2009). This may imply pulling apart  
2649 of a peri-Gondwanan terrane, perhaps at the late Neoproterozoic, and closure of the  
2650 intervening ocean during the Carboniferous. That suture would be that of NW Africa with a  
2651 peri-Gondwanan terrane approximately placed where the terrane called Florida-Suwannee

2652 (Dallmeyer, 1989; Matthews et al., 2016) or Carolina (Winchester et al., 2002), pulled apart  
1  
2 2653 from NW Africa during the Jurassic.

3  
4 2654  
5  
6 2655 *7.1.2 Links among Iberian and French autochthons (CZ, CIZ, OVD, OMZ, CAD, NAD, SAD,*  
7  
8 2656 *VM, SWM, MN, Sardinia)*

9  
10 2657 The Variscan zonation of the Iberian Peninsula is not fully represented in France. The  
11  
12 2658 CZ and WALZ do not crop except perhaps in the westernmost Pyrenees (Figs. 1 and 4). The  
13  
14 2659 OMZ and SPZ probably continue under the Meso- and Cenozoic cover of the Paris Basin, but  
15  
16 2660 only the OMZ may crop out north of Brest, in the western edge of the Armorican promontory.  
17  
18 2661 Conversely, the CIZ continues in the Armorican Massif and in the southern part of the Massif  
19  
20 2662 Central, and the NW Iberian Allochthon can be correlated with the same domain in all the  
21  
22 2663 French and related massifs.

23  
24 2664 The upper Brioverian of the CAD and the Schist-Greywacke Complex of the CIZ are  
25  
26 2665 similar. The Black Series of the OMZ, equivalent to the lower Brioverian, does not crop out  
27  
28 2666 in the CIZ, north of the OVD, but pebbles of black quartzite and amphibolite indicate erosion  
29  
30 2667 of the Black Series, which probably underlies the Schist-Greywacke Complex. For the  
31  
32 2668 Ordovician-Devonian sequence, a close correlation can be established between the CAD and  
33  
34 2669 CIZ (Henry et al., 1974; Paris and Robardet, 1977). A distribution of Middle Ordovician  
35  
36 2670 facies and fauna allowed Robardet et al. (1990) to separate 3 subdomains progressively more  
37  
38 2671 distal to the south in the Armorican Massif. A similar zonation exists in the southern part of  
39  
40 2672 the CIZ, where distality increases to the north, so that the subdomains may be correlated  
41  
42 2673 along the Ibero-Armorican Arc.

43 2674 The Paleozoic sequence is so similar in Buçaco (western Portugal) and Crozon  
44  
45 2675 (western Brittany) that both localities were probably very close to each other before the late  
46  
47 2676 Variscan strike-slip tectonics and the opening of the Bay of Biscay (Robardet et al., 1990;  
48  
49 2677 Young, 1990). Moreover, detrital zircon ages in Ordovician strata are similar in the CAD and  
50  
51 2678 CIZ (Dabard et al., 2021). On the other hand, the synorogenic Carboniferous in the CAD is,  
52  
53 2679 as in the CIZ, generally unconformable but often subparallel with the preorogenic sequence,  
54  
55 2680 and synsedimentary tectonism in the CAD may be related with early Carboniferous extension,  
56  
57 2681 as in southern Iberia.

58 2682 The correlation of the NAD with the CIZ is more problematic. The lower Brioverian,  
59  
60 2683 characterized by bedded black cherts, is well represented in the OMZ by the Black Series,

2684 while in the CIZ it does crop out only in the OVD. The southern CIZ, including the OVD, is  
1  
2685 characterized by more terrigenous and proximal Middle Ordovician facies, as the NAD  
3  
4  
2686 (Robardet et al., 1990). So, although a NAD/CIZ correlation can be envisaged, a more precise  
5  
6  
2687 link should be established only with the southern part of the CIZ (Figs. 1 to 5).

7  
8  
2688 There is not a clear equivalent to the OMZ in the Armorican Massif. A possible  
9  
10  
2689 candidate is the eclogite-bearing gneissic unit in the Léon, at the northwestern end of the  
11  
12  
2690 Armorican promontory. Balé and Brun, (1986) interpreted it as derived from the SAD and so,  
13  
14  
2691 representing a detached piece of the Allochthon. But its structural position is the same as that  
15  
16  
2692 of the Central Unit in the OMZ: at the contact with the OVD in Iberia and with the NAD in  
17  
18  
2693 Brittany. Rolet et al. (1986) consider the possibility of underthrusting of the Léon under the  
19  
20  
2694 rest of the CAD at the Upper Devonian. We will assume this idea and also follow Schulz et al.  
21  
22  
2695 (2007) regarding the eclogite-bearing unit in the Léon as a potential link between the OMZ  
23  
24  
2696 and the STZ of the Bohemian Massif (Fig. 1).

25  
26  
2697 The continuation of the OMZ may be found further to the east, in the relatively small  
27  
28  
2698 outcrops of the Vosges and Schwarzwald to the north of the Lalaye-Lubine and Baden-Baden  
29  
30  
2699 shear zones. There, low- to medium grade Cambro-Ordovician to Silurian deposits are  
31  
32  
2700 overlain by marine Middle and Upper Devonian marine facies and early Carboniferous flysch  
33  
34  
2701 ascribed to the STZ of the Bohemian Massif, which is considered equivalent to the OMZ  
35  
36  
2702 (Pereira et al., 2006a; Linnemann et al., 2008).

37  
38  
2703 In the SAD, the Autochthon can be compared with the Paleozoic of the northern part  
39  
40  
2704 of the CIZ by the occurrence of Cambro-Ordovician monotonous schists and porphyroids, the  
41  
42  
2705 possible existence of the Armorican Quartzite, the Middle Ordovician gray slates and the  
43  
44  
2706 Silurian black cherts. The latter, as well as some synorogenic deposits, could form part of the  
45  
46  
2707 Parautochthon, which includes metavolcanic Ordovician porphyroids, as in the Cabo Ortegal  
47  
48  
2708 and the Portuguese complexes.

49  
50  
2709 It is worth noting that while the Autochthon in the SAD correlates with that on the  
51  
52  
2710 northern CIZ east and south of the Iberian Allochthon, the CAD is rather comparable with the  
53  
54  
2711 central part of the CIZ. This correlation, as well as that of some allochthonous units, drove  
55  
56  
2712 Ballèvre et al. (1992) to propose the existence of a suture between the CAD and SAD which  
57  
58  
2713 would continue by NW and central Iberia. But in NW Iberia, the suture represented by the  
59  
60  
2714 Middle Allochthon, is rootless, only preserved in klippen, and does not continue to the SE of  
61  
62  
2715 the CIZ (Fig. 2a). This is one of the problems we try to solve in this contribution.

2716 In the FMC, the Montagne Noire (MN) can be correlated with the Pyrenees and  
1  
2 2717 continue, in the other side of the Bay of Biscay, with the branch of the CIZ limiting to the east  
3  
4 2718 and south the NW Iberian Allochthon (GTMZ) and forming also its relative autochthon. The  
5  
6 2719 Paleozoic sequence in the Pyrenees and MN shows differences with the CIZ and CAD as, for  
7  
8 2720 instance, the lack of the characteristic Armorican Quartzite, and younger or more lasting early  
9  
10 2721 Paleozoic felsic magmatism, which is here reported up to the Upper Ordovician. While the  
11  
12 2722 MN represents the only outcrop of the Autochthon in the FMC, the occurrence of the  
13  
14 2723 Parautochthon in several tectonic windows suggest that the massif is partially or totally  
15  
16 2724 underlain by an autochthonous crust comparable to that of the CIZ (Figs. 4 and 5b, c).

17 2725 In Sardinia, the Autochthon of Iglesias represents a less-deformed domain of the  
18  
19 2726 northern Gondwana foreland. The presence of the Upper Ordovician Sardinic unconformity, as  
20  
21 2727 in the Pyrenees (Casas, 2010) confirms that it forms part of the northern Gondwana  
22  
23 2728 Mediterranean branch. This, as younging of Ordovician magmatism only reflect lateral  
24  
25 2729 changes along the northern Gondwana paleomargin, whose western continuation through the  
26  
27 2730 Pyrenees and the Bay of Biscay reaches the part of the CIZ underthrust beneath the GTMZ.  
28  
29 2731 There are however differences with the Iberian Parautochthon, where no calc-alkaline  
30  
31 2732 Middle-Upper Ordovician arc is clearly represented.

### 32 2733 33 34 2734 *7.1.3. Links among Bohemian and western Variscan autochthons (STZ, OMZ, CIZ, RHZ, SPZ,* 35 36 2735 *MSZ)*

37  
38 2736 Several zones defined in the Bohemian Massif can be continued to the west into the  
39  
40 2737 French and Iberian Massifs. Starting with the STZ, its Autochthon has a similar structural  
41  
42 2738 relationship with its allochthonous complexes as the CIZ in NW Iberia in relation with the  
43  
44 2739 GTMZ Allochthon. This section discusses possible correlations following the order used to  
45  
46 2740 describe the zonation, highlighting similarities and signaling differences.

47  
48 2741 A key correlation can be established between the STZ and OMZ of SW Iberia.  
49  
50 2742 Ediacaran succesions, Cadomian arc magmatism and the transition to Cambro-Ordovician  
51  
52 2743 rift-related magmatism are quite similar on both zones (Pereira et al., 2006a; Linnemann et  
53  
54 2744 al., 2008) and also in the transitional OVD at the southern part of the CIZ (Bandrés et al.,  
55  
56 2745 2004). Moreover, the 565 Ma glaciation identified in the Lausitz Block of the STZ has its  
57  
58 2746 counterpart in the southern part of the CIZ, north of the transitional OVD (Linnemann et al.,  
59  
60 2747 2018). The Paleozoic successions are also comparable between the STZ and OMZ. Cambrian

2748 faunas in eastern Germany compare with those of France, Iberia and Morocco (Elicki, 2007),  
1  
2 2749 with links pointing to the CIZ and the Montagne Noire. Upper Ordovician glacigenics exist in  
3  
4 2750 the STZ and OMZ, as well as in the other autochthonous zones of Iberia (CIZ, WALZ and  
5  
6 2751 CZ) and in the Central and Northern domains of the Armorican Massif.

7  
8 2752 Subsidence patterns calculated for the Barrandian, the STZ and the eastern part of the  
9  
10 2753 CIZ in Iberia are comparable, less regarding the OMZ, but they are especially striking for the  
11  
12 2754 Cambrian, and start to diverge from the Lower Ordovician, when separation of the future  
13  
14 2755 Upper Allochthon took place (von Raumer and Stampfli, 2008). Even if the patterns are  
15  
16 2756 considered similar during the rest of the Paleozoic, this can be attributed to symmetrical  
17  
18 2757 evolutions of the continental margins of Gondwana on one side and the pulled apart terrane  
19  
20 2758 on the other.

21  
22 2759 With these data, a broad link can be established among the Autochthon of Iberia,  
23  
24 2760 France and Bohemia, namely the STZ, the CAD and NAD of western France and the Iberian  
25  
26 2761 OMZ and CIZ. A more accurate correlation can be attempted using detrital zircon age spectra.  
27  
28 2762 Linnemann et al. (2008) have shown that spectra are similar for Ediacaran, early Cambrian  
29  
30 2763 and Lower Ordovician metasediments of the STZ and SW Iberia (OMZ and OVD). The  
31  
32 2764 spectra in the CIZ, WALZ and CZ are also similar except for a significant Mesoproterozoic  
33  
34 2765 population centered at 1000 Ma (Gutiérrez-Alonso et al., 2003; Martínez Catalán et al.,  
35  
36 2766 2004b), which is absent or nearly so in the OMZ, STZ and NAD (Linnemann et al., 2008;  
37  
38 2767 Dabard et al., 2021). The source for this population is the East African-Arabian Zircon  
39  
40 2768 Province (Gómez Barreiro et al., 2007; Bea et al., 2010), fed by the eastern Gondwana super-  
41  
42 2769 fan system (Meinhold et al., 2013; Stephan et al., 2019). The abundance of this population in  
43  
44 2770 the CIZ, CAD, WALZ and CZ is related to the paleoposition of this part of the Iberian Massif  
45  
46 2771 close to present northern Africa, whereas its scarcity or absence indicates a more westward  
47  
48 2772 position of the OMZ and quite probably, of the STZ, both of which facing a more western  
49  
50 2773 segment of Northern Africa in agreement with the faunal record (Gutiérrez-Marco et al.,  
51  
52 2774 2002, 2016). Also it is worth noticing that STZ, NAD and WM share pieces of an Eburnean  
53  
54 2775 (c. 2.05 Ga) basement most likely derived from the West African Craton (Pereira et al.,  
55  
56 2776 2015b). This is in line with a relatively western derivation of the STZ of Bohemia, a character  
57  
58 2777 that might have been acquired since the Cadomian (Pérez-Cáceres et al., 2017), and amplified  
59  
60 2778 during the Variscan orogen.

61  
62 2779 Another affinity between STZ and OMZ is the existence of intrusives related with the  
63  
64 2780 closure of the Rheohercynian Ocean. In the STZ they were emplaced in the MGCH at 360-



2781 325 Ma, while equivalent rocks intruded at 355-335 Ma mostly in the SW of the OMZ and  
2782 eastern SPZ (Figs. 2, 4 and 6). Also supporting the correlation, the eclogites in the Odenwald  
2783 could have their counterpart in those of the Cubito-Moura Unit, in the southern OMZ.  
2784 Eclogite-facies metamorphism is probably older than 363-350 Ma in the Odenwald (Scherer  
2785 et al., 2002) and is dated at 371±17 Ma in the southern OMZ (Moita et al., 2005).

2786 Also, the high-P metamorphism of the Central Unit (377±19 Ma; Abati et al., 2018) is  
2787 probably older than the 360-335 Ma high-P granulites of the Granulitebirge (Franke and  
2788 Stein, 2000), the eclogites of the Erzgebirge (Schmädicke et al., 1995; Rötzler and Plessen,  
2789 2010) and the blueschists of the Krkonoše dome (Žáčková et al., 2010; Konopásek et al.,  
2790 2019). That suggests an early Carboniferous contrasting behavior: in the Bohemian Massif the  
2791 STZ underwent intracontinental subduction in relation to the emplacement of the Allochthon  
2792 and the continuation of convergence during the collisional stage (Závada et al., 2021 and  
2793 references therein). Conversely, in the OMZ an early Carboniferous extensional episode  
2794 produced normal faults and basins where detrital and carbonate rocks were deposited together  
2795 with volcanics. After, late folds developed during the middle-upper Carboniferous, largely  
2796 produced by transpression which was dextral in the STZ (Franke and Żelaźniewicz, 2002) and  
2797 sinistral in the OMZ (Simancas et al., 2001; Díaz Azpiroz and Fernández, 2005), where  
2798 reverse and left-lateral faulting continued until the Stephanian.

2799 While a correlation between the autochthonous STZ and OMZ is well established, an  
2800 equivalent zone is not properly identified in the Armorican Massif, except possibly in the  
2801 Léon region, although it may occur hidden under the cover of the Paris Basin (Fig. 4). For a  
2802 similar reason, and due to its relative position, no equivalent to the STZ occurs in the FMC.  
2803 Closer to the Bohemian Massif, limited outcrops in the northern part of the Vosges and  
2804 Schwarzwald massifs represent small pieces of a wide STZ covered by post-Variscan  
2805 sediments or submerged under the English Channel between the Iberian and Bohemian  
2806 massifs (Figs. 1, 4 and 6).

2807 Concerning the RHZ, it occupies the whole Rhenish Massif and continues to the west  
2808 in the southern part of the British Isles and in the SPZ of SW Iberia (Fig. 1). There, as in the  
2809 Bohemian and Rhenish massifs, the sutures of the Rheic and Rhenohercynian oceans are more  
2810 or less hidden by the complexity of Variscan tectonics. In the NW of the Bohemian Massif  
2811 the RHZ is mostly covered, with its main outcrop occurring at the Harz Mountains (Figs. 1  
2812 and 6). Further to the east, the MGCH and the Northern Phyllite Zone (Fig. 6) were continued

2813 by Franke and Żelaźniewicz (2000, 2002) following the gentle arc delineated by the  
2814 outcropping STZ, but the continuation of the RHZ to the east is uncertain.

2815 It has been proposed that the RHZ surrounds the rest of the Bohemian Massif and  
2816 continues by the MSZ (Kossmat, 1927; Tollmann, 1982), so tracing a tight Bohemian Arc.  
2817 This option was discussed by Franke and Żelaźniewicz (2002), who developed a model of  
2818 interaction of the Variscan Belt with Baltica that first formed the gentle Bohemian Arc,  
2819 opened about 90°, which was followed by a large dextral displacement along the Moldanubian  
2820 Thrust and then by NW-SE faults along the Baltic margin of Laurussia. In their model, the  
2821 Silesia Terrane Assemblage (the basement of the MSZ) was situated to the SE of Baltica and,  
2822 as Avalonia, represents the southern margin of Laurussia. These authors stress the  
2823 stratigraphic similarity and evolution between the RHZ and MSZ during the Devonian and  
2824 Carboniferous and the probable southern continuation of equivalent terranes in the Balkans  
2825 and northern Turkey.

2826 Avalonian affinities of the MSZ basement were described by Mazur et al. (2010), and  
2827 the suture between the Brunovistulian block and the Moldanubian Zone was placed at the  
2828 Upper Devonian by Mazur et al. (2010) and Jastrzębski et al. (2013), and interpreted as that of  
2829 the Rheic Ocean. However, flysch development continued during the Carboniferous, rather  
2830 pointing to the Rhenohercynian Ocean. As for the RHZ and the SPZ, that boundary could  
2831 include both sutures. Southward continuation of the Brunovistulian block terranes of  
2832 Avalonian derivation until the Serbo-Macedonian Massifs in the southern Carpathians and  
2833 Balkans was proposed by Mazur et al. (2010) and Spahić and Gaudenyi (2019).

## 2835 *7.2. Correlations in the Allochthon*

### 2836 *7.2.1. Links among Iberian and French allochthons (GTMZ, CAD, SAD, FMC, VM, SWM, 2837 MTM, Corsica, Sardinia)*

2838 Starting with the CAD, the characteristics described by Lardeux and Cavet (1994) for  
2839 the St. Georges-sur-Loire Unit, as well as those of the southern “blocky” subunit of Cartier  
2840 and Faure (2004) are also typical of the NW Iberian Parautochthon (Ribeiro, 1974; Dias da  
2841 Silva et al. 2014a, b; González Clavijo et al., 2016). So, this unit will be considered as  
2842 Parautochthon, overthrust upon the Autochthon of the rest of the CAD. However, there is  
2843 not a clear relationship between this Parautochthon and the contiguous Allochthon of the

2844 SAD to the south of the Nort-sur-Erdre Fault, as the strike-slip character of the fault may have  
1  
22845 put into contact pieces originally distant.

3  
42846 Slices of a Parautochthon comparable to that of the GTMZ in NW Iberia occur in the  
5  
62847 SAD in Vendée, SE of the Bois-de-Cené and underlying Lower Allochthon units (Figs. 4 and  
7  
82848 5a). It includes Lower Ordovician porphyroids, Silurian ampelites and black cherts, and  
9  
102849 synorogenic deposits. But the most striking similarities of this domain are established for the  
11  
122850 Allochthon. There are not significant differences between the Lower Allochthon in Galicia  
13  
142851 (Malpica-Tui and Órdenes complexes) and that of Champtoceaux and Vendée: same  
15  
162852 lithologies, protolith ages and metamorphic evolution. Only the age of high-P metamorphism  
17  
182853 seems to be younger by 10 Ma in France (360 vs. 370 Ma), but dating of high-P rocks by U-  
19  
202854 Pb methods is always challenging because zircon may grow close to the temperature peak, so  
21  
222855 postdating the pressure peak (Fernández-Suárez et al., 2007; Paquette et al., 2017).

232856 As in NW Iberia, the Middle Allochthon in the SAD is formed by ophiolitic  
24  
252857 complexes or units of oceanic affinity. Cambro-Ordovician ophiolites are represented in the  
26  
272858 Audierne Bay Complex, while the Ile-de-Groix and Bois-de-Cené units can be compared with  
28  
292859 the continental-oceanic transitional, upper crustal units of Malpica-Tui and Órdenes  
30  
312860 complexes. High-P metamorphism is in this case coeval (370-360 Ma). Middle Allochthon  
32  
332861 units of Lower Devonian age have not been dated in the SAD, although the age of two  
34  
352862 possible ophiolitic units is unknown. The ophiolitic unit bounding the Champtoceaux  
36  
372863 Complex is a good candidate to compare with Lower Devonian ophiolites in NW Iberia, but  
38  
392864 its protoliths seem 20 Ma younger (380 vs. 400 Ma). Would that be an indication of the  
40  
412865 lifespan of the Devonian Ocean? It is possible, because its closure has only a minimum age  
42  
432866 limit, given by the high-P metamorphism of the Lower Allochthon and Cambro-Ordovician  
44  
452867 Middle Allochthon, dated around 370 Ma.

46  
472868 Concerning the Upper Allochthon, the Essarts Unit is made of Cambro-Ordovician  
48  
492869 gabbroic and granitic intrusions and nearly contemporaneous high-T metamorphism perhaps  
50  
512870 resulting from magmatic underplating. This is comparable to the intermediate-P Upper  
52  
532871 Allochthon of NW Iberia. However, the eclogitic event suggests correlation with the high-  
54  
552872 P/high-T units. In NW Iberia, no high-P evidences have been found in the intermediate-P  
56  
572873 units, but traces of a Cambro-Ordovician high-T event in the high-P/high-T units are indicated  
58  
592874 by *c.* 500-485 Ma monazites (Fernández-Suárez et al., 2002, 2007). The fact that the Cambro-  
60  
612875 Ordovician and Devonian metamorphic events are so well preserved in the SAD supports the  
62  
632876 contention that intermediate-P/high-T (NW Iberia) or low-P/high-T (Armorican Massif) units

2877 form part of the same coherent terrane with the high-P/high-T units of both massifs, and that  
2878 no suture exists between the two groups.

2879 The Audierne Bay Complex includes a few tectonic slices with eclogites and high-P  
2880 granulites comparable to the high-P/high-T units in NW Iberia, and also an alternation of  
2881 metagreywackes and amphibolites that might present the intermediate-P units of the Upper  
2882 Allochthon. Two other units in the SAD representing the uppermost Allochthon (Mauges and  
2883 Roc-Cervelle) may have their equivalents in NW Iberia, but correlation is hindered because in  
2884 the Upper Allochthon of the GTMZ neither rocks younger than *c.* 510 Ma, nor Cadomian  
2885 basement have been found. Metamorphism does not help, as it is Cadomian in the SAD and  
2886 Cambro-Ordovician in Iberia. However, the intermediate-P event in the latter (495-482 Ma)  
2887 has been dated only in high-T rocks: it cannot be excluded that low-grade Cadomian  
2888 metamorphism affected the metasediments.

2889 For the FMC, the Parautochthon consists of Paleozoic, low-grade metasediments and  
2890 volcanics of northern Gondwana derivation, as in NW Iberia, where it was also locally  
2891 migmatized during late Variscan extension and voluminous granitic plutonism. The Lower  
2892 Gneiss Unit can be compared with the Iberian Lower Allochthon by its lithological  
2893 association, which includes tholeiitic and alkaline rocks revealing Cambro-Ordovician  
2894 extension. Although widely developed Barrovian metamorphism is dated from 360 Ma  
2895 onward, previous high-P metamorphism has been identified, and partial melting dated at 375-  
2896 365 Ma probably reflects exhumation following subduction. This points to a younger age for  
2897 the high-P event in the Lower Gneiss Unit in relation to the subduction-related event in the  
2898 Upper Gneiss Unit.

2899 There is a consensus that the two gneissic units are separated by a suture, which is  
2900 generally interpreted to occur in the Leptyno-Amphibolitic Complex, where the high-P rocks  
2901 abound (Burg and Matte, 1978; Ledru et al., 1989). Vanderhaeghe et al. (2020) individualize  
2902 a Middle Allochthon consisting of micaschists associated with an ophiolitic assemblage  
2903 preserving low-T eclogitic relicts (up to 2.9 GPa, 660 °C). But it seems included in the  
2904 Leptyno-Amphibolitic Complex or at least, the separation from it is unclear. The lithological  
2905 association and metamorphic conditions of their Middle Allochthon remind those of the  
2906 Cambro-Ordovician oceanic supracrustals in NW Iberia and the Armorican Massif (Ballèvre  
2907 et al., 2014). The Lower Devonian ophiolites of the GTMZ Middle Allochthon are also not or  
2908 poorly represented in the FMC, where an equivalent unit may exist in the Limousin above the  
2909 Lower Gneiss Unit (Girardeau et al., 1986, 1994; Berger et al., 2005).

2910 The best correlation can be established between the Upper Gneiss Unit and the Upper  
1  
2 2911 Allochthon: same lithologies, igneous protolith ages (Cambro-Ordovician) and metamorphic  
3  
4 2912 evolution. Parts of the Leptyno-Amphibolitic Complex share with the catazonal Iberian Upper  
5  
6 2913 Allochthon the Lower Devonian age of high-P metamorphism. No ultrahigh-P metamorphism  
7  
8 2914 has been described in NW Iberia, but at least 1.9-2.0 GPa were calculated for eclogites and  
9  
10 2915 ultramafics of the Cabo Ortegal Complex (Mendia, 2000; Mendia and Gil Ibarra, 2005).

11  
12 2916 Above the Leptyno-Amphibolitic Complex, but still in the Upper Gneiss Unit,  
13  
14 2917 migmatitic paragneisses and orthogneisses devoid of high-P relics may represent the high-  
15  
16 2918 grade upper units of the Upper Allochthon. The uppermost part of the nappe pile in the FMC,  
17  
18 2919 consisting of low- to medium grade Cambrian greywackes, quartzites and rhyolites, have also  
19  
20 2920 an equivalent in the Upper Allochthon of the Órdenes and Morais complexes.

21  
22 2921 The units of the Central Vosges and the Schwarzwald gneiss complexes have been  
23  
24 2922 compared with the Leptyno-Amphibolitic Complex of the FMC, particularly the part between  
25  
26 2923 the Varied and Granulite units (Pin and Vielzeuf, 1988; Fabriès and Latouche, 1988;  
27  
28 2924 Lardeaux et al., 2014). So, these units might be considered part of an Upper Allochthon  
29  
30 2925 similar to that of NW Iberia and to the Teplá-Barrandian Zone of the Bohemian Massif.  
31  
32 2926 However, the young age of high-P metamorphism in the Schwarzwald (*c.* 340 Ma; Kalt et al.,  
33  
34 2927 1994; Marschall et al., 2003), the fact that granulites possibly represent vertical extrusions at  
35  
36 2928 mid-crustal levels, and the ultra-potassic magmatism dated at 345-335 Ma rather suggest  
37  
38 2929 correlation with the Moldanubian Zone of the Bohemian Massif (Schulmann et al., 2002;  
39  
40 2930 Skrzypek et al., 2014).

41  
42 2931 Nevertheless, the Variscan evolution can still be correlated with that of the FMC  
43  
44 2932 because: i) the ophiolites of the Ligne des Klippes in the VM are equivalent to the Brévenne  
45  
46 2933 Unit, a back-arc related with the subduction of the Saxothuringian Ocean (Faure et al., 1997;  
47  
48 2934 Schulmann and Gayer, 2000; Lardeaux et al., 2014); ii) the overlying Visean flysch and the  
49  
50 2935 Devonian-Carboniferous sediments and volcanics of the metasedimentary belt separating the  
51  
52 2936 two gneiss complexes in the SWM can be equivalent to the Tuffs Anthracifères, related to the  
53  
54 2937 subduction of the Rhehercynian Ocean, whose influence was probably responsible for the  
55  
56 2938 subsequent voluminous granitic plutonism. Affinities of the VM and SWM with both the  
57  
58 2939 FMC and the Bohemian Massif are not surprising given their position. The differences and  
59  
60 2940 the possible causes have been discussed by Lardeaux et al. (2014), and will be dealt with  
61  
62 2941 below in the correlation with the Bohemian Massif.

2942 The massifs of the southern Variscan Belt occur in continuation of, and their units can  
1  
2 2943 be correlated with the southern FMC. The internal zones are represented in the MTM by the  
3  
4 2944 Central and Eastern domains which together seem to represent the Upper Allochthon,  
5  
6 2945 although they might also include a dismembered suture according to Schneider et al. (2014).  
7  
8 2946 In the Western Domain, one of the thrust sheets bears a rift-related succession with alkaline  
9  
10 2947 rocks possibly representing the Lower Allochthon, although no high-P has been described. In  
11  
12 2948 any case, the Middle Allochthon is missing or hidden in the Leptyno-Amphibolitic Complex,  
13  
14 2949 as in the FMC. The Central Domain presently underlies an inverted early Carboniferous  
15  
16 2950 synorogenic flysch which is in turn overlain by a Paleozoic sequence including Silurian black  
17  
18 2951 shales (Bronner and Bellot, 2000). The original stacking order was the opposite, with the  
19  
20 2952 Eastern Domain above and the Western Domain below. So, the Western Domain may  
21  
22 2953 represent the Parautochthon and/or the Autochthon.

23  
24 2954 In Corsica, most metamorphic outcrops represent a Leptyno-Amphibolitic Complex  
25  
26 2955 similar to that of the FMC, with eclogites and high-P/high-T granulites, which can be  
27  
28 2956 assimilated to the Upper Allochthon. The uppermost Allochthon crops out in northern Corsica  
29  
30 2957 as a low-grade Neoproterozoic and Paleozoic sequence that Rossi et al. (2009) interpreted as  
31  
32 2958 different from that of the Autochthon in SW Sardinia and the Montagne Noire, and deposited  
33  
34 2959 in a peri-Gondwanan microcontinent. It may find its equivalents in the uppermost Allochthon  
35  
36 2960 of NE Iberia (Órdenes and Morais complexes), the SAD (Mauges and Roc-Cervelle units) and  
37  
38 2961 the FMC (Thiviers-Payzac Unit).

39  
40 2962 In Sardinia, the Internal Zone represents the high-P/high-T part of the Upper  
41  
42 2963 Allochthon, whereas the Internal Nappes of the Nappe Zone may correlate with the Lower  
43  
44 2964 Allochthon on the basis of its eclogite-facies event in absence of high-P granulites. From a  
45  
46 2965 structural point of view, the External Nappes constitute a Parautochthon, which is coherent  
47  
48 2966 with their metamorphic Paleozoic sequence representing in this case only the preorogenic part  
49  
50 2967 of the succession.

51  
52 2968 In the External Massifs of the Alps, the metamorphic evolution of the third domain  
53  
54 2969 described by Ballèvre et al. (2018), characterized by the high-P eclogitic/granulitic event, may  
55  
56 2970 be compared to that of the FMC, VM and SWM (von Raumer and Neubauer, 1993).  
57  
58 2971 Consequently, it is correlated with the Upper Allochthon even if not all available ages of the  
59  
60 2972 high-P event yield the Lower Devonian age obtained in these and other Variscan massifs. The  
61  
62 2973 Chamrousse Ophiolite may represent the same ocean whose relicts have been preserved in the  
63  
64 2974 Middle Allochthon of NW Iberia and in the Audierne Bay Complex of the Armorican Massif.

2975 The ascription of the remaining domains is more problematic. The association of a Devono-  
1  
2 2976 Carboniferous bimodal suite with conglomerates underlying the ophiolite (second domain),  
3  
4 2977 suggest a correlation with the Morvan Arc of the FMC. Perhaps also with the migmatitic  
5  
6 2978 gneisses, early Carboniferous amphibolite and gabbro boudins in the southern SWM and/or  
7  
8 2979 with the Devono-Carboniferous sediments and volcanics of the metasedimentary belt  
9  
10 2980 separating the two gneiss complexes in the SWM. Finally, the undated low- to medium-grade  
11  
12 2981 schists of the first domain could represent the upper units of the Upper Allochthon (the option  
13  
14 2982 adopted in Fig. 4) because they are considered part of the polymetamorphic group by von  
15  
16 2983 Raumer et al. (1993), but might also represent the Parautochthon or even the Autochthon.

#### 17 2984 18 19 2985 *7.2.2. Links among Bohemian and western Variscan allochthons (STZ, TBZ, MZ, VM, SWM,* 20 21 2986 *FMC, SAD, GTMZ)*

22  
23 2987 The correlation described among the three groups of allochthonous units of the GTMZ  
24  
25 2988 and the SAD (Ballèvre et al., 2014) can be extended to the STZ allochthons based on the  
26  
27 2989 lithological association, structural sequence and ages. All the Iberian and Armorican groups  
28  
29 2990 are well represented in the STZ, although not always the three allochthons occur in one single  
30  
31 2991 massif.

32  
33 2992 In the western branch of the STZ, the Münchberg massif exhibits the most complete  
34  
35 2993 succession. Its nappe stack recalls that of Cabo Ortegal and Bragança complexes. There, as in  
36  
37 2994 Münchberg, the Parautochthon consists of a synorogenic flysch with an early Carboniferous  
38  
39 2995 maximum depositional age, overlain by a relatively distal preorogenic Paleozoic sequence  
40  
41 2996 (Dias da Silva et al. 2014a; Martínez Catalán et al., 2008, 2016). In Münchberg, the Lower  
42  
43 2997 Allochthon is not present while in Cabo Ortegal it is only represented by a small unit. The  
44  
45 2998 only identified oceanic units witnessing the Middle Allochthon are Devonian phyllites,  
46  
47 2999 prasinites and amphibolites equivalent to the Lower Devonian ophiolites of NW Iberia.  
48  
49 3000 Finally, the Upper Allochthon is represented mainly by the high-P/high-T units, with only a  
50  
51 3001 small unit of the intermediate-P group in Cabo Ortegal, and no equivalent in the western STZ.

52 3002 The three allochthons are also well represented along the eastern branch of the STZ,  
53  
54 3003 from the lower part of the nappe pile south of the Krkonoše Massif to the upper part in the  
55  
56 3004 Góry Sowie Massif. A small low-grade unit partially synorogenic represents the  
57  
58 3005 Parautochthon, while the South Krkonoše Unit depicts the lithological association and Late  
59  
60 3006 Devonian high-P and relatively low-T metamorphism of the Lower Allochthon in Iberia and

3007 the Armorican Massif. To the east, the Kaczawa Complex represents the Middle Allochthon,  
1  
2 3008 with the rocks of oceanic affinity being of Cambro-Ordovician, Silurian and Devonian age, of  
3  
4 3009 which, the first and the later are also identified in NW Iberia (Martínez Catalán et al., 2020).  
5  
6 3010 Upper Devonian-early Carboniferous flysch with chaotic assemblages and tectonic mélanges  
7  
8 3011 in the Kaczawa Complex may have an equivalent in the Cabo Ortegal mélange, formed in an  
9  
10 3012 Upper Devonian subduction zone (Martínez et al., 2012; Arenas and Sánchez Martínez,  
11  
12 3013 2015). A basaltic unit of probable Late Devonian age (Seston et al., 2000), may represent a  
13  
14 3014 series of young ophiolites existing in the French Massif Central (Brévenne; Génis; Pin and  
15  
16 3015 Paquette, 2002; Faure et al., 2009) and the Vosges (Ligne des Klippes; Skrzypek et al., 2012;  
17  
18 3016 Lardeaux et al., 2014), but not identified in NW Iberia. Further east, the Góry Sowie Massif  
19  
20 3017 represents the high-P/high-T part of the Upper Allochthon, with identical protolith ages,  
21  
22 3018 metamorphic evolution and structural position as the high-P/high-T units of the GTMZ in NW  
23  
24 3019 Iberia and the Münchberg Massif in Germany (Martínez Catalán et al., 2020; Tabaud et al.,  
25  
26 3020 2020).

27  
28 3021 In the STZ allochthons of Münchberg, Wildenfels, Frankenberg, Krkonoše and Góry  
29  
30 3022 Sowie massifs, Upper Allochthon units showing an intermediate-P Cambro-Ordovician event  
31  
32 3023 are absent. In NW Iberia, the Armorican Massif and French Massif Central, these units  
33  
34 3024 occupy the uppermost position of the nappe pile, so that their absence here can be explained  
35  
36 3025 by erosion. Moreover, this absence is compensated by the dominant occurrence of low-P  
37  
38 3026 Cambro-Ordovician metamorphism in the TBZ and MZ, which together represent the Upper  
39  
40 3027 Allochthon in the Bohemian Massif. Only in the Orlica-Šniežnik Dome the STZ autochthon is  
41  
42 3028 surrounded by rocks of the MZ which in the eastern part bear the imprint of Cambro-  
43  
44 3029 Ordovician medium-P/high-T metamorphism (Staré Město Unit; Štípská et al., 2001).

45  
46 3030 In the west of the TBZ, the basal association of low-grade metasediments, basic rocks,  
47  
48 3031 acid tuffs and serpentinites under the Mariánské Lázně and Erbendorf-Vohenstrauß units can  
49  
50 3032 be correlated with the phyllites and prasinities of Münchberg, and represent the Middle  
51  
52 3033 Allochthon. For the rest of the TBZ, a correlation may be established with the Upper  
53  
54 3034 Allochthon of the GTMZ (NW Iberia), SAD and FMC.

55  
56 3035 The Mariánské Lázně, Erbendorf-Vohenstrauß units and the Góry Sowie Massif  
57  
58 3036 underwent a high-P/high-T metamorphic event during the Lower Devonian, followed by  
59  
60 3037 Middle Devonian exhumation in amphibolite facies. The same happened in the lower units of  
61  
62 3038 the Upper Allochthon in the GTMA (Cabo Ortegal, Órdenes and Bragança complexes), SAD  
63  
64 3039 (Essarts and Audierne Bay units) and the FMC (Leptyno-Amphibolitic Complex of the Upper  
65



3040 Gneiss Unit). Above, the Teplá Crystalline Complex recorded a history similar to that of the  
1  
2 3041 upper group of the Upper Allochthon in the Órdenes and Morais complexes, with the  
3  
4 3042 difference that the Cambro-Ordovician metamorphic event (495-485 Ma) is of low-P in Teplá  
5  
6 3043 and of intermediate-P in NW Iberia. The Essarts Unit in the SAD did also record an  
7  
8 3044 Ordovician high-T event before Devonian eclogitization. In NW Iberia and the TBZ,  
9  
10 3045 Devonian shortening under Barrovian P/T conditions was followed by a low-P event  
11  
12 3046 connected with extension (Gómez Barreiro et al., 2006; Peřestý et al., 2017). The  
13  
14 3047 metamorphic contrast between the structurally upper and lower groups of the Upper  
15  
16 3048 Allochthon (Cambro-Ordovician low or intermediate-P above, Lower Devonian high-P/high-  
17  
18 3049 T below) is quite strong in all cases, accentuated by extensional shear zones and faults.

19 3050 A thick Neoproterozoic succession with Cadomian arc-related and Cambro-  
20  
21 3051 Ordovician rift-related magmatism characterizes the lower part of the TBZ (Dörr et al. 2002;  
22  
23 3052 Drost et al. 2004) whose uppermost unit is a rather complete and weakly metamorphosed  
24  
25 3053 Paleozoic succession preserved at the core of the Praha or Barrandian Syncline. The  
26  
27 3054 metamorphic grade decreases upward from the basal Mariánské Lázně and Erben-  
28  
29 3055 Vohenstrauß units through the Teplá Crystalline Complex (Peřestý et al., 2017) and a thick  
30  
31 3056 Neoproterozoic succession, until the core of the Praha Syncline.

32 3057 The Neoproterozoic sequence of the TBZ is compared with that of the Mauges Unit in  
33  
34 3058 the SAD, while in the GTMZ, the age of the high-grade metasediments is unconstrained. For  
35  
36 3059 the Paleozoic succession, several species of Middle Ordovician trilobites of the uppermost  
37  
38 3060 Allochthon in the SAD are also found in the TBZ, while only one is found in the Iberian  
39  
40 3061 Autochthon (Ballèvre, 2016), thus supporting separation from mainland Gondwana at  
41  
42 3062 Cambro-Ordovician times. In the FMC, the Paleozoic is represented by the Cambrian  
43  
44 3063 Thiviers-Payzac Unit. In the GTMZ, the Paleozoic succession is terrigenous and monotonous  
45  
46 3064 in the uppermost units of the Órdenes and Morais complexes, and its age is constrained to the  
47  
48 3065 middle-upper Cambrian by detrital zircons and intrusive magmatism (Fernández-Suárez et al.,  
49  
50 3066 2003; Fuenlabrada et al., 2010; Arenas et al., 2016). The latter, dated at 510-490 Ma, is  
51  
52 3067 bimodal, with arc affinities in the upper units (Andonaegui et al., 2002, 2012) and extension-  
53  
54 3068 related in the lower units of the Upper Allochthon (Galán and Marcos, 1997).

55 3069 A link of the TBZ with the Upper Allochthon of the northern small Variscan massifs  
56  
57 3070 has been proposed for the Central Vosges and Schwarzwald gneiss complexes (Pin and  
58  
59 3071 Vielzeuf, 1988; Fabriès and Latouche, 1988; Lardeaux et al., 2014), but also discussed, due  
60  
61 3072 in part to the younger ages of high-P metamorphism there (Schulmann et al., 2002; Skrzypek

3073 et al., 2014). However, correlation is straightforward with the southern small massifs: the  
1  
2 3074 Leptyno-Amphibolitic Complex is recognized in the Central and Eastern domains of the  
3  
4 3075 Maures, Corsica and the Internal Zone of Sardinia. That correlation can be extended at least to  
5  
6 3076 the third domain described in the External Massifs of the Alps by Ballèvre et al. (2018),  
7  
8 3077 characterized by a polymetamorphic evolution including eclogites or high-P granulites. Very  
9  
10 3078 interesting is the uppermost allochthonous unit of northern Corsica, with Neoproterozoic  
11  
12 3079 terrigenous sediments, interbedded metabasalts and a rather complete Paleozoic sequence,  
13  
14 3080 with a possible equivalent in the Mauges Unit of the SAD and perhaps also in the upper parts  
15  
16 3081 of the TBZ.

17 3082           Concerning the MZ, we consider it as a distinct element but still forming part of the  
18  
19 3083 Upper Allochthon. A back-arc setting has been proposed to explain its Silurian and Devonian  
20  
21 3084 volcano-sedimentary sequences, while the fore-arc could be represented by the TBZ and by  
22  
23 3085 the tectonic assemblage resulting from subduction of the Saxothuringian Ocean (Schulmann  
24  
25 3086 et al., 2009).

26 3087           Due to differences in the evolution between the Massif Central and Bohemian massifs,  
27  
28 3088 Lardeaux et al. (2014) proposed a division of the Moldanubian Zone between western and  
29  
30 3089 eastern parts, establishing as a possible limit the Bray Fault. That leaves the VM and SWM in  
31  
32 3090 the eastern Moldanubian, even when the authors interpret the northernmost FMC and the  
33  
34 3091 Southern Vosges as part of the same unit, as suggested by Jung and Roques (1952). However,  
35  
36 3092 similarities of the Central Vosges and the Schwarzwald gneiss complexes with the  
37  
38 3093 Moldanubian exist, namely the relatively young age of high-P metamorphism, the possible  
39  
40 3094 vertical extrusions of granulites to mid-crustal levels and the early-middle Carboniferous  
41  
42 3095 ultra-potassic magmatism (Kalt et al., 1994; Schulmann et al., 2002; Marschall et al., 2003;  
43  
44 3096 Skrzypek et al., 2014).

45 3097           It seems that the VM and SWM share characteristics and events with both the  
46  
47 3098 Bohemian and French Central massifs, in agreement with their relative geographic positions.  
48  
49 3099 Taken together, their tectonic, metamorphic and magmatic evolution seems to change  
50  
51 3100 gradually from east to west. For the Variscan magmatism, the change is abrupt between the  
52  
53 3101 eastern and western parts of the FMC, an additional argument against the role of the Bray  
54  
55 3102 Fault. These changes are related with the subduction of the Saxothuringian and  
56  
57 3103 Rhenohercynian zones under the Allochthon which to the west (SAD and GTMZ) apparently  
58  
59 3104 did not occur.

3105

1  
23106 7. 3. *Mid-Variscan suture and Mid-Variscan Ocean*

3  
43107 The Upper Allochthon was a peri-Gondwanan terrane and part of it was a Cambro-  
5  
63108 Ordovician magmatic arc. The possibility that it was formed by more than one terrane cannot  
7  
83109 be excluded. However, the ocean separating the Upper Allochthon from the Gondwanan  
9  
103110 Autochthon seems unique, as it exhibits a similar history in the Middle Allochthon of the  
11  
123111 whole Variscan Belt. This favors that the overlying Upper Allochthon was also a single  
13  
143112 terrane, even if it consisted of different paleogeographic environments, including fore arc,  
15  
163113 back-arc, thinned continental crust, shallow continental platform and emerged land.

17  
183114 The intervening ocean formed part of the Rheic realm, but was not the Rheic in a strict  
19  
203115 sense because the latter was defined as the ocean separating Laurussia and Gondwana, and  
21  
223116 Laurussia includes three continental masses of which Avalonia is the one in contact with the  
23  
243117 Variscan Belt to the south of the Midlands and Brabant massifs (Nance and Linnemann,  
25  
263118 2008). So, the Rheic suture is that of (or hidden by) the Rhenohercynian Zone and extends  
27  
283119 westward to the South Portuguese Zone. It has also been claimed as the suture between the  
29  
303120 Moldanubian and Moravo-Silesian zones (Mazur et al., 2010; Jastrzębski et al., 2013). The  
31  
323121 ocean represented by the Middle Allochthon can be called using the names of the massifs  
33  
343122 where it is identified, as for instance, the Galicia-Brittany-Massif Central Ocean of Matte  
35  
363123 (2001, 2007). But if the same suture continues up to the Bohemian Massif, Saxothuringian  
37  
383124 and Sudetian should be added. The resulting name would be exceedingly long.

393125 A short name would be more suitable. But for instance, Saxothuringian Ocean is of  
40  
413126 doubtful validity for the whole belt as the STZ was strictly defined in the Bohemian Massif  
42  
433127 and northernmost Schwarzwald and Vosges (Kossmat, 1927). Similarly, South Armorican  
44  
453128 Ocean (Paris and Robardet, 1994) refers only to one of the large Variscan massifs. A better  
46  
473129 name for the ocean represented by the Middle Allochthon was Medio-European (Ledru et al.,  
48  
493130 1989; Cartier and Faure, 2004; Faure et al., 2009; Lardeaux et al., 2014), used in contributions  
50  
513131 where the authors consider only one ocean in addition to the Rheic/Rhenohercynian.

523132 The common feature of the suture represented by the Middle Allochthon is that it  
53  
543133 exists in all the large massifs strictly representing the Variscan Belt, *i.e.* the large central and  
55  
563134 western European massifs. And the suture occurs roughly in the middle of the belt. Mid-  
57  
583135 Variscan suture would then be a better term, the disappeared sea could be referred to as the

3136 Mid-Variscan Ocean, and the whole ensemble of terranes forming the allochthonous  
1  
2 3137 accretionary prism may be called the Mid-Variscan Allochthon.

## 3138 5 6 3139 **8. Restoring late Variscan deformation**

### 8 3140 *8.1. Scope and revision of age data*

10  
11 3141 Crustal/lithospheric thickening characterizes the early Variscan (Devonian) and first  
12  
13 3142 stages of Variscan deformation (early Carboniferous) in Europe and Morocco. It is associated  
14  
15 3143 with convergence: early Variscan high-P metamorphism related with subduction and  
16  
17 3144 Barrovian metamorphism associated with collision. The late Variscan stages (late  
18  
19 3145 Carboniferous) recorded the extensional collapse of the orogen, as well as important wrench  
20  
21 3146 movements and orocline development. Extension is characterized by crustal thinning and low-  
22  
23 3147 P/high-T metamorphism, while wrenching did not cause significant changes in crustal  
24  
25 3148 thickness, neither a characteristic metamorphic imprint except retrogradation recorded locally.  
26  
27 3149 Nevertheless, transcurrence affected the orogenic crust by dislocations that hinder the original  
28  
29 3150 correlation among units and terranes, and also obscure the links between local and global  
30  
31 3151 processes.

32  
33 3152 A way to cope with the effects of transcurrence is carrying out a retrodeformation of  
34  
35 3153 wrench displacements and arcs. Ideally, it would show the position of the different massifs  
36  
37 3154 and zones before late Variscan movements, and inverting their sequence, the successive steps  
38  
39 3155 would show a part of the temporal evolution of the belt. However, going back by steps that  
40  
41 3156 represent real time snapshots would require more precise geochronology than available at  
42  
43 3157 time. As well, the amount of displacement or strain should be known for strike-slip faults and  
44  
45 3158 shear zones, and for the domains among them, and this is not the case for most of them.

46  
47 3159 Also important are the problems of partition of deformation to the scale of the belt,  
48  
49 3160 with more than one component involved. It is known that extension in the internal zones was  
50  
51 3161 contemporaneous with contraction in the more external ones (Faure et al.; 2009; Martínez  
52  
53 3162 Catalán et al., 2009), and that strike-slip shear zones were coeval with extensional and/or  
54  
55 3163 compressional structures (Martínez Catalán et al., 2014; Edel et al., 2018). Moreover, each  
56  
57 3164 particular shear zone may include different amounts of transpression, and may rotate during  
58  
59 3165 its activity in relation with oroclines or within wider shear zones whose limits may be  
60  
61 3166 imprecise.

3167 For these reasons, restoring wrenching deformation to the scale of the belt will be  
1  
2 3168 necessarily approximate, retrodeformation can only be partial and the successive steps might  
3  
4 3169 not represent the situation at a given time interval. The approach followed is to restore the  
5  
6 3170 main strike-slip shear zones and faults in steps marked by cross-cutting relationships to the  
7  
8 3171 map scale. The younger structures are restored first, and lately, the late Variscan internal  
9  
10 3172 deformation of a large part of the Variscan Belt is restored considering it as a broad dextral  
11  
12 3173 ductile shear zone based on the relationship of ductile shear zones with late folds (Iglesias  
13  
14 3174 Ponce de León and Choukroune, 1980; Gumiaux, 2003; Gumiaux et al., 2004) and the fact  
15  
16 3175 that they are always present in the Allochthon and the surrounding Autochthon. The  
17  
18 3176 restoration of arcuate geometries (oroclines) is very imprecise, but it is one of the goals of this  
19  
20 3177 contribution, and also one that yields the more interesting results.

21  
22 3178 Age data, although not always precise, provide a time frame to constrain Variscan  
23  
24 3179 wrench-type deformation. In the Massif Central, Armorican and Maures-Tanneron Massifs,  
25  
26 3180 plutonism related with Variscan convergence and collision started at the Middle-Upper  
27  
28 3181 Devonian and extended until the early Permian. Much of that magmatism was synkinematic  
29  
30 3182 with the activity of transcurrent shear zones, the oldest of which are dated at c. 370 Ma in the  
31  
32 3183 South Armorican Domain and the Massif Central (Rolin et al., 2009). These authors link the  
33  
34 3184 370-315 Ma wrenching activity with indentation of continental microplates during Variscan  
35  
36 3185 collisional tectonics. Shear zones coeval with the emplacement of old plutons were sealed by  
37  
38 3186 younger ones, and were frequently reactivated later. Rolin et al. (2009) distinguished two  
39  
40 3187 families, the older of which is mostly dextral, striking N100°-130° E, and formed during the  
41  
42 3188 Famennian-early Viséan (370-340 Ma). The younger is middle Viséan-Namurian in age (340-  
43  
44 3189 315 Ma) and includes dextral shear zones striking N150°-160° E and N130° E, and conjugate  
45  
46 3190 sinistral shear zones striking N0°-90° E.

47  
48 3191 The older family of Rolin et al. (2009) affects the allochthonous units and locally its  
49  
50 3192 relative autochthon, and can be related to the emplacement of the Mid-Variscan Allochthon,  
51  
52 3193 which in NW Iberia ended at 345-340 Ma (Dallmeyer et al., 1997). The younger family is  
53  
54 3194 represented in the other the Variscan massifs, but mostly clustering at the end of the middle  
55  
56 3195 Viséan-Namurian time interval or even later. Ductile deformation in the Elbe Shear Zone was  
57  
58 3196 dated by Hofmann et al. (2009) at 337-323 Ma (considering the maximum time span allowed  
59  
60 3197 by the error bars). The old age is based on the sigmoidal shape of a deformed granitic pluton,  
61  
62 3198 while the young age corresponds to an undeformed granite close to the EFZ and cross-cutting  
63  
64 3199 previous faults and cleavage. A wider time interval of 350-315 Ma is provided by Žák et al.  
65

3200 (2014) also based on relations with granitoids. In the Armorican Massif, granitoids  
1 3201 synkinematic with dextral shearing may span a 330-300 Ma interval in the northern part of the  
2 3202 SAD (Bernard-Griffiths et al., 1985b; Gumiaux et al., 2004), and are somewhat younger in  
3 3203 the south (310-290 Ma; Carron et al., 1994). The Bray Fault is dated around 320 Ma, but the  
4 3204 evidences are imprecise, based on Ar-Ar dating of biotite in a drilled mylonitic orthogneiss  
5 3205 (Matte et al., 1986), and on inversion of normal faults in the Culm Basin, not directly on the  
6 3206 Bray Fault itself (Leveridge and Hartley, 2006).

13 3207 The dextral PTSZ of western Iberia, which for half of its length limits the GTMZ  
14 3208 Allochthon, continues by the ductile dextral NEF and SASZ-N of the Armorican Massif, also  
15 3209 limiting the Mid-Variscan Allochthon there (Figs. 1, 2 and 4). In Iberia, ages of  
16 3210 metamorphism and synkinematic granites indicate that late folding related with dextral  
17 3211 transcurrence occurred at 315-305 Ma (Dallmeyer et al., 1997; Rubio Pascual et al., 2013a;  
18 3212 Martínez Catalán et al., 2014), while late dextral shear zones are dated at 310-305 Ma  
19 3213 (Gutiérrez-Alonso et al., 2015) and even continued until 290 Ma in the Pyrenees (Cochelin et  
20 3214 al., 2017). The PTSZ, NEF and SASZ-N were displaced during dextral transpression occurred  
21 3215 in the Pyrenees at 310-290 Ma, coeval with lateral flow, dome emplacement and upper crust  
22 3216 thickening (Cochelin et al., 2017).

31 3217 May be that the Ar-Ar dating in the CIZ reflects cooling ages a few million years  
32 3218 younger than shear zone motion. Also, isotopic dating of undeformed granitoids does not  
33 3219 necessarily yield a minimum age of fault activity, as later deformation can be concentrated  
34 3220 outside the igneous massifs. But still, significant deformation in the Elbe Shear Zone is older  
35 3221 than the mentioned Iberian equivalents. Perhaps, the Elbe zone was deformed by SW-NE  
36 3222 dextral shearing older than 310 Ma, which also affected NW Iberia and the Armorican Massif,  
37 3223 and was later reoriented to NW-SE during a younger shearing event as the one dated at *c.*  
38 3224 310-290 Ma in Iberia and France.

46 3225 Transpression in the Pyrenees was probably associated to the NPF, one of a group of  
47 3226 large NW-SE dextral faults and associated shear zones which also includes the SMF, SIF, BrF  
48 3227 and EFZ (Fig. 1). They are oblique to the general SW-NE trend of the belt and overprint all  
49 3228 previous structures. Consequently, they are thought to represent the latest significant  
50 3229 movements and must be restored before the folds and shear zones they cut across. Some of  
51 3230 these faults cannot be studied, because they are hidden or were reactivated as plate boundaries  
52 3231 later, as the SIF between Iberia and Africa, or the NPF. Others, like the Elbe Fault Zone and  
53 3232  
54 3233  
55 3234  
56 3235

3232 Bray Fault have been dated, but their age contradicts the structural evidence of being the  
1  
2 3233 latest significant Variscan structures.

3  
4 3234 Sinistral motion is of relatively minor importance in the Variscan Belt, except in  
5  
6 3235 southern Iberia. There, it is post Upper Namurian (Bashkirian), according to relationship with  
7  
8 3236 Carboniferous sedimentation (Simancas et al., 2001; Expósito et al., 2002; Martínez Poyatos,  
9  
10 3237 2002). This is somewhat older (*c.* 320-310 Ma) than dated motion in the PTSZ and SAD. But  
11 3238 even older dextral deformation has been reported in the latter (330 Ma; Bernard-Griffiths et  
12  
13 3239 al., 1985b; Guineberteau et al., 1987) and in the Elbe Shear Zone (Hofmann et al., 2009),  
14  
15 3240 while in the Massif Central, both dextral and sinistral movements yielded ages of 345-320  
16  
17 3241 (Gay et al., 1981; Costa et al., 1993; Rolin et al., 2009) and 320-300 Ma (Ledru et al., 1994b).

## 19 3242 20 21 3243 *8.2. Step by step restoration*

23  
24 3244 The process is illustrated in Fig. 11. It starts from a modified version of the late  
25  
26 3245 Carboniferous reconstruction of Figure 1, where the late-Variscan movement of the large  
27  
28 3246 NW-SE faults has been removed (Fig. 11a). While the real geometry and displacement of the  
29  
30 3247 late Variscan NPF in Figure 1 is rather hypothetical, its reconstruction by matching the GTMZ  
31 3248 and SAD is easy and dependable. Moreover, two clear magnetic anomalies that were probably  
32  
33 3249 in continuation to each other, one in the eastern part of Órdenes Complex (Martínez Catalán  
34  
35 3250 et al., 2012) and the other Baie d’Audierne (asterisks in Figs. 1 and 11a), help fitting both  
36  
37 3251 sides of the Bay of Biscay. For the rest of the large NW-SE Variscan faults, a simple  
38  
39 3252 translation has been applied to match the Variscan zones at each side.

40  
41 3253 This first step shows that the Ibero-Armorican Arc (IAA) is much tighter for the  
42  
43 3254 zonation of the Iberian and Armorican massifs than for a group of dextral shear zones which  
44  
45 3255 seem to occur in continuity to each other. The next step (Fig. 11b) consists of removing part  
46  
47 3256 of the IAA rotating these massifs in opposite directions to get the Porto-Tomar Shear Zone  
48 3257 (PTSZ) lined up with other significant dextral structures, the Nort-sur-Erdre Fault (NEF) and  
49  
50 3258 the Lalaye-Lubine and Baden-Baden shear zones (LLSZ-BBSZ).

51  
52 3259 The key for restoration is the similitude of the Paleozoic sequence between Buçaco  
53  
54 3260 (western Portugal) and Crozon (western Brittany), interpreted as reflecting proximity before  
55  
56 3261 the late Variscan strike-slip tectonics and the opening of the Bay of Biscay (Robardet et al.,  
57  
58 3262 1990; Young, 1990). These localities are separated in Figure 11a by *c.* 800 km, while in  
59  
60 3263 Figure 11b, the distance is reduced to *c.* 500 km due to the partial restoration of the IAA,

3264 which at this stage had a lesser amplitude. That slip has been removed in Figure 11c, as well  
1  
2 3265 as most of the curvature of the Bohemian Arc. The two sinistral shear zones of southern Iberia  
3  
4 3266 (BCSZ and SISZ) are continued to the north displacing the OMZ which would continue to the  
5  
6 3267 south of England filling a space under the waters of the Bristol Channel which connects the  
7  
8 3268 OMZ and STZ.

9  
10 3269 These two sinistral shear zones, which overprint the southern Iberian suture and the  
11  
12 3270 contact between the OMZ and CIZ, are an anomaly on the general dextral kinematics of late  
13  
14 3271 Variscan tectonics. Probably, they developed between two indentors, one to the west, related  
15  
16 3272 to the Grand Banks of Newfoundland and responsible for the hidden arc between Iberia and  
17  
18 3273 Morocco (Simancas et al., 2005, 2009), and the other to the east, along the north Gondwana  
19  
20 3274 margin, which would be at the origin of the Ibero-Armorican Arc. Removing the slip of the  
21  
22 3275 BCSZ and SISZ yields a still relatively complicated map (Fig. 11d) where the Mid-Variscan  
23  
24 3276 Allochthon looks as a triangular indentor splitting the CIZ in two branches which continue to  
25  
26 3277 the north by the CAD and NAD of the Armorican Massif and to the south by the  
27  
28 3278 Mediterranean province of the Autochthon.

29  
30 3279 The CAD is fully bounded by dextral shear zones, and the NAD probably too. We  
31  
32 3280 interpret the two domains as strike-slip duplexes, of which the first is more deformed than the  
33  
34 3281 latter (Le Gall, 1999; Gumiaux et al., 2004). Figure 11c shows that the two key localities of  
35  
36 3282 Buçaco and Crozon could have been adjacent to each other yet before restoring sinistral  
37  
38 3283 shearing, but Figure 11d shows that the NAD duplex has not been restored yet. This is done in  
39  
40 3284 Figure 11e, which places the NAD close to the Moroccan CB, in agreement with the  
41  
42 3285 correlation established between them and with the OVD of southern Iberia. Note that in the  
43  
44 3286 restoration, the OVD forms part of the NAD (Fig. 11d) before being displaced by the BCSZ.  
45  
46 3287 The translation of the little deformed NAD would have sheared the CAD, a deformation that  
47  
48 3288 has been restored in Figure 11e.

49  
50 3289 If that interpretation of the CAD and NAD is correct, joining Buçaco and Crozon does  
51  
52 3290 not account for the full dextral slip along the main shear zone or zones, because a previous  
53  
54 3291 slip is necessary to move the NAD to the north of the CAD. The restoration shows that this  
55  
56 3292 must have occurred before motion in the BCSZ and SISZ, because they came from the west  
57  
58 3293 of these two sinistral shear zones and rest presently to the east. But the BCSZ, and most  
59  
60 3294 probably the SISZ were later cut across and dragged by the dextral PTSZ.



3295 In addition to late Variscan shear zones and faults, the whole Variscan Belt was  
1  
23296 affected by relatively tight late Variscan folds with a well developed axial planar cleavage,  
3  
43297 with the exception of the NAD. In the CIZ for instance, late folds are similar in wavelength  
5  
63298 and amplitude to those of the CAD, and coeval slaty cleavage is widely developed in pelitic  
7  
83299 formations. Late folds and associated slaty cleavage are commonly recognized structures also  
9  
103300 in the STZ and the TBZ. In areas where metamorphism had reached the high-T greenschist  
11  
123301 facies and higher, late folds are also common, and the associated fabric is a well-developed  
13  
143302 crenulation cleavage.

153303 On the grounds of plate tectonics evolution (dealt with in the next section), we  
16  
173304 consider that late folding reflects distributed dextral shearing, while strike-slip shear zones  
18  
193305 and faults reflect more localized deformation of the same generalized dextral shearing. In the  
20  
213306 CAD, a shear value  $\gamma = 1.5$ , equivalent to a shear angle of  $56.3^\circ$ , has been calculated from the  
22  
233307 angular relationship between the shearing direction and the mean attitude of the associated  
24  
253308 cleavage (Gumiaux, 2003; Gumiaux et al., 2004). This implies 50 % shortening perpendicular  
26  
273309 to the cleavage if deformation took place only by simple shear.

283310 A 10-25% shortening is necessary to develop an incipient cleavage (Ramsay and  
29  
303311 Huber, 1983), 30 % until it becomes apparent (Siddans, 1972), and 50 % is considered a  
31  
323312 starting value for a well developed slaty cleavage (Wood, 1974). Because late folds are  
33  
343313 widespread and their axial planar cleavage is generally well developed, Gumiaux's shear  
35  
363314 value is used for the last step: restoring distributed dextral shearing along the Variscan Belt  
37  
383315 (Fig. 11f).

39  
403316 The new picture shows a Mid-Variscan Allochthon that is wedge-shaped in map view,  
41  
423317 but the wedge is open and realistic, although not necessarily so much open. A right or acute  
43  
443318 angle shape may have resulted only from mechanisms related to the emplacement.  
45  
463319 Famennian-Lower Carboniferous dextral shearing at the northern limb of the wedge (Rolin et  
47  
483320 al., 2009) may have contributed to make it more acute during its emplacement. Also, in terms  
49  
503321 of the critically tapered wedge models (Davis et al., 1983), the thicker is a thrust sheet relative  
51  
523322 to thinner adjacent parts, the more probabilities it has of spreading above its relative  
53  
543323 autochthon forming salients (Boyer, 1995). The Mid-Variscan Allochthon was really thick,  
55  
563324 especially by the contribution of the Upper Allochthon, which in turn was a microcontinent of  
57  
583325 limited lateral extent. This may have created a wedge shaped, even tongue shaped salient  
59  
603326 simply during the emplacement. So, the actual shape of the Allochthon before late Variscan

3327 folding may be that of Figure 11f if the later, generalized ductile dextral shear had a value  $\gamma =$   
1  
23328 1.5, and more acute if that value was lower.

3  
43329 The last step of restoration represents a stage just before the onset of generalized late-  
5  
63330 Variscan dextral shearing, when late folds had not developed and early folds wrap around the  
7  
83331 indenter delineating an open arc which later became the CIA-EMA. An approximate position  
9  
103332 of the CAD, NAD and CB is indicated. At this stage, the Allochthon had been emplaced and  
11  
123333 the SPZ and RHZ were developing thrust belts, which occurred after 340 Ma. Previous  
133334 wrench deformation dominantly dextral, described in the SAD, FMZ and the Bohemian  
14  
153335 Massif, was probably related to the emplacement of the Allochthon. A comment on available  
16  
173336 ages for transcurrent deformation is given in the previous subsection, and an attempt to fit the  
18  
193337 different steps of late Variscan deformation in a time frame is done in the next section.

## 213338 22 233339 **9. Plate tectonics and Variscan evolution**

### 243340 *9.1. Sources and approach*

25  
263341 The Pangea configuration proposed by Wegener (1929) for the late Carboniferous,  
27  
283342 commonly known as Pangea A is generally accepted before the opening of the Atlantic  
29  
303343 Ocean. However, inconsistency between previous paleomagnetic poles of Laurentia and  
31  
323344 Gondwana led Irving (1977) to propose an alternative Pangea B model where Laurentia  
33  
343345 occupied a more western position, implying large dextral shearing to explain the transition  
35  
363346 from models B to A. Relative dextral displacement between Laurussia and Gondwana  
37  
383347 continued in principle from the late Carboniferous to the Permian and perhaps up to the  
39  
403348 Lower Triassic (Muttoni et al., 2009; Gallo et al., 2017).

41  
42  
433349 Various plate reconstructions have been attempted in the last decades and are  
44  
453350 particularly useful in combination with software utilities allowing the user to introduce  
46  
473351 changes in plate kinematics, such as GMap and GPLates. However, while abundant for the  
48  
493352 Mesozoic and Cenozoic, reconstructions are scarce and show significant differences for the  
50  
513353 Paleozoic. As a way to validate the partial retrodeformation of the Variscan Belt, it has been  
52  
533354 checked against one of such a models: the Domeier and Torsvik (2014) reconstruction for the  
54  
553355 late Paleozoic (410-250 Ma). Figure 12 was built using GPLates  
56  
573356 (<https://sourceforge.net/projects/gplates/files/gplates/2.2/>, accessed 5/5/2021). For information  
583357 concerning GPLates, see Boyden et al. (2011).

3358 The reconstruction is based on Domeier and Torsvik (2014) and uses the following  
1  
2 3359 reconstruction geometries and tree of Matthews et al. (2016):

3  
4 3360 Matthews\_etal\_GPC\_2016\_ContinentalPolygons.gpmlz

5  
6 3361 Matthews\_etal\_GPC\_2016\_Coastlines.gpmlz

7  
8 3362 Matthews\_etal\_GPC\_2016\_410-0Ma\_GK07.rot. The latter allows reconstruction from  
9  
10 3363 420 Ma. For the Cambro-Ordovician maps (500-470 Ma), the reconstruction tree  
11  
12 3364 Master2010\_II.rot and animations 500.A97 and 470.A97 of GMap2015 were used  
13  
14 3365 (<http://www.iggl.no/resources.html>, accessed 5/5/2021).

15  
16 3366 The choice of Domeier and Torsvik (2014) reconstruction is because it is mostly based  
17  
18 3367 on paleomagnetism, although this method does not allow establishing paleolongitudes. The  
19  
20 3368 authors acknowledge that paleomagnetic poles are not abundant for the time interval of their  
21  
22 3369 reconstruction, and they also use eruptions in Large Igneous Provinces and kimberlite  
23  
24 3370 emplacements in relation with a mantle reference frame for provisionally establishing  
25  
26 3371 paleolongitudes, as well as additional geological and paleontological data. Moreover, the  
27  
28 3372 reconstruction of Domeier and Torsvik (2014) counts on the work done by Mathews et al.  
29  
30 3373 (2016) in the files ready to use for GPlates. We prefer this reconstruction also because it fits  
31  
32 3374 better our knowledge about the Variscan evolution in comparison with, for instance, one of  
33  
34 3375 the most popular alternatives, that of Stampfli et al. (2013).

35  
36 3376 Domeier and Torsvik (2014) stated that a number of Gondwana paleomagnetic data  
37  
38 3377 reveal a relatively stationary position about the South Pole near Angola during the Middle and  
39  
40 3378 Upper Devonian. Meanwhile, Devonian paleomagnetic data for the main Variscan massifs,  
41  
42 3379 although scarce, indicate that they remained at constant latitude. Then, to explain early  
43  
44 3380 Carboniferous collision with Baltica, they move them thousands of kilometers from northern  
45  
46 3381 Africa to Laurentia during the Devonian and turn them back to northern Africa during the  
47  
48 3382 Carboniferous, with the Iberian Massif returning to practically to the same position but after  
49  
50 3383 having experienced a counterclockwise rotation of 90°. And all that happened without  
51  
52 3384 changes in the shape of the massifs, which behaved as rigid elements.

53  
54 3385 According to stratigraphic similarities between the Autochthon of the Iberian Massif  
55  
56 3386 and Morocco, the existence of a suture between them had not been considered (Michard et al.,  
57  
58 3387 2008, 2010a). However, high-P metamorphism and new ages of high-T metamorphism in the  
59  
60 3388 Rif Domain and Betics point to a convergent plate boundary being active there toward the end  
61  
62 3389 of the Variscan cycle. Even so, correlation among zones of both sides suggests that relative  
63  
64 3390 movements did not modified essentially the relative position of Iberia and Africa. Based on  
65

3391 that correlation and in the evidence that strong deformation characterizes the Variscan  
1  
2 3392 Massifs, we will keep the model of Domeier and Torsvik (2014) for the major plates,  
3  
4 3393 inserting our own model regarding more specifically the evolution of the Variscan Belt.

## 5 6 3394 7 8 3395 *9.2. Reconstruction*

9  
10 3396 The main continental masses and previously described significant elements of the  
11  
12 3397 Variscan Belt are shown in Figure 12 in orthographic projection for different ages. For the  
13  
14 3398 two Cambro-Ordovician reconstructions, a projection centered in the South Pole has been  
15  
16 3399 used, while for the tothers, covering the 400-290 Ma time interval in 10 stages, a fixed  
17  
18 3400 geographic grid shows the absolute and relative motions of the elements (“features” in  
19  
20 3401 GPlates’ slang). Features unrelated to Variscan evolution, such as northern and eastern  
21  
22 3402 territories (Siberia, China, etc.) are omitted. For a better understanding of the Variscan  
23  
24 3403 evolution, Figure 13 shows cross-section snapshots of continents, terranes and plate  
25  
26 3404 boundaries corresponding to the time frames of Figure 12. The sections vary for each frame in  
27  
28 3405 that figure to show different aspects of the tectonic evolution until 320 Ma.

### 29 30 3406 31 32 3407 *9.2.1. Terrane individualization*

33  
34 3408 The reconstruction starts at 500 Ma, when future Avalonia was still part of Gondwana  
35  
36 3409 and a wide passive continental margin developed to the north and NW of present Africa. A  
37  
38 3410 piece of the outermost margin of NW Gondwana was being pulled apart by slab roll back of a  
39  
40 3411 subduction zone which created a magmatic arc in the side facing the Iapetus Ocean. This was  
41  
42 3412 probably the same responsible for the Avalonia volcanic arc (Pickering and Smith, 1995,  
43  
44 3413 1997), which continued further to the south along more than 2000 km in present South  
45  
46 3414 America forming the Famatinia-Puna Ordovician arc (Ducea et al., 2017). The detached piece  
47  
48 3415 formed later the Mid-Variscan Upper Allochthon. It was a microcontinent whose  
49  
50 3416 individualization may have started at 520-510 Ma and where magmatic and metamorphic  
51  
52 3417 peaks were reached around 500 Ma.

53 3418 Placing the future Upper Allochthon microcontinent in the western part of present  
54  
55 3419 northern Africa is based on the absence of a *c.* 1 Ga Mesoproterozoic detrital zircon  
56  
57 3420 population (Fernández-Suárez et al., 2003), compared with their abundance in the central and  
58  
59 3421 northern Iberian Autochthon (Fernández-Suárez et al., 1999, 2000; Martínez Catalán et al.,  
60  
61 3422 2004b; Gómez Barreiro et al., 2007) and the Central Armorican Domain (Dabard et al., 2021;

Stephan et al., 2019). The zircon age spectra of the Upper Allochthon are compatible with provenance from the West African Craton, while those of the Autochthon in Iberia suggest a more eastern paleoposition, closer to the Saharan Metacraton and the adjacent Arabian-Nubian Shield. Note the proximity at 500 Ma of the future Upper Allochthon with the Saxothuringian and Ossa-Morena Zones, where the Mesoproterozoic zircon population is also absent or very rare (Linnemann et al., 2008; Martínez Catalán et al., 2020). Moreover, faunistic similarities between the Teplá-Barrandian and Iberian Autochthon include Ordovician species found in the Ossa-Morena Zone (Gutiérrez-Marco et al., 1999b).

The microcontinent has been placed to the north of, and partly outboard from future Avalonia because its separation from Gondwana predates that of Avalonia, which occurred after 480 Ma (Pickering and Smith, 1997; Stampfli et al., 2013). Its location is conditioned by the paleoposition of Avalonia, Baltica and Gondwana in the reconstruction of GMap2015 for 500 Ma (Fig. 12). If the position of Baltica was more to the east or north, the terrane may have been located in the eastern continuation of Avalonia instead of partly outboard of it.

For the sake of simplicity, we have considered Avalonia as a unique feature instead of including Avalon-Acadia and England-Brabant separately. Moreover, we have included the Rhenohercynian and Moravo-Silesian zones in Avalonia and prolonged it to the NE to explain its probable continuation to the Balkans and Turkey. However it is possible that the latter were different entities.

At 470 Ma, separation of Avalonia had been completed with the opening of the Rheic Ocean, while the location of the future Upper Allochthon is unconstrained, but perhaps never too far from Gondwana. Figure 13 shows with a question mark the possible position of northern Avalonia at that time assuming that the reconstruction at 500 Ma is correct.

Meanwhile, the northern and NW marine platform of Gondwana continued to extend, as rift-related bimodal and alkaline magmatism took place until at least 460 Ma in the future Lower Allochthon (Santos Zalduegui et al., 1995; Díez Fernández et al., 2012b), the Parautochthon (Dias da Silva et al., 2016) and the boundary between de Ossa-Morena and Central Iberian zones (Galindo, 1989; Ochsner, 1993).

### 9.2.2. Early Variscan convergence

By the Lower Devonian, a wide water realm existed north of Gondwana. Domeier and Torsvik (2014) divided it in two oceanic domains, the Rheic to the west and the Paleotethys to

3455 the east, with one and three mid-ocean ridges respectively, and both separated by a subduction  
1  
2 3456 zone dipping to the east. In their text, the authors place the opening of the Paleotethys in the  
3  
4 3457 Lower Devonian, but in their figures, this is an older, very large ocean at 410 Ma. In Figure  
5  
6 3458 12, this hypothetical large Paleotethys of Domeier and Torsvik (2014) is labeled at 400 Ma  
7  
8 3459 between brackets with a question mark. Actually, opening of the Paleotethys occurred at the  
9  
10 3460 Eifelian (390 Ma) according to Stampfli et al. (2013), which suggest that it did not exist or  
11  
12 3461 was rather narrow at 400 Ma. A large region in present northern Africa recorded an Upper  
13  
14 3462 Devonian-early Carboniferous thermal uplift and rifting (Frizon de Lamotte et al., 2013)  
15  
16 3463 probably representing the inception of the true Paleotethys.

17 3464 At 400 Ma, the oceanic lithosphere between Gondwana and the future Upper  
18  
19 3465 Allochthon is that of the Mid-Variscan Ocean preserved in the Middle Allochthon. It was  
20  
21 3466 partly the lithosphere of the Ordovician Rheic Ocean and partly new, created by the relative  
22  
23 3467 movements between Gondwana and the microcontinent during the Silurian and Lower  
24  
25 3468 Devonian. Details are unknown, but suprasubduction signatures have been found in some  
26  
27 3469 oceanic rocks of these ages, suggesting that intra-oceanic subduction zones and perhaps  
28  
29 3470 incipient volcanic arcs developed close to the microcontinent (Díaz García et al., 1999a; Pin  
30  
31 3471 et al., 2002, 2006; Sánchez Martínez et al., 2007b, 2011; Arenas et al., 2014).

32 3472 The first early Variscan events were recorded in the Upper Allochthon during the  
33  
34 3473 Lower Devonian: high-P/high-T metamorphism reaching eclogite facies and dated at (415?)  
35  
36 3474 400-380 Ma is identified in the lower group of all Variscan Massifs where the Upper  
37  
38 3475 Allochthon occurs (Schäfer et al., 1993b; Santos Zalduegui et al., 1996; Franke, 2000;  
39  
40 3476 Lardeaux et al., 2001; Ordóñez Casado et al., 2001; Kryza and Fanning, 2007; Godard, 2009;  
41  
42 3477 Koglin et al., 2018; Collett et al., 2018; Martínez Catalán et al., 2020). This event reflects  
43  
44 3478 subduction of the Upper Allochthon lower group under the units presently forming the upper  
45  
46 3479 group (Martínez Catalán et al., 2009). If this subduction zone was the same as that proposed  
47  
48 3480 by Domeier and Torsvik (2014), its polarity should be the opposite, (*i.e.*, to the NW; Fig. 13)  
49  
50 3481 because the part of the microcontinent subducted at *c.* 400 Ma was the rifted margin of the  
51  
52 3482 microcontinent, facing Gondwana, while the upper plate was the active Cambro-Ordovician  
53  
54 3483 margin, facing the Rheic Ocean (Fig. 12, 400 Ma).

54 3484 That early subduction initiated the building of an accretionary wedge by incorporation  
55  
56 3485 of new elements. The Mid-Variscan Ocean was closed by oceanic subduction, underthrusting  
57  
58 3486 and imbrication by 380 Ma. This was followed by continental subduction of the extended  
59  
60 3487 external part of the northern Gondwana margin. Exhumation of the previously subducted part

3488 of the microcontinent took place between 395-360 Ma, while oceanic imbricates formed the  
1  
2 3489 Middle Allochthon and high-P metamorphism affected the more external part of the northern  
3  
4 3490 Gondwana margin at 375-360 Ma, which later was incorporated to the upper plate as the  
5  
6 3491 Lower Allochthon during the collisional stage. An oblique subduction with an eastward  
7  
8 3492 component is suggested in Figure 12 (compare 400 and 370 Ma images) based on kinematic  
9  
10 3493 criteria observed in the Lower Allochthon of NW Iberia (Malpica-Tui Complex; Díez  
11  
12 3494 Fernández and Martínez Catalán, 2012). Once the subduction of the Lower Allochthon was  
13  
14 3495 blocked by underthrusting of thicker Gondwanan crust, the convergence regime changed from  
15  
16 3496 subductive to collisional.

17 3497           Meanwhile, the western part of the Rheic Ocean recorded renewed activity. An arc  
18  
19 3498 developed at the late Silurian-Lower Devonian (425-392 Ma; Zeh and Will, 2010) in eastern  
20  
21 3499 Avalonia, and relics of it are preserved in the Mid German Crystalline High and the Northern  
22  
23 3500 Phyllite Zone, at the boundary between the Rhenish and Bohemian massifs. Laurussia had  
24  
25 3501 been amalgamated by 420 Ma (Ludlow; Stampfli et al., 2013), and a ribbon microcontinent  
26  
27 3502 and/or island arc was pulled apart from Laurussia (Hanseatic terrane of Stampfli et al., 2013),  
28  
29 3503 opening the Rhehercynian Ocean. Its existence spans ~410-380 Ma for Franke (2000),  
30  
31 3504 ~410-350 Ma for Zeh and Gerdes (2010) and ~370-320 Ma for Stampfli et al. (2013). We  
32  
33 3505 have chosen the interval given by Zeh and Gerdes (2010) and Zeh and Will (2010) for central  
34  
35 3506 Europe, adapting their reconstruction, shown in a series of cross sections, to ours (Figs. 12  
36  
37 3507 and 13). The result is an unexpectedly wide Rhehercynian Ocean between Avalonia and the  
38  
39 3508 Silurian-Devonian arc, whose reliability depends on the reconstruction by Domeier and  
40  
41 3509 Torsvik (2014). But it finds support in the fact that present west-dipping subduction zones are  
42  
43 3510 characterized by large back-arc spreading (Doglioni et al., 2007).

44 3511           The reconstruction is coherent with the evolution of SW Iberia at the contact between  
45  
46 3512 the OMZ and SPZ. There, an ophiolite dated at 480 Ma represents the original lithosphere of  
47  
48 3513 the Rheic Ocean (Fonseca et al., 1999; Pedro et al., 2010). But it is included in a high-P  
49  
50 3514 mélange forming part of an orogenic wedge and representing the closure of an ocean by SW-  
51  
52 3515 directed subduction at *c.* 400 Ma (Rubio Pascual et al., 2013b). An arc and back-arc pair,  
53  
54 3516 another high-P unit and a NE-verging accretionary wedge developed later and complex  
55  
56 3517 continent/ocean interactions, including an extensional event, occurred before a thin-skinned  
57  
58 3518 thrust belt developed in the South Portuguese Zone between 340-310 Ma (Simancas et al.,  
59  
60 3519 2004). Note that because the *c.* 90° late-Variscan counterclockwise rotation of SW Iberia,  
61  
62 3520 present SW-directed subduction and NE-verging thrusting correspond, before 340 Ma, to  
63  
64  
65

3521 NW-directed and SE-verging respectively, fitting the reconstruction of Fig. 12. The opening of  
1  
2 3522 the Rhenohercynian or Lizard-Giessen Ocean occurred in the latest Silurian-Lower Devonian  
3  
4 3523 (425-392 Ma; Zeh and Will, 2010; 405-390 Ma; Clark et al., 1998; Woodcock et al., 2007),  
5  
6 3524 causing the closure of the Rheic Ocean by the Upper Devonian-early Carboniferous. Later,  
7  
8 3525 the closure of the Rhenohercynian Ocean is indicated by eclogites of 350 Ma, and the  
9  
10 3526 collision and underthrusting of Avalonia started probably around *c.* 345 Ma in the South  
11  
12 3527 Portuguese Zone (Simancas, 2004), the Rhenohercynian Zone (Oncken et al., 2000; Zeh and  
13  
14 3528 Will, 2010), and the Moravo-Silesian Zone (Tomek et al., 2019).

### 15 3529 16 17 3530 *9.2.3. Variscan collision*

18  
19  
20 3531 The collision of the accretionary wedge with Gondwana emplaced the Mid-Variscan  
21  
22 3532 Allochthon and was accompanied by the incorporation of the Parautochthon and of  
23  
24 3533 generalized compressional deformation. Recumbent folds formed in NW Iberia, and the first  
25  
26 3534 folds in the Central Iberian Zone and the Moroccan Eastern Meseta started developing in the  
27  
28 3535 earliest Carboniferous. The Saxothuringian Zone was covered by the Allochthon and partly  
29  
30 3536 subducted beneath. But there is no evidence that the same occurred to the west, in the Ossa-  
31  
32 3537 Morena Zone or in Morocco, where compression was probably related with collision of the  
33  
34 3538 Silurian-Devonian arc of Avalonian derivation. This is supported by zircon age spectra in  
35  
36 3539 Upper Devonian synorogenic flysch in the southern Ossa-Morena Zone and the northern part  
37  
38 3540 of Eastern Meseta, which points to an Avalonian source (Pereira et al., 2012; Accotto et al.,  
39  
40 3541 2020, 2021). That source may have been a piece of the Silurian-Devonian arc obducted at *c.*  
41  
42 3542 360 Ma not far from the flysch occurrences (Fig. 12), while arc collision may explain the  
43  
44 3543 recumbent folds in the central part of the Ossa-Morena Zone and the subduction of the  
45  
46 3544 Cubito-Moura Unit in the south and of the Central Unit in the north. Both the latter occurred  
47  
48 3545 at the Upper Devonian (380-360 Ma) and are coeval with high-P metamorphism of the  
49  
50 3546 eclogitic unit in the Pays de Léon and in the Mid German Crystalline High.

51  
52 3547 The collisions of the accretionary prism and of the Silurian-Devonian arc were  
53  
54 3548 apparently unrelated with push by Laurussia, the large continent formed by Laurentia, Baltica  
55  
56 3549 and Avalonia, as it was far away at that time (370-360 Ma) according to the reconstruction of  
57  
58 3550 Domeier and Torsvik (2014) that we have used. A fact supporting this hypothesis is that no  
59  
60 3551 other allochthon was emplaced on top of the Upper Allochthon, which excludes obduction  
61  
62 3552 and/or overthrusting by Laurussia.



3553 According to the reconstruction provided by Matthews et al. (2016) for GPlates,  
1  
2 3554 Laurussia moved to the east in relation to Gondwana some 50-55° in longitude between 360-  
3  
4 3555 340 Ma. Then both migrated together to the NE between 340-330 Ma, which was followed at  
5  
6 3556 330-320 Ma by a new relative eastward displacement of Laurussia of roughly 15° in  
7  
8 3557 longitude. The first relative dextral translation explains the closure of the Rhenohercynian  
9  
10 3558 Ocean as well as much of the activity mentioned in the previous paragraph. But it would have  
11  
12 3559 been insufficient for provoking a collision with the Variscan Belt at *c.* 345 Ma if the latter had  
13  
14 3560 remained attached to northern Gondwana. An additional motion of the Variscan Belt was  
15  
16 3561 needed, which in our model is solved by a counterclockwise rotation due to the opening of a  
17  
18 3562 small ocean to the south.

19 3563 Such ocean is a good candidate for being named the Paleotethys. Its birth coincides  
20  
21 3564 with an Upper Devonian-early Carboniferous extensional event recorded in southern Iberia  
22  
23 3565 and northern Africa (Simancas et al., 2003; Frizon de Lamotte et al., 2013; Rubio Pascual et  
24  
25 3566 al., 2013b; Lahfid et al., 2019). In the model, the Paleotethys began to open at 365 Ma and  
26  
27 3567 reached its maximum width at 345 Ma, when the Rhenohercynian Ocean had closed (Zeh and  
28  
29 3568 Gerdes, 2010) and a thrust belt initiated its development in the South Portuguese,  
30  
31 3569 Rhenohercynian and Moravo-Silesian zones. No oceanic lithosphere was apparently created  
32  
33 3570 in Morocco (Michard et al., 2008, 2010a; Simancas et al., 2009).

34 3571 The progressive closure of the Mid-Variscan Ocean, coeval with the initial rifting  
35  
36 3572 stage that will lead to the opening of the Paleotethys, provides an explanation for  
37  
38 3573 simultaneous contraction and extension in the Variscan Belt (Fig. 12, 370-350 Ma interval)  
39  
40 3574 which is an alternative to the mantle plume hypothesis (Simancas et al., 2003, 2006), although  
41  
42 3575 both are not mutually exclusive.

43 3576 The middle Carboniferous Variscan suture in the Mauritanides (Caby and Kienast,  
44  
45 3577 2009), might be that of the Rheic, Rhenohercynian or Paleotethys oceans, but also due to the  
46  
47 3578 collision of a peri-Gondwanan terrane approximately located where plate reconstructions  
48  
49 3579 place the Mesozoic Florida-Suwannee terrane. The reconstructions of Domeier and Torsvik  
50  
51 3580 (2014) and Matthews et al. (2016) do not include such terrane, and keep Florida-Suwannee  
52  
53 3581 fixed to Gondwana during the Paleozoic. Consequently, the same is done here, being aware  
54  
55 3582 that pulling apart and docking of some terrane could have occurred in NW Africa and new  
56  
57 3583 data might provide a precise correlation with European Variscan sutures.

58  
59 3584

3585 9.2.4. Late Variscan deformation

1  
23586 The final emplacement of the Iberian Allochthon has been dated at 345-340 Ma,  
3 including thrusting onto the Parautochthon and of the whole ensemble onto the Autochthon  
43587 (Dallmeyer et al., 1997; Martínez Catalán et al., 2007, 2009). This can be related to the  
5  
63588 closure of the Rhehercynian Ocean and final collision with Laurussia. The continental  
7  
83589 subduction of the Saxothuringian Zone is dated between 370-340 Ma (Franke and Stein,  
9  
103590 2000; Žáčková et al., 2010; Konopásek et al., 2019), although the peak of high-P  
113591 metamorphism occurred at 360-350 Ma (Schmädicke et al., 1995; Rötzler and Plessen, 2010;  
12  
133592 Závada et al., 2021). Continuation of convergence until 340 Ma suggests a relationship with  
14  
153593 Laurussian push, which may also be the cause of propagation of early Variscan folds and  
16  
173594 thrust faults toward the foreland, and of the initial curvature of the fold axes that ultimately  
18  
193595 led to the Central Iberian Arc and possibly the Eastern Meseta Arc (Figs. 1, 2 and 8), creating  
20  
213596 a configuration similar to that of Figure 11f. The reconstruction at 350-330 Ma indicates that  
223597 most of the northern boundary of the Mid-Variscan Allochthon came into contact with  
23  
243598 Avalonia and supports the contention that the Brunovistulian block derives from, or formed  
25  
263599 part of that ribbon continent.  
27  
283600

29  
303601 Subsequent relative dextral displacement of Laurussia and Gondwana was responsible  
31  
323602 for the late Variscan deformation restored in Figure 11, whose successive steps are  
33  
343603 approximately reflected in Figure 12 between 330 and 290 Ma. They show that the suture  
35  
363604 related with the emplacement of the Mid-Variscan Allochthon derives from an ocean situated  
37  
383605 to the NW, but after strong dextral shearing involving rotational deformation, the root of the  
393606 suture was moved to a N-S attitude in the east of the Variscan Belt.  
40

41  
423607 Placing the root in the center of the Bohemian Massif makes sense, because: i) this is  
43  
443608 the only place where part of the Moho may be that of the Allochthon (Fig. 7b); ii) no Middle  
453609 or Lower Allochthon units have been described (Fig. 6). The latter is what can be expected in  
46  
473610 the root zone of a large thrust fault, while in the periphery, detached fragments of its relative  
48  
493611 autochthon can be commonly found as imbricates. The probable continuation of the root zone  
50  
513612 to the south is an area where the Variscan basement is mostly covered, and probably includes  
52  
533613 a terrane or terranes different from that of the Mid-Variscan Upper Allochthon.  
54

553614 In that interpretation, the Mediterranean province of the Variscan Belt does not  
56  
573615 represent an individual terrane, but simply the eastern part of the extended northern  
58  
593616 Gondwana platform, which recorded a somewhat different evolution (younger Ordovician  
60  
61  
62  
63  
64  
65

3617 magmatism, Sardinian unconformity, along margin facies changes). The transition from the  
1  
2 3618 Iberian and central Europe province to the Mediterranean province occurs between the two  
3  
4 3619 flanks of the Ibero-Armorican Arc (IAA; Fig. 1). But the reconstruction shows that it occurs  
5  
6 3620 also between the two sides of the more or less acute angle of the tongue-shaped Mid-Variscan  
7  
8 3621 Allochthon (Fig. 11e). The microcontinent whose collision formed the Mid-Variscan  
9  
10 3622 Allochthon impinged the northern Gondwana platform at a place where some lateral  
11  
12 3623 variations existed previously, but changes are progressive and occurred along hundreds of  
13  
14 3624 km: the separation from the Central Iberian Zone under the Cabo Ortegal Complex in NW  
15  
16 3625 Iberia and the western Pyrenees was at least of 500 km, and from there to the Montagne Noire  
17  
18 3626 another 300 km must be added.

19 3627 The Balkanides and Pontides, include significant pieces of the Variscan Belt. They  
20  
21 3628 presently surround the Black Sea Upper Cretaceous back-arc basin, and in the reconstruction  
22  
23 3629 of Matthews et al. (2016) for GPlates, they occur in the eastern continuation of the Variscan  
24  
25 3630 Mediterranean province. Okay and Topuz (2017) compare the evolution of the Balkanides  
26  
27 3631 and Pontides with that of central Europe during the Carboniferous, finding close similarities  
28  
29 3632 for the metamorphic evolution and granite magmatism, and propose continuity among them at  
30  
31 3633 least from the Upper Devonian. Conversely, the future Anatolides and Taurides, where no  
32  
33 3634 Variscan deformation is recorded, remained attached to Gondwana (*i.e.*, the southern margin  
34  
35 3635 of Paleotethys) during the whole upper Paleozoic.

36 3636 In the reconstruction, the small Paleotethys closed at 320 Ma following north-directed  
37  
38 3637 subduction. This is in agreement with the two classical provinces established in the Caucasus  
39  
40 3638 and Turkey for the late Paleozoic (Adamia et al., 1987, 2011): the northern province  
41  
42 3639 representing an active margin and the southern one a passive margin. A third province exist  
43  
44 3640 farther to the north, from Moesia to the Istanbul Zone, interpreted as the southern margin of  
45  
46 3641 Laurussia during the late Paleozoic (Okay and Topuz, 2017). This corresponds to the eastern  
47  
48 3642 part of the Avalonia terrane, which joined the Pontides much later, during the Upper Triassic.

49 3643 The space between the Mediterranean province and the Anatolides and Taurides was  
50  
51 3644 occupied, at least partially, by Gondwanan continental crust: the Alpine terranes of Figure 12,  
52  
53 3645 which were later incorporated to the Alpine chains. These include for instance Adria,  
54  
55 3646 Calabria, the Dinaride platform, Greece, and the Peloponnese. According to Matthews et al.  
56  
57 3647 (2016), they stayed tied to Gondwana until the Alpine collision, while Stampfli et al. (2013)  
58  
59 3648 include them in the continuation of the Variscan Belt to the east, separated at the Middle  
60  
61  
62  
63  
64  
65

3649 Devonian by the opening of the Paleotethys and attached to the south of Laurasia during the  
1  
2 3650 Upper Carboniferous.

3  
4 3651 The IAA and probably the hidden arc between Iberia and Morocco developed at the  
5  
6 3652 late stages of collision. For the first of them, an age of 305-295 Ma has been proposed based  
7  
8 3653 on paleomagnetic data (Weil, 2006; Weil et al., 2010), while structural data fixed the interval  
9  
10 3654 at 310-299 Ma (Pastor-Galán et al., 2011). Although a buckling model has been proposed by  
11  
12 3655 Weil et al. (2010) to explain the origin of the IAA, we consider more reasonable the  
13  
14 3656 indentation hypothesis proposed by Matte and Ribeiro (1975) and Matte (1986, 1991). The  
15  
16 3657 reason is that structures such as the very large recumbent folds and thrust sheets of the West  
17  
18 3658 Asturian-Leonese and Cantabrian zones occur only at the arc's core, and fade away to the  
19  
20 3659 southern limb in the WALZ and its continuation to La Demanda and Iberian Chains, and to  
21  
22 3660 the northern limb in the Basque Massifs of western Pyrenees. The large horizontal translations  
23  
24 3661 at the hinge zone of the arc are more compatible with underthrusting of some relatively rigid  
25  
26 3662 indentor than with a tangential longitudinal strain at the core of a large buckle fold.

27 3663 It can be argued that the folds and most of the thrust faults predate the development of  
28  
29 3664 the IAA, which is true. But possibly some of these structures were reactivated during the  
30  
31 3665 formation of the arc. This may be the case of the recumbent folds and basal thrust fault of the  
32  
33 3666 Mondoñedo Nappe (Fig. 3a), where the two largest recumbent folds share a reverse limb of  
34  
35 3667 20-30 km (Matte, 1968; Bastida et al., 1986; Martínez Catalán et al., 2003) and Ar-Ar ages of  
36  
37 3668 cleavage yielded abnormally young values (300-280 Ma; Dallmeyer et al., 1997). In the CZ,  
38  
39 3669 piggy-back and out-of-sequence thrusting remained active until 300 Ma (Pérez-Estaún et al.,  
40  
41 3670 1988, 1991; Alonso et al., 2009; Merino-Tomé et al., 2009), so overlapping the time span of  
42  
43 3671 arc development. On the other side, the tangential translations at the hinge of the arc should  
44  
45 3672 be accompanied by wrench movements at the limbs. For the northern limb, coeval (310-290  
46  
47 3673 Ma) dextral transurrence in the southern branch of the South Armorican Shear Zone and the  
48  
49 3674 Pyrenees (Carron et al., 1994; Cochelin et al., 2017) may account for that displacement. The  
50  
51 3675 counterpart in the southern limb may include the sinistral Juzbado-Penalva Shear Zone (Figs.  
52  
53 3676 1 and 2).

54  
55 3677 For the hidden arc between Iberia and Morocco, indentation by the Grand Banks of  
56  
57 3678 Newfoundland has been proposed by Simancas et al. (2005, 2009). A more detailed model by  
58  
59 3679 Simancas et al. (2013) considers that curvatures of the Central Iberian Arc (CIA) and the  
60  
61 3680 hidden arc were originally the same, nucleated around a paleogeographic salient in Avalonia  
62  
63 3681 and amplified, cut across and superposed during the Variscan collision.

3682 In our model, both arcs are different and of different age, as explained in the section  
1 devoted to retrodeformation (Fig. 11) and shown in Figure 12. The CIA was nucleated by the  
2 3683 emplacement of the Mid-Variscan Allochthon and closed by dextral shearing, partly during  
3 3684 emplacement and partly during late-Variscan transcurrence. The hidden arc is linked to the  
4 3685 activity of a wide sinistral shear zone whose motion took place during a short interval,  
5 3686 intercalated in the generally dextral transcurrent regime dominant during the late  
6 3687 Carboniferous. The Grand Banks indenter moved during the late Carboniferous, although the  
7 3688 existence of initial smooth salients in Avalonia are not excluded, neither possible  
8 3689 reactivations of older structures producing indentors there. That motion probably overlapped  
9 3690 in time with the development of the IAA, and can be related with indentors in the two major  
10 3691 plates confining the Variscan Belt: a northern indenter developed in Avalonia and a southern  
11 3692 one in NE Gondwana, probably a promontory formed by deformation of the future Alpine  
12 3693 terranes. That motion, coeval with continuity of dextral shearing, remained active during the  
13 3694 early Permian.  
14 3695

15 3696 Pereira et al. (2015a, 2017b) interpreted late Variscan (315-280 Ma) calc-alkaline  
16 3697 granitoids of Iberia as related to subduction of the Paleotethys linked to the development of  
17 3698 the IAA, and unrelated to the Variscan collision. However, the same granitoids have been  
18 3699 interpreted as resulting from partial melting of the lower crust with variable mantelic heat and  
19 3700 magmatic input and also variable contribution of orogenic crustal thickening (Castiñeiras et  
20 3701 al., 2008; Carracedo et al., 2009; Orejana et al., 2012; Villaseca et al., 2017). Even assuming a  
21 3702 crustal origin with variable mantle contribution, Gutiérrez-Alonso et al. (2011) defended  
22 3703 delamination of thickened mantle lithosphere during the closure of the IAA orocline as the  
23 3704 source of heat necessary for massive granite production. And Alcock et al. (2015) calculate  
24 3705 that heat production due to crustal thickening could had contributed significantly to heat  
25 3706 input for NW Iberian granite production, without discarding an additional source due to  
26 3707 asthenospheric upwelling.  
27

28 3708 Our model does not back the Paleotethys oceanic subduction hypothesis of Pereira et  
29 3709 al. (2015a, 2017b) for late Variscan granitoids, because south of the Iberian Peninsula, the  
30 3710 small Paleotethys closed at 320 Ma, and in Matthews et al. (2016) reconstruction, no oceanic  
31 3711 crust existed south of Iberia between 325-280 Ma. This does not mean that the model by  
32 3712 Pereira et al. (2015a, 2017b) should be discarded, because the reconstruction may be  
33 3713 incorrect. Meanwhile, we find that our model of the Variscan Belt implies a late Variscan  
34  
35  
36  
37  
38  
39  
40  
41  
42  
43  
44  
45  
46  
47  
48  
49  
50  
51  
52  
53  
54  
55  
56  
57  
58  
59  
60  
61  
62  
63  
64  
65

3714 narrowing and associated crustal thickening which rather supports the alternative of crustal  
1  
2 3715 thickening and melting with variable amounts of mantle involvement.

3  
4 3716 Figure 13 shows the late Variscan evolution of the belt in relation with the relative  
5  
6 3717 position of Laurussia and Gondwana. Successive positions of these plates are based on the  
7  
8 3718 model by Domeier and Torsvik (2014) and the reconstruction of Matthews et al. (2016). The  
9  
10 3719 Variscan Belt became progressively squeezed between the major plates as shown by the angle  
11  
12 3720 formed by two reference lines, which decreases between 340 and 290 Ma. This imposed an  
13  
14 3721 internal deformation similar to trishear (Erslev, 1991), a kinematic model of fault-propagation  
15  
16 3722 folding where the decrease in displacement along a fault induces heterogeneous shear in a  
17  
18 3723 triangular zone radiating from the tip line (Hardy and Allmendinger, 2011). The trishear  
19  
20 3724 model was initially applied to the triangular area in front of a propagating thrust fault (Erslev,  
21  
22 3725 1991; Zehnder and Almendinger, 2000; Cristallini and Allmendinger, 2011) and was  
23  
24 3726 extended to normal faults and 3D models by Cardozo (2008).

25 3727 The late Variscan evolution of the belt in relation with the relative position of the  
26  
27 3728 major, supposedly rigid plates, was conditioned by the eastward and southward translation  
28  
29 3729 and clockwise rotation of Laurussia relative to Gondwana and by internal heterogeneities  
30  
31 3730 inside the mobile zone. The eastward relative translation of Laurussia between 340 and 320  
32  
33 3731 Ma, calculated for a longitudinal displacement of *c.* 15° (continuous and dashed red lines at  
34  
35 3732 340 Ma), is around 1660 km at the Equator and 1440 km at 30° south latitude. This explains  
36  
37 3733 the strong dextral component of late Variscan deformation. Relative northward translation of  
38  
39 3734 Gondwana and *c.* 12° clockwise rotation are responsible for the closure of the small  
40  
41 3735 Paleotethys Ocean, indentation leading to orocline development (Ibero-Armorican Arc and a  
42  
43 3736 hidden arc between Iberia and Morocco), and to late, NW-SE dextral oblique faulting. In  
44  
45 3737 addition, early to middle Permian conjugate strike-slip brittle faulting was put in relation with  
46  
47 3738 such a megashear and the NW-SE oblique faulting by Arthaud and Matte (1977).

## 48 49 3740 **10. Conclusions**

50  
51  
52 3741 The non-cylindrical geometry of the Variscan Belt derives from the lack of continuity  
53  
54 3742 of one of its zones, the Mid-Variscan Allochthon, while other zones essentially maintain their  
55  
56 3743 continuity along the overall belt from the Bohemian Massif to Morocco. The geometry of the  
57  
58 3744 Mid-Variscan Allochthon, together with that of the whole ensemble, is partially restored for  
59  
60 3745 the late Variscan deformation in a series of steps that yield a picture of the geometry at the

3746 end of the early Variscan stage. Based on that picture, the Mid-Variscan Allochthon is  
1 3747 explained by overthrusting of a microcontinent, a peri-Gondwanan terrane detached from a  
2 3748 region close to NW Africa and collided with more eastern parts of northern Gondwana  
3 3749 platform.  
4  
5  
6

7 3750 What is preserved of the microcontinent presently forms the Upper Allochthon, but its  
8 3751 collision involved the closure of an intervening Mid-Variscan Ocean whose lithosphere partly  
9 3752 belongs to the initial (Cambro-Ordovician) Rheic Ocean and partly was created later, during  
10 3753 the Silurian and Devonian. Some of these oceanic lithospheres were incorporated to an  
11 3754 accretionary prism during closure of the Mid-Variscan Ocean, and were later overthrust onto  
12 3755 the northern Gondwana platform, presently forming the Middle Allochthon. Outer parts of  
13 3756 that continental platform were also incorporated to the accretionary prism and later emplaced  
14 3757 to more internal parts of it, forming the Lower Allochthon and the Parautochthon.  
15  
16  
17  
18  
19  
20  
21

22 3758 The available knowledge of pre-Variscan and early Variscan evolution and the results  
23 3759 of late Variscan retrodeformation have been integrated in a calibrated plate-tectonics  
24 3760 reconstruction covering the late Cambrian to early Permian, which is shown with a focus on  
25 3761 the Variscan deformation. The resulting model explains the non-cylindrical geometry by: i)  
26 3762 the small size of the Upper Allochthon microcontinent compared with the extent of the  
27 3763 deformed northern Gondwana and Avalonia plates and ii) large intracontinental dextral  
28 3764 shearing caused by the relative eastward displacement of Laurussia relative to Gondwana. The  
29 3765 latter also explains the rotation of the Mid-Variscan Allochthon root zone from an original  
30 3766 position to the NW of the belt to its proposed present location in the central and southern parts  
31 3767 of the Bohemian Massif.  
32  
33  
34  
35  
36  
37  
38  
39  
40

41 3768 Southward translation and moderate clockwise rotation of Laurussia relative to  
42 3769 Gondwana explain indentation leading to formation of the Ibero-Armorican Arc and a hidden  
43 3770 arc between Iberia and Morocco. The open Massif Central Arc may be a side effect of the  
44 3771 Ibero-Armorican Arc. However, the Central Iberian Arc is primarily related to the indentation  
45 3772 of the Mid-Variscan Allochthon, although it was strongly amplified by late-Variscan dextral  
46 3773 shearing. The Bohemian Arc is also related to dextral shearing, resolved there in the Elbe  
47 3774 Shear Zone and the Moldanubian Thrust.  
48  
49  
50  
51  
52  
53  
54  
55  
56

## 57 3776 **Acknowledgements**

58  
59  
60  
61  
62  
63  
64  
65

3777 This contribution has been funded by the research projects CGL2011-22728 of the  
1 3778 Spanish Ministry of Science and Innovation), and CGL2016-78560-P of the Spanish Ministry  
2  
3 3779 of Economy and Competitiveness, as part of the National Program of Promotion of Scientific  
4  
5 3780 and Technical Research of Excellence, in the frame of the National Plan of Scientific and  
6  
7 3781 Technical Research and Innovation 2013-2016. JRMC acknowledges a Program XII grant of  
8  
9 3782 the University of Salamanca that allowed research stays at universities and laboratories of  
10  
11 3783 Rennes, Strasbourg, Praha, Dresden and Wrocław during the academic year 2017-18. KS  
12  
13 3784 acknowledges GAČR grant No 19-25035. Discussions with M. Ballèvre, P. Aleksandrowsky,  
14  
15 3785 S. Mazur, J. Szczepański, S. Collet and U. Linnemann contributed to clarify many aspects  
16  
17 3786 related with correlations among Variscan massifs. The manuscript has benefited from the  
18  
19 3787 input of the editor and reviewers, Zuo Chen Li and especially André Michard, whose  
20  
21 3788 corrections, comments and suggestions were highly appreciated.  
22  
23 3789

## 24 **References**

- 25 3790
- 26
- 27 3791 Abad, I., Nieto, F. and Velilla, N. 2001. The phyllosilicates in diagenetic-metamorphic rocks  
28  
29 3792 of the South Portuguese Zone, southwestern Portugal. *Canadian Mineralogist*, 39,  
30  
31 3793 1571-1589.  
32
- 33 3794 Abad, I., Nieto, F., Velilla, N. and Simancas, J.F. 2004. Zona Sudportuguesa: Metamorfismo.  
34  
35 3795 In: Vera, J.A. (Ed.), *Geología de España*, SGE-IGME, Madrid, Cap. 2, 209-211.  
36
- 37 3796 Ábalos, B. and Díaz Cusí, J. 1995. Correlation between seismic anisotropy and major  
38  
39 3797 geological structures in SW Iberia: a case study on continental lithosphere  
40  
41 3798 deformation. *Tectonics*, 14, 1012-1040.  
42
- 43 3799 Abalos, B., Gil Ibarra, J.I. and Eguíluz, L. 1991. Cadomian subduction/collision and  
44  
45 3800 Variscan transpression in the Badajoz-Córdoba shear belt, southwest Spain.  
46  
47 3801 *Tectonophysics*, 199, 51-72.  
48
- 49 3802 Abati, J. and Dunning, G.R. 2002. Edad U-Pb en monacitas y rutilos de los paragneises de la  
50  
51 3803 Unidad de Agualada (Complejo de Órdenes, NW del Macizo Ibérico). *Geogaceta*, 32,  
52  
53 3804 95-98.  
54
- 55 3805 Abati, J., Dunning, G.R., Arenas, R., Díaz García, F., González Cuadra, P., Martínez Catalán,  
56  
57 3806 J.R. and Andonaegui, P. 1999. Early Ordovician orogenic event in Galicia (NW  
58  
59 3807 Spain): evidence from U-Pb ages in the uppermost unit of the Ordenes Complex. *Earth*  
60  
61  
62  
63  
64  
65



- 3808 and Planetary Science Letters, 165, 213-228. <https://doi.org/10.1016/S0012->  
1  
23809 821X(98)00268-4.  
3
- 43810 Abati, J., Arenas, R., Martínez Catalán, J.R. and Díaz García, F. 2003. Anticlockwise P-T  
5  
63811 path of granulites from the Monte Castelo Gabbro (Órdenes Complex, NW Spain).  
7  
83812 Journal of Petrology, 44, 305-327.  
9
- 103813 Abati, J., Castiñeiras, P., Arenas, R., Fernández-Suárez, J. Gómez Barreiro, J. and Wooden,  
11  
123814 J.L. 2007. Using SHRIMP zircon dating to unravel tectonothermal events in arc  
13  
143815 environments. The early Paleozoic arc of NW Iberia revisited. Terra Nova, 19, 432-  
15  
163816 439. <https://doi.org/10.1111/j.1365-3121.2007.00768.x>.  
17
- 183817 Abati, J., Gerdes, A., Fernández-Suárez, J., Arenas, R., Whitehouse, M.J. and Díez  
19  
203818 Fernández, R. 2010. Magmatism and early-Variscan continental subduction in the  
21  
223819 northern Gondwana margin recorded in zircons from the basal units of Galicia, NW  
23  
243820 Spain. Geological Society of America Bulletin, 122 (1/2), 219-235.  
253821 <https://doi.org/10.1130/B26572.1>.  
26
- 273822 Abati, J., Arenas, R., Díez Fernández, R., Albert, R. and Gerdes, A. 2018. Combined zircon  
28  
293823 U-Pb and Lu-Hf isotopes study of magmatism and high-P metamorphism of the basal  
30  
313824 allochthonous units in the SW Iberian Massif (Ossa-Morena complex). Lithos, 322,  
32  
333825 20-37. <https://doi.org/10.1016/j.lithos.2018.07.032>.  
34
- 353826 Accotto, C., Martínez Poyatos, D.J., Azor, A., Talavera, C., Evans, N.J., Jabaloy-Sánchez, A.,  
36  
373827 Azdimousa, A., Tahiri, A. and El Hadi, H. 2019. Mixed and recycled detrital zircons  
38  
393828 in the Paleozoic rocks of the Eastern Moroccan Meseta: Paleogeographic inferences.  
40  
413829 Lithos, 338-339, 73-86. <https://doi.org/10.1016/j.lithos.2019.04.011>.  
42
- 433830 Accotto, C., Martínez Poyatos, D., Azor, A., Jabaloy-Sánchez, A., Talavera, C., Evans, N.J.  
44  
453831 and Azdimousa, A. 2020. Tectonic evolution of the Eastern Moroccan Meseta: from  
46  
473832 Late Devonian fore-arc sedimentation to Early Carboniferous collision of an  
48  
493833 Avalonian promontory. Tectonics, 38, e2019TC005976.  
50  
513834 <https://doi.org/10.1029/2019TC005976>.  
52
- 533835 Accotto, C., Martínez Poyatos, D., Azor, A., Talavera, C., Evans, N.J., Jabaloy-Sánchez, A.,  
54  
553836 Azdimousa, A., Tahiri, A. and El Hadi, H. 2021. Syn-collisional detrital zircon source  
56  
573837 evolution in the northern Moroccan Variscides. Gondwana Research, (in press).  
583838 <https://doi.org/10.1016/j.gr.2021.02.001>.  
59  
60  
61  
62  
63  
64  
65

- 3839 Ackerman, L., Hajná, J., Žák, J., Erban, V., Sláma, J., Polák, L., Kachlík, V., Strnad, L. and  
1  
23840 Trubač, J. 2020. Architecture and composition of ocean floor subducted beneath  
3  
43841 northern Gondwana during Neoproterozoic to Cambrian: A palinspastic reconstruction  
5  
63842 based on Ocean Plate Stratigraphy (OPS). *Gondwana Research*, 76, 77-97.
- 7  
83843 Acosta-Vigil, A., Rubatto, D., Bartoli, O., Cesare, B., Meli, S., Pedrera, A., Azor, A.,  
9  
103844 Tajčmanová, L. 2014. Age of anatexis in the crustal footwall of the Ronda peridotites,  
11  
123845 S Spain. *Lithos*, 210-211, 147-167.
- 13  
143846 Adamia, S.A., Belov, A.A., Kekelia, M.A. and Shavishvili, I.D. 1987. Paleozoic tectonic  
15  
163847 development of the Caucasus and Turkey (Geotraverse C). In: Flügel, H.V., Sassi, F.P.  
17  
183848 and Grecula, P. (Eds.), *Pre-Variscan and Variscan events in the Alpine-Mediterranean*  
19  
203849 *Mountain Belts. Mineralia slovacica, Monography, Alfa Bratislava*, 23-50.
- 21  
223850 Adamia, S., Zakariadze, G., Chkhotua, T., Sadradze, N., Tsereteli, N., Chabukiani, A. and  
23  
243851 Gventsadze, A. 2011. Geology of the Caucasus: a review. *Turkish Journal of Earth*  
25  
263852 *Sciences*, 20, 489-544.
- 27  
283853 Aït Lahna A., Youbi, N., Tassinari, C.C.G., Basei, M.A.S., Ernst, R.E., Chaib, L., Barzouk,  
29  
303854 A., Mata J., Gärtner, A., Admou, H., Boumehdi, M.A., Söderlund, U., Bensalah, M.K.,  
31  
323855 Bodinier, J.-L., Maacha L. and Bekker, A. 2020. *Journal of African Earth Sciences*,  
33  
343856 171, 103946.
- 35  
363857 Ajaji, T., Weis, D., Giret, A. and Bouabdellah, M. 1998. Coeval potassic and sodic  
37  
383858 calcalkaline series in post-collisional Hercynian Tanncherfi intrusive complex,  
39  
403859 northeastern Morocco: geochemical, isotopic and geochronological evidence. *Lithos*,  
41  
423860 45, 371-393.
- 43  
443861 Albert, R., Arenas, R., Gerdes, A., Sánchez Martínez, S., Fernández-Suárez, J. and  
45  
463862 Fuenlabrada, J.M. 2015. Provenance of the Variscan Upper Allochthon (Cabo Ortegal  
47  
483863 Complex, NW Iberian Massif). *Gondwana Research*, 28, 1434-1448.  
49  
503864 <https://doi.org/10.1016/j.gr.2014.10.016>.
- 51  
523865 Alcock, J.E., Martínez Catalán, J.R., Arenas, R. and Díez Montes, A. 2009. Use of thermal  
53  
543866 modeling to assess the tectono-metamorphic history of the Lugo and Sanabria gneiss  
55  
563867 domes, Northwest Iberia. *Bulletin de la Société Géologique de France*, 180 (3), 179-  
57  
583868 197.

- 3869 Alcock, J.E., Martínez Catalán, J.R., Rubio Pascual, F.J., Díez Montes, A., Díez Fernández,  
1  
23870 R., Gómez Barreiro, J., Arenas, R., Dias da Silva, Í. and González Clavijo, E. 2015. 2-  
3  
43871 D thermal modeling of HT-LP metamorphism in NW and Central Iberia: Implications  
5  
63872 for Variscan magmatism, rheology of the lithosphere and orogenic evolution.  
73873 *Tectonophysics*, 657, 21-37. <https://doi.org/10.1016/j.tecto.2015.05.022>.
- 8  
93874 Aleksandrowski, P. and Mazur, S. 2002. Collage tectonics in the northeasternmost part of the  
10  
113875 Variscan Belt: the Sudetes, Bohemian Massif. In: Winchester, J.A., Pharaoh, T.C. and  
12  
133876 Verniers (Eds.), *Palaeozoic Amalgamation of Central Europe*. Geological Society,  
14  
153877 London, Special Publication 201, 237-277.
- 16  
173878 Aller, J., Bastida Aller, J., Valín, M. L., García-López, S., Brime, C., and Bastida, F. 2005.  
18  
193879 Superposition of tectono-thermal episodes in the southern Cantabrian Zone (foreland  
20  
213880 thrust and fold belt of the Iberian Variscides, NW Spain), *Bulletin de la Société*  
22  
233881 *Géologique de France*, 176, 503-514.
- 24  
253882 Alonso, J.L., Marcos, A. and Suárez, A. 2009. Paleogeographic inversion resulting from large  
26  
273883 out of sequence breaching thrusts: The León Fault (Cantabrian Zone, NW Iberia). A  
28  
293884 new picture of the external Variscan Thrust Belt in the Ibero-Armorican Arc.  
30  
313885 *Geologica Acta*, 7, 451-473. <https://doi.org/10.1344/105.000001449>.
- 32  
333886 Alonso-Chaves, F.M., Andreo, B., Azañón, J.M., Balanyá, J.C., Booth-Rea, G., Crepo-Blanc,  
34  
353887 A., Delgado, F., Estévez, A., García-Casco, A., García-Deñas, V., López-Garrido,  
36  
373888 A.C., Martín-Algarra, A., Orozco, M., Sánchez-Gómez, M., Sánchez-Navas, A., Sand  
38  
393889 de Galdeano, C. and Torres-Roldán, R.L. 2004. Complejo Alpujárride. Sucesiones  
40  
413890 litológicas, petrología y estratigrafía. In: Vera, J.A. (Ed.), *Geología de España*, SGE-  
423891 IGME, Cap. 4, Madrid, 409-414.
- 43  
443892 Álvarez-Marrón, J. 1995. Three dimensional geometry and interference of fault-bend folds:  
45  
463893 examples from the Ponga Unit, Variscan Belt, NW Spain. *Journal of Structural*  
47  
483894 *Geology*, 17, 549-560, 1995.
- 49  
503895 Álvarez-Marrón, J., Pérez-Estaún, A., Dañobeitia, J.J., Pulgar, J.A., Martínez Catalán, J.R.,  
51  
523896 Marcos, A., Bastida, F., Aller, J., Ayarza Arribas, P., Gallart, J., González-Lodeiro, F.,  
53  
543897 Banda, E., Comas, M.C. and Córdoba, D. 1995. Results from the ESCI-N3.1 and  
55  
563898 ESCI-N3.2 marine deep seismic profiles in the northwestern Galicia Margin. *Revista*  
57  
583899 *de la Sociedad Geológica de España*, 8 (4), 331-339.
- 59  
60  
61  
62  
63  
64  
65

- 3900 Álvarez-Marrón, J., Pérez-Estaún, A., Dañobeitia, J.J., Pulgar, J.A., Martínez Catalán, J.R.,  
1  
23901 Marcos, A., Bastida, F., Ayarza Arribas, P., Aller, J. Gallart, J., González-Lodeiro, F.,  
3  
43902 Banda, E., Comas, M.C. and Córdoba, D. 1996. Seismic structure of the northern  
5  
63903 continental margin of Spain from ESCIN deep seismics profiles. *Tectonophysics*, 264,  
73904 153-174.  
8  
93905 Álvarez Valero, A.M., Gómez Barreiro, J., Alampi, A., Castiñeiras, P. and Martínez Catalán,  
10  
113906 J.R. 2014. Local isobaric heating above an extensional detachment in the middle crust  
12  
133907 of a Variscan allochthonous terrane (Órdenes complex, NW Spain). *Lithosphere*, 6 (6),  
14  
153908 409-418. <https://doi.org/10.1130/L369.1>.  
16  
173909 Alvaro, J.-J., Aretz, M., Benhareff, M., Hbiti, M., Puclet, A., El Hadi, H., Koukaya, A.,  
18  
193910 Ettachfani, E.M. and Boudad, L. 2014. Carte géologique du Maroc au 1/50 000, feuille  
20  
213911 Tawz - Mémoire explicatif. Notes et Mémoires du Service Géologique du Maroc, n°  
22  
233912 551bis, 127 pp.  
24  
253913 Álvaro, J.J., Casas, J.M. and Clausen, S. 2017. Ordovician geodynamics: the Sardinian Phase in  
26  
273914 the Pyrenees, Mouthoumet and Montagne Noire massifs. *Géologie de la France*, 1 (4),  
28  
293915 1-83.  
30  
313916 Ancochea, E., Arenas, R., Brandle, J.L., Peinado, M. and Sagredo, J. 1988. Caracterización de  
32  
333917 las rocas metavolcánicas silúricas del Noroeste del Macizo Ibérico. *Geociências*,  
34  
353918 Aveiro 3, 1-2, 23-34.  
36  
373919 Andonaegui, P., González del Tánago, J., Arenas, R., Abati, J., Martínez Catalán, J.R.,  
38  
393920 Peinado, M. and Díaz García, F. 2002. Tectonic setting of the Monte Castelo gabbro  
40  
413921 (Ordenes Complex, northwestern Iberian Massif): Evidence for an arc-related terrane  
42  
433922 in the hanging wall to the Variscan suture. In: Martínez Catalán, J.R., Hatcher Jr.,  
44  
453923 R.D., Arenas, R. and Díaz García, F. (Eds.), *Variscan-Appalachian Dynamics: The*  
463924 *Building of the Late Paleozoic Basement*, Geological Society of America Special  
47  
483925 Paper 364, 37-56.  
49  
503926 Andonaegui, P., Castiñeiras, P., González Cuadra, P., Arenas, R., Sánchez Martínez, S.,  
51  
523927 Abati, J., Díaz García, F. and Martínez Catalán, J.R. 2012. The Corredoiras  
53  
543928 orthogneiss (NW Iberian Massif): Geochemistry and geochronology of the Paleozoic  
55  
563929 magmatic suite developed in a peri-Gondwanan arc. *Lithos*, 128-131, 84-99.  
57  
583930 <https://doi.org/10.1016/j.lithos.2011.11.005>.  
59  
60  
61  
62  
63  
64  
65

- 3931 Andonaegui, P., Sánchez-Martínez, S., Castiñeiras, P., Abati, J. and Arenas, R. 2016.  
1  
2 3932 Reconstructing subduction polarity through the geochemistry of mafic rocks in a  
3  
4 3933 Cambrian magmatic arc along the Gondwana margin (Órdenes Complex, NW Iberian  
5  
6 3934 Massif). *International Journal of Earth Sciences*, 105, 713-725.  
7  
8 3935 <https://doi.org/10.1007/s00531-015-1195-x>.
- 9  
10 3936 Andrade, A.A.S., 1985. Les deux associations basiques-ultrabasiques de Beja (Portugal  
11  
12 3937 méridional) sont-elles des ophiolites hercyniennes? *Ofioliti* 10, 147-160.
- 13  
14 3938 Apalategui, O., Borrero, J.D. and Higuera, P. 1985. División en grupos de rocas en Ossa-  
15  
16 3939 Morena Oriental. 5ª Reunión del Grupo de Ossa-Morena (1983). *Temas Temas*  
17  
18 3940 *Geológico-Mineros, IGME*, 73-80.
- 19  
20 3941 Apalategui Isasa, O. and Higuera, P. 1980. Mapa Geológico Nacional 1:50.000, Hoja 855,  
21  
22 3942 Usagre. Instituto Geológico y Minero de España, Madrid.
- 23  
24 3943 Araújo, A.A. and Ribeiro, A. 1996. Estrutura dos domínios meridionais da Zona de Ossa-  
25  
26 3944 Morena. *Estudos sobre a Geologia da Zona de Ossa-Morena (Maciço Ibérico)*. Livro  
27  
28 3945 de homenagem ao Prof. Francisco Gonçalves, Évora, 169-182.
- 29  
30 3946 Arenas, R. and Martínez Catalán, J.R. 2002. Prograde development of corona textures in  
31  
32 3947 metagabbros of the Sobrado window (Ordenes Complex, NW Iberian Massif). In:  
33  
34 3948 Martínez Catalán, J.R., Hatcher Jr., R.D., Arenas, R. and Díaz García, F. (Eds.),  
35  
36 3949 *Variscan-Appalachian Dynamics: The Building of the Late Paleozoic Basement*,  
37  
38 3950 *Geological Society of America Special Paper*, 364, 73-88.
- 39  
40 3951 Arenas, R. and Martínez Catalán, J.R. 2003. Low-P metamorphism following a Barrovian-  
41  
42 3952 type evolution. Complex tectonic controls for a common transition, as deduced in the  
43  
44 3953 Mondoñedo thrust sheet (NW Iberian Massif). *Tectonophysics*, 365, 143-164.
- 45  
46 3954 Arenas, R. and Sánchez Martínez, S. 2015. Variscan ophiolites in NW Iberia: Tracking lost  
47  
48 3955 Paleozoic oceans and the assembly of Pangea. *Episodes*, 38, 315-333.
- 49  
50 3956 Arenas, R., Rubio Pascual, F.J., Díaz García, F. and Martínez Catalán, J.R. 1995. High-  
51  
52 3957 pressure micro-inclusions and development of an inverted metamorphic gradient in the  
53  
54 3958 Santiago Schists (Ordenes Complex, NW Iberian Massif, Spain): evidence of  
55  
56 3959 subduction and syn-collisional decompression. *Journal of Metamorphic Geology*, 13,  
57  
58 3960 141-164.

- 3961 Arenas, R., Martínez Catalán, J.R., Sánchez Martínez, S., Díaz García, F., Abati, J.,  
1  
23962 Fernández-Suárez, J., Andonaegui, P. and Gómez-Barreiro, J. 2007a. Paleozoic  
3  
43963 ophiolites in the Variscan suture of Galicia (northwest Spain): distribution,  
5  
63964 characteristics and meaning. In: Hatcher, R.D., Jr., Carlson, M.P., McBride, J.H. and  
7  
83965 Martínez Catalán, J.R. (Eds.), 4-D framework of continental crust. Geological Society  
9  
103966 of America, Memoir 200, 425-444. [https://doi.org/10.1130/2007.1200\(22\)](https://doi.org/10.1130/2007.1200(22)).
- 113967 Arenas, R., Martínez Catalán, J.R., Sánchez Martínez, S., Fernández-Suárez, J., Andonaegui,  
12  
133968 P., Pearce, J.A. and Corfu, F. 2007b. The Vila de Cruces Ophiolite: A remnant of the  
14  
153969 early Rheic Ocean in the Variscan suture of Galicia (NW Iberian Massif). *Journal of*  
16  
173970 *Geology*, 115 (2), 129-148.
- 18  
193971 Arenas, R., Sánchez Martínez, S., Castiñeiras, P., Jeffries, T.E., Díez Fernández, R. and  
20  
213972 Andonaegui, P. 2009. The basal tectonic mélange of the Cabo Ortegal Complex (NW  
22  
233973 Iberian Massif): a key unit in the suture of Pangea. *Journal of Iberian Geology*, 35, 85-  
24  
253974 125.
- 26  
273975 Arenas, R., Sánchez Martínez, S., Gerdes, A., Albert, R., Díez Fernández, R. and  
28  
293976 Andonaegui, P. 2014. Re-interpreting the Devonian ophiolites involved in the  
30  
313977 Variscan suture: U-Pb and Lu-Hf zircon data of the Moeche Ophiolite (Cabo Ortegal  
32  
333978 Complex, NW Iberia). *International Journal of Earth Sciences*, 103, 1385-1402.  
34  
353979 <https://doi.org/10.1007/s00531-013-0880-x>.
- 36  
373980 Arenas, R., Sánchez Martínez, S., Díez Fernández, R., Gerdes, A., Abati, J., Fernández-  
38  
393981 Suárez, J., Andonaegui, P., González Cuadra, P., López Carmona, A., Albert, R.,  
40  
413982 Fuenlabrada, J.M. and Rubio Pascual, F.J. 2016. Allochthonous terranes involved in  
42  
433983 the Variscan suture of NW Iberia: A review of their origin and tectonothermal  
44  
453984 evolution. *Earth-Science Reviews*, 161, 140-178.  
46  
473985 <https://doi.org/10.1016/j.earscirev.2016.08.010>.
- 483986 Arriola, A., Chacón, J., Eraso, A., Eguíluz, L., Garrote, A., Sánchez, R. and Vargas, I. 1981.  
49  
503987 Mapa Geológico Nacional 1:50.000, Hoja 829, Villafranca de los Barros. Instituto  
51  
523988 Geológico y Minero de España, Madrid.
- 53  
543989 Arthaud, F. and Matte, P. 1977. Late Paleozoic strike-slip faulting in southern Europe and  
55  
563990 northern Africa: result of a right-lateral shear zone between the Appalachians and the  
57  
583991 Urals. *Geological Society of America Bulletin*, 88, 1305-1320.

- 3992 Ayarza, P., Martínez Catalán, J.R., Gallart, J., Dañobeitia, J.J. and Pulgar, J.A. 1998. Estudio  
1 Sísímico de la Corteza Ibérica Norte 3.3: a seismic image of the Variscan crust in the  
2 3993 hinterland of the NW Iberian Massif. *Tectonics*, 17, 171-186.
- 3 3994  
4  
5  
6 3995 Azor, A., González Lodeiro, F. and Simancas, F. 1994. Tectonic evolution of the boundary  
7 between the Central Iberian and Ossa-Morena zones (Variscan belt, southwest Spain).  
8 3996 *Tectonics*, 13, 45-61.
- 9 3997  
10  
11  
12 3998 Azor, A., Rubatto, D., Simancas, J.F., González Lodeiro, F., Martínez Poyatos, D., Martín  
13 Parra, L.M. and Matas, J. 2008. Rheic Ocean ophiolitic remnants in Southern Iberia  
14 3999 questioned by SHRIMP U-Pb zircon ages on the Beja-Acebuches Amphibolites.  
15 4000 *Tectonics*, 27, TC5006, 1-11. <https://doi.org/10.1029/2008TC002306>.
- 17 4001  
18  
19 4002 Azor, A., Rubatto, D., Marchesi, C., Simancas, J.F., González Lodeiro, F., Martínez Poyatos,  
20 D., Martín Parra, L.M. and Matas, J. 2009. A reply to the comment by C. Pin and J.  
21 4003 Rodríguez Aller on “Rheic Ocean ophiolitic remnants in southern Iberia questioned by  
22 SHRIMP U-Pb zircon ages on the Beja-Acebuches amphibolites”. *Tectonics*, 28.
- 23 4004  
24  
25 4005  
26  
27 4006 Azor Pérez, A. 1997. Evolución tectonometamórfica del límite entre las Zonas Centroibérica  
28 y de Ossa-Morena (Cordillera Varisca, SO de España). Universidad de Granada, 312  
29 4007 pp.
- 30 4008  
31  
32  
33 4009 Baidder, L., Raddi, Y., Tahiri, M. and Michard, A. 2008. Devonian extension of the Pan-  
34 African crust north of the West African Craton and its bearing on the Variscan  
35 4010 foreland deformation: evidence from eastern Anti-Atlas (Morocco). In: Ennih, N. and  
36 Liégeois, J.P. (Eds.). *The Boundaries of the West African Craton*. Geological Society,  
37 4011 London, Special Publication 297, 453-465.
- 38 4012  
39 4013  
40  
41 4014 Baidder, L., Michard, A., Soulaïmani, A., Fekkak, A., Eddebbi, A., Rjimati, E.C. and Raddi,  
42 Y. 2016. Fold interference pattern in thick-skinned tectonics; a case study from the  
43 4015 external Variscan belt of Eastern Anti-Atlas, Morocco. *Journal of African Earth  
44 Sciences*, 119, 204-225.
- 46 4016  
47 4017  
48  
49 4018 Balé, P. and Brun, J.P. 1983. Les chevauchements cadomiens de la Baie de Saint-Brieuc  
50 (Massif Armoricaïn). *Comptes Rendus de l'Académie des Sciences, Paris*, 297, 359-  
51 4019 362.
- 52 4020  
53  
54  
55  
56  
57  
58  
59  
60  
61  
62  
63  
64  
65

- 4021 Balé, P. and Brun, J.P. 1986. Les complexes métamorphiques du Léon (NW Bretagne): un  
1  
24022 segment du domain éo-hercynien sud armoricain translaté au Dévonien. Bulletin de la  
3  
44023 Société Géologique de France, 8, (2), 471-477.
- 5  
64024 Ballèvre, M. 2016. Provinces fauniques et domaines continentaux à l'Ordovicien. Fossiles,  
7  
84025 hors-série VII, 78-87. Editions du Piat, Saint-Julien-du-Pinet, France.
- 9  
104026 Ballèvre, M. and Lardeux, H. 2005. Signification paléoécologique et paléogéographique des  
11  
124027 bivalves du Carbonifère inférieur du bassin d'Ancenis (Massif armoricain). Comptes  
13  
144028 Rendus Palevol, 4, 109-121.
- 15  
164029 Ballèvre, M. and Marchand, J. 1991. Zonation du métamorphisme écolitique dans la nappe  
17  
184030 de Champtoceaux (Massif armoricain, France). Comptes Rendus de l'Académie des  
19  
204031 Sciences de Paris, II-312, 705-711.
- 21  
224032 Ballèvre, M., Kiénast, J.-R. and Paquette, J.-L. 1987. Le métamorphisme écolitique dans la  
23  
244033 nappe hercynienne de Champtoceaux (Massif armoricain). Comptes Rendus de  
25  
264034 l'Académie des Sciences, Paris, II-305, 127-131.
- 27  
284035 Ballèvre, M., Pinardon, J.-L., Kiénast, J.-R. and Vuichard, J.-P. 1989. Reversal of Fe-Mg  
29  
304036 partitioning between garnet and staurolite in eclogite-facies metapelites from the  
31  
324037 Champtoceaux nappe (Brittany, France). Journal of Petrology, 30, 1321-1349.
- 33  
344038 Ballèvre, M., Paris, F. and Robardet, M. 1992. Corrélations ibéro-armoricaines au  
35  
364039 Paléozoïque: une confrontation des données paléobiogéographiques et  
37  
384040 tectonométamorphiques. Comptes-Rendus de l'Académie des Sciences de Paris, 315,  
39  
404041 II, 1783-1789.
- 41  
424042 Ballèvre, M., Marchand, J., Godard, G., Goujou, J.C. and Wyns, R. 1994. The Variscan  
43  
444043 Orogeny in the Armorican Massif. Structure and metamorphism. Eo-Hercynian events  
45  
464044 in the Armorican Massif. In: Keppie, J.D. (Ed.), Pre-Mesozoic Geology in France and  
47  
484045 related areas. Springer-Verlag, Berlin, 183-194.
- 49  
504046 Ballèvre, M., Pitra, P. and Bohn, M. 2003. Lawsonite growth in the epidote blueschists from  
51  
524047 the Ile de Groix (Armorican Massif, France): a potential barometer. Journal of  
53  
544048 Metamorphic Geology, 21, 723-735.
- 55  
564049 Ballèvre, M., Bosse, V., Ducassou, C. and Pitra, P. 2009. Palaeozoic history of the Armorican  
57  
584050 Massif: Models for the tectonic evolution of the suture zones. Comptes Rendus  
59  
604051 Geoscience, 341, 174-201.



- 4052 Ballèvre, M., Fourcade, S., Capdevila, R., Peucat, J.-J., Cocherie, A. and Fanning, C.M. 2012.  
1  
24053 Geochronology and geochemistry of Ordovician felsic volcanism in the Southern  
3  
44054 Armorican Massif (Variscan belt, France): Implications for the breakup of Gondwana.  
54055 Gondwana Research, 21, 1019-1036. <https://doi.org/10.1016/j.gr.2011.07.030>.  
6
- 7  
84056 Ballèvre, M., Martínez Catalán, J.R., López-Carmona, A., Pitra, P., Abati, J., Díez Fernández,  
9  
104057 R., Ducassou, C., Arenas, R., Bosse, V., Castiñeiras, P., Fernández-Suárez, J., Gómez  
114058 Barreiro, J., Paquette, J.L., Peucat, J.J., Poujol, M., Ruffet, G. and Sánchez Martínez,  
12  
134059 S. 2014. Correlation of the nappe stack in the Ibero-Armorican arc across the Bay of  
14  
154060 Biscay: a joint French-Spanish project. In: Schulmann, K., Martínez Catalán, J.R.,  
16  
174061 Lardeaux, J.M., Janousek, V. and Oggiano, G. (Eds.), The Variscan Orogeny: Extent,  
18  
194062 Timescale and the Formation of the European Crust. Geological Society, London,  
20  
214063 Special Publication 405, 77-113, <http://dx.doi.org/10.1144/SP405.13>.  
22
- 234064 Ballèvre, M., Manzotti, P. and Dal Piaz, G.V. 2018. Pre-Alpine (Variscan) inheritance: A key  
24  
254065 for the location of the future Valaisan Basin (Western Alps). *Tectonics*, 37, 786-817.  
264066 <https://doi.org/10.1002/2017TC004633>.  
27
- 28  
294067 Bandrés, A., Eguíluz, L., Pin, C., Paquette, J.L., Ordóñez, B., Le Fèvre, B., Ortega, L.A. and  
30  
314068 Gil Ibarguchi, J.I. 2004. The northern Ossa-Morena Cadomian batholith (Iberian  
32  
334069 Massif): magmatic arc origin and early evolution. *International Journal of Earth  
344070 Sciences*, 93, 860-885. <https://doi.org/10.1007/s00531-004-0423-6>.  
35
- 36  
374071 Baptiste, J. 2016. Cartographie structurale et lithologique du substratum du Bassin parisien et  
38  
394072 sa place dans la chaîne varisque de l'Europe de l'Ouest. *Approches combinées:  
404073 géophysiques, pétrophysiques, géochronologiques et modélisations 2D*. PhD Thesis,  
41  
424074 Université d'Orléans, 367 pp.  
43
- 44  
454075 Barich, A., Acosta-Vigil, A., Garrido, C.J., Cesare, B., Tajčmanová, T. and Bartoli, O. 2014.  
464076 Microstructures and petrology of melt inclusions in the anatexis sequence of Jubrique  
47  
484077 (Betic Cordillera, S Spain): Implications for crustal anatexis. *Lithos*, 206-207, 303-  
49  
504078 320.  
51
- 524079 Barrois, C. 1899. Brioverian system in a sketch of the geology of Central Brittany.  
53  
544080 *Proceedings of the Geological Association*, 16, 101-132.  
55
- 56  
574081 Bastida, F., Marcos, A., Pérez-Estaún, A. and Pulgar, J.A. 1984. Geometría y evolución  
584082 estructural del Manto de Somiedo (Zona Cantábrica, NO España). *Boletín Geológico y  
59  
604083 Minero*, 95, 517-539.  
61  
62  
63  
64  
65

- 4084 Bastida, F., Martínez Catalán, J.R. and Pulgar, J.A. 1986. Structural, metamorphic and  
1 4085 magmatic history of the Mondoñedo nappe (Hercynian belt, NW Spain). *Journal of*  
2  
3 4086 *Structural Geology*, 8, 415-430.  
4
- 5  
6 4087 Baudin, T., Chèvremont, P., Razin, P., Youbi, N., Andriès, D., Hoepffner, C., Thiéblemont,  
7 4088 D., Chihani, E.M. and Tegye, M. 2003. Carte géologique du Maroc au 1/50 000,  
8  
9 4089 feuille de Skhour des Rehamna. Mémoire explicatif. Notes et Mémoires du  
10  
11 4090 Service Géologique du Maroc, 435 bis, 1-114.  
12
- 13  
14 4091 Bea, F., Montero, P., Talavera, C. and Zinger, T. 2006. A revised Ordovician age for the  
15  
16 4092 Miranda do Douro orthogneiss, Portugal. Zircon U-Pb ion-microprobe and LA-ICPMS  
17  
18 4093 dating. *Geologica Acta*, 4 (3), 395-401. <https://doi.org/10.1344/105.000000353>.  
19
- 20 4094 Bea, F., Montero, P., Talavera, C., Abu Anbar, M., Scarrow, J.H., Molina, J.F. and Moreno,  
21  
22 4095 J.A. 2010. The palaeogeographic position of Central Iberia in Gondwana during the  
23  
24 4096 Ordovician: evidence from zircon chronology and Nd isotopes. *Terra Nova*, 22, 341-  
25  
26 4097 346. <https://doi.org/10.1111/j.1365-3121.2010.00957.x>.  
27
- 28 4098 Belka, Z., Ahrendt, H., Franke, W. and Wemmer, K. 2000. The Baltica-Gondwana suture in  
29  
30 4099 central Europe: evidence from K-Ar ages of detrital muscovites and biogeographical  
31  
32 4100 data. In: Franke, W., Haak, V., Oncken, O. and Tanner, D. (Eds.), *Orogenic Processes:*  
33  
34 4101 *Quantification and Modelling in the Variscan Belt*. Geological Society, London,  
35  
36 4102 Special Publication 179, 87-102.  
37
- 38 4103 Bellot, J.P., Bronner, G. and Laverne, C.. 2002. Transcurrent strain partitioning along a suture  
39  
40 4104 zone in the Maures massif (France): Result of eastern indenter tectonics in European  
41  
42 4105 Variscides? In: Martínez Catalán, J.R., Hatcher Jr., R.D., Arenas, R. and Díaz García,  
43  
44 4106 F. (Eds.), *Variscan-Appalachian Dynamics: The Building of the Late Paleozoic*  
45  
46 4107 *Basement*. Geological Society of America Special Paper, 364, 223-237.  
47
- 48 4108 Benyoucef, M., Malti, F.Z., Adaci, M., Fellah, A.H., Abbache A., Cherif, A., Sidhoum, R.  
49  
50 4109 and Bensalah, M. 2015. Evolution lithostratigraphique, paléoenvironnemental et  
51  
52 4110 paléogéographique du flysch de Ben-Zireg (Viséen inférieur, Algérie). *Geodiversitas*,  
53  
54 4111 37, 5-29.  
55
- 56 4112 Berger, J., Féménias, O., Mercier, J.C.C. and Demaiffe, D. 2005. Ocean-floor hydrothermal  
57  
58 4113 metamorphism in the Limousin ophiolites (western French Massif Central):  
59  
60  
61  
62  
63  
64  
65

- 4114 evidence of a rare preserved Variscan oceanic marker. *Journal of Metamorphic*  
1  
24115 *Geology*, 23, 795-812.  
3
- 44116 Berger, J., Féménias, O., Ohnenstetter, D., Bruguier, O., Plissart, G., Mercier, J.C. and Demaiffe,  
5  
64117 D. 2010. New occurrence of UHP eclogites in Limousin (French Massif Central):  
7  
84118 age, tectonic setting and fluid-rock interactions. *Lithos*, 118, 365-382.  
9
- 104119 Bernard-Griffiths, J. and Cornichet, J. 1985. Origin of eclogites from South Brittany, France:  
11  
124120 A Sm-Nd isotopic and REE study. *Chemical Geology*, 52, 185-201.  
13
- 144121 Bernard-Griffiths, J., Gebauer, D., Grünenfelder, M. and Piboule, M. 1985a. The tonalite belt  
15  
164122 of Limousin (French Central Massif): U-Pb zircon ages and geotectonic implications.  
17  
184123 *Bulletin de la Société Géologique de France*, (8) I, 523-529.  
19
- 204124 Bernard-Griffiths, J., Peucat, J.J., Sheppard, S. and Vidal, P. 1985b. Petrogenesis of Hercynian  
21  
224125 leucogranites from the southern Armorican Massif: contribution of REE and isotopic  
23  
244126 (Sr, Nb, Pb and O) geochemical data to the study of source rock characteristics and  
25  
264127 ages. *Earth and Planetary Science Letters*, 74, 235-250.  
27
- 284128 Bernard-Griffiths, J., Carpenter, M.S.N., Peucat, J.J. and Jahn, B.-M. 1986 Geochemical and  
29  
304129 isotopic characteristics of blueschist facies rocks from the Ile de Groix, Armorican  
31  
324130 Massif (northwest France), *Lithos*, 19, 235-253.  
33
- 344131 Bertrand, J.M., Leterrier, J., Cuney, M., Brouand, M., Stussi, M., Delaperrière, E. and  
35  
364132 Virlogeux, D. 2001. Géochronologie U-Pb sur zircons de granitoïdes du Confolentais,  
37  
384133 du massif de Charroux-Civray (seuil du Poitou) et de Vendée. *Géologie de la France*,  
39  
404134 2001 (1-2), 167-189.  
41
- 424135 BGR. 1993. Geologische Karte der Bundesrepublik Deutschland 1:1 000 000. Bundesanstalt  
43  
444136 für Geowissenschaften und Rohstoffe., Hannover.  
45
- 464137 BGR. 2005. The 1:5 Million International Geological Map of Europe and Adjacent Areas.  
47  
484138 Bundesanstalt für Geowissenschaften und Rohstoffe., Hannover. Asch, K. (Compiler).  
49
- 504139 Bitri, A., Brun, J.P., Truffert, C. and Guennoc, P. 2001. Deep seismic imager of the Cadomian  
51  
524140 thrust wedge of Northern Brittany. *Tectonophysics*, 331, 65-80.  
53
- 544141 Bitri, A., Ballèvre, M., Brun, J.P., Chantraine, J., Gapais, D., Guennoc, P., Gumiaux, C. and  
55  
564142 Truffert, C. 2003. Imagerie sismique de la zone de collision hercynienne dans le Sud-  
57  
584143 Est du Massif armoricain (projet Armor 2/programme GéoFrance 3D). *Comptes*  
59  
604144 *Rendus Geoscience*, 335, 969-979. <https://doi.org/10.1016/j.crte.2003.09.002>.  
61  
62  
63  
64  
65

- 4145 Bitri, A., Brun, J.P., Gapais, D., Cagnard, F., Gumiaux, C., Chantraine, J., Martelet, G. and  
1 4146 Truffert, C. 2010. Deep reflection seismic imaging of the internal zone of the South  
2 4147 Armorican Hercynian belt (western France) (ARMOR 2/programme GéoFrance 3D).  
3 4148 Comptes Rendus Geoscience, 342, 448-452.  
4 4149 <https://doi.org/10.1016/j.crte.2010.03.006>.  
5 4150  
6  
7  
8  
9 4151 Blanco-Ferrera, S., Sanz-López, J., Garcia-López, S. and Bastida, F. 2017. Tectonothermal  
10 4152 evolution of the northeastern Cantabrian zone (Spain). International Journal of Earth  
11 4153 Sciences, 106, 1539-1555. <https://doi.org/10.1007/s00531-016-1365-5>.  
12 4154  
13 4155 Blatrix, P. and Burg, J.P. 1981.  $^{40}\text{Ar}/^{39}\text{Ar}$  dates from Sierra Morena (Southern Spain):  
14 4156 Variscan metamorphism and Cadomian Orogeny. Neues Jahrbuch für Mineralogie  
15 4157 Monatshefte, 10, 470-478.  
16 4158  
17 4159 Blümel, P. 1990. The Moldanubian region in Bavaria. International Conference on Paleozoic  
18 4160 Orogens in Central Europe. Göttingen-Giessen. Field Guide: Bohemian Massif, 143-  
19 4161 179.  
20 4162  
21 4163 Blümel, P., Franke, W. and Stein, E. 1990. Saxothuringian Zone. International Conference on  
22 4164 Paleozoic Orogens in Central Europe. Göttingen-Giessen. Field Guide: Bohemian  
23 4165 Massif, 181-205.  
24 4166  
25 4167 Boillot, G., Montadert, L., Lemoine, M. and Biju Duval, B. 1984. Les marges continentales  
26 4168 actuelles et fossiles autour de la France. Masson, Paris, 342 pp.  
27 4169  
28 4170 Boogaard, M., Van den and Vázquez, F. 1981. Conodont faunas from Portugal and  
29 4171 Southwestern Spain. Part 5. Lower Carboniferous conodonts at Santa Olalla de Cala  
30 4172 (Spain). Scripta Geologica, 61, 1-8.  
31 4173  
32 4174 Bosse, V., Féraud, G., Ruffet, G., Ballèvre, M., Peucat, J.J. and de Jong, K. 2000. Late  
33 4175 Devonian subduction and early orogenic exhumation of eclogite-facies rocks from the  
34 4176 Champtoceaux complex (Variscan belt, France). Geological Journal, 35, 297-325.  
35 4177  
36 4178 Bosse, V., Ballèvre, M. and Vidal, O. 2002. Ductile thrusting recorded by the garnet isograd  
37 4179 from blueschist-facies metapelites of the Ile de Groix, Armorican Massif, France.  
38 4180 Journal of Petrology, 43, 485-510.  
39 4181  
40 4182 Bosse, V., Féraud, G., Ballèvre, M., Peucat, J.J. and Corsini, M. 2005. Rb-Sr and  $^{40}\text{Ar}/^{39}\text{Ar}$   
41 4183 ages in blueschists from the Ile de Groix (Armorican Massif, France): Implications for  
42 4184 closure mechanisms in isotopic systems. Chemical Geology, 220, 21-45.  
43 4185  
44  
45  
46  
47  
48  
49  
50  
51  
52  
53  
54  
55  
56  
57  
58  
59  
60  
61  
62  
63  
64  
65

- 4176 Bouton, P. and Branger, P. 2007. Notice explicative de la carte géologique de France au 1:50  
1  
24177 000, feuille Coulonges-sur-l'Autize, 587. BRGM, Orléans.  
3
- 44178 Bouton, P. and Camuzard, J.P. 2012. Le Givétien de la Villedé d'Ardin (Sud du Massif  
5  
64179 armoricain, France): une série discordante sur un socle cadomien? Annales de la  
7  
84180 Société Géologique du Nord, 19, 25-34.  
9
- 104181 Bouybaouene, M., Michard, A. and Goffé, B. 1998. High-pressure granulites on top of the  
11  
124182 Beni Bousera peridotites, Rif Belt, Morocco; a record of an ancient thickened crust in  
13  
144183 the Alboran Domain. Bulletin de la Société Géologique de France, 169, 153-162.  
15
- 164184 Boyden, J.A., Müller, R.D., Gurnis, M., Torsvik, T.H., Clark, J.A., Turner, M., Ivey-Law, H.,  
17  
184185 Watson, R.J. and Cannon, J.S. 2011. Next-generation plate-tectonic reconstructions  
19  
204186 using GPlates. In: Keller, G.R. and Baru, C. (Eds.), Geoinformatics:  
21  
224187 Cyberinfrastructure for the Solid Earth Sciences. Cambridge University Press,  
23  
244188 Cambridge, 95-114.  
25
- 264189 Boyer, S.E. 1995. Sedimentary basin taper as a factor controlling the geometry and advance  
27  
284190 of thrust belts. American Journal of Science, 295, 1220-1254.  
29
- 304191 Brahimi, S., Liégeois, J.P., Ghienne J.F., Munsch, M. and Bourmatte, A. 2018. The Tuareg  
31  
324192 shield terranes revisited and extended towards the northern Gondwana margin:  
33  
344193 Magnetic and gravimetric constraints. Earth-Science Reviews, 185, 572-599.  
35  
364194 <https://doi.org/10.1016/j.earscirev.2018.07.002>.  
37
- 384195 Braid, J.A., Murphy, J.B., Quesada, C. and Mortensen, J. 2011. Tectonic escape of a crustal  
39  
404196 fragment during the closure of the Rheic Ocean: U-Pb detrital zircon data from the  
41  
424197 Late Palaeozoic Pulo do Lobo and South Portuguese zones, southern Iberia. Journal of  
43  
444198 the Geological Society, 168 (2), 383-392.  
45
- 464199 BRGM. 1972. Carte magnétique de la France. Anomalies détaillées du champ total à l'échelle  
47  
484200 du 1/1000 000. Ministère du Développement Industriel et Scientifique, Bureau de  
49  
504201 Recherches Géologiques et Minières, Service, Géologique National. Orléans, col. map  
51  
524202 106 x 112 cm, 2 feuilles 64 x 120 cm et 60 x 120 cm. G5831 .C93 1971 .F7 North  
53  
544203 Sheet; G5831 .C93 1971 .F7 South Sheet.  
55
- 564204 BRGM. 1996. Carte Géologique de la France à l'échelle du millionième, 6<sup>e</sup> édition. Bureau de  
57  
584205 Recherches Géologiques et Minières. Chantraine, J., Autran, A., Cavelier, C. et al.  
59  
604206 (Eds.).  
61  
62  
63  
64  
65

- 4207 Briand, B. 1978. Métamorphisme inverse et chevauchement de type "himalayen" dans la  
1  
24208 vallée du Lot (Massif Central français). Comptes Rendus de l'Académie des  
3  
44209 Sciences, Paris, 286, D, 729-731.
- 5  
64210 Briand, B. and Santallier, D. 1994. Basic and ultrabasic magmatism: Metabasites and  
7  
84211 Paleozoic openings in the French Massif Central. Highly transformed metabasites. In:  
9  
104212 Keppie, J.D. (Ed.), Pre-Mesozoic Geology in France and related areas. Springer-  
11  
124213 Verlag, Berlin, 343-349.
- 13  
144214 Bröcker, M., Żelaźniewicz, A. and Enders, M. 1998. Rb-Sr and U-Pb geochronology of  
15  
164215 migmatitic gneisses from the Góry Sowie (West Sudetes, Poland): the importance of  
17  
184216 Mid-Late Devonian metamorphism. Journal of the Geological Society, London, 155  
19  
204217 (6):1025-1036.
- 21  
224218 Bronner, G. and Bellot, J.P. 2000. The inverted nodule-rich Bagaud-Malalongue Formation:  
23  
244219 an Early Carboniferous synorogenic flysch in the Maures massif (SE France):  
25  
264220 paleogeographic, structural and geodynamic implications. In: Variscan-Appalachian  
27  
284221 dynamics: the building of the Upper Paleozoic basement. Basement Tectonics 15, A  
29  
304222 Coruña, Spain, Program and Abstracts, 73-74.
- 31  
324223 Brun, J.P. and Burg, J.P. 1982. Combined thrusting and wrenching in the Ibero-Armorican  
33  
344224 arc: a corner effect during continental collision. Earth and Planetary Science Letters,  
35  
364225 61, 319-332.
- 37  
384226 Buła, Z., Habryn, R., Jachowicz-Zdanowska, M. and Żaba, J. 2015. Precambrian and Lower  
39  
404227 Paleozoic of the Brunovistulicum (eastern part of the Upper Silesian Block, southern  
41  
424228 Poland) – the state of the art. Geological Quarterly, 59 (1), 123-134.
- 43  
444229 Burg, J.P. and Matte, P. 1978. A cross section through the french Massif Central and the  
45  
464230 scope of its Variscan geodynamic evolution. Zeitschrift der Deutschen Geologischen  
47  
484231 Gesellschaft, 129, 429-460.
- 49  
504232 Burkhard, M., Caritg, S., Helg, U., Robert-Charrue, Ch. and Soulimani, A. 2006. Tectonics  
51  
524233 of the Anti-Atlas of Morocco. In: Saddiqi, O., Michard, A. and Frizon de Lamotte, D.  
53  
544234 (Eds.), Recent Developments on the Maghreb Geodynamics. Comptes Rendus  
55  
564235 Geoscience, Special Volume 338, 11-24.

- 4236 Cabanis, B. and Godard, G. 1987. Les eclogites du Pays de Léon (Nord-Ouest du Massif  
1 4237 Armoricain): étude pétrologique et géochimique, implications géodynamiques.  
2 4238 Bulletin de la Société Géologique de France, 8 (3), 1133-1142.  
3  
4  
5  
6 4239 Capdevila, R. 1969. Le métamorphisme régional progressif et les granites dans le segment  
7 4240 hercynien de Galice nord oriental (NW de l'Espagne). PhD Thesis, Université de  
8 4241 Montpellier, 430 pp.  
9  
10  
11  
12 4242 Capdevila, R. and Floor, P. 1970. Les différents types de granites hercyniens et leur  
13 4243 distribution dans le Nord-Ouest de l'Espagne. Boletín Geológico y Minero, Instituto  
14 4244 Geológico y Minero de España, 81, 215-225.  
15  
16  
17  
18 4245 Cappelli, B., Carmignani, L., Castorina, F., Di Pisa, A., Oggiano, G. and Petrini, R.A. 1992.  
19 4246 Hercynian suture zone in Sardinia: geological and geochemical evidence.  
20 4247 Geodinamica Acta, 5, 101-118.  
21  
22  
23  
24 4248 Cardozo, N. 2008. Trishear in 3D. Algorithms, implementation, and limitations. Journal of  
25 4249 Structural Geology, 30 (3), 327-340.  
26  
27  
28 4250 Carlé, W. 1945. Ergebnisse geologischer Untersuchungen im Grundgebirge von Galicien  
29 4251 (Norwest Spanien). Geotektonische Forschungen, 6, 13-36. (Translated to Spanish in:  
30 4252 Publicaciones Extranjeras sobre Geología de España, 1950, V, 61-90).  
31  
32  
33  
34 4253 Carls, P., Gozalo, R., Valenzuela-Ríos, J.I. and Truyols-Massoni, M. 2004. Cordilleras Ibérica  
35 4254 y Costero-Catalana: El basamento prealpino. La sedimentación marina devono-  
36 4255 carbonífera. In: Vera, J.A. (Ed.), Geología de España. SGE-IGME, Madrid, 475-479.  
37  
38  
39  
40 4256 Carosi, R., Petroccia, A., Iaccarino, S., Simonetti, M., Langone, A. and Montomoli, C. 2020.  
41 4257 Kinematics and Timing Constraints in a Transpressive Tectonic Regime: The Example  
42 4258 of the Posada-Asinara Shear Zone (NE Sardinia, Italy). Geosciences, 10, 288, 1-26.  
43 4259 <https://doi.org/10.3390/geosciences10080288>.  
44  
45  
46  
47  
48 4260 Carracedo, M., Paquette, J.L., Alonso Olazabal, A., Santos Zalduegui, J.F., García de  
49 4261 Madinabeitia, S., Tiepolo, M. and Gil Ibarguchi, J.I. 2009. U-Pb dating of granodiorite  
50 4262 and granite units of the Los Pedroches batholith. Implications for geodynamic models  
51 4263 of the southern Central Iberian Zone (Iberian Massif). International Journal of Earth  
52 4264 Sciences, 98 (7), 1609-1624. <https://doi.org/10.1007/s00531-008-0317-0>.  
53  
54  
55  
56  
57  
58 4265 Carreras, J. and Druguet, E. 2014. Framing the tectonic regime of the NE Iberian Variscan  
59 4266 segment. In: Schulmann, K., Martínez Catalán, J.R., Lardeaux, J.M., Janousek, V. and  
60  
61  
62  
63  
64  
65

- 4267 Oggiano, G. (Eds.), *The Variscan Orogeny: Extent, Timescale and the Formation of*  
1 4268 *the European Crust*. Geological Society, London, Special Publications, 405, 249-264,  
2  
3 4269 <http://dx.doi.org/10.1144/SP405.7>.  
4
- 5  
6 4270 Carron, J.P., Le Guen de Kerneizon, M. and Nachit, H. 1994. Variscan Granites from  
7  
8 4271 Brittany. In: Keppie, J.D. (Ed.), *Pre-Mesozoic Geology in France and related areas:*  
9  
10 4272 *Springer-Verlag, Berlin, 231-239.*
- 11  
12 4273 Cartier, C. and Faure, M. 2004. The Saint-Georges-sur-Loire olistostrome, a key zone to  
13  
14 4274 understand the Gondwana-Armorica boundary in the Variscan belt (Southern Brittany,  
15  
16 4275 France). *International Journal of Earth Sciences*, 93, 945-958.  
17 4276 <https://doi.org/10.1007/s00531-004-0398-3>.  
18
- 19  
20 4277 Casas, J.M. 2010. Ordovician deformations in the Pyrenees: new insights into the significance  
21  
22 4278 of pre-Variscan ('sardic') tectonics. *Geological Magazine*, 147 (5), 674-689.  
23 4279 <https://doi.org/10.1017/S0016756809990756>.  
24
- 25  
26 4280 Casas, J.M., Sánchez-García, T., Álvaro, J.J., Puddu, C. and Liesa, M. 2017. Ordovician  
27  
28 4281 magmatism in the Pyrenees. In: *Ordovician Geodynamics: the Sardic Phase in the*  
29  
30 4282 *Pyrenees, Mouthoumet and Montagne Noire massifs*. Álvaro, J.J., Casas, J.M. and  
31 4283 Clausen, S. (Eds.), *Géologie de la France*, 1 (4), 12.  
32
- 33  
34 4284 Casas, J.M. and Murphy, J.B. 2018. Unfolding the arc: The use of pre-orogenic constraints to  
35  
36 4285 assess the evolution of the Variscan belt in Western Europe. *Tectonophysics*, 736, 47-  
37 4286 61. <https://doi.org/10.1016/j.tecto.2018.04.012>.  
38
- 39  
40 4287 Casquet, C. and Galindo, C. 2004. Zona Sudportuguesa: Magmatismo varisco y postvarisco  
41  
42 4288 en la Zona de Ossa-Morena. In: Vera, J.A. (Ed.), *Geología de España*, SGE-IGME,  
43 4289 Madrid, Cap. 2, 194-199.  
44
- 45  
46 4290 Castiñeiras, P., Villaseca, C., Barbero, L. and Martín Romera, C. 2008. SHRIMP U–Pb zircon  
47  
48 4291 dating of anatexis in high-grade migmatite complexes of Central Spain: implications  
49  
50 4292 in the Hercynian evolution of Central Iberia. *International Journal of Earth Sciences*,  
51 4293 97, 35-50. <https://doi.org/10.1007/s00531-006-0167-6>.  
52
- 53  
54 4294 Castiñeiras, P., Díaz García, F. and Gómez Barreiro, J. 2010. REE-assisted U-Pb zircon age  
55  
56 4295 (SHRIMP) of an anatectic granodiorite: constraints on the evolution of the A Silva  
57 4296 granodiorite, Iberian Allochthonous Complexes. *Lithos*, 116 (1-2), 153-166.  
58  
59 4297 <https://doi.org/10.1016/j.lithos.2010.01.013>.  
60  
61  
62  
63  
64  
65



- 4298 Castro, A., Fernández, C., De la Rosa, J.D., Moreno-Ventas, I., El-Hmidi, H., El-Biad, M.,  
1  
24299 Bergamín, J.F. and Sánchez, N. 1996a. Triple-junction migration during Paleozoic  
3  
44300 plate convergence: the Aracena metamorphic belt, Hercynian massif, Spain.  
54301 *Geologische Rundschau*, 85, 180-185.  
6
- 7  
84302 Castro, A., Fernandez, C., de la Rosa, J.D., Moreno-Ventas, I. and Rogers, G. 1996b.  
9  
104303 Significance of MORB-derived amphibolites from the Aracena metamorphic belt, SW  
114304 Spain. *Journal of Petrology*, 37, 235-260.  
12
- 13  
144305 Castro, A., Fernández, C., El-Hmidi, H., El-Biad, M., Díaz Azpiroz, M., De La Rosa, J.D. and  
154306 Stuart, F. 1999. Age constraints to the relationships between magmatism,  
16  
174307 metamorphism and tectonism in the Aracena metamorphic belt, southern Spain.  
18  
194308 *International Journal of Earth Sciences*, 88, 26-37.  
20
- 21  
224309 Cavet, P., Gruet, M. and Pillet, J. 1966. Sur la présence du Cambrien à Paradoxides à Cléré-  
234310 sur-Layon (M.-et-L.) dans le Nord-Est du Bocage Vendéen (Massif armoricain).  
24  
254311 *Comptes Rendus de l'Académie des Sciences, Paris*, D-263, 1685-1688.  
26
- 27  
284312 Cavet, P., Lardeux, H. and Philippot, A. 1971. Ordovicien et Silurien aux environs de  
294313 Montjean et Chalonnes (Maine-et-Loire, Sud-Est du Massif armoricain). *Mémoires du*  
30  
314314 *Bureau de Recherches Géologiques et Minières*, 73, 199-212.  
32
- 33  
344315 Cerrina Feroni, A., Ellero, A., Malusà, M.G., Musumeci, G., Ottria, G., Polino, R. and Leoni,  
354316 L. 2010. Transpressional tectonics and nappe stacking along the Southern Variscan  
36  
374317 Front of Morocco. *International Journal of Earth Sciences*, 99, 1111-1122.  
38  
394318 <https://doi.org/10.1007/s00531-009-0449-x>.  
40
- 41  
424319 Chantraine, J., Auvray, B., Brun, J.P., Chauvel, J.J. and Rabu, D. 1994a. The Cadomian  
434320 Orogeny in the Armorican Massif. Introduction. In: Keppie, J.D. (Ed.), *Pre-Mesozoic*  
44  
454321 *Geology in France and related areas*: Springer-Verlag, Berlin, 75-80.  
46
- 47  
484322 Chantraine, J., Chauvel, J.J. and Rabu, D. 1994b. The Cadomian Orogeny in the Armorican  
494323 Massif, Lithostratigraphy. In: Keppie, J.D. (Ed.), *Pre-Mesozoic Geology in France and*  
50  
514324 *related areas*. Springer-Verlag, Berlin, 81-95.  
52
- 53  
544325 Chantraine, J., Auvray, B. and Rabu, D. 1994c. The Cadomian Orogeny in the Armorican  
554326 Massif, Igneous activity. In: Keppie, J.D. (Ed.), *Pre-Mesozoic Geology in France and*  
56  
574327 *related areas*. Springer-Verlag, Berlin, 111-125.  
58

- 4328 Chardon, D., Aretz, M. and Roques, D. 2020. Reappraisal of Variscan thrust tectonics in the  
1  
24329 southern French Massif Central. *Tectonophysics*, 787, 1-16, 228477.  
3  
44330 <https://doi.org/10.1016/j.tecto.2020.228477>.  
5  
64331 Chelle-Michou, C., Laurent, O., Moyen, J.F., Block, S., Paquette, J.L., Couzinié, S., Gardien,  
7  
84332 V., Vanderhaeghe, O., Villaros, A. and Zeh, A. 2017. Pre-Cadomian to late-Variscan  
9  
94333 odyssey of the eastern Massif Central, France: Formation of the West European crust  
10  
114334 in a nutshell. *Gondwana Research*, 46, 170-190.  
12  
134335 <http://dx.doi.org/10.1016/j.gr.2017.02.010>.  
14  
154336 Chlupáč, I. 1989. Fossil communities in the metamorphic Lower Devonian of the Hrubý  
16  
174337 Jeseník Mts., Czechoslovakia. *Neues Jahrbuch für Geologie und Paläontologie*,  
18  
194338 *Abhandlungen* 177, 367-392.  
20  
214339 Chlupáčová, M. and Švancara, J., 1994. Hustotní model geologické stavby podél geotraverzu  
22  
234340 9HR a nadstavbové zpracování tíhového pole západní části Českého masívu, č0  
24  
254341 1028/02-b. Czech Geological Survey report.  
26  
274342 Chopin, F., Corsini, M., Schulmann, K, El Houicha, M., Ghienne, J.F. and Edel, J.B. 2014.  
28  
294343 Tectonic evolution of the Rehamna metamorphic dome (Morocco) in the context of  
30  
314344 the Alleghanian-Variscan orogeny. *Tectonics*, 33, 1154-1177.  
32  
334345 <https://doi.org/10.1002/2014TC003539>.  
34  
354346 Chopin, F., Schulmann, K., Skrzypek, E., Lehmann, J., Dujardin, J.R., Martelat, J.E., Lexa,  
36  
374347 O., Corsini, M., Edel, J.B., Štípská, P. and Pitra, P. 2012. Crustal influx, indentation,  
38  
394348 ductile thinning and gravity redistribution in a continental wedge: Building a  
40  
414349 Moldanubian mantled gneiss dome with underthrust Saxothuringian material  
42  
434350 (European Variscan belt). *Tectonics*, 31, TC1013, 1-27.  
44  
454351 <https://doi.org/10.1029/2011TC002951>.  
46  
474352 Choukroune, P., Le Pichon, X., Seguret, M. and Sibuet, J.C. 1973a. Bay of Biscay and  
48  
494353 Pyrenees. *Earth and Planetary Science Letters*, 18, 109-118.  
50  
514354 Choukroune, P., Seguret, M. and Galdeano, A. 1973b. Caractéristiques et evolution  
52  
534355 structurale des Pyrénées: un modèle de relation entre zone orogénique et mouvement  
54  
554356 des plaques. *Bulletin de la Société Géologique de France*, 7, XV, 601-611.

- 4357 Clark, A.H., Scott, D.J., Sandeman, H.A., Bromley, A.V. and Farrar, E. 1998. Siegenian  
1 generation of the Lizard ophiolite: U-Pb zircon age data for plagiogranite, Porthkerris,  
2 4358 Cornwall. *Journal of the Geological Society, London*, 155, p. 595-598.
- 3 4359  
4  
5  
6 4360 Clariana, P., Valverde-Vaquero, P., Rubio, Á., Beranoaguirre, A. and García-Sanseguendo, J.  
7  
8 4361 2017. Upper Ordovician magmatism in the Central Pyrenees: First U-Pb zircon age  
9  
10 4362 from the Pallaresa Massif. In: *Ordovician Geodynamics: the Sardinic Phase in the*  
11 4363 *Pyrenees, Mouthoumet and Montagne Noire massifs*. Álvaro, J.J., Casas, J.M. and  
12  
13 4364 Clausen, S. (Eds.), *Géologie de la France*, 1 (4), 15-16.
- 14  
15 4365 Cochelin, B., Chardon, D., Denèle, Y., Gumiaux, C. and Le Bayon, B. 2017. Vertical strain  
16  
17 4366 partitioning in hot Variscan crust: Syn-convergence escape of the Pyrenees in the  
18  
19 4367 Iberian-Armorican syntax. *Bulletin de la Société Géologique de France*, 188, 39, 1-25,  
20  
21 4368 doi.org/10.1051/bsgf/2017206.
- 22  
23 4369 Cocherie, A., Baudin, T., Autran, A., Guerrot, C., Fanning, M. and Laumonier, B. 2005. U-Pb  
24  
25 4370 zircon (ID-TIMS and SHRIMP) evidence for the early Ordovician intrusion of  
26  
27 4371 metagranites in the late Proterozoic Canaveilles Group of the Pyrenees and the  
28  
29 4372 Montagne Noire (France). *Bulletin de la Société Géologique de France*, 176, 269-  
30  
31 4373 282.
- 32  
33 4374 Cocco, F., Oggiano, G., Funedda, A., Loi, A. and Casini, L. 2018. Stratigraphic, magmatic  
34  
35 4375 and structural features of Ordovician tectonics in Sardinia (Italy): a review. *Journal of*  
36  
37 4376 *Iberian Geology*, 44 (4), 619-639. <https://doi.org/10.1007/s41513-018-0075-1>.
- 38  
39 4377 Colchen, M. 1974. *Géologie de la Sierra de la Demanda, Burgos-Logroño (Espagne)*.  
40  
41 4378 *Memorias del Instituto Geológico y Minero de España*, 85, 1-436.
- 42  
43 4379 Collett, S., Štípská, P., Kusbach, V., Schulmann, K. and Marciniak, G. 2017. Dynamics of  
44  
45 4380 Saxothuringian subduction channel/wedge constrained by phase-equilibria modelling  
46  
47 4381 and micro-fabric analysis. *Journal of Metamorphic Geology*, 35, 253-280.  
48  
49 4382 <https://doi.org/10.1111/jmg.12226>.
- 50  
51 4383 Collett, S., Štípská, P., Schulmann, K., Peřestý, V., Soldner, J., Anczkiewicz, R., Lexa, O.,  
52  
53 4384 Kylander-Clark, A. 2018. Combined Lu-Hf and Sm-Nd geochronology of the  
54  
55 4385 Mariánské Lázně Complex: New constraints on the timing of eclogite-and granulite-  
56  
57 4386 facies metamorphism. *Lithos*, 304, 74-94.

- 4387 Collett, S., Štípská, P., Schulmann, K., Míková, J. and Kröner, A. 2021. Tectonic significance of the  
1 4388 Variscan suture between Brunovistulia and the Bohemian Massif. *Journal of the*  
2 Geological Society, London. <https://doi.org/10.1144/jgs2020-176>.  
3 4389  
4  
5  
6 4390 Corretgé, L.G. and Suárez, O. 1990. Cantabrian and Palentian Zones. *Igneous Rocks*. In:  
7 4391 Dallmeyer R.D. and Martínez García E. (Eds.), *Pre-Mesozoic Geology of Iberia*.  
8 Springer-Verlag. Berlin, 72-79.  
9 4392  
10  
11  
12 4393 Corsini, M. and Rolland, Y. 2009. Late evolution of the southern European Variscan belt:  
13 4394 Exhumation of the lower crust in a context of oblique convergence. *Comptes Rendus*  
14 Geoscience, 341, 214-223. <https://doi.org/10.1016/j.crte.2008.12.002>.  
15 4395  
16  
17  
18 4396 Cortesogno, L., Gaggero, L., Oggiano, G. and Paquette, J.L. 2004. Different tectonothermal  
19 4397 evolutionary paths in eclogitic rocks from the axial zone of the Variscan Chain in  
20 Sardinia (Italy) compared with the Ligurian Alps. *Ofioliti*, 29, 125-144.  
21 4398  
22  
23  
24 4399 Costa, S. 1989. Age radiométrique  $^{39}\text{Ar}/^{40}\text{Ar}$  du métamorphisme des séries du Lot et du  
25 4400 charriage du groupe leptynoamphibolique de Marvejols (MCF). *Comptes Rendus de*  
26 l'Académie des Sciences, Paris, II, 309, 561-567.  
27 4401  
28  
29  
30 4402 Costa, S., Maluski, H. and Lardeaux, J.M. 1993.  $^{40}\text{Ar}/^{39}\text{Ar}$  chronology of Variscan tectono-  
31 4403 metamorphic events in an exhumed crustal nappe: the Monts du Lyonnais complex  
32 (Massif Central, France). *Chemical Geology (Isotope Geoscience section)*, 105, 339-  
33 4404 359.  
34  
35 4405  
36  
37  
38 4406 Crespo-Blanc, A. and Orozco, M. 1988. The Southern Iberian Shear Zone: a major boundary  
39 4407 in the Hercynian folded belt. *Tectonophysics*, 148, 221-227.  
40  
41  
42 4408 Crespo-Blanc, A. and Orozco, M. 1991. The boundary between the Ossa-Morena and  
43 4409 Southportuguese Zones (Southern Iberian Massif): a major suture in the European  
44 Hercynian Chain. *Geologische Rundschau*, 80, 691-702.  
45 4410  
46  
47  
48 4411 Cristallini, E.O. and Allmendinger, R.W. 2001. Pseudo-3D modeling of trishear fault  
49 4412 propagation folding. *Journal of Structural Geology*, 23 (12), 1883-1899.  
50  
51  
52 4413 Cuney, M., Stussi, J.M., Brouand, M., Dautel, D., Michard, A., Gros, Y., Poncet, D., Bouton,  
53 4414 P., Colchen, M. and Vervialle, J.P. 1993. Géochimie et géochronologie U-Pb des  
54 4415 diorites quartziques du Tallud et de Montcoutant: nouveaux arguments pour une  
55 extension de la «Ligne Tonalitique Limousine» en Vendée. *Comptes Rendus de*  
56 4416 l'Académie des Sciences, Paris, II-316, 1383-1390.  
57 4417  
58  
59  
60  
61  
62  
63  
64  
65

- 4418 Czech Geological Survey. 2007. Geological Map of the Czech Republic, 1:500 000. Cháb, J.,  
1  
24419 Stráník, Z. and Eliáš, M. (Compilers).  
3  
44420 Dabard, M.P., Loi, A., Pavanetto, P., Meloni, M.A., Hauser, N., Matteini, M. and Funedda, A.  
5  
64421 2021. Provenance of Ediacarian-Ordovician sediments of the Medio Armorican  
7  
84422 Domain, Brittany, West France: Constraints from U/Pb detrital zircon and Sm-Nd  
9  
94423 isotope data. *Gondwana Research*, 90, 63-76. <https://doi.org/10.1016/j.gr.2020.11.004>.  
10  
11  
124424 Dallmeyer, R.D. and Martínez García, E. (Eds.). 1990. Pre-Mesozoic Geology of Iberia.  
13  
144425 Springer-Verlag. Berlín, 416 pp.  
15  
164426 Dallmeyer, R.D. and Quesada, C. 1992. Cadomian vs. Variscan evolution of the Ossa-Morena  
17  
184427 zone (SW Iberia): field and  $^{40}\text{Ar}/^{39}\text{Ar}$  mineral age constraints. *Tectonophysics*, 216,  
19  
204428 339-364.  
21  
224429 Dallmeyer, R.D. and Tucker, R.D. 1993. U-Pb zircon age for the Lagoa augen gneiss, Morais  
23  
244430 Complex, Portugal: tectonic implications. *Journal of the Geological Society, London*,  
25  
264431 150, 405-410.  
27  
284432 Dallmeyer, R.D., Ribeiro, A. and Marques, F. 1991. Polyphase Variscan emplacement of  
29  
304433 exotic terranes (Morais and Bragança Massifs) onto Iberian successions: Evidence  
31  
324434 from  $^{40}\text{Ar}/^{39}\text{Ar}$  mineral ages. *Lithos*, 27, 133-144.  
33  
344435 Dallmeyer, R.D., Fonseca, P., Quesada, C. and Ribeiro, A. 1993.  $^{40}\text{Ar}/^{39}\text{Ar}$  mineral age  
35  
364436 constraints for the tectonothermal evolution of a Variscan suture in southwest Iberia.  
37  
384437 *Tectonophysics*, 222, 177-194.  
39  
404438 Dallmeyer, R.D., Martínez Catalán, J.R., Arenas, R., Gil Ibarguchi, J.I., Gutiérrez Alonso, G.,  
41  
424439 Farias, P., Aller, J. and Bastida, F. 1997. Diachronous Variscan tectonothermal  
43  
444440 activity in the NW Iberian Massif: Evidence from  $^{40}\text{Ar}/^{39}\text{Ar}$  dating of regional fabrics.  
45  
464441 *Tectonophysics*, 277, 307-337.  
47  
484442 Davis, D., Suppe, J. and Dahlen, F.A. 1983. Mechanics of fold-and-thrust belts and  
49  
504443 accretionary wedges. *Journal of Geophysical Research*, 88, 1153-1172.  
51  
524444 de Hoÿm de Marien, L., Le Bayon, B., Pitra, P., Van Den Driessche, J., Poujol, M. and  
53  
544445 Cagnard, F. 2019. Two- stage Variscan metamorphism in the Canigou massif:  
55  
564446 Evidence for crustal thickening in the Pyrenees. *Journal of Metamorphic Geology*, 37,  
57  
584447 863-888. <https://doi.org/10.1111/jmg.12487>.  
59  
60  
61  
62  
63  
64  
65

- 4448 Deiller, P., Štípská, P., Ulrich, M., Schulmann, K., Collett, S., Peřestý, V., Hacker, B.,  
1 4449 Kylander-Clark, A., Whitechurch, H., Lexa, O., Pelt, E. and Míková, J. (submitted).  
2 4450 Evidence for an Early to Late Devonian arc in the eastern Variscan belt (Bohemian  
3 4451 Massif). *Journal of Petrology*.  
4  
5  
6  
7 4452 de la Rosa, J.D. 1992. *Petrología de las rocas básicas y granitoides del Batolito de la Sierra*  
8 4453 *Norte de Sevilla. Zona Sudportuguesa. Macizo Ibérico*. PhD Thesis, Universidad de  
9 4454 Sevilla, 312 pp.  
10  
11  
12  
13 4455 de la Rosa, J.D., Rogers, G., Castro, A. 1993. Relaciones  $87\text{Sr}/86\text{Sr}$  de rocas básicas y  
14 4456 granitoides del batolito de la Sierra Norte de Sevilla. *Revista de la Sociedad Geologica*  
15 4457 *de España*, 6, 141-149.  
16  
17  
18  
19 4458 de la Rosa, J., Jenner, J. and Castro, A. 2002. A study of inherited zircons in granitoid rocks  
20 4459 from the South Portuguese and Ossa-Morena Zones, Iberian Massif: support for the  
21 4460 exotic origin of the South Portuguese Zone. *Tectonophysics*, 352, 245-256.  
22  
23  
24  
25 4461 de la Rosa, J.D. and Castro, A. 2004. Zona Sudportuguesa: Magmatismo de la Zona  
26 4462 Sudportuguesa. In: Vera, J.A. (Ed.), *Geología de España*, SGE-IGME, Madrid, Cap. 2,  
27 4463 215-222.  
28  
29  
30  
31 4464 Delchini, S., Lahfid, A., Lacroix, B., Baudin, T., Hoepffner, C., Guerrot, C., Lach, P.,  
32 4465 Saddiqi, O. and Ramboz, C. 2018. The geological evolution of the Variscan Jebilet  
33 4466 Massif, Morocco, inferred from new structural and geochronological analyses.  
34 4467 *Tectonics*, 37, 4470-4493. <https://doi.org/10.1029/2018TC005002>.  
35  
36  
37  
38  
39 4468 Delfour J. 1989. Données lithostratigraphiques et géochimiques sur le Dévono-Dinantien de la  
40 4469 partie sud du faisceau du Morvan (nord-est du Massif central français). *Géologie de la*  
41 4470 *France*, 1989 (4), 49-77.  
42  
43  
44  
45 4471 Delgado, J.F.N. 1908. *Système Silurique du Portugal. Étude de stratigraphie paléontologique*.  
46 4472 *Mémoire de la Commission du Service Géologique du Portugal*, 1-245.  
47  
48  
49  
50 4473 Demay, A. 1942. *Microtectonique et tectonique profonde. Mémoires du Service de la Carte*  
51 4474 *Géologique de France*, Paris, 247 pp.  
52  
53  
54 4475 Demoux, A., Schärer, U. and Corsini, M. 2008. Variscan evolution of the Tanneron massif,  
55 4476 SE-France, examined through U-Pb monazite ages. *Journal of the Geological Society*,  
56 4477 *London*, 165, 467-478.  
57  
58  
59  
60  
61  
62  
63  
64  
65

- 4478 de Poulpiquet, J. 1988. Etude magnétique et sismique du massif basique et ultrabasique de la  
1  
24479 Baie d'Audierne (Massif armoricain). *Géologie de la France*, 1988 (4), 11-22.  
3
- 44480 Destombes, J., Hollard, H. and Willefert, S. 1985. Lower Palaeozoic rocks of Morocco. In:  
5  
64481 Holland, C.H. (Ed.), *Lower Palaeozoic of North-western and West Central Africa*.  
7  
84482 John Wiley, New York., 91-336.  
9
- 104483 Dewey, J.F., Helman, M.L., Turco, E., Hutton, D.H.W. and Knott, S.D. 1989. Kinematics of  
11  
124484 western Mediterranean. In: Coward, M.P., Dietrich, D. and Park, R.G. (Eds.), *Alpine*  
13  
144485 *Tectonics*, Geological Society, London, Special Publication 45, 265-283.  
15
- 164486 Dezes, P. and Ziegler, P.A. 2002. Map of the European Moho. EUCOR URGENT, University  
17  
184487 Basel.  
19
- 204488 Dias da Silva, Í., Linnemann, U., Hofmann, M., González Clavijo, E., Díez-Montes, A. and  
21  
224489 Martínez Catalán, J.R. 2014a. Detrital zircon and tectonostratigraphy of the  
23  
244490 Parautochthon under the Morais Complex (NE Portugal): implications for the Variscan  
25  
264491 accretionary history of the Iberian Massif. *Journal of the Geological Society*, London,  
27  
284492 172, 45-61. <https://doi.org/10.1144/jgs2014-005>.  
29
- 304493 Dias da Silva, I.F., González Clavijo, E., Gutiérrez Alonso, G. and Gómez Barreiro, J. 2014b.  
31  
324494 Large Upper Cambrian rhyolite olistoliths locked in the Early Carboniferous Variscan  
33  
344495 syn-orogenic melange of the parautochthonous realm of the NW Iberian Massif. In:  
35  
364496 Pankhurst, R.J., Castiñeiras, P. and Sánchez Martínez, S. (Eds.), *Gondwana 15. North*  
37  
384497 *meets South. Madrid. Abstracts Book*, 52.  
39
- 404498 Dias da Silva, I., Valverde-Vaquero, P., González-Clavijo, E., Díez-Montes, A. and Martínez  
41  
424499 Catalán, J.R. 2014c. Structural and stratigraphical significance of U-Pb ages from the  
43  
444500 Mora and Saldanha volcanic complexes (NE Portugal, Iberian Variscides). In:  
45  
464501 Schulmann, K., Martínez Catalán, J.R., Lardeaux, J.M., Janousek, V. and Oggiano, G.  
47  
484502 (Eds.), *The Variscan Orogeny: Extent, Timescale and the Formation of the European*  
49  
504503 *Crust*. Geological Society, London, Special Publication 405, 115-135.  
51  
524504 <https://doi.org/10.1144/SP405.3>.  
53
- 544505 Dias da Silva, Í., Díez Fernández, R., Díez-Montes, A., González Clavijo, E. and Foster, D.A.  
55  
564506 2016. Magmatic evolution in the N-Gondwana margin related to the opening of the  
57  
584507 Rheic Ocean—evidence from the Upper Parautochthon of the Galicia-Trás-os-Montes  
59  
604508 Zone and from the Central Iberian Zone (NW Iberian Massif). *International Journal of*  
61  
624509 *Earth Sciences*, 105, 1127-1151. <https://doi.org/10.1007/s00531-015-1232-9>.  
63  
64  
65

- 4510 Dias da Silva, Í., Pereira, M.F., Silva, J.B. and Gama, C. 2018. Time-space distribution of  
1  
24511 silicic plutonism in a gneiss dome of the Iberian Variscan Belt: The Évora Massif  
3  
44512 (Ossa-Morena Zone, Portugal). *Tectonophysics*, 747-748, 298-317.  
54513 <https://doi.org/10.1016/j.tecto.2018.10.015>.  
6
- 7  
84514 Díaz Alvarado, J., Fernández, C., Castro, A. and Moreno-Ventas, I. 2013. SHRIMP U-Pb  
9  
104515 zircon geochronology and thermal modeling of multilayer granitoid intrusions.  
114516 Implications for the building and thermal evolution of the Central System batholith,  
12  
134517 Iberian Massif, Spain. *Lithos*, 175-176, 104-123.  
14  
154518 <https://doi.org/10.1016/j.lithos.2013.05.006>.  
16
- 174519 Díaz Azpiroz, M. and Fernández, C. 2005. Kinematic analysis of the southern Iberian shear  
18  
194520 zone and tectonic evolution of the Acebuches metabasites (SW Variscan Iberian  
20  
214521 Massif). *Tectonics*, 24, TC3010, 1-19. <https://doi.org/10.1029/2004TC00168>.  
22
- 234522 Díaz Azpiroz, M., Fernández, C., Castro, A. and El-Biad, M. 2006. Tectonometamorphic  
24  
254523 evolution of the Aracena metamorphic belt (SW Spain) resulting from ridge-trench  
26  
274524 interaction during Variscan plate convergence. *Tectonics*, 25, 1-20, TC1001.  
28  
294525 <https://doi.org/10.1029/2004TC001742>.  
30
- 314526 Díaz García, F., Arenas, R., Martínez Catalán, J.R., González del Tánago, J. and Dunning, G.  
32  
334527 1999a. Tectonic evolution of the Careón ophiolite (Northwest Spain): a remnant of  
34  
354528 oceanic lithosphere in the Variscan belt. *Journal of Geology*, 107, 587-605.  
36
- 374529 Díaz García, F., Martínez Catalán, J.R., Arenas, R. and González Cuadra, P. 1999b. Structural  
38  
394530 and kinematic analysis of the Corredoiras Detachment: evidence for early variscan  
40  
414531 orogenic extension in the Ordenes Complex, NW Spain. *International Journal of Earth  
42  
434532 Sciences*, 88, 337-351.  
44
- 454533 Díaz García, F., Sánchez Martínez, S., Castiñeiras P., Fuenlabrada J.M. and Arenas, R. 2010.  
46  
474534 A peri-Gondwanan arc in NW Iberia. II: Assessment of the intra-arc tectonothermal  
48  
494535 evolution through U-Pb SHRIMP dating of mafic dykes. *Gondwana Research*, 17 (2-  
50  
514536 3), 352-362. <https://doi.org/10.1016/j.gr.2009.09.010>.  
52
- 534537 Díez Balda, M.A., Vegas, R. and González Lodeiro, F. 1990. Central-Iberian Zone.  
54  
554538 Autochthonous Sequences. Structure. In: Dallmeyer, R.D. and Martínez García, E.  
56  
574539 (Eds.), *Pre-Mesozoic Geology of Iberia*, Springer-Verlag, Berlín, 172-188.  
58  
59  
60  
61  
62  
63  
64  
65



- 4540 Díez Balda, M.A., Martínez Catalán, J.R. and Ayarza, P. 1995. Syn-collisional extensional  
1  
2 4541 collapse parallel to the orogenic trend in a domain of steep tectonics: the Salamanca  
3  
4 4542 detachment zone (Central Iberian Zone, Spain). *Journal of Structural Geology*, 17 (2),  
5  
6 4543 163-182.
- 7  
8 4544 Díez Fernández, R. and Martínez Catalán, J.R. 2012. Stretching lineations in high-pressure  
9  
10 4545 belts: the fingerprint of subduction and subsequent events (Malpica-Tui complex, NW  
11  
12 4546 Iberia). *Journal of the Geological Society, London*, 169, 531-543.  
13  
14 4547 <https://doi.org/10.1144/0016-76492011-101>.
- 15  
16 4548 Díez Fernández, R., Martínez Catalán, J.R., Gerdes, A., Abati, J., Arenas, R. and Fernández-  
17  
18 4549 Suárez, J. 2010. U-Pb ages of detrital zircons from the Basal allochthonous units of  
19  
20 4550 NW Iberia: Provenance and paleoposition on the northern margin of Gondwana during  
21  
22 4551 the Neoproterozoic and Paleozoic. *Gondwana Research*, 18 (2-3), 385-399.  
23  
24 4552 <https://doi.org/10.1016/j.gr.2009.12.006>.
- 25  
26 4553 Díez Fernández, R., Martínez Catalán, J.R., Arenas, R., Abati, J., Gerdes, A. and Fernández-  
27  
28 4554 Suárez, J. 2012a. U-Pb detrital zircon analysis of the lower allochthon of NW Iberia:  
29  
30 4555 age constraints, provenance and links with the Variscan mobile belt and Gondwanan  
31  
32 4556 cratons. *Journal of the Geological Society, London*, 169, 655-665.  
33  
34 4557 <https://doi.org/10.1144/jgs201>.
- 35  
36 4558 Díez Fernández, R., Castiñeiras, P. and Gómez Barreiro, J. 2012b. Age constraints on Lower  
37  
38 4559 Paleozoic convection system: Magmatic events in the NW Iberian Gondwana margin.  
39  
40 4560 *Gondwana Research*, 21 (4), 1066-1079. <https://doi.org/10.1016/j.gr.2011.07.028.1-146>.
- 41  
42  
43 4562 Díez Montes, A., Martínez Catalán, J.R. and Bellido Mulas, F. 2010. Role of the Ollo de Sapo  
44  
45 4563 massive felsic volcanism of NW Iberia in the Early Ordovician dynamics of northern  
46  
47 4564 Gondwana. *Gondwana Research*, 17 (2-3), 363-376.  
48  
49 4565 <https://doi.org/10.1016/j.gr.2009.09.001>.
- 50  
51 4566 Do Couto, D., Gorini, C., Jolivet, L., Le Bret, N., Augier, R., Gumiaux, C., d'Acremont, E.,  
52  
53 4567 Ammar, A., Jabour, H. and Auxietre, J.L. 2016. Tectonic and stratigraphic evolution  
54  
55 4568 of the Western Alboran Sea Basin in the last 25 Myrs. *Tectonophysics*, 677-678, 280-  
56  
57 4569 311.

- 4570 Doglioni, C., Carminati, E., Cuffaro, M. and Scrocca, D. 2007. Subduction kinematics and  
1  
24571 dynamic constraints. *Earth-Science Reviews*, 83, 125-175.  
3  
44572 <https://doi.org/10.1016/j.earscirev.2007.04.001>.
- 5  
64573 Domeier, M. and Torsvik, T.H. 2014. Plate tectonics in the late Paleozoic. *Geoscience*  
7  
84574 *Frontiers*, 5, 303-350.
- 9  
104575 Don, J., Dumicz, M., Wojciechowska, I. and Żelaźniewicz, A. 1990. Lithology and tectonics  
11  
124576 of the Orlica-Śnieżnik Dome, Sudetes – Recent State of Knowledge. *Neues Jahrbuch*  
13  
144577 *für Geologie und Paläontologie, Abhandlungen* 197, 159-188.
- 15  
164578 Dörr, W., Zulauf, G., Fiala, J., Franke, W. and Vejnar, Z. 2002. Neoproterozoic to Early  
17  
184579 Cambrian history of an active plate margin in the Teplá-Barrandian unit—a  
19  
204580 correlation of U-Pb isotopic dilution-TIMS ages (Bohemia, Czech Republic).  
21  
224581 *Tectonophysics*, 352, 65-85.
- 23  
244582 Drost, K., Linnemann, U., McNaughton, N., Fatka, O., Kraft, P., Gehmlich, M., Tonk, C. and  
25  
264583 Marek, J. 2004. New data on the Proterozoic-Cambrian geotectonic setting of the  
27  
284584 Teplá-Barrandian volcano-sedimentary successions: geochemistry, U-Pb zircon ages,  
29  
304585 and provenance (Bohemian Massif, Czech Republic). *International Journal of Earth*  
31  
324586 *Sciences*, 93 (5), 742-757. <https://doi.org/10.1007/s00531-004-0416-5>.
- 33  
344587
- 35  
364588 Dubińska, E., Bylina, P., Kozłowski, A., Dörr, W., Nejbort, K., Schastok, J. and Kulicki, C.  
37  
384589 2004. U-Pb dating of serpentinization: hydrothermal zircon from a metasomatic  
39  
404590 rodingite shell (Sudetic ophiolite, SW Poland). *Chemical Geology*, 203 (3-4), 183-  
41  
424591 203.
- 43  
444592 Ducassou, C., 2010. Age et origine des premiers reliefs de la chaîne varisque: Le Dévono-  
45  
464593 Carbonifère du Bassin d'Ancenis. *Mémoires de Géosciences Rennes*, 135, 513 pp.
- 47  
484594 Ducassou, C., Strullu-Derrien, C., Ballèvre, M., Dabard, M.P., Gerrienne, P., Lardeux, H. and  
49  
504595 Robin, C. 2009. Age and depositional environment of the Sainte-Anne Formation  
51  
524596 (Armorican Massif, France): the oldest (Emsian) evidence for mountain erosion in the  
53  
544597 Variscan belt. *Bulletin de la Société Géologique de France*, 180, 529-544.
- 55  
564598 Ducassou, C., Poujol, M., Ruffet, G., Bruguier, O. and Ballèvre, M. 2014. Relief variation and  
57  
584599 erosion of the Variscan belt: detrital geochronology of the Palaeozoic sediments from

- 4600 the Mauges Unit (Armorican Massif, France). Geological Society, London, Special  
1  
24601 Publication 405, 137-167. <https://doi.org/10.1144/SP405.6>.
- 3  
44602 Ducea, M.N., Bergantz, G.W., Crowley, J.L. and Otamendi, J. 2017. Ultrafast magmatic  
5  
64603 buildup and diversification to produce continental crust during subduction. *Geology*,  
7  
84604 45 (3), 235-238. <https://doi.org/10.1130/G38726.1>.
- 9  
104605 Dudek, A. 1980. The crystalline basement block of the Outer Carpathians in Moravia: Bruno-  
11  
124606 Vistulicum. *Rozprawy Československá akademie věd - řada matematických a*  
13  
144607 *přírodních věd*, 90, 8, 3-85. Praha.
- 15  
164608 Dunning, G.R., Díez Montes, A., Matas, J., Martín Parra, L.M., Almarza, J. y Donaire, M.  
17  
184609 2002. Geocronología U/Pb del vulcanismo ácido y granitoides de la Faja Pirítica  
19  
204610 Ibérica. *Geogaceta*, 32, 127-130.
- 21  
224611 Duretz, T., Kaus, B.J.P., Schulmann, K., Gapais, D. and Kermarrec, J.J. 2011. Indentation as  
23  
244612 an extrusion mechanism of lower crustal rocks: Insight from analogue and numerical  
25  
264613 modelling, application to the Eastern Bohemian Massif. *Lithos*, 124 (1-2), 158-168.
- 27  
284614 Dymant, J., Sibouet, J.C. and Pinet, B. 1990. Deep structure of the Celtic Sea: a discussion on  
29  
304615 the formation of basins. *Tectonophysics*, 173, 435-444.
- 31  
324616 Edel, J.B. and Schulmann, K. 2009. Geophysical constraints and model of the  
33  
344617 'Saxothuringian and Rhenohercynian subductions – magmatic arc system' in NE  
35  
364618 France and SW Germany. *Bulletin de la Société Géologique de France*, 180, 545-558.
- 37  
384619 Edel, J.-B., Schulmann, K., Skrzypek, E. and Cocherie, A. 2013. Tectonic evolution of the  
39  
404620 European Variscan belt constrained by palaeomagnetic, structural and anisotropy of  
41  
424621 magnetic susceptibility data from the Rhenohercynian magmatic arc (Northern  
43  
444622 Vosges, Eastern France). *Journal of the Geological Society, London*, 170, 785-804.  
45  
464623 <https://doi.org/10.1144/jgs2011-138>.
- 47  
484624 Edel, J.B., Casini, L., Oggiano, G., Rossi P. and Schulmann, K. 2014. Early Permian  
49  
504625 clockwise 90° rotation of the Maures-Estérel-Corsica-Sardinia block confirmed by  
51  
524626 new palaeomagnetic data and followed by a Triassic 60° clockwise rotation. In:  
53  
544627 Schulmann, K., Martínez Catalán, J.R., Lardeaux, J.M., Janousek, V. and Oggiano, G.  
55  
564628 (Eds.), *The Variscan Orogeny: Extent, Timescale and the Formation of the European*  
574629 *Crust*. Geological Society, London, Special Publication 405, 333-361.  
58  
594630 <https://doi.org/10.1144/SP405.10>.

- 4631 Edel, J.B., Schulmann, K., Lexa, O. and Lardeaux, J.-M. 2018. Late Palaeozoic  
1  
2 4632 palaeomagnetic and tectonic constraints for amalgamation of Pangea supercontinent in  
3  
4 4633 the European Variscan belt. *Earth-Science Reviews*, 177, 589-612.  
5 4634 <https://doi.org/10.1016/j.earscirev.2017.12.007>.  
6
- 7 4635 Eden, C.P. and Andrews, J.R. 1990. Middle to Upper Devonian mélanges in SW Spain and  
8  
9 4636 their relationship to the Meneage Formation in South Cornwall. *Proceedings of the*  
10  
11 4637 *Ussher Society*, 7, 217-222.  
12
- 13 4638 El Hadi, H., Tahiri, A., Simancas, F., González Lodeiro, F., Azor, A. and Martínez Poyatos,  
14  
15 4639 D. 2014. Pillow lavas of Rabat (northwestern Moroccan Meseta): Transitional  
16  
17 4640 geochemical signature of magmas set up in an Early Ordovician extending platform.  
18  
19 4641 *European Journal of Scientific Research*, ISSN 1450-216X / 1450-202X, Vol.122  
20  
21 4642 No.1, 45-57. <http://www.europeanjournalofscientificresearch.com>.  
22
- 23 4643 El Houicha, M., Pereira, M.F., Jouhari, A., Gama, C., Ennih, N., Fekkak, A., Ezzouhairi, H.,  
24  
25 4644 El Attari, A. and Silva, J.B. 2018. Recycling of the Proterozoic crystalline basement in  
26  
27 4645 the Coastal Block (Moroccan Meseta): New insights for understanding the  
28  
29 4646 geodynamic evolution of the northern peri-Gondwanan realm. *Precambrian Research*,  
30  
31 4647 306, 129-154. <https://doi.org/10.1016/j.precamres.2017.12.039>.  
32
- 33 4648 Elicki, O. 2007. Paleontological data from the Early Cambrian of Germany and  
34  
35 4649 paleobiogeographical implications for the configuration of central Perigondwana. In:  
36  
37 4650 Linnemann, U., Nance, R.D., Kraft, P. and Zulauf, G. (Eds.), *The evolution of the*  
38  
39 4651 *Rheic Ocean: From Avalonian-Cadomian active margin to Alleghenian-Variscan*  
40  
41 4652 *collision. Geological Society of America Special Paper*, 423, 143-152.  
42 4653 [https://doi.org/10.1130/2007.2423\(05\)](https://doi.org/10.1130/2007.2423(05)).  
43
- 44 4654 El Kamel, F., Remmal, T. and Mohsine, A. 1998. Mise en évidence d'un magmatisme alcalin  
45  
46 4655 d'intraplaque post-Calédonien dans le bassin silurien des Ouled Abbou (Meseta  
47  
48 4656 côtière, Maroc *Comptes Rendus de l'Académie des Sciences, Paris, Science de la*  
49  
50 4657 *Terre et des Planètes*, 327, 309-314.  
51
- 52 4658 El Korh, A., Schmidt, S.T., Ulianov, A. and Potel S. 2009. Trace element partitioning in HP-  
53  
54 4659 LT metamorphic assemblages during subduction-related metamorphism, Ile de Groix,  
55  
56 4660 France: a detailed LA-ICPMS study. *Journal of Petrology*, 50, 1107-1148.  
57
- 58 4661 El Korh, A., Schmidt, S.T., Ballèvre, M., Ulianov, A. and Bruguier, O. 2012. Discovery of an  
59  
60 4662 albite gneiss from the Ile de Groix (Armorican Massif, France): geochemistry and LA-  
61  
62  
63  
64  
65

- 4663 ICP-MS U-Pb geochronology of its Ordovician protolith. *International Journal of*  
1  
2 4664 *Earth Sciences*, 101, 1169-1190.
- 3  
4 4665 Engel, W., Feist, R. and Franke, W. 1980. Le Carbonifère ante-Stéphanien de la Montagne  
5  
6 4666 Noire: rapports entre mise en place des nappes et sédimentation. *Bulletin du Bureau de*  
7  
8 4667 *Recherches Géologiques et Minières*, 2 (1), 341-389.
- 9  
10 4668 Ennih, N. and Liégeois, J.P. 2001. The Moroccan Anti-Atlas: the West African craton passive  
11  
12 4669 margin with limited Pan-African activity. Implications for the northern limit of the  
13  
14 4670 craton. *Precambrian Research*, 112, 289-302.
- 15  
16 4671 Erslev, E.A. 1991. Trishear fault-propagating folding. *Geology*, 19, 617-620.
- 17  
18 4672 Escuder Viruete, J., Arenas, R. and Martínez Catalán, J.R. 1994. Tectonothermal evolution  
19  
20 4673 associated with Variscan crustal extension in the Tormes Gneiss Dome (NW  
21  
22 4674 Salamanca, Iberian Massif, Spain). *Tectonophysics*, 238, 117-138.
- 23  
24 4675 Expósito, I., Simancas, J.F., González Lodeiro, F., Azor, A. and Martínez Poyatos, D.J. 2002.  
25  
26 4676 Estructura de la mitad septentrional de la Zona de Ossa-Morena: deformación en el  
27  
28 4677 bloque inferior de un cabalgamiento cortical de evolución compleja. *Revista de la*  
29  
30 4678 *Sociedad Geológica de España*, 15 (1-2), 3-14.
- 31  
32 4679 Expósito, I., Simancas, J.F., González Lodeiro, F., Bea, F., Montero, P. and Salman, K. 2003.  
33  
34 4680 Metamorphic and deformational imprint of Cambrian-Lower Ordovician rifting in the  
35  
36 4681 Ossa-Morena Zone (Iberian Massif, Spain). *Journal of Structural Geology*, 25 (12),  
37  
38 4682 2077-2087.
- 39  
40 4683 Fabre, J. 2005. *Géologie du Sahara occidental et central*. Tervuren African Geoscience  
41  
42 4684 Collection 18. Musée Royal de l’Afrique Centrale, Tervuren, 572 pp.
- 43  
44 4685 Fabriès, J. and Latouche, L. 1988. Granulite facies conditions in the Ste-Marie-aux-Mines  
45  
46 4686 ‘Varied Group’ (Central Vosges). *Terra Cognita*, 8, 249.
- 47  
48 4687 Farias, P. and Marcos, A. 2019. Geodynamic evolution of the San Vitero basin, a foreland-  
49  
50 4688 type basin developed in the hinterland of the Variscan Orogen (Zamora, NW Spain).  
51  
52 4689 *Journal of Iberian Geology*, 45 (3), 529-551. [https://doi.org/10.1007/s41513-019-](https://doi.org/10.1007/s41513-019-00108-w)  
53  
54 4690 [00108-w](https://doi.org/10.1007/s41513-019-00108-w).
- 55  
56 4691 Farias, P., Gallastegui, G., González Lodeiro, F., Marquínez, J., Martín Parra, L.M., Martínez  
57  
58 4692 Catalán, J.R., Pablo Maciá, J.G. de, and Rodríguez Fernández, L.R. 1987.

- 4693 Aportaciones al conocimiento de la litoestratigrafía y estructura de Galicia Central.  
1  
24694 Memórias da Faculdade de Ciências, Universidade do Porto, 1, 411-431.  
3  
44695 Faure, M., Leloix, C. and Roig, J.Y. 1997. L'évolution polycyclique de la chaîne hercynienne.  
5  
64696 Bulletin de la Société Géologique de France, 168, 695-705.  
7  
84697 Faure, M., Bé Mézème, E., Cocherie, A., Rossi, P., Chemenda, A. and Boutelier, D. 2008.  
9  
104698 Devonian geodynamic evolution of the Variscan Belt, insights from the French Massif  
11  
124699 Central and Massif Armoricaïn. *Tectonics*, 27 (2), TC2005, 1-19.  
13  
144700 <http://dx.doi.org/10.1029/2007TC002115>.  
15  
164701 Faure, M., Lardeaux, J.M. and Ledru, P. 2009. A review of the pre-Permian geology of the  
17  
184702 Variscan French Massif Central. *Comptes Rendus Geosciences*, 341, 202-213.  
19  
204703 <https://doi.org/10.1016/j.crte.2008.12.001>.  
21  
224704 Faure, M., Sommers, C., Melleton, J., Cocherie, A. and Lautout, O. 2010a. The Léon Domain  
23  
244705 (French Massif Armoricaïn): a westward extension of the Mid-German Crystalline  
25  
264706 Rise? Structural and geochronological insights. *International Journal of Earth  
27  
284707 Sciences*, 99, 65-81. <https://doi.org/0.1007/s00531-008-0360-x>.  
29  
304708 Faure, M., Cocherie, A., Bé Mézène, E., Charles, N. and Rossi, P. 2010b. Middle  
31  
324709 Carboniferous crustal melting in the Variscan belt: new insights from U-Th-Pb<sub>tot</sub>  
33  
344710 monazite and U-Pb zircon ages of the Montagne Noire Axial Zone (southern French  
35  
364711 Massif Central). *Gondwana Research*, 18, 653-673.  
37  
384712 Faure, M., Cocherie, A., Gaché, J., Esnault, C., Guerrot, C., Rossi, P., Wei, L. and Qiuli, L.  
39  
404713 2014. Middle Carboniferous intracontinental subduction in the outer zone of the  
41  
424714 Variscan belt (Montagne Noire Axial Zone, French Massif Central): multimethod  
43  
444715 geochronological approach of polyphase metamorphism. In: Schulmann, K., Martínez  
45  
464716 Catalán, J.R., Lardeaux, J.M., Janousek, V. and Oggiano, G. (Eds.), *The Variscan  
47  
484717 Orogeny: Extent, Timescale and the Formation of the European Crust*. Geological  
49  
504718 Society, London, Special Publication 405, 289-311.  
51  
524719 <http://dx.doi.org/10.1144/SP405.2>.  
53  
544720 Fernández-Suárez, J., Gutiérrez-Alonso, G., Jenner, G.A. and Jackson, S.E. 1998.  
55  
564721 Geochronology and geochemistry of the Pola de Allande granitoids (northern Spain).  
57  
584722 Their bearing on the Cadomian/Avalonian evolution of NW Iberia. *Canadian Journal  
59  
604723 of Earth Sciences*, 35, 1439-1453.  
61  
62  
63  
64  
65

- 4724 Fernández-Suárez, J., Gutiérrez-Alonso, G., Jenner, G.A. and Tubrett, M.N. 1999. Crustal  
1  
24725 sources in Lower Paleozoic rocks from NW Iberia: insights from laser ablation U-Pb  
3  
44726 ages of detrital zircons. *Journal of the Geological Society, London*, 156, 1065-1068.
- 5  
64727 Fernández-Suárez, J., Dunning, G.R., Jenner, G.A. and Gutiérrez-Alonso, G. 2000. Variscan  
7  
84728 collisional magmatism and deformation in NW Iberia: constraints from U-Pb  
9  
104729 geochronology of granitoids. *Journal of the Geological Society, London*, 157, 565-  
11  
124730 576.
- 13  
144731 Fernández-Suárez, J., Corfu, F., Arenas, R., Marcos, A., Martínez Catalán, J.R., Díaz García,  
15  
164732 F., Abati, J. and Fernández, F.J. 2002. U-Pb evidence for a polyorogenic evolution of  
17  
184733 the HP-HT units of the NW Iberian Massif. *Contributions to Mineralogy and  
19  
204734 Petrology*, 143, 236-253.
- 21  
224735 Fernández-Suárez, J., Díaz García, F., Jeffries T.E., Arenas, R. and Abati, J. 2003. Constraints  
23  
244736 on the provenance of the uppermost allochthonous terrane of the NW Iberian Massif:  
25  
264737 Inferences from detrital zircon U-Pb ages. *Terra Nova*, 15, 138-144.
- 27  
284738 Fernández-Suárez, J., Arenas, R., Abati, J., Martínez Catalán, J.R., Whitehouse, M.J. and  
29  
304739 Jeffries, T.E. 2007. U-Pb chronometry of polymetamorphic high-pressure granulites:  
31  
324740 An example from the allochthonous terranes of the NW Iberian Variscan belt. In:  
33  
344741 Hatcher Jr., R.D., Carlson, M.P., McBride, J.H. and Martínez Catalán, J.R. (Eds.), 4-D  
35  
364742 framework of continental crust. *Geological Society of America, Memoir* 200, 469-488.  
37  
384743 [https://doi.org/10.1130/2007.1200\(24\)](https://doi.org/10.1130/2007.1200(24)).
- 39  
404744 Ferragne, A. 1972. Le Précambrien et le Paléozoïque de la province d'Orense (Nord-ouest de  
41  
424745 l'Espagne). *Stratigraphie-tectonique-métamorphisme*. PhD Thesis, Université de  
43  
444746 Bordeaux, 249 pp.
- 45  
464747 Floor, P. 1966. Petrology of an aegirine-riebeckite gneiss-bearing part of the Hesperian  
47  
484748 Massif: the Galiñeiro and surrounding areas, Vigo, Spain. *Leidse Geologische  
49  
504749 Mededelingen*, 36, 1-204.
- 51  
524750 Floyd, P.A., Kryza, R., Crowley, Q.G., Winchester, J.A. and Abdel Wahed, M. 2002. Sleza  
53  
544751 Ophiolite: geochemical features and relationship to lower Paleozoic rift magmatism in  
55  
564752 the Bohemian Massif. In: Winchester, J.A., Pharaoh, T.C. and Verniers, J. (Eds.),  
57  
584753 *Palaeozoic Amalgamation of Central Europe*. Geological Society, London, Special  
59  
604754 Publication 201, 197-215.

- 4755 Fonseca, P., Munhá, J., Pedro, J., Rosas, F., Moita, P., Araújo, A. and Leal, N. 1999. Variscan  
1 4756 ophiolites and high-pressure metamorphism in southern Iberia. *Ofioliti*, 24 (2), 259-  
3 4757 268.
- 5  
6 4758 Forestier, F.H. 1963. Métamorphisme hercynien et antéhercynien dans le bassin du Haut-  
7 4759 Allier (Massif Central français). *Bulletin des services de la carte géologique de la*  
9 4760 *France*, 271 (LIX), 294 pp.
- 11  
12 4761 Franke, W. 1989. Tectonostratigraphic units in the Variscan belt of central Europe. In:  
13 4762 Dallmeyer, R.D. (Ed.), *Terranes in the Circum-Atlantic Paleozoic Orogens*.  
15 4763 *Geological Society of America Special Paper*, 230, 67-90.
- 17  
18 4764 Franke, W. 1990. Tectonostratigraphic units in the W part of the Bohemian Massif. An  
19 4765 Introduction. *International Conference on Paleozoic Orogens in Central Europe*.  
21 4766 *Göttingen-Giessen. Field Guide: Bohemian Massif*, 1-23.
- 23  
24 4767 Franke, W. 2000. The mid-European segment of the Variscides: tectonostratigraphic units,  
25 4768 terrane boundaries and plate tectonic evolution. In: Franke, W., Haak, V., Oncken, O.  
27 4769 and Tanner, D. (Eds.), *Orogenic Processes: Quantification and Modelling in the*  
29 4770 *Variscan Belt*. *Geological Society, London, Special Publication* 179, 35-61.
- 31  
32 4771 Franke, W. 2014. Topography of the Variscan Orogen in Europe: failed – not collapsed.  
33 4772 *International Journal of Earth Sciences*, 103, 1471-1499.  
35 4773 <https://doi.org/10.1007/s00531-014-1014-9>.
- 37  
38 4774 Franke, W. and Dulce, J.C. 2017. Back to sender: tectonic accretion and recycling of Baltica-  
39 4775 derived Devonian clastic sediments in the Rheno-Hercynian Variscides. *International*  
41 4776 *Journal of Earth Sciences*, 106, 377-386. <https://doi.org/10.1007/s00531-016-1408-y>.
- 43  
44 4777 Franke, W. and Engel, W. 1986. Synorogenic sedimentation in the Variscan Belt of Europe.  
45 4778 *Bulletin de la Société Géologique de France*, 8<sup>e</sup> serie, II (1), 25-33.
- 47  
48 4779 Franke, W. and Stein, E. 2000. Exhumation of high-grade rocks in the Saxo-Thuringian Belt:  
49 4780 geological constraints and geodynamic concepts. In: Franke, W., Haak, V., Oncken, O.  
51 4781 and Tanner, D. (Eds.), *Orogenic Processes: Quantification and Modelling in the*  
53 4782 *Variscan Belt*. *Geological Society, London, Special Publication* 179, 63-86.
- 55  
56 4783 Franke, W. and Żelaźniewicz, A. 2000. The eastern termination of the Variscides: terrane  
57 4784 correlation and kinematic evolution. In: Franke, W., Haak, V., Oncken, O. and Tanner,  
59  
60  
61  
62  
63  
64  
65



- 4785 D. (Eds.), *Orogenic Processes: Quantification and Modelling in the Variscan Belt*.  
1 Geological Society, London, Special Publication 179, 63-86.  
24786  
3
- 44787 Franke, W. and Żelaźniewicz, A. 2002. Structure and evolution of the Bohemian Arc. In:  
5  
64788 Winchester, J.A., Pharaoh, T.C. and Verniers, J. (Eds.), *Palaeozoic Amalgamation of*  
7  
84789 *Central Europe*. Geological Society, London, Special Publication 201, 279-293.  
9
- 104790 Franke, W., Doublier, M.P., Klama, K., Potel, S. and Wemmer, K. 2011. Hot metamorphic  
11  
124791 core complex in a cold foreland. *International Journal of Earth Sciences*, 100, 753-785.  
13  
144792 <https://doi.org/10.1007/s00531-010-0512-7>.  
15
- 164793 Franke, W., Cocks, L.R.M. and Torsvik, T.H. 2017. The Palaeozoic Variscan oceans  
17  
184794 revisited. *Gondwana Research*, 48, 257-284. <https://doi.org/10.1016/j.gr.2017.03.005>.  
19
- 204795 Franke, W., Ballèvre, M., Cocks, L.R.M., Torsvik, T.H. and Żelaźniewicz, A. 2020. Variscan  
21  
224796 Orogeny. *Encyclopedia of Geology*, 2nd edition, 12 pp. Elsevier.  
23  
244797 <https://doi.org/10.1016/B978-0-08-102908-4.00022-9>.  
25
- 264798 Friedl, G., Finger, F., Paquette, J.L., von Quadt, A., McNaughton, N.J., and Fletcher, I.R.  
27  
284799 2004. Pre-Variscan geological events in the Austrian part of the Bohemian Massif  
29  
304800 deduced from U-Pb zircon ages: *International Journal of Earth Sciences*, 93, 802-823.  
31
- 324801 Frizon de Lamotte, D., Tavakoli-Shirazi, S., Leturmy, P., Averbuch, O., Mouchot, N., Raulin,  
33  
344802 C., Leparmentier, F., Blanpied, C. and Ringenbach, J.C. 2013. Evidence for Late  
35  
364803 Devonian vertical movements and extensional deformation in northern Africa and  
37  
384804 Arabia: Integration in the geodynamics of the Devonian world. *Tectonics*, 32, 107-  
39  
404805 132.  
41
- 424806 Fuchs, G. 1976. Zur Entwicklung der Böhmisches Masse. *Jahrbuch der Geologischen*  
43  
444807 *Bundelsansalt*, 119, 45-61.  
45
- 464808 Fuchs, G. 1986. Zur Diskussion um den Deckenbau der Böhmisches Masse. *Jahrbuch der*  
47  
484809 *Geologischen Bundelsansalt* 127, 41-49.  
49
- 504810 Fuenlabrada, J.M., Arenas, R., Sánchez Martínez, S., Díaz García, F. and Castiñeiras, P. 2010.  
51  
524811 A peri-Gondwanan arc in NW Iberia. I: isotopic and geochemical constraints to the  
53  
544812 origin of the arc-A sedimentary approach. *Gondwana Research*, 17 (2-3), 338-351.  
55  
564813 <https://doi.org/10.1016/j.gr.2009.09.007>.  
57
- 584814 Fuenlabrada, J.M., Arenas, R., Díez Fernández, R., Sánchez Martínez, S., Abati, J. and López  
59  
604815 Carmona, A. 2012. Sm-Nd isotope geochemistry and tectonic setting of the  
61  
62  
63  
64  
65

- 4816 metasedimentary rocks from the basal allochthonous units of NW Iberia (Variscan  
1 4817 suture, Galicia). *Lithos*, 148, 196-208. <https://doi.org/10.1016/j.lithos.2012.06.002>.  
3  
4 4818 Furnes, H-, Kryza, R., Muszynski, A., Pin, C., and Garmann, L.B. 1994. Geochemical  
5 4819 evidence for progressive, rift-related early Palaeozoic volcanism in the western  
7 4820 Sudetes. *Journal of the Geological Society, London*, 151 (1), 91-109.  
9  
10 4821 Galán, G., Pin, C. and Duthou, J.L. 1996. Sr-Nd isotopic record of multi-stage interactions  
11 4822 between mantle-derived magmas and crustal components in a collision context - The  
13 4823 ultramafic-granitoid association from Vivero (Hercynian belt, NW Spain). *Chemical  
15 4824 Geology*, 131, 67-91.  
16  
17 4825 Galán, G. and Marcos, A. 1997. Geochemical evolution of high-pressure mafic granulites  
19 4826 from the Bacariza formation (Cabo Ortegal complex, NW Spain): an example of a  
21 4827 heterogeneous lower crust. *Geologische Rundschau*, 86, 539-355.  
22  
23 4828 Galindo, C. 1989. *Petrología y geocronología del complejo plutónico Táliga-Barcarrota  
25 4829 (Badajoz)*. PhD Thesis, Universidad Complutense, Madrid, 343 pp.  
27  
28 4830 Galindo, C., Portugal Ferreira, M.R., Casquet, C. and Priem, H.N.A. 1990. Dataciones Rb-Sr  
29 4831 en el Complejo plutónico Táliga-Barcarrota (CPTB) (Badajoz). *Geogaceta*, 8, 7-10.  
31  
32 4832 Gallastegui, G. 2005. *Petrología del macizo granodiorítico de Bayo-Vigo (Provincia de  
33 4833 Pontevedra, España): Laboratorio Xeolóxico de Laxe, Instituto Universitario de  
35 4834 Xeoloxía, A Coruña, Spain, Serie Nova Terra*, 26, 414 pp.  
37  
38 4835 Gallastegui, G., Martín Parra, L.M., Pablo Maciá, J.G. de, and Rodríguez Fernández, L.R.  
39 4836 1988. Las metavulcanitas del Dominio Esquistoso de Galicia-Tras-os-Montes:  
41 4837 petrografía, geoquímica y ambiente geotectónico (Galicia, NO de España). *Cuadernos  
43 4838 do Laboratorio Xeolóxico de Laxe, Coruña*, 12, 127-139.  
45  
46 4839 Gallo, L.C., Tomezzoli, R.N. and Cristallini, E.O. 2017. A pure dipole analysis of the  
47 4840 Gondwana apparent polar wander path: Paleogeographic implications in the evolution  
49 4841 of Pangea. *Geochemistry, Geophysics, Geosystems*, 18, 21 pp.  
51 4842 <https://doi.org/10.1002/2016GC006692>.  
52  
53 4843 García Casquero, J.L., Boelrijk, N.A.I.M., Chacón, J. and Priem, H.N.A. 1985. Rb-Sr  
55 4844 evidence for the presence of Ordovician granites in the deformed basement of the  
57 4845 Badajoz-Córdoba Belt, SW Spain. *Geologische Rundschau*, 74, 379-384.  
58  
59  
60  
61  
62  
63  
64  
65

- 4846 García Garzón, J., Pablo Maciá, J.G. de, and Llamas Borrajo, J.F. 1981. Edades absolutas  
1  
24847 obtenidas mediante el método Rb/Sr en dos cuerpos de ortoneises en Galicia  
3  
44848 Occidental. *Boletín Geológico y Minero*, 92, 463-466.
- 5  
64849 García-López, S., Bastida, F., Brime, C., Aller, J., Valín, M.L., Sanz-López, J., Méndez, C.A.  
7  
84850 and Menéndez-Álvarez, J.R. 1999. Los episodios metamórficos de la Zona Cantábrica  
9  
94851 y su contexto estructural. *Trabajos de Geología, Universidad de Oviedo*, 21, 177-187.
- 10  
11  
124852 Gay, M., Peterlongo, J.M. and Caen-Vachette, M. 1981. Age radiométrique des granites en  
13  
144853 massifs allongés et en feuillets minces syn-tectoniques dans les Monts du  
15  
164854 Lyonnais (Massif Central Français). *Comptes Rendus de l'Académie des Sciences*,  
17  
184855 Paris, 293, 993-996.
- 19  
204856 Gerdes, A., Wörner, G. and Henk, A. 2000. Post- collisional granite generation and HT-LP  
21  
224857 metamorphism by radiogenic heating: the Variscan South Bohemian Batholith. *Journal*  
23  
244858 *of the Geological Society, London*, 157 (3), 577-587.  
254859 <https://doi.org/10.1144/jgs.157.3.577>.
- 26  
274860 Ghienne, J.F., Monod , O., Kozlu, H. and Dean, W.T. 2010. Cambrian-Ordovician  
28  
294861 depositional sequences in the Middle East: A perspective from Turkey. *Earth-Science*  
30  
314862 *Reviews*, 101, 101-146. <https://doi.org/10.1016/j.earscirev.2010.04.004>.
- 32  
33  
344863 Ghienne, J.F., Desrochers, A., Vandembroucke, T.R.A., Achab, A., Asselin, E., Dabard, M.-  
35  
364864 P., Farley, C., Loi, A., Paris, F., Wickson, S. and Veizer, J. 2014. A Cenozoic-style  
374865 scenario for the end-Ordovician glaciation. *Nature Communications*, 5, 4485.  
38  
394866 <https://doi.org/10.1038/ncomms5485>.
- 40  
414867 Ghienne, J.F., Benvenuti, A., El Houicha, M., Girard, F., Kali, E., Khoukhi, Y., Langbour, C.,  
42  
434868 Magna, T., Míková, J., Moscariello, A. and Schulmann K. 2018. The impact of the  
44  
454869 end-Ordovician glaciation on sediment routing systems: A case study from the Meseta  
46  
474870 (northern Morocco). *Gondwana Research*, 63, 169-178.  
48  
494871 <https://doi.org/10.1016/j.gr.2018.07.001>.
- 50  
514872 Giacomini, F., Bomparola, R.M., Ghezzi, C. and Guldbransen, H. 2006. The geodynamic  
52  
534873 evolution of the Southern European Variscides: constraints from the U/Pb  
54  
554874 geochronology and geochemistry of the lower Palaeozoic magmatic-sedimentary  
56  
574875 sequences of Sardinia (Italy). *Contributions to Mineralogy and Petrology*, 152 (1), 19-  
584876 42. <https://doi.org/10.1007/s00410-006-0092-5>.
- 59  
60  
61  
62  
63  
64  
65

- 4877 Giacomini, F., Dallai, L., Carminati, E., Tiepolo, M. and Ghezzo, C. 2008. Exhumation of a  
1  
2 4878 Variscan orogenic complex: insights into the composite granulitic–amphibolitic  
3  
4 4879 metamorphic basement of south-east Corsica (France). *Journal of Metamorphic  
5  
6 4880 Geology*, 26, 403-436. <https://doi.org/10.1111/j.1525-1314.2008.00768.x>.
- 7  
8 4881 Gibbons, W. and Moreno, T. (Eds.). 2002. *The Geology of Spain*. Geological Society of  
9  
10 4882 London, *Geology of... series*, 632 pp.
- 11  
12 4883 Giese, W., Hoegen, R.V., Hollmann, G. and Walter, R. 1994. Geology of the southwestern  
13  
14 4884 Iberian Meseta I. The Palaeozoic of the Ossa Morena Zone north and south of the  
15  
16 4885 Olivenza-Monesterio Anticline (Huelva province, SW Spain). *Neues Jahrbuch für  
17  
18 4886 Geologie und Paläontologie, Abhandlungen*, 192 (3), 293-331.
- 19  
20 4887 Gil Ibarguchi, J.I. 1981. A comparative study of vaugnerites and metabasic rocks from the  
21  
22 4888 Finisterre region (NW Spain). *Neues Jarbuch für Mineralogie, Abhandlungen (N. Jb.  
23  
24 4889 Mineral. Abh.)*, 143, 91-101.
- 25  
26 4890 Gil Ibarguchi, J.I., Mendia, M., Girardeau, J. and Peucat, J.J. 1990. Petrology of eclogites and  
27  
28 4891 clinopyroxene-garnet metabasites from the Cabo Ortegal Complex (northwestern  
29  
30 4892 Spain). *Lithos*, 25, 133-162.
- 31  
32 4893 Gil Ibarguchi, J.I. and Dallmeyer, R.D. 1991. Hercynian blueschist metamorphism in North  
33  
34 4894 Portugal: tectonothermal implications. *Journal of Metamorphic Geology*, 9, 539-549.
- 35  
36 4895 Gil-Peña, I. and Barnolas, A. 2004. El ciclo varisco de los Pirineos: etapas y materiales:  
37  
38 4896 Introducción al ciclo varisco en los Pirineos Madrid, (Ed.), *Geología de España*, SGE-  
39  
40 4897 IGME, Cap. 3, 241-242.
- 41  
42 4898 Gimeno-Vives, O., Frizon de Lamotte, D., Leprêtre, R., Haissen F., Atouabat, A. and Mohn,  
43  
44 4899 G. 2020. The structure of the Central-Eastern External Rif (Morocco); Poly-phased  
45  
46 4900 deformation and role of the under-thrusting of the North-West African paleo-margin.  
47  
48 4901 *Earth-Science Reviews*, 205, 103-198.
- 49  
50 4902 Girardeau, J. and Gil Ibarguchi, J.I. 1991. Pyroxenite-rich peridotites of the Cabo Ortegal  
51  
52 4903 Complex (Northwestern Spain): Evidence for large-scale upper-mantle heterogeneity.  
53  
54 4904 *Journal of Petrology*, 32 (Spec. Lherzolites Issue), 135-154.
- 55  
56 4905 Girardeau, J., Dubuisson, G. and Mercier, J.C.C. 1986. Cinématique de mise en place des  
57  
58 4906 ophiolites et nappes cristallophylliennes du Limousin, Ouest du Massif Central  
59  
60 4907 français. *Bulletin de la Société Géologique de France*, (8), II 5, 849-860.

- 4908 Girardeau, J., Dubuisson, G. and Mercier, J.C. 1994. Early Paleozoic mantle formations,  
1  
24909 Western Massif Central, a discussion. The Limousin ophiolite complexes: evidence for  
3  
44910 oceanic lithosphere. In: Keppie, J.D. (Ed.), Pre-Mesozoic Geology in France and  
54911 related areas: Berlin, Springer-Verlag, 349-354.  
6
- 7  
84912 Gladney, E.R., Braid, J.A., Murphy, J.B., Quesada, C. and McFarlane, C.R.M. 2014. U-Pb  
9  
104913 geochronology and petrology of the late Paleozoic Gil Marquez pluton: magmatism in  
114914 the Variscan suture zone, southern Iberia, during continental collision and the  
12  
134915 amalgamation of Pangea. *International Journal of Earth Sciences*, 103, 1433-1451.  
14  
154916 <https://doi.org/10.1007/s00531-014-1034-5>.
- 16  
174917 Gloaguen, E. 2006. Apports d'une étude intégrée sur les relations entre granites et  
18  
194918 minéralisations filoniennes (Au et Sn-W) en contexte tardiorogénique (Chaîne  
20  
214919 Hercynienne, Galice centrale, Espagne). PhD Thesis, Université d'Orléans, 572 pp.  
22  
234920 <http://tel.archives-ouvertes.fr/tel-00107391>.
- 24  
254921 Gloaguen, E., Ruffet, G., Monie, P., Barbanson, L., Branquet, Y., Chauvet, A. and Bouchot,  
26  
274922 V. 2006. Geochronological constraints on the magmatic and hydrothermal evolution of  
28  
294923 the Tras-os-Montes Hercynian domain (Galicia, Spain): Position of the Au, Sn-W  
30  
314924 mineralizing events. In: Colloque Transmet, 2006, France. Societe Francaise de  
32  
334925 Mineralogie et de Cristallographie, 111-114.
- 34  
354926 Godard, G. 1983. Dispersion tectonique des éclogites de Vendée lors d'une collision  
36  
374927 continent-continent. *Bulletin de Minéralogie*, 106, 719-722.
- 38  
394928 Godard, G. 1988. Petrology of some eclogites in the Hercynides: The eclogites from the  
40  
414929 southern Armorican Massif. In: Smith, D.C. (Ed.), *Eclogites and eclogite-facies rocks*.  
42  
434930 Elsevier, Amsterdam, 451-519.
- 44  
454931 Godard, G. 2001. The Les Essarts eclogite-bearing metamorphic Complex (Vendée, southern  
46  
474932 Armorican Massif, France): Pre-Variscan terrains in the Hercynian belt? *Géologie de*  
48  
494933 *la France*, 2001 (1-2), 19-51.
- 50  
514934 Godard, G. 2009. Two orogenic cycles recorded in eclogite-facies gneiss from the southern  
52  
534935 Armorican Massif (France). *European Journal of Mineralogy*, 21, 1173-1190.
- 54  
554936 Godard, G., Kiénast, J.-R. and Lasnier, B. 1981. Retrogressive development of glaucophane  
56  
574937 in some eclogites from the "Massif Armoricain" (east of Nantes, France).  
58  
594938 *Contributions to Mineralogy and Petrology*, 78, 126-135.

- 4939 Gómez Barreiro, J., Wijbrans, J.R., Castiñeiras, P., Martínez Catalán, J.R., Arenas, R., Díaz  
1  
24940 García, F. and Abati, J. 2006.  $^{40}\text{Ar}/^{39}\text{Ar}$  laserprobe dating of mylonitic fabrics in a  
3  
44941 polyorogenic terrane of NW Iberia. *Journal of the Geological Society, London*, 163  
54942 (1), 61-73.  
6
- 7  
84943 Gómez Barreiro, J., Martínez Catalán, J.R., Arenas, R., Castiñeiras, P., Abati, J., Díaz García,  
9  
104944 F. and Wijbrans, J.R. 2007. Tectonic evolution of the upper allochthon of the Órdenes  
114945 Complex (northwestern Iberian Massif): structural constraints to a polyorogenic peri-  
12  
134946 Gondwanan terrane. In: Linnemann, U., Nance, R.D., Kraft, P. and Zulauf, G. (Eds.),  
14  
154947 The evolution of the Rheic Ocean: From Avalonian-Cadomian active margin to  
16  
174948 Alleghenian-Variscan collision. *Geological Society of America, Special Paper* 423,  
18  
194949 315-332. [https://doi.org/10.1130/2007.2423\(15\)](https://doi.org/10.1130/2007.2423(15)).  
20
- 214950 Gómez Pugnaire, M.T., Azor, A., Fernández-Soler, J.M. and López Sánchez-Vizcaíno, V.  
22  
234951 2003. The amphibolites from the Ossa-Morena/Central Iberian Variscan suture  
24  
254952 (Southwestern Iberian Massif): Geochemistry and tectonic interpretation. *Lithos*, 68,  
264953 23-42.  
27
- 28  
294954 Gonçalves, F. 1971. Subsídios para o conhecimento geológico do nordeste Alentejano.  
30  
314955 *Serviços Geológicos de Portugal, Memória* 18 (Nova Serie), 62 pp., 7 plates, 1 map.  
32
- 334956 González Clavijo, E., Dias da Silva, Í., Gutiérrez-Alonso, G. and Díez Montes, A. 2016. U/Pb  
34  
354957 age of a large dacitic block locked in an Early Carboniferous synorogenic mélangé in  
36  
374958 the Parautochthon of NW Iberia: New insights on the structure/sedimentation Variscan  
38  
394959 interplay. *Tectonophysics*, 681, 159-169. <https://doi.org/10.1016/j.tecto.2016.01.001>.  
40
- 414960 González-Clavijo, E., Díez-Montes, A., Dias da Silva, Í.F. and Sánchez-García, T. 2017. An  
42  
434961 overview on the Ordovician volcanic rocks and unconformities in the Central Iberian  
44  
454962 and Galicia-Trás-os-Montes Zones of the Iberian Variscan Massif. In: *Ordovician  
464963 Geodynamics: the Sardinic Phase in the Pyrenees, Mouthoumet and Montagne Noire  
47  
484964 massifs*. Álvaro, J.J., Casas, J.M. and Clausen, S. (Eds.), *Géologie de la France*, 1 (4),  
49  
504965 22-24.  
51
- 524966 González Clavijo, E., Dias da Silva, I., Martínez Catalán, J.R., Gómez Barreiro, J., Gutiérrez-  
53  
544967 Alonso, G., Díez Montes, A., Hofmann, M., Gärtner, A. and Linnemann, U. 2021. A  
55  
564968 tectonic carpet of Variscan flysch at the base of a rootless accretionary prism in  
57  
584969 northwestern Iberia: U–Pb zircon age constrains from sediments and volcanic  
59  
604970 olistoliths. *Solid Earth*, 12, 835-867. <https://doi.org/10.5194/se-12-835-2021>.  
61  
62  
63  
64  
65

- 4971 Guineberteau, B., Bouchez, J.L. and Vignerese, J.L. 1987. The Mortagne granite pluton  
1 4972 (France) emplaced by pull-apart along a shear zone: structural and gravimetric  
2 arguments and regional implication. Geological Society of America Bulletin, 99, 763-  
3 4973 770.  
4 4974  
5 4975 Guitard, G., Vielzeuf, D. and Martinez, F. 1995. Métamorphisme hercynien. Synthèse  
6 4976 Géologique et Géophysique des Pyrénées - Edition BRGM - ITGE - Volume 1,  
7 Chapter 10, 501-584.  
8 4977  
9 4978 Gumiaux, C. 2003. Modélisation du cisaillement hercynien de Bretagne centrale: déformation  
10 crustale et implications lithosphériques. PhD Thesis, Université de Rennes. 267 pp.  
11 4979  
12 4980 Gumiaux, C., Gapais, D., Brun, J.P., Chantraine, J. and Ruffet, G. 2004. Tectonic history of  
13 the Hercynian Armorican shear Belt (Brittany, France). Geodinamica Acta, 17, 289-  
14 4981 397.  
15 4982  
16 4983 Gunia, T. 1999 Microfossils from the high-grade metamorphic rocks of the Góry Sowie Mts.  
17 (Sudetes area) and their stratigraphic importance. Geological Quarterly, 43 (4), 519-  
18 4984 536.  
19 4985  
20 4986 Gutiérrez-Alonso, G., Fernández-Suárez, J., Jeffries, T.E., Jenner, G.A., Tubrett, M.N., Cox,  
21 R. and Jackson, S.E. 2003. Terrane accretion and dispersal in the northern Gondwana  
22 4987 margin. An Early Paleozoic analogue of a long-lived active margin. Tectonophysics,  
23 365, 221-232. [https://doi.org/10.1016/S0040-1951\(03\)00023-4](https://doi.org/10.1016/S0040-1951(03)00023-4).  
24 4988  
25 4989 Gutiérrez-Alonso, G., Fernández-Suárez, J. and Weil, A.B. 2004. Orocline-triggered  
26 lithospheric delamination. In: Sussman, A.J. and Weil, A.B. (Eds.), Orogenic  
27 4990 curvature: Integrating Paleomagnetic and Structural Analyses. Geological Society of  
28 America Special Paper 383, 121-130. [https://doi.org/10.1130/0-8137-2383-  
29 4991 3\(2004\)383\[121:OTLD\]2.0.CO;2](https://doi.org/10.1130/0-8137-2383-3(2004)383[121:OTLD]2.0.CO;2).  
30 4992  
31 4993 Gutiérrez-Alonso, G., Fernández-Suárez, J., Jeffries, T.E., Johnston, S.T., Pastor-Galán, D.,  
32 Murphy, J.B., M. Franco, P. and Gonzalo, J.C. 2011. Diachronous post-orogenic  
33 4994 magmatism within a developing orocline in Iberia, European Variscides. Tectonics,  
34 30, TC5008, 1-17. <https://doi.org/10.1029/2010TC002845>.  
35 4995  
36 4996 Gutiérrez-Alonso, G., Collins, A.S., Fernández-Suárez, J., Pastor-Galán, D., González-  
37 Clavijo, E., Jourdan, F., Weil, A.B. and Johnston, S.T. 2015. Dating of lithospheric  
38 5000  
39  
40  
41  
42  
43  
44  
45  
46  
47  
48  
49  
50  
51  
52  
53  
54  
55  
56  
57  
58  
59  
60  
61  
62  
63  
64  
65

- 5001 buckling:  $^{40}\text{Ar}/^{39}\text{Ar}$  ages of syn-oroclinal strike-slip shear zones in northwestern Iberia.  
1  
25002 Tectonophysics, 643, 44-54. <https://doi.org/10-1016/j.tecto.2014.12.009>.  
3  
45003 Gutiérrez-Alonso, G., Fernández-Suárez, J., López-Carmona, A. and Gärtner, A. 2018.  
5  
65004 Exhuming a cold-case: The early granodiorites of the northwest Iberian Variscan Belt-  
7  
85005 A Visean magmatic flare up? Lithosphere, 10 (2), 194-216.  
9  
105006 <https://doi.org/10.1130/L706.1>.  
11  
125007 Gutiérrez-Marco, J.C. 2004a. Cordilleras Ibérica y Costero-Catalana: El basamento prealpino.  
13  
145008 In: Vera, J.A. (Ed.), Geología de España. SGE-IGME, Madrid, 470.  
15  
165009 Gutiérrez-Marco, J.C. 2004b. El Ordovícico Inferior de los Macizos Vascos. In: Vera, J.A.  
17  
185010 (Ed.), Geología de España. SGE-IGME, Madrid, Cap. 3, 245.  
19  
205011 Gutiérrez-Marco, J.C., Aramburu, C., Arbizu, M., Bernárdez, E., Hacar Rodríguez, M.P.,  
21  
225012 Méndez-Bedia, I., Montesinos López, R., Rábano, I., Truyols, J., and Villas, E. 1999a.  
23  
245013 Revisión bioestratigráfica de las pizarras del Ordovícico Medio en el noroeste de  
25  
265014 España (zonas Cantábrica, Asturoccidental-leonesa y Centroibérica septentrional).  
27  
285015 Acta Geologica Hispanica, 34 (1), 3-87.  
29  
305016 Gutiérrez-Marco, J.C., Rábano, I., Sarmiento, G.N., Aceñolaza, G.F., San José, M.A., Pieren,  
31  
325017 A.P., Herranz, P., Couto, H.M. and Piçarra, J.M. 1999b. Faunal dynamics between  
33  
345018 Iberia and Bohemia during the Oretanian and Dobrotivian (late Middle-earliest Upper  
35  
365019 Ordovician), and biogeographic relations with Avalonia and Baltica. Acta  
37  
385020 Universitatis Carolinae-Geologica, 43 (1/2), 487-490.  
39  
405021 Gutiérrez-Marco, J.C., Robardet, M., Rábano, I., Sarmiento, G.N., San José Lancha, M.A.,  
41  
425022 Herranz Araújo, P. and Pieren Pidal, A.P. 2002. Ordovician. In: Gibbons, W. and  
43  
445023 Moreno, T. (Eds.), The Geology of Spain. Geological Society, London, 31-49.  
45  
465024 Gutiérrez-Marco, J.C., Herranz, P., Pieren, A., Rábano, I., Sarmiento, G.N., San José, M.A.,  
47  
485025 Barnolas, A. and Villas, E. 2004. Cordilleras Ibérica y Costero-Catalana: El basamento  
49  
505026 prealpino. El margen pasivo ordovícico-silúrico. In: Vera, J.A. (Ed.), Geología de  
51  
525027 España. SGE-IGME, Madrid, 473-475.  
53  
545028 Gutiérrez-Marco, J.C., Ghienne, J.F., Bernárdez, E. and Hacar, M.P. 2010. Did the Late  
55  
565029 Ordovician African ice sheet reach Europe? Geology, 38 (3), 279-282.  
57  
585030 <https://doi.org/10.1130/G30430.1>.  
59  
60  
61  
62  
63  
64  
65



- 5031 Gutiérrez-Marco, J.C., Sá, A.A., García-Bellido, D.C. and Rábano, I. 2016: The Bohemo-  
1  
25032 Iberian regional chronostratigraphical scale for the Ordovician System and  
3  
45033 palaeontological correlations within South Gondwana. *Lethaia*.  
5034 <https://doi.org/10.1111/let.12197>.  
6
- 7  
85035 Gutiérrez-Marco, J.C., Piçarra, J.M., Meireles, C.A., Cózar, P., García-Bellido, D.C., Pereira,  
9  
105036 Z., Vaz, N., Pereira, S., Lopes, G., Oliveira, J.T., Quesada, C., Zamora, S., Esteve, J.,  
115037 Colmenar, J., Bernárdez, E., Coronado, I., Lorenzo, S., Sá, A.A., Dias da Silva, Í.,  
12  
135038 González-Clavijo, E., Díez-Montes, A. and Gómez-Barreiro, J. 2019. Early  
14  
155039 Ordovician–Devonian passive margin Stage in the Gondwanan units of the  
16  
175040 Iberian Massif. In: Quesada, C. and Oliveira, J.T. (Eds.), *The Geology of Iberia: A*  
18  
195041 *Geodynamic Approach, Regional Geology Reviews*, Springer Nature.  
205042 [https://doi.org/10.1007/978-3-030-10519-8\\_3](https://doi.org/10.1007/978-3-030-10519-8_3).  
21
- 22  
235043 Guy, A., Edel, J.-B., Schulmann, K., Tomek, Č. and Lexa, O. 2011. A geophysical model of  
24  
255044 the Variscan orogenic root (Bohemian Massif): Implications for modern collisional  
26  
275045 orogens. *Lithos*, 124 (1-2), 144-157. <https://doi.org/10.1016/j.lithos.2010.08.008>.  
28
- 295046 Habryn, R., Krzeminska, E., Krzeminski, L., Markowiak, M. and Zielinski, G. 2020. Detrital  
30  
315047 zircon age data from the conglomerates in the Upper Silesian and Małopolska blocks,  
32  
335048 and their implications for the pre-Variscan tectonic evolution (S Poland). *Geological*  
34  
355049 *Quarterly*, 64 (2), 321-341.
- 36  
375050 Hacker, B.R., Kelemen, P.B. and Behn, M.D. 2011. Differentiation of the continental crust by  
38  
395051 relamination. *Earth and Planetary Science Letters*, 307, 501-516.  
405052 <https://doi.org/10.1016/j.epsl.2011.05.024>.  
41
- 42  
435053 Hajná, J., Žák, J. and Kachlík, V. 2011. Structure and stratigraphy of the Teplá–Barrandian  
44  
455054 Neoproterozoic, Bohemian Massif: A new plate-tectonic reinterpretation. *Gondwana*  
46  
475055 *Research*, 19, 495-508.
- 48  
495056 Hajná, J., Žák, J., Kachlík, V. and Chadima, M. 2012. Deciphering the Variscan tectonothermal  
50  
515057 overprint and deformation partitioning in the Cadomian basement of the Teplá–  
52  
535058 Barrandian unit, Bohemian Massif. *International Journal of Earth Sciences*, 101, 1855-  
54  
555059 1873.
- 56  
575060 Hajná, J., Žák, J., Dörr, W., Kachlík, V. and Sláma, J. 2018. New constraints from detrital  
58  
595061 zircon ages on prolonged, multiphase transitiv from the Cadomian accretionary orogen  
605062 to a passive margin of Gondwana. *Precambrian Research*, 317, 159-178.  
61  
62  
63  
64  
65

- 5063 Hanmer, S.K. 1977. Age and tectonic implications of the Baie d'Audierne basic-ultrabasic  
1 5064 complex. *Nature*, 270, 336-338.  
2  
3  
4 5065 Hardy, S. and Allmendinger, R.W. 2011. Trishear: A review of kinematics, mechanics and  
5  
6 5066 applications. In McClay, K., Shaw, J.H. and Suppe, J. (Eds.), Thrust fault related  
7  
8 5067 folding. American Association of Petroleum Geologists, Memoir 94, 95-121.  
9  
10 5068 Hefferan, K., Soullaimani, A., Samson, S.D., Admou, H., Inglis, J., Saquaque, A., Latifa, C.  
11  
12 5069 and Heywood, N. 2014. A reconsideration of Pan African orogenic cycle in the Anti-  
13  
14 5070 Atlas Mountains, Morocco. *Journal of African Earth Sciences*, 98, 34-46.  
15  
16 5071 Henry, J.L., Nion, J., Paris, F. and Thadeu, D. 1974. Chitinozoaires, Ostracodes et Trilobites  
17  
18 5072 de l'Ordovicien du Portugal (Serra de Buçaco) et du Massif Armoricaïn: essai de  
19  
20 5073 comparaison et signification paléogéographique. *Comunicaçoes dos Serviços*  
21  
22 5074 *Geológicos de Portugal*, 57, 303-345.  
23  
24 5075 Hoepffner, C., Houari, M.R. and Bouabdelli, M. 2006. Tectonics of the North African  
25  
26 5076 Variscides (Morocco, western Algeria), an outline. Recent developments on the  
27  
28 5077 Maghreb geodynamics. *Comptes Rendus Geoscience*, Special Volume 338, 25-40.  
29  
30 5078 Hofmann, M. and Linnemann, U. 2013. The Late Ordovician (Hirnantian) Lederschiefer  
31  
32 5079 Formation in Thuringia – Evidences for a glaciomarine origin from the Berga  
33  
34 5080 Antiform (Saxo-Thuringian Zone). *Geologica Saxonica*, 59, 133-139.  
35  
36 5081 Hofmann, M., Linnemann, U., Gerdes, A., Ullrich, B. and Schauer, M. 2009. Timing of  
37  
38 5082 dextral strike-slip processes and basement exhumation in the Elbe Zone (Saxo-  
39  
40 5083 Thuringian Zone): the final pulse of the Variscan Orogeny in the Bohemian Massif  
41  
42 5084 constrained by LA-SF-ICP-MS U-Pb zircon data. In: Murphy, J.B., Keppie, J.D. and  
43  
44 5085 Hynes, A.J. (Eds.), *Ancient orogens and modern analogues*, Geological Society,  
45  
46 5086 London, 327, 197-214. <https://doi.org/10.1144/SP327.10>.  
47  
48 5087 Hubregtse, J.J.M.W. 1973. Petrology of the Mellid area, a Precambrian polymetamorphic  
49  
50 5088 rock complex, Galicia, N.W. Spain. *Leidse Geologische Mededelingen*, 49, 9-31.  
51  
52 5089 Iglesias Ponce de León, M. and Choukroune, P. 1980. Shear zones in the Iberian arc. *Journal*  
53  
54 5090 *of Structural Geology*, 2, 63-68.  
55  
56 5091 IGME-LNEG. 2015. Mapa geológico de España y Portugal. Escala 1:1.000.000. Instituto  
57  
58 5092 Geológico y Minero de España - Laborarorio Nacional de Energía y Geología de  
59  
60 5093 Portugal. Rodríguez Fernández, L.R. and Oliveira, J.T. (Eds.).  
61  
62  
63  
64  
65

- 5094 Irving, E. 1977. Drift of the major continental blocks since the Devonian. *Nature*, 270, 97-  
1 5095 112.  
2  
3
- 45096 Janoušek, V. and Holub, F.V. 2007. The causal link between HP–HT metamorphism and  
5 5097 ultrapotassic magmatism in collisional orogens: case study from the Moldanubian  
6 5098 Zone of the Bohemian Massif. *Proceedings of the Geologists' Association*, 118,75-86.  
7  
8  
9
- 105099 Janoušek, V., Braithwaite, C.J R., Bowes, D.R. and Gerdes, A. 2004. Magma-mixing in the  
11 5100 genesis of Hercynian calc-alkaline granitoids: an integrated petrographic and  
12 5101 geochemical study of the Sázava intrusion, Central Bohemian Pluton, Czech Republic.  
13  
14 5102 *Lithos*, 78 (1-2), 67-99.  
15  
16
- 17 5103 Janoušek, V., Krenn, E., Finger, F., Míková, J. and Frýda, J. 2007. Hyperpotassic granulites  
18 5104 from the Blanský les Massif (Moldanubian Zone, Bohemian Massif) revisited. *Journal*  
19 5105 *of Geosciences* 52, 73-112. <https://doi.org/10.3190/jgeosci.010>.  
20  
21  
22
- 23 5106 Janoušek, V., Vrána, S., Erban, V., Vokurka, K. and Drábek, M. 2008. Metabasic rocks in the  
24 5107 Varied Group of the Moldanubian Zone, southern Bohemia – their petrology,  
25 5108 geochemical character and possible petrogenesis. *Journal of Geosciences*, 53, 31-  
26  
27  
28  
29 5109 64.  
30
- 31 5110 Janoušek, V., Wiegand, B.A. and Žák, J. 2010. Dating the onset of Variscan crustal  
32 5111 exhumation in the core of the Bohemian Massif: new U–Pb single zircon ages from  
33 5112 the high-K calc-alkaline granodiorites of the Blatná suite, Central Bohemian Plutonic  
34  
35  
36  
37 5113 Complex. *Journal of the Geological Society, London*, 167, 347-360.  
38
- 39 5114 Janoušek, V., Aichler, J., Hanžl, P., Gerdes, A., Erban, V., Žáček, V., Pecina, V., Pudilová,  
40 5115 M., Hrdličková, K., Mixa, P. and Žáčková, E. 2014. Constraining genesis and  
41 5116 geotectonic setting of metavolcanic complexes: a multidisciplinary study of the  
42  
43  
44  
45 5117 Devonian Vrbno Group (Hrubý Jeseník Mts., Czech Republic). *International Journal*  
46 5118 *of Earth Sciences*, 103, 455-483.  
47  
48
- 49 5119 Janoušek, V., Hanžl, P., Svojtka, M., Hora, J.M., Erban, V., Kochergina, Y., Gadas, P., Holub,  
50 5120 F.V., Gerdes, A., Verner, K., Hrdličková, K., Daly, J.S. and Buriánek, D., 2020.  
51 5121 Ultrapotassic magmatism in the heyday of the Variscan Orogeny: the story of the  
52 5122 Třebíč Pluton, the largest durbachitic body in the Bohemian Massif. *International*  
53 5123 *Journal of Earth Sciences*, 109, 1767-1810.  
54  
55  
56  
57  
58  
59  
60  
61  
62  
63  
64  
65

- 5124 Jastrzębski, M., Żelaźniewicz, A., Majka, J., Murtezi, M., Bazarnik, J. and Kapitonov, I.  
1  
25125 2013. Constrains on the Devonian-Carboniferous closure of the Rheic Ocean from a  
3  
45126 multi-method geochronology study on the Staré Město Belt in the Sudetes (Poland and  
5127 the Czech Republic). *Lithos*, 170-171, 54-72.  
6  
75128 <https://doi.org/10.1016/j.lithos.2013.02.021>.  
8  
95129 Jeřábek, P., Konopásek, J. and Záčková, E. 2016. Two-stage exhumation of subducted  
10  
115130 Saxothuringian continental crust records underplating in the subduction channel and  
12  
135131 collisional forced folding (Krkonoše-Jizera Mts., Bohemian Massif). *Journal of*  
14  
155132 *Structural Geology*, 89, 214-229. <https://doi.org/10.1016/j.jsg.2016.06.008>.  
16  
175133 Jesus, A.P., Munhá, J., Mateus, A., Tassinari, C. and Nutman, A.P. 2007. The Beja layered  
18  
195134 gabbroic sequence (Ossa-Morena Zone, southern Portugal): Geochronology and  
20  
215135 geodynamic implications. *Geodinamica Acta*, 20, 139-157.  
22  
235136 <https://doi.org/10.3166/ga.20.139-157>.  
24  
255137 Julivert, M., Fontboté, J.M., Ribeiro, A. and Conde, L. 1972. Mapa Tectónico de la Península  
26  
275138 Ibérica y Baleares E. 1: 1 000 000. Instituto Geológico y Minero de España, Madrid.  
28  
295139 Julivert, M., Fontboté, J.M., Ribeiro, A. and Conde, L. 1980. Mapa Tectónico de la Península  
30  
315140 Ibérica y Baleares (Memoria). Instituto Geológico y Minero de España, Madrid. 113  
32  
335141 pp.  
34  
355142 Jung, J. and Roques, M. 1952. Introduction à la zonéographie des formations  
36  
375143 cristallophylliennes. *Bulletin des services de la carte géologique de la France*, 235, 62.  
38  
395144 Kachlík, V. 1997. The Kladská Unit. In: Vrána, S. and Štědrá, V. (Eds.), *Geological model of*  
40  
415145 *western Bohemia related to the KTB borehole in Germany*. Czech Geological Survey,  
42  
435146 Prague, 70-80.  
44  
455147 Kalt, A., Hanel, M., Schleicher, H. and Kramm, U. 1994. Petrology and geochronology of  
46  
475148 eclogites from the Variscan Schwarzwald (F.R.G.). *Contributions to Mineralogy and*  
48  
495149 *Petrology*, 115, 287-302.  
50  
515150 Katzung, G. 1961. Die Geröllführung des Lederschiefers (Ordovizium) an der SE-Flanke des  
52  
535151 Schwarzbürger Sattels (Thüringen). *Geologie*, 10 (7), 778-802, Berlin.  
54  
555152 Keppie, J.D. 1994 (Ed.). *Pre-Mesozoic geology in France and related areas*. Springer-Verlag,  
56  
575153 Berlin, 514 pp.  
58  
59  
60  
61  
62  
63  
64  
65

- 5154 Kharbouch, F., 1994. Le volcanisme dévono-dinantien du Massif central et de la Meseta  
1  
25155 orientale. Géologie du Paléozoïque du Maroc central et de la Meseta orientale.  
3  
45156 Bulletin de l'Institut Scientifique (Rabat), Numero Spécial, 18, 191-199.
- 5  
65157 Kharbouch, F., Juteau, T., Treuil, M., Joron, J.L., Piqué, A. and Hoepffner, C. 1985. Le  
7  
85158 volcanisme dinantien de la Meseta marocaine nord-occidentale et orientale. Caractères  
9  
95159 pétrographiques et géochimiques et implications géodynamiques. Sciences  
10  
115160 Géologiques, Bulletins et mémoires, 38, 155-163.
- 12  
13  
145161 Klemm, R. 2010. Early Variscan allochthonous domains: the Münchberg Complex,  
15  
165162 Frankenberg, Wildenfels, and Góry Sowie. In: Linnemann, U. and Romer, R.L. (Eds.),  
175163 Pre-Mesozoic Geology of Saxo-Thuringia-From the Cadomian Active Margin to the  
18  
195164 Variscan Orogen. Schweizerbart, Stuttgart, 221-232.
- 20  
215165 Koglin, N., Zeh, A., Franz, G., Schüssler, U., Glodny, J, Gerdes, A. and Brätz, H. 2018. From  
22  
235166 Cadomian magmatic arc to Rheic ocean closure: the geochronological-geochemical  
24  
255167 record of nappe protoliths of the Münchberg Massif, NE Bavaria (Germany).  
26  
275168 Gondwana Research, 55, 135-152.
- 28  
295169 Konopásek, J., Schulmann, K. and Johan, V. 2002. Eclogite-facies metamorphism at the  
30  
315170 eastern margin of the Bohemian Massif—subduction prior to continental  
32  
335171 underthrusting?. European Journal of Mineralogy, 14, 701-713.
- 34  
355172 Konopásek, J., Anczkiewicz, R., Jeřábek, P., Corfu, F. and Žáčková, E. 2019. Chronology of  
36  
375173 the Saxothuringian subduction in the West Sudetes (Bohemian Massif, Czech  
38  
395174 Republic and Poland). Journal of the Geological Society, London, 176 (1), 492-504.  
40  
415175 <https://doi.org/10.1144/jgs.2018-173>.
- 42  
435176 Košler, J., Aftalion, M. and Bowes, D.R. 1993. Mid-late Devonian plutonic activity in the  
44  
455177 Bohemian Massif: U-Pb zircon isotopic evidence from the Staré Sedlo and Mirotice  
46  
475178 gneiss complexes. Neues Jahrbuch für Mineralogie Monatshefte, 417-431.
- 48  
495179 Košler, J., Konopásek, J., Sláma, J. and Vrána, S. 2014. U–Pb zircon provenance of  
50  
515180 Moldanubian metasediments in the Bohemian Massif. Journal of the Geological  
52  
535181 Society, London, 171, 83-95.
- 54  
555182 Kossmat, F. 1921. Die mediterranen Kettengebirge in ihrer Beziehung zum  
56  
575183 Gleichgewichtszustande der Erde. Abhandlungen der Sächsische Akademie der  
58  
59  
60  
61  
62  
63  
64  
65

- 5184            Wissenschaften, Mathematisch-Physischen, (Abhandl. Sächs. Akad. Wiss., math.-  
1  
25185            phys.) Kl., 38 (2). Leipzig.
- 3  
45186            Kossmat, F. 1927. Gliederung des varistischen Gebirgsbaues. Abhandlungen des Sächsischen  
5  
65187            Geologuschen Landesamts, Leipzig, Heft 1, 39 pp., 2 tafeln.
- 7  
85188            Kotková, J., Gerdes, A., Parrish, R.R. and Novák, M. 2007. Clasts of Variscan high-grade  
9  
105189            rocks within upper Visean conglomerates—constraints on exhumation history from  
11  
125190            petrology and U-Pb chronology. *Journal of Metamorphic Geology*, 25 (7), 781-801.
- 13  
145191            Krawczyk, C.M., Stein, E., Choi, S., Oettinger, G., Schuster, K., Götze, H.J., Haak, V.,  
15  
165192            Oncken, O., Prodehl, C., and Schulze, A. 2000. Geophysical constraints on the  
17  
185193            exhumation mechanisms of high pressure rocks: the Saxo-Thuringian case between the  
19  
205194            Franconian Line and Elbe Zone. In: Franke, W., Haak, V., Oncken, O. and Tanner, D.  
21  
225195            (Eds.), *Orogenic Processes: Quantification and modelling in the Variscan Belt*.  
235196            Geological Society, London, Special Publication 179, 303-322.
- 24  
255197            Krecher, M., Behrmann, J.H. and Müller-Sigmund, H. 2007. Sedimentology and tectonic  
26  
275198            setting of Devonian-Carboniferous turbidites and debris flow deposits in the Variscan  
28  
295199            Vosges Mountains (Markstein Group, NE-France). *Zeitschrift der Deutschen*  
30  
315200            *Gesellschaft für Geowissenschaften*, 158, 1063-1087.
- 32  
335201            Kreuzer, H., Seidel, E., Schüssler, U., Okrusch, M., Lenz, K.L. and Raschka, H. 1989. K-Ar  
34  
355202            geochronology of different tectonic units at the northwestern margin of the Bohemian  
36  
375203            Massif. *Tectonophysics*, 157, 149-178.
- 38  
395204            Krohe, A. 1996. Variscan tectonics of central Europe: Postaccretionary intraplate deformation  
40  
415205            of weak continental lithosphere. *Tectonics*, 15 (6), 1364-1388.
- 42  
435206            Kroner, U. 1995. Postkollisionale Extension am Nordrand der Böhmisches Masse – die  
44  
455207            Exhumierung des Sächsischen Granulitgebirges. *Freiberger Forschungshefte*, C457, 1-  
46  
475208            114.
- 48  
495209            Kroner, U. and Romer, R.L. 2013. Two plates - Many subduction zones: The Variscan  
50  
515210            orogeny reconsidered. *Gondwana Research*, 24, 298-329.  
52  
535211            <https://doi.org/10.1016/j.gr.2013.03.001>.
- 54  
555212            Kroner, U., Romer, R.L. and Linnemann, U. 2010. The Saxo-Thuringian Zone of the Variscan  
56  
575213            Orogen as part of Pangea. In: Linnemann, U. and Romer, R.L. (Eds.), *Pre-Mesozoic*

- 5214 Geology of Saxo-Thuringia - From the Cadomian Active Margin to the Variscan  
1  
25215 Orogen. Stuttgart, 3-16.  
3
- 45216 Kröner, A. and Hegner, E. 1998. Geochemistry, single zircon ages and Sm-Nd systematics of  
5  
65217 granitoid rocks from the Góry Sowie (Owl Mts.), Polish West Sudetes: evidence for  
7  
85218 early Paleozoic arc-related plutonism. *Journal of the Geological Society, London*, 155  
9  
105219 (4), 711-724.
- 11  
125220 Kröner, A., Jaeckel, P., Hegner, E. and Opletal, M. 2001. Single zircon ages and whole-rock  
13  
145221 Nd isotopic systematic of early Paleozoic granitoid gneisses from the Czech and  
15  
165222 Polish Sudetes (Jizerske hory, Karkonosze Mountains and Orlica-Śnieżnik Complex).  
17  
185223 *International Journal of Earth Sciences*, 90, 304-324.
- 19  
205224 Kryza, R. and Fanning, C.M. 2007. Devonian deep-crustal processes and uplift in the  
21  
225225 Variscan Orogen: evidence from SHRIMP zircon ages from the HT-HP granulites and  
23  
245226 migmatites of the Góry Sowie (Polish Sudetes). *Geodinamica Acta*, 20, 159-175.
- 25  
265227 Kryza, R., Muszynski, A. and Vielzeuf, D. 1990. Glaucofanite-bearing assemblage  
27  
285228 overprinted by greenschist-facies metamorphism in the Variscan Kaczawa complex,  
29  
305229 Sudetes, Poland. *Journal of Metamorphic Geology*, 8 (3), 345-355.
- 31  
325230 Kryza, R., Mazur, S. and Pin, C. 1995. The Leszczyńiec meta-igneous Complex in the eastern  
33  
345231 part of the Karkonosze-Izera Block, Western Sudetes: trace element and Nd isotope  
35  
365232 study. *Neues Jahrbuch für Mineralogie-Abhandlungen*, 170, 59-74.
- 37  
385233 Kryza, R., Mazur, S. and Oberc-Dziedzic, T. 2004. The Sudetic geological mosaic: insights  
39  
405234 into the root of the Variscan orogen. *Przegląd Geologiczny*, 52 (8/2), 761-773.
- 41  
425235 Kryza, R. and Zalasiewicz, J. 2008. Records of Precambrian–Early Palaeozoic volcanic and  
43  
445236 sedimentary processes in the Central European Variscides: A review of SHRIMP  
45  
465237 zircon data from the Kaczawa succession (Sudetes, SW Poland). *Tectonophysics*, 461,  
47  
485238 60-71. <https://doi.org/10.1016/j.tecto.2008.04.003>.
- 49  
505239 Kryza, R., Willner, A.P., Massonne, H.J., Muszyński, A. and Schertl, H.P. 2011. Blueschist-  
51  
525240 facies metamorphism in the Kaczawa Mountains (Sudetes, SW Poland) of the Central-  
53  
545241 European Variscides: PT constraints from a jadeite-bearing metatrachyte.  
55  
565242 *Mineralogical Magazine*, 75, 241-263.
- 57  
585243 Kryza, R., Schaltegger, U., Oberc-Dziedzic, T., Pin, C. and Ovtcharova, M. 2014.  
59  
605244 Geochronology of a composite granitoid pluton: a high-precision ID-TIMS U-Pb

- 5245 zircon study of the Variscan Karkonosze Granite (SWPoland). *International Journal of*  
1 Earth Sciences, 103, 683-696.  
2
- 3  
45247 Kusbach, V., Janoušek, V., Hasalová, P., Schulmann, K., Fanning, C.M., Erban, V. and  
5  
65248 Ulrich, S. 2015. Importance of crustal relamination in origin of the orogenic mantle  
7  
85249 peridotite–high-pressure granulite association: example from the Náměšť Granulite  
9  
95250 Massif (Bohemian Massif, Czech Republic). *Journal of the Geological Society,*  
10  
115251 London, 172, 479-490. <https://doi.org/10.1144/jgs2014-070>.  
12
- 13  
145252 Lahfid, A., Baidder, L., Ouanaïmi, H., Soulaïmani, A., Hoepffner, C., Farah, A., Saddiqi, O.  
15  
165253 and Michard, A. 2019. From extension to compression: high geothermal gradient  
17  
185254 during the earliest Variscan phase of the Moroccan Meseta; a first structural and  
19  
205255 RSCM thermometric study. *European Journal of Mineralogy*, 31, 695-713.  
21
- 225256 Lahondère, D., Chèvremont, P., Béchenec, F., Bouton, P., Godard, G., Stussi, J.-M., Viaud,  
23  
245257 J.-M., Roy, C., Cocherie, A. and Rebay, G. 2009. Notice explicative de la carte  
25  
265258 géologique de France au 1:50000, feuille Palluau (535). BRGM, Orléans, 176 pp.  
27
- 285259 Lange, U., Bröcker, M., Armstrong, R., Żelaźniewicz, A., Trapp, E. and Mezger, K. 2005.  
29  
305260 The orthogneisses of the Orlica-Śnieżnik complex (West Sudetes, Poland):  
31  
325261 geochemical characteristics, the importance of pre-Variscan migmatization and  
33  
345262 constraints on the cooling history. *Journal of the Geological Society, London*, 162,  
35  
365263 973-984.  
37
- 385264 Lardeaux, J.M., Ledru, P., Daniel, I. and Duchene, S. 2001. The Variscan French Massif  
39  
405265 Central—a new addition to the ultra-high pressure metamorphic ‘club’: exhumation  
41  
425266 processes and geodynamic consequences. *Tectonophysics*, 332, 143-167.  
43
- 445267 Lardeaux, J.M., Schulmann, K., Faure, M., Janoušek, V., Lexa, O., Skrzypek, E., Edel, J.B.  
45  
465268 and Štípská, P. 2014. The Moldanubian Zone in French Massif Central,  
47  
485269 Vosges/Schwarzwald and Bohemian Massif revisited: Differences and similarities. In:  
49  
505270 Schulmann, K., Martínez Catalán, J.R., Lardeaux, J.M., Janousek, V. and Oggiano, G.  
51  
525271 (Eds.), *The Variscan Orogeny: Extent, Timescale and the Formation of the European*  
52  
535272 *Crust*. Geological Society, London, Special Publication 405, 7-44.  
54  
555273 <https://doi.org/10.1144/SP405.14>.  
56
- 575274 Lardeux, H. and Cavet, P. 1994. Paleozoic of the Ligerian Domain, The Variscan Orogeny in  
58  
595275 the Armorican Massif, In: Keppie, J.D. (Ed.), *Pre-Mesozoic Geology in France and*  
60  
615276 *related areas*. Springer-Verlag, Berlin, 152-156.  
62  
63  
64  
65



- 5277 Ledru, P., Lardeaux, J.M., Santallier, D., Autran, A., Quenardel, J.M., Floc'h J.P., Lerouge,  
1 5278 G., Maillet, N., Marchand, J. and Ploquin, A. 1989. Où sont les nappes dans le Massif  
2  
3 5279 Central Français? Bulletin de la Société Géologique de France, 3, 605-618.  
4  
5 5280 <https://doi.org/10.2113/gssgfbull.V.3.605>.  
6
- 7 5281 Ledru, P. Autran, A. and Santallier, D. 1994a. Lithostratigraphy of Variscan Terranes in the  
8  
9 5282 French Massif Central: A basis for paleogeographical reconstruction, The Massif  
10  
11 5283 Central. In: Keppie, J.D. (Ed.), Pre-Mesozoic Geology in France and related areas:  
12  
13 5284 Berlin, Germany, Springer-Verlag, Berlin, 276-288.  
14
- 15 5285 Ledru, P. Costa, S. and Echtler, H. 1994b. Structure, The Massif Central. In: Keppie, J.D.  
16  
17 5286 (Ed.), Pre-Mesozoic Geology in France and related areas: Berlin, Germany, Springer-  
18  
19 5287 Verlag, Berlin, 305-323.  
20
- 21 5288 Ledru, P., Courrioux, G., Dallain, C., Lardeaux, J.M. Montel, J.M., Vanderhaeghe, O. and  
22  
23 5289 Vitel, 2001. The Velay dome (French Massif Central): melt generation and granite  
24  
25 5290 emplacement during orogenic evolution, Tectonophysics, 342, 207-237.  
26
- 27 5291 Lefèvre C., Lakhrissi M. and Schneider J.L. 1994. Les affinités magmatiques du volcanisme  
28  
29 5292 dinantien des Vosges méridionales (France): approche géochimique et interprétation.  
30  
31 5293 Comptes Rendus de l'Académie des Sciences, Paris, II-319, 79-86.  
32
- 33 5294 Le Gall, J. 1999. Les dolérites et basaltes tholéiitiques du domaine nord-armoricain. Géologie  
34  
35 5295 de la France, 4, 3-26.  
36
- 37 5296 Le Heron, D.P., Ghienne, J.F., El Houicha, M., Khoukhi, Y. and Rubino, J.L. 2007.  
38  
39 5297 Maximum extent of ice sheets in Morocco during the Late Ordovician glaciation.  
40  
41 5298 Paleogeography, Paleoclimatology, Paleoecology, 245, 200-226.  
42
- 43 5299 Leloix, C., Faure, M. and Feybesse, J.L. 1999. Hercynian polyphase tectonics in north-east  
44  
45 5300 French Massif Central: the closure of the Breévenne Devonian-Dinantian rift.  
46  
47 5301 International Journal of Earth Sciences, 88, 409-421.  
48
- 49 5302 Le Maître, D. 1937. Étude de la faune corallienne des calcaires givétiens de la Ville-Dé  
50  
51 5303 d'Ardin (Deux-Sèvres). Bulletin de la Société Géologique de France, (5) VII, 105-128.  
52
- 53 5304 Le Pichon, X., Sibuet, J.D. and Francheteau, J. 1977. The fit of the continents around the  
54  
55 5305 North Atlantic Ocean. Tectonophysics, 28, 169-209.  
56
- 57 5306 Letsch, D., El Houicha, M., von Quadt, A. and Winkler, W. 2018. A missing link in the peri-  
58  
59 5307 Gondwanan terrane collage: the Precambrian basement of the Moroccan Meseta and  
60  
61  
62  
63  
64  
65

- 5308 its lower Paleozoic cover. *Canadian Journal of Earth Sciences*, 55, 33-51,  
1  
2 5309 [dx.doi.org/10.1139/cjes-2017-0086](https://doi.org/10.1139/cjes-2017-0086).  
3
- 4 5310 Leveridge, B.E. and Hartley, A.J. 2006. The Variscan orogeny: the development and  
5  
6 5311 deformation of Devonian/Carboniferous basins in SW England and South Wales. In:  
7  
8 5312 Brenchley, P.J. and Rawson, P.F. (Eds.) *The Geology of England and Wales*, 2<sup>nd</sup> edn.  
9  
10 5313 The Geological Society, London, pp 225-255.
- 11  
12 5314 Lexa, O., Schulmann, K., Janoušek, V., Štípská, P., Guy, A., and Racek, M. 2011. Heat  
13  
14 5315 sources and trigger mechanisms of exhumation of HP granulites in Variscan orogenic  
15  
16 5316 root: *Journal of Metamorphic Geology*, 29, 79-102. <https://doi.org/10.1111/j.1525-1314.2010.00906.x>.
- 17 5317  
18  
19 5318 Lindner, M., Dörr, W., Reither, D. and Finger, F. 2020. The Dobra Gneiss and the Drosendorf  
20  
21 5319 Unit in the south-eastern Bohemian Massif, Austria: West-Amazonian crust in the  
22  
23 5320 heart of Europe. *Geological Society, London, Special Publications*, 503, 20.
- 24  
25 5321 Lindner, M. and Finger, F. 2018. Geochemical characteristics of the Late Proterozoic Spitz  
26  
27 5322 granodiorite gneiss in the Drosendorf Unit (southern Bohemian Massif, Austria) and  
28  
29 5323 implications for regional tectonic interpretations. *Journal of Geosciences*, 63, 345-362.  
30
- 31 5324 Linnemann, U. and Romer, R.L. (Eds.). 2010. *Pre-Mesozoic geology of Saxo-Thuringia*.  
32  
33 5325 From the Cadomian active margin to the Variscan orogen. Schweizerbart Science  
34  
35 5326 Publishers, 485 pp., 1 fold out and 1 sheet map.
- 36  
37 5327 Linnemann, U., Elicki, O. and Gaitzsch, B. 2003. Die Stratigraphie des Saxothuringikums. In:  
38  
39 5328 Linnemann, U. (Ed.), *Das Saxothuringikum*, Kapitel 3. *Geologica Saxonica*, 48/49,  
40  
41 5329 29-70.  
42
- 43 5330 Linnemann, U., Gerdes, A., Drost, K. and Buschmann, B. 2007. The continuum between  
44  
45 5331 Cadomian orogenesis and opening of the Rheic Ocean: Constraints from LA-ICP-MS  
46  
47 5332 U-Pb zircon dating and analysis of plate-tectonic setting (Saxo-Thuringian zone,  
48  
49 5333 northeastern Bohemian Massif, Germany). In: Linnemann, U., Nance, R.D., Kraft, P.  
50  
51 5334 and Zulauf, G. (Eds.), *The evolution of the Rheic Ocean: From Avalonian-Cadomian*  
52  
53 5335 *active margin to Alleghenian-Variscan collision*. *Geological Society of America*  
54  
55 5336 *Special Paper*, 423, 61-96. [https://doi.org/10.1130/2007.2423\(03\)](https://doi.org/10.1130/2007.2423(03)).  
56
- 57 5337 Linnemann, U., Pereira, F., Jeffries, T.E., Drost, K. and Gerdes, A. 2008. The Cadomian  
58  
59 5338 Orogeny and the opening of the Rheic Ocean: The diacrony of geotectonic processes  
60  
61  
62  
63  
64  
65

- 5339 constrained by LA-ICP-MS U–Pb zircon dating (Ossa-Morena and Saxo-Thuringian  
1  
25340 Zones, Iberian and Bohemian Massifs). *Tectonophysics*, 461, 21-43.  
3  
45341 <https://doi.org/10.1016/j.tecto.2008.05.002>.
- 5  
65342 Linnemann, U., Pieren, A., Hofmann, M., Drost, K., Quesada, C., Gerdes, A., Marko, L.,  
7  
85343 Gärtner, A., Ulrich, J., Krause, R., Vickers-Rich, P. and Horak, J. 2018. A ~565 Ma  
9  
105344 old glaciation in the Ediacaran of peri-Gondwanan West Africa. *International Journal*  
11  
125345 *of Earth Sciences*, 107, 885-911. <https://doi.org/10.1007/s00531-017-1520-7>.
- 13  
145346 Liñán, E., Gozalo, R., Palacios, T., Gámez-Vintaned, J.A., Ugidos, J.M. y Mayoral, E. 2002.  
15  
165347 Cambrian. En: Gibbons W., Moreno T. (Eds): *The Geology of Spain*. Geological  
17  
185348 Society, London, pp. 17-29.
- 19  
205349 Liñán, E., Gámez-Vintaned, J.A., San José, M.A. and Tejero, R. 2004. Cordilleras Ibérica y  
21  
225350 Costero-Catalana: El basamento prealpino. El sustrato prepaleozoico. In: Vera, J.A.  
23  
245351 (Ed.), *Geología de España*. SGE-IGME, Madrid, 470-471.
- 25  
265352 López-Carmona, A., Abati, J. and Reche, J. 2010. Petrologic model of chloritoid-glaucophane  
27  
285353 schists from the NW Iberian Massif. *Gondwana Research*, 17 (2-3), 377-391.  
29  
305354 <https://doi.org/10.16/j.gr.2009.10.003>.
- 31  
325355 López-Carmona, A., Pitra, P. and Abati, J. 2013. Blueschist-facies metapelites from the  
33  
345356 Malpica-Tui Unit (NW Iberian Massif): phase equilibria modelling and H<sub>2</sub>O and  
35  
365357 Fe<sub>2</sub>O<sub>3</sub> influence in high-pressure assemblages. *Journal of Metamorphic Geology*, 31,  
37  
385358 263-280.
- 39  
405359 López-Carmona, A., Abati, J., Pitra, P. and Lee, J.K.W. 2014. Retrogressed lawsonite  
41  
425360 blueschists from the NW Iberian Massif: P-T-t constraints from thermodynamic  
43  
445361 modelling and <sup>40</sup>Ar/<sup>39</sup>Ar geochronology. *Contributions to Mineralogy and Petrology*,  
45  
465362 167, 1-20. <https://doi.org/10.1007/s00410-014-0987-5>.
- 47  
485363 López-Moro, F.J. and López-Plaza, M. 2004. Monzonitic series from the Variscan Tormes  
49  
505364 Dome (Central Iberian Zone): petrogenetic evolution from monzogabbro to granite  
51  
525365 magmas. *Lithos*, 72, 19-44.
- 53  
545366 López-Guijarro, R., Armendáriz, M., Quesada, C., Fernández-Suárez, Murphy, J.B., Pin, C.  
55  
565367 and Bellido, F. 2008. Ediacaran–Palaeozoic tectonic evolution of the Ossa Morena and  
57  
585368 Central Iberian zones (SW Iberia) as revealed by Sm-Nd isotope systematics.  
59  
605369 *Tectonophysics*, 461, 202- 214. <https://doi.org/10.1016/j.tecto.2008.06.006>.

- 5370 López-Moro, F.J., López-Plaza, M., Gutiérrez-Alonso, G., Fernández-Suárez, J., López-  
1 Carmona, A., Hofmann, M. and Romer, R.L. 2017. Crustal melting and recycling:  
25371 geochronology and sources of Variscan syn-kinematic anatectic granitoids of the  
3  
45372 Tormes Dome (Central Iberian Zone). A U-Pb LA-ICP-MS study. International  
5  
65373 Journal of Earth Sciences, 107 (3), 985-1004. <https://doi.org/10.1007/s00531-017-1483-8>.  
75374  
8  
95375
- 10  
115376 López Sánchez-Vizcaíno, V., Gómez-Pugnaire, M.T., Azor, A. and Fernández-Soler, J.M.  
12  
135377 2003. Phase diagram sections applied to amphibolites: a case study from the Ossa-  
14  
155378 Morena/Central Iberian Variscan suture (southwestern Iberian massif). Lithos, 68, 1-  
16  
175379 21.
- 18  
195380 Lotout, C., Pitra, P., Poujol, M., Anczkiewicz, R. and Van Den Driessche, J. 2018. Timing  
20  
215381 and duration of Variscan high-pressure metamorphism in the French Massif Central: A  
22  
235382 multimethod geochronological study from the Najac Massif. Lithos, 308-309, 381-  
24  
255383 394. <https://doi.org/10.1016/j.lithos2018.03.022>.
- 26  
275384 Lotze, F. 1929. Stratigraphie und Tektonik des Keltiberischen Grundgebirges (Spanien).  
28  
295385 Abhandlungen Gesellschaft der Wissenschaften zu Göttingen, Mathematisch-  
30  
315386 Physischen, 14 (2), 143-462.
- 32  
335387 Lotze, F. 1945. Zur Gliederung der Varisziden der Iberischen Meseta. Geotektonische  
34  
355388 Forschungen, 6, 78-92.
- 36  
375389 Lubedser, S. 2008. Palaeozoic low-oxygen, high-latitude carbonates: Silurian and Lower  
38  
395390 Devonian nautiloid and scyphocrinoid limestones of the Anti-Atlas (Morocco).  
40  
415391 Palaeogeography, Palaeoclimatology, Palaeoecology, 264, 195-209.
- 42  
435392 Lucks, H., Schulz, B., Audren, C. and Triboulet C., 2002. Variscan pressure-temperature  
44  
455393 evolution of garnet-pyroxenites and amphibolites in the Baie d'Audierne metamorphic  
46  
475394 series, Brittany (France). In: Martínez Catalán, J.R., Hatcher Jr., R.D., Arenas, R. and  
48  
495395 Díaz García, F. (Eds.), Variscan-Appalachian Dynamics: the Building of the Late  
50  
515396 Paleozoic Basement, Geological Society of America Special Paper, 364, 89-103.
- 52  
535397 Macaya, J., González Lodeiro, F., Martínez Catalán, J.R. and Álvarez, F. 1991. Continuous  
54  
555398 deformation, ductile thrusting and backfolding in the basement of the Hercynian  
56  
575399 orogen and their relationships with structures in the metasedimentary cover in the  
58  
595400 Spanish Central System. Tectonophysics, 191, 291-309.

- 5401 Majka, J., Mazur, S., Kosminska, K., Dudek, K. and Klonowska, I. 2016. Pressure-  
1 5402 temperature estimates of the blueschists from the Kopina Mt., northern Bohemian  
2 5403 Massif, Poland - constraints on subduction of the Saxothuringian continental margin.  
3 5404 European Journal of Mineralogy, 28, 1047-1057.  
4 5405  
5 5406  
6 5407  
7 5408  
8 5409  
9 5410  
10 5411  
11 5412  
12 5413  
13 5414  
14 5415  
15 5416  
16 5417  
17 5418  
18 5419  
19 5420  
20 5421  
21 5422  
22 5423  
23 5424  
24 5425  
25 5426  
26 5427  
27 5428  
28 5429  
29 5430  
30 5431  
31 5432  
32 5433  
33 5434  
34 5435  
35 5436  
36 5437  
37 5438  
38 5439  
39 5440  
40 5441  
41 5442  
42 5443  
43 5444  
44 5445  
45 5446  
46 5447  
47 5448  
48 5449  
49 5450  
50 5451  
51 5452  
52 5453  
53 5454  
54 5455  
55 5456  
56 5457  
57 5458  
58 5459  
59 5460  
60 5461  
61 5462  
62 5463  
63 5464  
64 5465  
65
- Malavieille, J., Guihot, P., Costa, S., Lardeaux, J.M. and Gardien, V. 1990. Collapse of the thickened Variscan crust in the French Massif Central: Mont Pilat extensional shear zone and St. Étienne Upper Carboniferous basin. *Tectonophysics*, 177, 139-149.
- Malod, J.A. 1982. Comparaison de l'évolution des marges continentales au Nord et au Sud de la Péninsule Ibérique. PhD Thesis, Université de Paris, 235 pp.
- Maluski, H. and Patočka, F. 1997. Geochemistry and  $^{40}\text{Ar}$ - $^{39}\text{Ar}$  geochronology of the metavolcanics from the Rýchory Mts Complex (W Sudetes, Bohemian Massif): paleotectonic significance. *Geological Magazine*, 134, 703-716.
- Marchand, J. 1982. Une véritable éclogite en Bretagne occidentale (Baie d'Audierne, France). *Terra Cognita*, 2/3, 312.
- Marcoux, E., Cocherie, A., Ruffet, G., Darboux, J.R. and Guerrot, C. 2009. Géochronologie revisitée du dôme du Léon (Massif armoricain, France). *Géologie de la France*, 2009 (1), 17-37.
- Marheine, D., Kachlík, V., Maluski, H., Patočka, F. and Żelaźniewicz, A. 2002. The  $^{40}\text{Ar}/^{39}\text{Ar}$  ages from the West Sudetes (NE Bohemian Massif): constraints on the Variscan polyphase tectonothermal development. In: Winchester, J.A., Pharaoh, T.C. and Verniers, J. (Eds.), *Palaeozoic amalgamation of Central Europe*. Geological Society, London, Special Publication 201, 133-155.
- Marques, F.G., Ribeiro, A. and Pereira, E. 1991-1992. Tectonic evolution of the deep crust: Variscan reactivation by extension and thrusting of Precambrian basement in the Bragança and Morais massifs (Trás-os-Montes, NE Portugal). *Geodinamica Acta*, 5 (1-2), 135-151.
- Marschall, H.R., Kalt, A. and Hanel, M. 2003. P-T evolution of a Variscan lower-crustal segment: a study of granulites from the Schwarzwald, Germany. *Journal of Petrology*, 44, 227-253.

- 5431 Martín-Algarra, A., Rodríguez-Cañero, R., O'Doguerty, L., Sánchez-Navas, A. and Ruiz-  
1 5432 Cruz, M.D. 2004. Complejo Maláguide. Estratigrafía. Paleozoico ¿y más antiguo?  
2 5433 (Grupo Piar). In: Vera, J.A. (Ed.), Geología de España, SGE-IGME, Cap. 4, Madrid,  
3 5434 401-406.  
4 5435
- 7 5435 Martín Parra, L.M., González Lodeiro, F., Martínez Poyatos, D. and Matas, J. 2006. The  
8 5436 Puente Génave-Castelo de Vide shear zone (southern Central Iberian Zone, Iberian  
9 5437 Massif): geometry, kinematics and regional implications. Bulletin de la Société  
10 5438 Géologique de France, 177, 191-202.  
11 5439
- 15 5439 Martínez, S.S., Gerdes, A., Arenas, R. and Abati, J. 2012. The Bazar Ophiolite of NW Iberia:  
16 5440 a relic of the Iapetus-Tornquist Ocean in the Variscan suture. Terra Nova, 24 (4), 283-  
17 5441 294. <https://doi.org/10.1111/j.1365-3121.2012.01061.x>.  
18 5442
- 21 5442 Martínez Catalán, J.R. 1990. A non-cylindrical model for the northwest Iberian allochthonous  
22 5443 terranes and their equivalents in the Hercynian belt of Western Europe.  
23 5444 Tectonophysics, 179, 253-272.  
24 5445
- 27 5445 Martínez Catalán, J.R. 2011. Are the oroclines of the Variscan belt related to late Variscan  
28 5446 strike-slip tectonics? Terra Nova, 23, 241-247. <https://doi.org/10.1111/j.1365-3121.2011.01005.x>.  
29 5447  
30 5448
- 33 5448 Martínez Catalán, J.R. 2012. The Central Iberian arc, an orocline centered in the Iberian  
34 5449 Massif and some implications for the Variscan belt. International Journal of Earth  
35 5450 Sciences, 101 (5), 1299-1314. <https://doi.org/10.1007/s00531-011-0715-6>.  
36 5451
- 39 5451 Martínez Catalán, J.R., Hacar Rodríguez, M.P., Villar Alonso, P., Pérez-Estaún, A. and  
40 5452 González Lodeiro, F. 1992. Lower Paleozoic extensional tectonics in the limit between  
41 5453 the West Asturian-Leonese and Central Iberian Zones of the Variscan Fold-Belt in  
42 5454 NW Spain. Geologische Rundschau, 81, 545-560.  
43 5455
- 47 5455 Martínez Catalán, J.R., Ayarza Arribas, P., Pulgar, J.A., Pérez-Estaún, A., Gallart, J., Marcos,  
48 5456 A., Bastida, F., Álvarez-Marrón, J., González Lodeiro, F., Aller, J., Dañobeitia, J.J.,  
49 5457 Banda, E., Cordoba, D. and Comas, M.C. 1995. Results from the ESCI-N3.3 marine  
50 5458 deep seismic profile along the Cantabrian continental margin. Revista de la Sociedad  
51 5459 Geológica de España, 8 (4), 341-354.  
52 5460
- 57 5460 Martínez Catalán, J.R., Arenas, R., Díaz García, F., Rubio Pascual, F.J., Abati, J. and  
58 5461 Marquínez, J. 1996. Variscan exhumation of a subducted Paleozoic continental  
59 5462  
60 5463  
61 5464  
62 5465

- 5462 margin: The basal units of the Ordenes Complex, Galicia, NW Spain. *Tectonics*, 15,  
1 5463 106-121.  
3
- 45464 Martínez Catalán, J.R., Díaz García, F., Arenas, R., Abati, J., Castiñeiras, P., González  
5 5465 Cuadra, P., Gómez Barreiro, J. and Rubio Pascual, F. 2002. Thrust and detachment  
7 5466 systems in the Ordenes Complex (northwestern Spain): Implications for the Variscan-  
9 5467 Appalachian geodynamics. In: Martínez Catalán, J.R., Hatcher Jr., R.D., Arenas, R.  
10 5468 and Díaz García, F. (Eds.), *Variscan-Appalachian Dynamics: The Building of the Late*  
12 5469 *Paleozoic Basement*. Geological Society of America Special Paper, 364, 163-182.  
14
- 15 5470 Martínez Catalán, J.R., Arenas, R. and Díez Balda, M.A. 2003. Large extensional structures  
16 5471 developed during emplacement of a crystalline thrust sheet: the Mondoñedo nappe  
17 5472 (NW Spain). *Journal of Structural Geology*, 25, 1815-1839.  
18
- 19 5473 Martínez Catalán, J.R., Martínez Poyatos, D. y Bea, F. 2004a. Zona Centroibérica:  
21 5474 Introducción. In: Vera, J.A. (Ed.), *Geología de España*, SGE-IGME, Madrid, Cap. 2,  
22 5475 68-69.  
26
- 27 5476 Martínez Catalán, J.R., Fernández-Suárez, J., Jenner, G.A., Belousova, E. and Díez Montes,  
28 5477 A. 2004b. Provenance constraints from detrital zircon U-Pb ages in the NW Iberian  
29 5478 Massif: implications for Paleozoic plate configuration and Variscan evolution. *Journal*  
30 5479 *of the Geological Society, London*, 161 (3), 463-476.  
34
- 35 5480 Martínez Catalán, J.R., Arenas, R., Díaz García, F., Gómez-Barreiro, J., González Cuadra, P.,  
36 5481 Abati, J., Castiñeiras, P., Fernández-Suárez, J., Sánchez Martínez, S., Andonaegui, P.,  
37 5482 González Clavijo, E., Díez Montes, A., Rubio Pascual, F.J. and Valle Aguado, B.  
38 5483 2007. Space and time in the tectonic evolution of the northwestern Iberian Massif:  
39 5484 Implications for the Variscan belt. In: Hatcher Jr., R.D., Carlson, M.P., McBride, J.H.  
40 5485 and Martínez Catalán, J.R. (Eds.), *4-D framework of continental crust*. Geological  
41 5486 Society of America, *Memoir* 200, 403-423. [https://doi.org/10.1130/2007.1200\(21\)](https://doi.org/10.1130/2007.1200(21)).  
42 5487  
43 5488  
44 5489  
45 5490  
46 5491  
47 5492
- 48 5493 Martínez Catalán, J.R., Fernández-Suárez, J., Meireles, C., González Clavijo, E., Belousova,  
49 5494 E. and Saeed, A. 2008. U-Pb detrital zircon ages in synorogenic deposits of the NW  
50 5495 Iberian Massif (Variscan belt): interplay of Devonian-Carboniferous sedimentation  
51 5496 and thrust tectonics. *Journal of the Geological Society, London*, 165, 687-698.  
52 5497  
53 5498  
54 5499  
55 5500
- 56 5491 Martínez Catalán, J.R., Arenas, R., Abati, J., Sánchez Martínez, S., Díaz García, F.,  
57 5492 Fernández-Suárez, J., González Cuadra, P., Castiñeiras, P., Gómez Barreiro, J., Díez  
58 5493 Montes, A., González Clavijo, E., Rubio Pascual, F.J., Andonaegui, P., Jeffries, T.E.,  
59 5494  
60 5495  
61 5496  
62 5497  
63 5498  
64 5499  
65 5500

- 5494 Alcock, J.E., Díez Fernández, R. and López Carmona, A. 2009. A rootless suture and  
1 5495 the loss of the roots of a mountain chain: the Variscan belt of NW Iberia. *Comptes*  
2 Rendus Geoscience, 341 (2-3), 114-126. <https://doi.org/10.1016/j.crte.2008.11.004>.
- 3 5496  
4  
5  
6 5497 Martínez Catalán, J.R., Álvarez Lobato, F., Pinto, V., Gómez Barreiro, J., Ayarza, P.,  
7 5498 Villalaín, J.J. and Casas, A. 2012. Gravity and magnetic anomalies in the  
8 allochthonous Órdenes Complex (Variscan belt, NW Spain): Assessing its internal  
9 5499 structure and thickness. *Tectonics*, 31, TC5007, 1-18.  
10  
11 5500 <https://doi.org/10.1029/2011TC003093>.
- 12 5501  
13  
14  
15 5502 Martínez Catalán, J.R., Rubio Pascual, F.J., Díez Montes, A., Díez Fernández, R., Gómez  
16 Barreiro, J., Dias da Silva, I., González Clavijo, E., Ayarza, P. and Alcock, J.E. 2014.  
17 5503 The late Variscan HT/LP metamorphic event in NW and Central Iberia: relationships  
18 to crustal thickening, extension, orocline development and crustal evolution. In:  
19 5504 Schulmann, K., Martínez Catalán, J.R., Lardeaux, J.M., Janousek, V. and Oggiano, G.  
20 (Eds.), *The Variscan Orogeny: Extent, Timescale and the Formation of the European*  
21 5505 *Crust*. Geological Society, London, Special Publication 405, 225-247.  
22 <https://doi.org/10.1144/SP405.1>.
- 23 5506  
24  
25 5507  
26 5508  
27  
28 5509  
29  
30 5510 Martínez Catalán, J.R., Aerden, D.G.A.M. and Carreras, J. 2015. The “Castilian bend” of  
31 Rudolf Staub (1926): Historical perspective of a forgotten orocline in Central Iberia.  
32 5511 *Swiss Journal of Geosciences*, 108, 289-303. [https://doi.org/10.1007/s00015-015-](https://doi.org/10.1007/s00015-015-0202-3)  
33 5512 [0202-3](https://doi.org/10.1007/s00015-015-0202-3).
- 34 5513  
35  
36 5514  
37  
38 5514 Martínez Catalán, J.R., González Clavijo, E., Meireles, C., Díez Fernández, R. and Bevis, J.  
39 5515 2016. Relationships between syn-orogenic sedimentation and nappe emplacement in  
40 the hinterland of the Variscan belt in NW Iberia deduced from detrital zircons.  
41 5516 *Geological Magazine*, 153 (1), 38-60. <https://doi.org/10.1017/S001675681500028X>.
- 42 5517  
43  
44 5518 Martínez Catalán, J.R., Collett S., Schulmann, K., Aleksandrowski, P. and Mazur, S. 2020.  
45 Correlation of allochthonous terranes and major tectonostratigraphic domains between  
46 5519 NW Iberia and the Bohemian Massif, European Variscan belt. *International Journal of*  
47 Earth Sciences, 109, 1105-1131. <https://doi.org/10.1007/s00531-019-01800-z>.
- 48 5520  
49  
50 5520 Martínez Poyatos, D.J. 2002. Estructura del borde meridional de la Zona Centroibérica y su  
51 relación con el contacto entre las Zonas Centroibérica y de Ossa-Morena. Laboratorio  
52 5521 Xeológico de Laxe, Instituto Universitario de Xeoloxía, A Coruña, Spain, Serie Nova  
53 Terra, 18, 295 pp.
- 54 5522  
55  
56 5523  
57  
58 5524  
59  
60 5525  
61  
62  
63  
64  
65



- 5526 Martínez Poyatos, D., Azor, A., González Lodeiro, F. and Simancas, J.F. 1995. Timing of the  
1  
25527 Variscan structures on both sides of the Ossa Morena/Central Iberian contact (south-  
3  
45528 west Iberian Massif). *Comptes Rendus de l'Académie des Sciences, Paris*, 321 (II),  
5529 609-615.  
6
- 7  
85530 Martínez Poyatos, D., Simancas, J.F., Azor, A. and González Lodeiro, F. 1998. Evolution of a  
9  
105531 Carboniferous piggyback basin in the southern Central Iberian Zone (Variscan Belt,  
115532 SE Spain). *Bulletin de la Société Géologique de France*, 169, 573-578.  
12
- 13  
145533 Martínez Poyatos, D., Nieto, F., Azor, A. and Simancas, J.F. 2001. Relationships between  
155534 very low-grade metamorphism and tectonic deformation: examples from the southern  
16  
175535 Central Iberian Zone (Iberian Massif, Variscan Belt). *Journal of the Geological*  
18  
195536 *Society, London*, 158, 953-968.  
20
- 215537 Martínez Poyatos, D., Gutiérrez-Marco, J.C., Pardo Alonso, M.V., Rábano, I. and Sarmiento,  
22  
235538 G. 2004. Dominio del Complejo Esquisto-grauváquico: La secuencia paleozoica  
24  
255539 postcámbrica. In: Vera, J.A. (Ed.), *Geología de España, SGE-IGME, Madrid, Cap. 2,*  
26  
275540 *Macizo Ibérico.* 81-83.  
28
- 295541 Martínez Poyatos, D., Carbonell, R., Palomeras, I., Simancas, J.F., Ayarza, P., Martí, D.,  
30  
315542 Azor, A., Jabaloy, A., González Cuadra, P., Tejero, R., Martín Parra, L.M., Matas, J.,  
32  
335543 González Lodeiro, F., Pérez-Estaún, A., García Lobón, J.L. and Mansilla, L. 2012.  
34  
355544 Imaging the crustal structure of the Central Iberian Zone (Variscan Belt): The  
36  
375545 ALCUDIA deep seismic reflection transect. *Tectonics*, 31, TC3017, 1-21.  
38  
395546 <https://doi.org/10.1029/2011TC002995>.  
40
- 415547 Massone, H.J. 2001. First find of coesite in the ultrahigh-pressure metamorphic area of the  
42  
435548 central Erzgebirge, Germany. *European Journal of Mineralogy*, 13, 565-570.  
44
- 455549 Massonne, H.J., 2014. Wealth of P-T-t information in medium-high grade metapelites:  
46  
475550 Example from the Jubrique Unit of the Betic Cordillera, S Spain. *Lithos*, 208-209,  
48  
495551 137-157.  
50
- 515552 Massonne, H.J., Kennedy, A., Nasdala, L. and Theye, T. 2007. Dating of zircon and monazite  
52  
535553 from diamondiferous quartzofeldspathic rocks of the Saxonian Erzgebirge – hints at  
54  
555554 burial and exhumation velocities. *Mineralogical Magazine*, 7 (4), 407-425.  
56  
57  
58  
59  
60  
61  
62  
63  
64  
65

- 5555 Mattauer, M. and Etchecopar, A. 1976. Arguments en faveur de chevauchements de type  
1  
25556 himalayen dans la chaîne hercynienne du Massif Central français. In: Ecologie et  
3  
45557 géologie de l'Himalaya. CNRS International Colloque Paris, 268, 261-267.
- 5  
65558 Matte, P. 1968. La structure de la virgation hercynienne de Galice (Espagne). Revue de  
7  
85559 Géologie Alpine, 44, 1-128.
- 9  
105560 Matte, P. 1986. Tectonics and plate tectonics model for the Variscan belt of Europe.  
11  
125561 Tectonophysics, 126, 329-374.
- 13  
145562 Matte, P. 1991. Accretionary history and crustal evolution of the Variscan belt in Western  
15  
165563 Europe. Tectonophysics, 196, 309-337.
- 17  
185564 Matte, P. 2001. The Variscan collage and orogeny (480-290 Ma) and the tectonic definition of  
19  
205565 the Armorica microplate: a review. Terra Nova, 13, 122-128.
- 21  
225566 Matte, P. 2002. Variscides between the Appalachians and the Urals: Similarities and  
23  
245567 differences between Paleozoic subduction and collision belts. In: Martínez Catalán,  
25  
265568 J.R., Hatcher Jr., R.D., Arenas, R. and Díaz García, F. (Eds.), Variscan-Appalachian  
27  
285569 Dynamics: The Building of the Late Paleozoic Basement, Geological Society of  
29  
305570 America Special Paper, 364, 237-248.
- 31  
325571 Matte, P. 2007. Variscan thrust nappes, detachments, and strike-slip faults in the French  
33  
345572 Massif Central: Interpretation of the lineations. In: Hatcher Jr., R.D., Carlson, M.P.,  
35  
365573 McBride, J.H. and Martínez Catalán, J.R. (Eds.), 4-D framework of continental crust.  
37  
385574 Geological Society of America, Memoir 200, 391-402.  
39  
405575 [https://doi.org/10.1130/2007.1200\(20\)](https://doi.org/10.1130/2007.1200(20)).
- 41  
425576 Matte, P. and Burg, J.P. 1981. Sutures, thrusts and nappes in the Variscan Arc of western  
43  
445577 Europe: plate tectonics implications. In: McClay, K.R. and Price, N.J. (Eds.), Thrust  
45  
465578 and Nappe Tectonics. Geological Society, London, Special Publication 9, 353-358.
- 47  
485579 Matte, P. and Hirn, A. 1988. Seismic signature and tectonic cross section of the variscan crust  
49  
505580 in western France. Tectonics 7 (2), 141-155.
- 51  
525581 Matte, P. and Ribeiro, A. 1975. Forme et orientation de l'ellipsoïde de déformation dans la  
53  
545582 virgation hercynienne de Galice. Relations avec le plissement et hypothèses sur la  
55  
565583 genèse de l'arc ibéro-armoricain. Comptes Rendus de l'Académie des Sciences, Paris,  
57  
585584 280, 2825-2828.

- 5585 Matte, P., Respaut, J.P., Maluski, H., Lancelot, J.R. and Brunel, M. 1986. La faille NW-SE du  
1  
2 5586 Pays de Bray, un décrochement ductile dextre hercynien: déformation à 330 Ma d'un  
3  
4 5587 granite à 570 Ma dans le sondage Pays de Bray 201. Bulletin de la Société Géologique  
5  
6 5588 de France, (8), II (1), 69-77.
- 7  
8 5589 Matte, P., Maluski, H., Rajlich, P. and Franke, W. 1990. Terrane boundaries in the  
9  
10 5590 Bohemian Massif: result of large-scale Variscan shearing. Tectonophysics, 177, 151-  
11  
12 5591 170.
- 13  
14 5592 Matthews, K.J., Maloney, K.T., Zahirovic, S., Williams, S.E., Seton, M. and Müller, R.D.  
15  
16 5593 2016. Global plate boundary evolution and kinematics since the late Paleozoic: Global  
17  
18 5594 and Planetary Change. <https://doi.org/10.1016/j.gloplacha.2016.10.002>.
- 19  
20 5595 Maurel, O., Monié, P., Respaut, J.P., Leyreloup, A.F. and Maluski, H. 2003. Pre-metamorphic  
21  
22 5596  $^{40}\text{Ar}/^{39}\text{Ar}$  and U-Pb ages in HP metagranitoids from the Hercynian belt (France).  
23  
24 5597 Chemical Geology, 193, 195-214.
- 25  
26 5598 Mazur, S. and Aleksandrowski, P. 2001. The Teplá(?) / Saxothuringian suture in the  
27  
28 5599 Karkonosze-Izera massif, western Sudetes, central European Variscides. International  
29  
30 5600 Journal of Earth Sciences, 90, 341-360. <https://doi.org/10.1007/s005310000146>.
- 31  
32 5601 Mazur, S., Kroner, A., Szczepański, J., Turniak, K., Hanzl, P., Melichar, R., Rodionov, N.V.,  
33  
34 5602 Paderin, I. and Sergeev, S.A. 2010. Single zircon U-Pb ages and geochemistry of  
35  
36 5603 granitoid gneisses from SW Poland: Evidence for an Avalonian affinity of the Brunian  
37  
38 5604 microcontinent. Geological Magazine, 147, 508-526.
- 39  
40 5605 Mazur, S., Szczepański, J., Turniak, K. and McNaughton, N.J. 2012. Location of the Rheic  
41  
42 5606 suture in the eastern Bohemian Massif: evidence from detrital zircon data. Terra Nova,  
43  
44 5607 24, 199-206.
- 45  
46 5608 Mazur, S., Turniak, K., Szczepański, J. and McNaughton, N.J. 2015. Vestiges of  
47  
48 5609 Saxothuringian crust in the Central Sudetes, Bohemian Massif: Zircon evidence of a  
49  
50 5610 recycled subducted slab provenance. Gondwana Research, 27, 825-839.  
51  
52 5611 <https://doi.org/10.1016/j.gr.2013.11.005>.
- 53  
54 5612 Meinhold, G., Morton, A.C. and Avigad, D. 2013. New insights into peri-Gondwana  
55  
56 5613 paleogeography and the Gondwana super-fan system from detrital zircon U-Pb ages.  
57  
58 5614 Gondwana Research, 23, 661-665. <https://doi.org/10.1016/j.gr.2012.05.003>.

- 5615 Meinhold, G. 2017. Franz Kossmat – Subdivision of the Variscan Mountains – a translation  
1  
2 5616 of the German text with supplementary notes. *History of Geo- and Space Sciences*, 8.,  
3  
4 5617 29-51. <https://doi.org/10.5194/hgss-8-29-2017>.
- 5  
6 5618 Meireles, C. 2013. Litoestratigrafía do Paleozóico do Sector a Nordeste de Bragança (Trás-os-  
7  
8 5619 Montes). *Laboratorio Xeolóxico de Laxe, Instituto Universitario de Xeoloxía, A*  
9  
10 5620 *Coruña, Spain, Serie Nova Terra*, 42, 471 pp.
- 11  
12 5621 Mendia, M.S. 2000. Petrología de la Unidad Eclogítica del Complejo de Cabo Ortegal (NW  
13  
14 5622 de España). *Laboratorio Xeolóxico de Laxe, Nova Terra*, 16, 424 pp.
- 15  
16 5623 Mendia, M. and Gil Ibarguchi, J.I. 2005. Petrografía y condiciones de formación de las rocas  
17  
18 5624 ultramáficas con granate asociadas a las eclogitas de Cabo Ortegal. *Geogaceta*, 37, 31-  
19  
20 5625 34.
- 21  
22 5626 Ménot, R.P. 1988. Magmatismes paléozoïques et structuration carbonifère du Massif de  
23  
24 5627 Belledonne (Alpes Françaises). PhD Thesis, Université de Lyon (1987). *Mémoires et*  
25  
26 5628 *Documents du Centre Armoricaïn d'Etudes Structurales des Socles, Rennes*, 21, 465  
27  
28 5629 pp.
- 29  
30 5630 Ménot, R.P., Peucat, J.J., Scarenzi, D. and Piboule, M. 1988. 496 My age of plagiogranites in  
31  
32 5631 the Chamrousse ophiolite complex (external crystalline massifs in the French Alps):  
33  
34 5632 evidence of a Lower Paleozoic oceanization. *Earth and Planetary Science Letters*, 88,  
35  
36 5633 82-92.
- 37  
38 5634 Mercier, L., Lardeaux, J.M. and Davy, P. 1991. On the tectonic significance of the  
39  
40 5635 retromorphic P-T paths of the French Massif Central eclogites. *Tectonics*, 10, 131-  
41  
42 5636 140.
- 43  
44 5637 Merino-Tomé, O.A., Bahamonde, J.R., Colmenero, J.R., Heredia, N., Villa, E. and Farias, P.  
45  
46 5638 2009. Emplacement of the Cuera and Picos de Europa imbricate thrust system at the  
47  
48 5639 core of the Iberian-Armorican arc (Cantabrian zone, north Spain): New precisions  
49  
50 5640 concerning the timing of arc closure. *Geological Society of America Bulletin*, 121,  
51  
52 5641 729-751. <https://doi.org/10.1130/B26366.1>.
- 53  
54 5642 Michard, A., Goffé, B., Bouybaouene, M. and Saddiqi, O. 1997. Late Hercynian-Mesozoic  
55  
56 5643 thinning in the Alboran domain: metamorphic data from the northern Rif, Morocco.  
57  
58 5644 *Terra Nova*, 9, 171-174.

- 5645 Michard, A., Hoepffner, C., Soulaïmani, A. and Baidder, L. 2008. The Variscan Belt. In:  
1  
2 5646 Continental evolution: The geology of Morocco. Lecture Notes in Earth Sciences, 116,  
3  
4 5647 65-132. Springer-Verlag, Berlin Heidelberg.
- 5  
6 5648 Michard, A., Soulaïmani, A., Hoepffner, C., Ouanaimi, H., Baidder, L., Rjimati, E.C. and  
7  
8 5649 Saddiqi, O. 2010a. The South-Western Branch of the Variscan Belt: Evidence from  
9  
9 5650 Morocco. Tectonophysics, 492 (1-4), 1-24.  
10  
11 5651 <https://doi.org/10.1016/j.tecto.2010.05.021>.
- 12  
13  
14 5652 Michard, A., Ouanaimi, H., Hoepffner, C., Soulaïmani, A., and Baidder, L. 2010b. Comment  
15  
16 5653 on Tectonic relationships of Southwest Iberia with the allochthons of Northwest Iberia  
17  
18 5654 and the Moroccan Variscides by J.F. Simancas et al. [C.R. Geoscience 341 (2009)  
19  
19 5655 103-113]. Comptes Rendus Geoscience, 342, 170-174.
- 20  
21  
22 5656 Michard, A., Soulaïmani, A., Ouanaimi, H., Raddi, Y., Aït Brahim, L., Rjimati, E., Baidder,  
23  
24 5657 L. and Saddiqi, O. 2017. Saghro Group in the Ougnat Massif (Morocco), an evidence  
25  
26 5658 for a continuous Cadomian basin along the northern West African Craton. Comptes  
27  
28 5659 Rendus Geoscience, 349, 81-90.
- 29  
30 5660 Moita, P., Munhá, J., Fonseca, P.E., Pedro, J., Tassinari, C.C.G., Araújo, A. and Palacios, T.  
31  
32 5661 2005. Phase equilibria and geochronology of Ossa-Morena eclogites. XIV Semana de  
33  
34 5662 Geoquímica, VIII Congresso de Geoquímica dos Países de Língua Portuguesa, Aveiro,  
35  
36 5663 Portugal, 2, 471-474.
- 37  
38 5664 Molli, G., Brogi, A., Caggianelli, A., Capezzuoli, E., Liotta, D., Spina, A. and Zibra, I. 2020.  
39  
40 5665 Late Palaeozoic tectonics in Central Mediterranean: a reappraisal. Swiss Journal of  
41  
42 5666 Geosciences, 113:23, 1- 32. <https://doi.org/10.1186/s00015-020-00375-1>.
- 43  
44 5667 Moreno, T., Gibbons, W., Prichard, H.M. and Lunar, R. 2001. Platiniferous chromitites and  
45  
46 5668 the tectonic setting of ultramafic rocks in Cabo Ortegal (North West Spain). Journal of  
47  
48 5669 the Geological Society, London, 158, 601-614.
- 49  
50 5670 Montero, P., Salman, K., Bea, F., Azor, A., Expósito, I., González Lodeiro, F., Martínez-  
51  
52 5671 Poyatos, D. and Simancas, J.F. 2000. New data on the geochronology of the Ossa-  
53  
54 5672 Morena zone, Iberian Massif. In: Variscan-Appalachian dynamics: The building of the  
55  
56 5673 Upper Paleozoic basement. Basement Tectonics 15, A Coruña, Spain, Abstracts, 136-  
57  
58 5674 138.

- 5675 Montero, P., Talavera, C., Bea, F., Lodeiro, F.G. and Whitehouse, M.J. 2009a. Zircon  
1  
25676 geochronology of the Ollo de Sapo Formation and the age of the Cambro-Ordovician  
3  
45677 rifting in Iberia. *Journal of Geology*, 117, 174-191. <https://doi.org/10.1086/595017>.
- 5  
65678 Montero, P., Bea, F., Corretgé, L.G., Floor, P. and Whitehouse, M.J. 2009b. U-Pb ion  
7  
85679 microprobe dating and Sr and Nd isotope geology of the Galiñeiro Igneous Complex:  
9  
105680 A model for the peraluminous/peralkaline duality of the Cambro-Ordovician  
115681 magmatism of Iberia. *Lithos*, 107 (3-4), 227-238.  
12  
135682 <https://doi.org/10.1016/j.lithos.2008.10.009>.
- 14  
155683 Montigny, R. and Allègre, C. 1974. A la recherche des océans perdus: les éclogites de Vendée  
16  
175684 témoins métamorphisés d'une ancienne croûte océanique. *Comptes Rendus de*  
18  
195685 *l'Académie des Sciences, Paris*, D-279, 543-545.
- 20  
215686 Moreno, T., Gibbons, W., Prichard, H.M. and Lunar, R. 2001. Platiniferous chromitites and  
22  
235687 the tectonic setting of ultramafic rocks in Cabo Ortegal (North West Spain). *Journal of*  
24  
255688 *the Geological Society, London*, 158, 601-614.
- 26  
275689 Munhá, J., Ribeiro, A. and Ribeiro, M.L. 1984. Blueschists in the Iberian Variscan Chain  
28  
295690 (Trás-os-Montes: NE Portugal). *Comunicações dos Serviços Geológicos de Portugal*,  
30  
315691 70, 31-53.
- 32  
335692 Muttoni, G., Gaetani, M., Kent, D.V., Sciunnach, D., Angiolini, L., Berra, F., Garzanti, E.,  
34  
355693 Mattei, M. and Zanchi, A. 2009. Opening of the Neo-Tethys Ocean and the Pangea B  
36  
375694 to Pangea A transformation during the Permian. *GeoArabia*, 14 (4), 17-48. Gulf  
38  
395695 PetroLink, Bahrain.
- 40  
415696 Nahodilová, R., Hasalová, P., Štípská, P., Schulmann, K., Závada, P., Míková, J., Kylander-  
42  
435697 Clark, A. and Maierová, P. 2020. Exhumation of subducted continental crust along the  
44  
455698 arc region. *Gondwana Research*, 80, 157-187.
- 46  
475699 Nance, R.D. and Linnemann, U. 2008. The Rheic Ocean: Origin, evolution and significance.  
48  
495700 *GSA Today*, 18 (12), 4-12. <https://doi.org/10.1130/GSATG24A.1>.
- 50  
515701 Neubauer, F. and Von Raumer, J.F. 1993. The Alpine basement - Linkage between Variscides  
52  
535702 and Esat-Mediterranea mountain belts. In: von Raumer, J.F. and Neubauer, F. (eds):  
54  
555703 *Pre-Mesozoic geology in the Alps*. Springer, Berlin, 641-663.
- 56  
575704 Nirrengarten, M, Manatschal, G., Tugend, J., Kusznir, N. and Sauter, D. 2018. Kinematic  
58  
595705 evolution of the southern North Atlantic: Implications for the formation of  
60  
61  
62  
63  
64  
65

- 5706 hyperextended rift systems. *Tectonics*, 37, 1-30.  
1  
25707 <https://doi.org/10.1002/2017TC004495>.  
3  
45708 Nysaether, E., Torsvik, T.H., Feist, R., Walderhaug, H.J. and Eide, E.A. 2002. Ordovician  
5  
65709 palaeogeography with new palaeomagnetic data from the Montagne Noire (Southern  
7  
85710 France). *Earth and Planetary Science Letters*, 203, 329-341.  
9  
105711 Obrador, A., Pomar, L. and Ramos, E. 2004. Menorca: Síntesis estratigráfica. In: Vera, J.A.  
11  
125712 (Ed.), *Geología de España*. SGE-IGME, Madrid, 460-461.  
13  
145713 O'Brien, P.J., Corner, A., Jaekel, P., Hegner, E., Zelazniewicz, A. and Kryza, R. 1997.  
15  
165714 Petrological and isotopic studies on Paleozoic high pressure granulites, Góry Sowie  
17  
185715 Mts. Polish Sudetes. *Journal of Petrology*, 38, 433-456.  
19  
205716 Ochsner, A. 1993. U-Pb geochronology of the Upper Proterozoic-Lower Paleozoic  
21  
225717 geodynamic evolution in the Ossa-Morena Zone (SW Iberia): constraints on the timing  
23  
245718 of the Cadomian orogeny. PhD Thesis, University of Zurich, Diss. ETH 10, 392, 249  
25  
265719 pp.  
27  
285720 Oczlon, M.S. 2006. Terrane Map of Europe. *GAEA heidelbergensis*, 15. Geologisch-  
29  
305721 Paläontologisches Institut Ruprecht-Karls Universität, Heidelberg.  
31  
325722 <https://katalog.ub.uni-heidelberg.de/titel/66145031>.  
33  
345723 Okay, A.I. and Topuz, G. 2017. Variscan orogeny in the Black Sea region. *International*  
35  
365724 *Journal of Earth Sciences*, 106, 569-592. <https://doi.org/10.1007/s00531-016-1395-z>.  
37  
385725 Oliver, G., Corfu, F. and Krogh, T. 1993. U-Pb ages from southwest Poland: evidence for a  
39  
405726 Caledonian suture zone between Baltica and Gondwana. *Journal of the Geological*  
41  
425727 *Society*, London, 150, 355-369.  
43  
445728 Olivier, P. and Paquette, J.L. 2018. Early Permian age of granite pebbles from an Eocene or  
45  
465729 Oligocene conglomerate of the Internal Rif belt (Alboran domain, Morocco):  
47  
485730 hypothesis on their origin. *Bulletin de la Société Géologique de France*, 189, 13.  
49  
505731 Oncken, O., Plesch, A., Weber, J., Ricken, W. and Schrader, S. 2000. Passive margin  
51  
525732 detachment arc-continent collision (Central European Variscides). In: Franke, W.,  
53  
545733 Haak, V., Oncken, O. and Tanner, D. (Eds.), *Orogenic Processes: Quantification and*  
55  
565734 *Modelling in the Variscan Belt*. Geological Society, London, Special Publication 179,  
57  
585735 199-216.  
59  
60  
61  
62  
63  
64  
65

- 5736 Onézime, J., Charvet, J., Faure, M., Chauvet, A. and Panis, D. 2002. Structural evolution of  
1 the southernmost segment of the West European Variscides: the South Portuguese  
2 5737 Zone (SW Iberia). *Journal of Structural Geology*, 24, 451-468.  
3 5738  
4  
5  
6 5739 Ordóñez Casado, B. 1998. Geochronological studies of the Pre-Mesozoic basement of the  
7 Iberian Massif: The Ossa-Morena zone and the Allochthonous Complexes within the  
8 5740 Central Iberian zone. PhD Thesis, Swiss Federal Institute of Technology, Zürich,  
9 Switzerland, 235 pp.  
10 5741  
11 5742  
12  
13 5743 Ordóñez Casado, B., Gebauer, D., Schäfer, H.J., Gil Ibarguchi, J.I. and Peucat, J.J. 2001. A  
14 5744 single Devonian subduction event for the HP/HT metamorphism of the Cabo Ortegal  
15 5745 complex within the Iberian Massif. *Tectonophysics*, 332, 359-385.  
16  
17  
18  
19 5746 Orejana, D., Villaseca, C., Pérez-Soba, C., López-García, J.A. and Billström, K. 2009. The  
20 5747 Variscan gabbros from the Spanish Central System: A case for crustal recycling in the  
21 5748 sub-continental lithospheric mantle? *Lithos*, 110, 262-276.  
22  
23 5749 <https://doi.org/10.1016/j.lithos.2009.01.003>.  
24  
25  
26  
27 5750 Orejana, D., Villaseca, C., Valverde-Vaquero, P., Belousova, E.A. and Armstrong, R.A.  
28 5751 2012. U-Pb geochronology and zircon composition of late Variscan S- and I-type  
29 5752 granitoids from the Spanish Central System batholith. *International Journal of Earth  
30 5753 Sciences*, 101, 1789-1815. <https://doi.org/10.1007/s00531-012-0750-y>.  
31  
32  
33  
34  
35 5754 Ouanaïmi, H., Soulaïmani, A., Hoepffner, C., Michard, A. and Baidder, L. 2016. The Atlas-  
36 5755 Meseta red beds basin (Morocco) and the Lower Ordovician rifting of NW-Gondwana.  
37 5756 *Bulletin de la Société Géologique de France*, 187 (3), 155-168.  
38  
39  
40  
41 5757 Ouanaïmi, H., Soulaïmani, A., Baidder, L., Eddebbi, A. and Hoepffner, C. 2018. Unraveling a  
42 5758 distal segment of the West African Craton Paleozoic margin: Stratigraphy of the  
43 5759 Mougueur inlier of the eastern High Atlas, Morocco. *Comptes Rendus Geoscience*,  
44 5760 350, 289-298.  
45  
46  
47  
48  
49 5761 Ouanaïmi, H., Soulaïmani, A., Hoepffner, C. and Michard, A. 2019. The “Eovariscan  
50 5762 Synmetamorphic Phase” of the Moroccan Meseta Domain revisited; a hint for Late  
51 5763 Devonian extensional geodynamics prior to the Variscan orogenic evolution. In: F.  
52 5764 Rossetti et al. (Eds.), *The structural geology contribution to the Africa-Eurasia  
53 5765 geology: Basement and reservoir structure, ore mineralisation and tectonic modelling.*  
54 5766 *Advances in Science, Technology & Innovation*, Springer Nature, Switzerland AG  
55 5767 2019, 259-261. [https://doi.org/10.1007/978-3-030-01455-1\\_56](https://doi.org/10.1007/978-3-030-01455-1_56).  
56  
57  
58  
59  
60  
61  
62  
63  
64  
65



- 5768 Oukemeni, D., Bourne, J. and Krogh, T.E. 1995. Géochronologie U-Pb sur zircon du pluton  
1  
2 5769 d'Aouli, Haute Moulouya, Maroc. Bulletin de la Société Géologique de France, 166,  
3  
4 5770 15-21.
- 5  
6 5771 Palacios, T., Jensen, S., Eguíluz, S., Apalategui, O., Martí, M., Martínez-Torres, L.M.,  
7  
8 5772 Carracedo, M., Gil Ibarguchi, J.I., Sarrionandía, F., Lobo, P.J. and Junguitu, I. 2010.  
9  
10 5773 Memoria del Mapa Geológico de Extremadura a Escala 1:250.000. Junta de  
11  
12 5774 Extremadura, Consejería de Industria, Energía y Medio Ambiente, 218 pp.
- 13  
14 5775 Paquette, J.L. 1987. Comportement des systèmes isotopiques U-Pb et Sm-Nd dans le  
15  
16 5776 métamorphisme éclogitique. Chaîne hercynienne et chaîne alpine. Mémoires et  
17  
18 5777 Documents du Centre Armoricaïn d'Etudes Structurales des Socles, 14, 1-190.
- 19  
20 5778 Paquette, J.L., Peucat, J.J., Bernard-Griffiths, J. and Marchand, J. 1985. Evidence for old  
21  
22 5779 Precambrian relics shown by U-Pb zircon dating of eclogites and associated rocks in  
23  
24 5780 the Hercynian belt of South Brittany, France. Chemical Geology, 52, 203-216.
- 25  
26 5781 Paquette, J.L., Balé, P., Ballèvre, M. and Georget, Y. 1987. Géochronologie et géochimie des  
27  
28 5782 éclogites du Léon: nouvelles contraintes sur l'évolution géodynamique du Nord-Ouest  
29  
30 5783 du Massif Armoricaïn. Bulletin de Minéralogie, 110, 683-696.
- 31  
32 5784 Paquette, L., Ménot, R.P. and Peucat, J.J. 1989. REE, Sm-Nd and U-Pb zircon study of  
33  
34 5785 eclogites from the Alpine External massifs (Western Alps): Evidence for crustal  
35  
36 5786 contamination. Earth and Planetary Science Letters, 96, 181-198.
- 37  
38 5787 Paquette, J.L., Monchoux, P. and Couturier, M. 1995. Geochemical and isotopic study of a  
39  
40 5788 norite-eclogite transition in the European Variscan Belt. Implications for U-Pb zircon  
41  
42 5789 systematics in metabasic rocks. Geochimica et Cosmochimica Acta, 59, 1611-1622.
- 43  
44 5790 Paquette, J.L., Ballèvre, M., Peucat, J.J., and Cornen, G. 2017. From opening to subduction of  
45  
46 5791 an oceanic domain constrained by LA-ICP-MS U-Pb zircon dating (Variscan belt,  
47  
48 5792 Southern Armoricaïn Massif, France). Lithos, 294-295, 418-437.  
49  
50 5793 <https://doi.org/10.1016/j.lithos.2017.10.005>.
- 51  
52 5794 Paris, F. and Le Pochat, G. 1994. The Aquitaine Basin. In: Keppie, J.D. (Ed.), Pre-Mesozoic  
53  
54 5795 Geology in France and related areas. Springer-Verlag, Berlin, 405-415.
- 55  
56 5796 Paris, F. and Robardet, M. 1977. Paléogéographie et relations ibéro-armoricaïnes au  
57  
58 5797 Paléozoïque anté-carbonifère. Bulletin de la Société Géologique de France, 19, 1121-  
59  
60 5798 1126.

- 5799 Paris, F. and Robardet, M. 1994. The Variscan Orogeny in the Armorican Massif.  
1 5800 Paleogeographic synthesis. In: Keppie, J.D. (Ed.), Pre-Mesozoic Geology in France  
2 and related areas. Springer-Verlag, Berlin, 172-176.  
3 5801  
4  
5 5802 Paris, F., Le Herisse, A., Pelhate, A. and Weyant, M. 1982. Les déformations carbonifères et  
6 la phase Bretonne dans le synclinorium du Ménez-Bélaïr: Essai de Synthèse. Bulletin  
7 5803 de la Société Géologique et Minéralogique de Bretagne, 14 (2), 19-32.  
8 5804  
9  
10 5805 Pastor-Galán, D., Gutiérrez-Alonso, G. and Weil, A.B. 2011. Orocline timing through joint  
11 analysis: Insights from the Ibero-Armorican Arc. Tectonophysics, 507 (1-4), 31-46.  
12 5806 <https://doi.org/10.1016/j.tecto.2011.05.005>.  
13 5807  
14  
15 5808 Pavanetto, P., Funedda, A., Northup, C.J., Schmitz, M.D., Crowley, J.L. and Loi, A. 2012.  
16 Structure and U-Pb zircon geochronology in the Variscan foreland of SW Sardinia,  
17 Italy. Geological Journal, 47 (4), 426-445. <http://dx.doi.org/10.1002/gj.1350>.  
18 5809  
19 5810  
20 5811 Pedro, J., Araújo, A., Fonseca, P., Tassinari, C. and Ribeiro, A. 2010. Geochemistry and U-Pb  
21 zircon age of the internal Ossa-Morena zone ophiolite sequences: A remnant of Rheic  
22 5812 Ocean in SW Iberia. Ofioliti, 35 (2), 117-130.  
23 5813  
24  
25 5814 Peiffer, M.T. 1986. La signification de la ligne tonalitique du Limousin. Son implication dans  
26 la structuration varisque du Massif central français. Comptes Rendus de l'Académie  
27 5815 des Sciences, Paris, II 303, 305-310.  
28 5816  
29  
30 5817 Pelhate, A. 1994. Carboniferous of the Armorican Massif. In: Keppie, J.D. (Ed.), Pre-  
31 Mesozoic Geology in France and related areas. Springer-Verlag, Berlin, 162-168.  
32 5818  
33  
34 5819 Pereira, E., Ribeiro, A., Oliveira, D.P.S., Machado, M.J., Moreira, M.E. and Castro, P. 2003.  
35 Unidade de Pombais: Ofiolito inferior do Maciço de Morais (NE de Trás-os-Montes  
36 5820 Portugal). Ciências da Terra (UNL), nº esp. V, CD-ROM B76-B80.  
37 5821  
38  
39 5822 Pereira, M.F., Chichorro, M., Linnemann, U., Eguiluz, L. and Silva, J.B. 2006a. Inherited arc  
40 signature in the Ediacaran and Early Cambrian basins of the Ossa-Morena Zone  
41 5823 (Iberian Massif, Portugal): paleogeographic link with West-Central European and  
42 North African Cadomian correlatives. Precambrian Research, 144, 297-315.  
43 5824  
44  
45 5825 Pereira, M.F., Silva, J.B., Chichorro, M., Moita, P., Santos, J.F., Apraiz, A. and Ribeiro, C.  
46 2007a. Crustal growth and deformational processes in the northern Gondwana margin:  
47 5826 constraints from the Évora Massif (Ossa-Morena zone, southwest Iberia, Portugal). In:  
48 Linnemann, U., Nance, R.D., Kraft, P. and Zulauf, G. (Eds.), The evolution of the  
49 5827  
50  
51  
52  
53  
54  
55  
56  
57  
58  
59  
60  
61  
62  
63  
64  
65

- 5830 Rheic Ocean: From Avalonian-Cadomian active margin to Alleghenian-Variscan  
1  
25831 collision. Geological Society of America Special Paper, 333-358.  
3  
45832 [https://doi.org/10.1130/2007.2423\(16\)](https://doi.org/10.1130/2007.2423(16)).  
5  
65833 Pereira, M.F., Apraiz, A., Chichorro, M., Silva, J.B. and Armstrong, R.A. 2010. Exhumation  
7  
85834 of high-pressure rocks in northern Gondwana during the Early Carboniferous  
9  
105835 (Coimbra-Córdoba shear zone, SW Iberian massif): tectonothermal analysis and U-Th-  
115836 Pb SHRIMP in-situ zircon geochronology. *Gondwana Research*, 17, 440-460.  
12  
13  
145837 Pereira, M.F., Chichorro, M., Johnston, S.T., Gutiérrez-Alonso, G., Silva, J.B., Linnemann,  
155838 U., Hofmann, M. and Drost, K. 2012. The missing Rheic Ocean magmatic arcs:  
16  
175839 Provenance analysis of Late Paleozoic sedimentary clastic rocks of SW Iberia.  
18  
195840 *Gondwana Research*, 22 (3-4), 882-891. <https://doi.org/10.1016/j.gr.2012.03.010>.  
20  
215841 Pereira, M.F., Ribeiro, C., Vilallonga, F., Chichorro, M., Drost, K., Silva, J.B., Albardeiro, L.,  
225842 Hofmann, M. and Linnemann, U. 2014. Variability over time in the sources of South  
235843 Portuguese Zone turbidites: evidence of denudation of different crustal blocks during  
24  
255844 the assembly of Pangaea. *International Journal of Earth Sciences*, 103, 1453-1470.  
26  
275845 <https://doi.org/10.1007/s00531-013-0902-8>.  
28  
295846  
30  
315847 Pereira, M.F., Castro, A. and Fernández, C. 2015a. The inception of a Paleotethyan magmatic  
32  
335848 arc in Iberia. *Geoscience Frontiers*, 6, 297-306.  
34  
355849 <https://doi.org/10.1016/j.gsf.2014.02.006>.  
36  
375850 Pereira, M.F., El Houicha, M., Chichorro, M., Armstrong, R., Jouhari, A., El Attari, A.,  
38  
395851 Ennih, N. and Silva, J.B. 2015b. Evidence of a Paleoproterozoic basement in the  
40  
415852 Moroccan Variscan Belt (Rehamna Massif, Western Meseta). *Precambrian Research*,  
42  
435853 268, 61-73.  
44  
455854 Pereira, M.F., Gutiérrez-Alonso, G., Murphy, J.B., Drost, K., Gama, C. and Silva J.B. 2017a.  
46  
475855 Birth and demise of the Rheic Ocean magmatic arc(s): Combined U-Pb and Hf isotope  
48  
495856 analyses in detrital zircon from SW Iberia siliciclastic strata. *Lithos*, 278-281, 383-  
50  
515857 399, <http://dx.doi.org/10.1016/j.lithos.2017.02.009>.  
52  
535858 Pereira, M.F., Gama, C. and Rodríguez, C. 2017b. Coeval interaction between magmas of  
54  
555859 contrasting composition (Late Carboniferous-Early Permian Santa Eulália-Monforte  
56  
575860 massif, Ossa-Morena Zone): field relationships and geochronological constraints.  
58  
59  
60  
61  
62  
63  
64  
65

- 5861 Pereira, M.F., Díez Fernández, R., Gama C., Hofmann, M., Gärtner, A. and Linnemann, U.  
1  
25862 2018. S-type granite generation and emplacement during a regional switch from  
3  
45863 extensional to contractional deformation (Central Iberian Zone, Iberian autochthonous  
5  
65864 domain, Variscan Orogeny). *International Journal of Earth Sciences*, 107, 251-267.  
75865 <https://doi.org/10.1007/s00531-017-1488-3>.  
8
- 9  
105866 Pereira, Z., Piçarra, J.M. and Oliveira, J.T. 1998. Palinomorfos do Devónico Inferior da  
11  
125867 região de Barrancos (Zona de Ossa Morena). *Actas do V Congresso Nacional de*  
135868 *Geologia. Instituto Geológico e Mineiro*, 84, A-18-A-21.  
14
- 15  
165869 Pereira, Z., Oliveira, V. and Oliveira, J.T. 2006b. Palynostratigraphy of the Toca da Moura  
17  
185870 and Cabrela Complexes, Ossa Morena Zone, Portugal. *Geodynamic implications.*  
195871 *Review of Palaeobotany and Palynology*, 139, 227-240.  
20
- 21  
225872 Pereira, Z., Matos, J., Fernandes, P. and Oliveira, J.T. 2007b. Devonian and Carboniferous  
235873 palynostratigraphy of the South Portuguese Zone, Portugal. *Comunicações Geológicas*,  
245874 94, 53-79.  
25  
26
- 27  
285875 Peřestý, V., Lexa, O., Holder, R., Jeřábek, P., Racek, M., Štípská, P., Schulmann, K. and  
29  
305876 Hacker, B. 2017. Metamorphic inheritance of Rheic passive margin evolution and its  
315877 early-Variscan overprint in the Teplá-Barrandian Unit, Bohemian Massif. *Journal of*  
325878 *Metamorphic Geology*, 35, 327-355. <https://doi.org/10.1111/jmg.12234>.  
33  
34
- 35  
365879 Peřestý, V., Lexa, O., Jeřábek, P., 2020. Restoration of early-Variscan structures exposed  
375880 along the Teplá shear zone in the Bohemian Massif: constraints from kinematic  
38  
395881 modelling. *International Journal of Earth Sciences*, 109, 1189-1211.  
40
- 41  
425882 Pérez-Cáceres, I., Simancas, J.F., Martínez Poyatos, D., Azor, A. and González Lodeiro, F.  
435883 2016. Oblique collision and deformation partitioning in the SW Iberian Variscides.  
445884 *Solid Earth*, 7, 857-872. <https://doi.org/10.5194/se-7-857-2016>.  
45  
46
- 47  
485885 Pérez-Cáceres, I., Martínez Poyatos, D., Simancas, J.F. and Azor, A. 2017. Testing the  
495886 Avalonian affinity of the South Portuguese Zone and the Neoproterozoic evolution of  
505887 SW Iberia through detrital zircon populations. *Gondwana Research*, 42, 177-192.  
515887  
525888 <https://doi.org/10.1016/j.gr.2016.10.010>.  
53  
54
- 555889 Pérez-Cáceres, I., Martínez Poyatos, D.J., Vidal, O., Beyssac, O., Nieto, F., Simancas, J.F.,  
565890 Azor, A. and Bourdelle, F. 2020. Deciphering the metamorphic evolution of the Pulo  
575890  
58  
59  
60  
61  
62  
63  
64  
65

- 5891 do Lobo metasedimentary domain (SW Iberian Variscides). *Solid Earth*, 11, 469-488.  
1  
25892 <https://doi.org/10.5194/se-11-469-2020>.  
3
- 45893 Pérez-Estaún, A., Bastida, F., Alonso, J.L., Marquínez, J., Aller, J., Álvarez-Marrón, J.,  
5  
65894 Marcos, A. and Pulgar, J.A. 1988. A thin-skinned tectonics model for an arcuate fold  
7  
85895 and thrust belt: The Cantabrian Zone (Variscan Ibero-Armorican Arc). *Tectonics*, 7,  
9  
95896 517-537.  
10
- 11  
125897 Pérez-Estaún, A., Bastida, F., Martínez Catalán, J.R., Gutierrez Marco, J.C., Marcos, A. and  
13  
145898 Pulgar, J.A. 1990. West Asturian-Leonese Zone. *Stratigraphy*. In: Dallmeyer, R.D.,  
15  
165899 and Martínez García, E. (Eds.), *Pre-Mesozoic Geology of Iberia*. Springer-Verlag.  
175900 Berlin, 92-102.  
18
- 19  
205901 Pérez-Estaún, A., Martínez Catalán, J.R. and Bastida, F. 1991. Crustal thickening and  
21  
225902 deformation sequence in the footwall to the suture of the Variscan Belt of northwest  
235903 Spain. *Tectonophysics*, 191, 243-253.  
24
- 25  
265904 Pérez-Estaún, A., Pulgar, J.A., Banda, E., Álvarez-Marrón, J. and ESCI-N Research Group.  
275905 1994. Crustal structure of the external Variscides in NW Spain from deep seismic  
28  
295906 reflection profiling, *Tectonophysics*, 232, 91-118.  
30
- 31  
325907 Pérez-Estaún, A., Pulgar, J.A., Álvarez-Marrón, J. and ESCI-N group. ESCI-N Group:  
335908 Marcos, A., Bastida, F., Aller, J., Marquínez, J., Farias, P., Alonso, J.L., Gutiérrez, G.,  
34  
355909 Gallastegui, J., Rodríguez, R., Heredia, N., Bulnes, M., Banda, E., Martínez Catalán,  
36  
375910 J.R., Córdoba, D., Dañobeitia, J.J., Comas, M.C. 1995. Crustal structure of the  
38  
395911 Cantabrian Zone: seismic image of a Variscan foreland thrust and fold belt (NW  
40  
415912 Spain). *Revista de la Sociedad Geológica de España*, 8 (4), 307-319.  
42
- 435913 Pérez-Estaún, A., Aramburu, C., Méndez-Bedia, I., Arbizu, M., García-López, S., Fernández,  
44  
455914 L.P., Bahamonde, J.R., Barba, P., Colmenero, J.R., Heredia, N., Rodríguez-Fernández,  
46  
475915 L.R., Salvador, C., Sánchez de Posada, L.C., Villa, E., Merino-Tomé, O. and Motis, K.  
48  
495916 2004. Zona Cantábrica: Estratigrafía. In: Vera, J.A. (Ed.), *Geología de España*, SGE-  
50  
515917 IGME, Madrid, Cap. 2, 26-42.  
52
- 535918 Perraki, M. and Faryad, S.W. 2014. First finding of microdiamond, coesite and other UHP  
54  
555919 phases in felsic granulites in the Moldanubian Zone: Implications for deep subduction  
56  
575920 and a revised geodynamic model for Variscan Orogeny in the Bohemian Massif.  
585921 *Lithos*, 202-203, 157-166.  
59  
60  
61  
62  
63  
64  
65

- 5922 Perroud, H. and van der Voo, R. 1985. Paleomagnetism of the late Ordovician Thouars  
1  
25923 massif, Vendée province, France. *Journal of Geophysical Research*, 90, 4611-4625.  
3
- 45924 Perroud, H., Bonhommet, N. and Ribeiro, A. 1985. Paleomagnetism of Late Paleozoic  
5  
65925 igneous rocks from southern Portugal. *Geophysical Research Letters*, 12 (1), 45-48.  
7
- 85926 Perroud, H., Bonhommet, N. and Thebault, J.-P. 1986. Palaeomagnetism of the Ordovician  
9  
105927 Moulin de Chateaupanne Formation, Vendée, western France. *Geophysical Journal of*  
11  
125928 *the Royal Society of Astronomy*, 85, 573-582.  
13
- 145929 Peucat, J.J. 1973. Les schistes cristallins de la baie d'Audierne: étude pétrographique et  
15  
165930 structurale. PhD thesis, Université de Rennes, 108 pp.  
17
- 185931 Peucat, J.J. 1983. Géochronologie des roches métamorphiques (Rb-Sr et U-Pb). Exemples  
19  
205932 choisis au Groënland, en Laponie, dans le massif Armoricaïn et en Grande Kabylie.  
21  
225933 *Mémoires de la Société Géologique et Minéralogique de Bretagne*, 28, 158.  
23
- 245934 Peucat, J.J. and Cogné, J. 1974. Les schistes cristallins de la Baie d'Audierne (Sud Finistère):  
25  
265935 un jalon intermédiaire entre la Meseta ibérique et les régions sud-armoricaines.  
27  
285936 *Comptes Rendus de l'Académie des Sciences, Paris*, D-278, 1809-1812.  
29
- 305937 Peucat, J.J., Bernard-Griffiths, J., Gil Iburguchi, J.I., Dallmeyer, R.D., Menot, R.P.,  
31  
325938 Cornichet, J. and Iglesias Ponce de León, M. 1990. Geochemical and geochronological  
33  
345939 cross section of the deep Variscan crust: The Cabo Ortegal high-pressure nappe  
35  
365940 (northwestern Spain). *Tectonophysics*, 177, 263-292.  
37
- 385941 Piçarra, J.M. 1997. Nota sobre a descoberta de graptólitos do Devónico Inferior na Formação  
39  
405942 de Terena, em Barrancos (Zona de Ossa-Morena). In: Araújo A.A. and Pereira M.F.  
41  
425943 (Eds.), *Estudo sobre a Geologia da Zona de Ossa-Morena (Maciço Ibérico)*,  
43  
445944 *Homenagem ao Prof. Francisco Gonçalves*. Universidade de Évora, 27-36.  
45
- 465945 Piçarra, J.M., Pereira, Z. and Oliveira, J.T. 1998. Novos dados sobre a idade da sucessão  
47  
485946 Silúrico-Devónica do Sinclinal de Terena, na região de Barrancos. Implicações  
49  
505947 geodinâmicas. *Actas do V Congresso Nacional de Geologia*. Instituto Geológico e  
51  
525948 Mineiro, 84, A-15-A-17.  
53
- 545949 Piçarra, J.M., Robardet, M., Bourahrouh, A., Paris, F., Pereira, Z., Le Menn, J., Gourvennec,  
55  
565950 R., Oliveira, T. and Lardeux, H. 2002. Le passage Ordovicien-Silurien et la partie  
57  
585951 inférieure du Silurien (Sud-Est du Massif armoricaïn, France). *Comptes Rendus*  
59  
605952 *Géoscience*, 334, 1177-1183.  
61  
62  
63  
64  
65

- 5953 Piçarra, J.M., Robardet, M., Oliveira, J.T., Paris, F. and Lardeux, H. 2009. Graptolite faunas  
1 of the Llandovery «phtanites» at Les Fresnaies (Chalonnnes-sur-Loire, southeastern  
2 5954 of the Llandovery «phtanites» at Les Fresnaies (Chalonnnes-sur-Loire, southeastern  
3 5955 Armorican Massif): Palaeontology and biostratigraphy. *Bulletin of Geosciences*, 84,  
4 41-50.  
5 5956  
6
- 7 5957 Pickering, K.T. and Smith, A.G. 1995. Arcs and backarc basins in the Early Paleozoic Iapetus  
8 Ocean. *The Island Arc*, 4, 1-67.  
9 5958
- 10 5959 Pickering, K.T. and Smith, A.G. 1997. The Caledonides. In: van der Pluijm, B.A. and  
11 Marshak, S. *Earth structure: An introduction to Structural Geology and Tectonics*.  
12 5960 WBC/McGraw-Hill, 435-444.  
13  
14 5961
- 15 5962 Pin, C. and Lancelot, J.R. 1982. U-Pb dating of an early Paleozoic bimodal magmatism in the  
16 French Massif Central and of its further metamorphic evolution. *Contributions to  
17 Mineralogy and Petrology*, 79, 1-12.  
18 5963  
19  
20 5964
- 21 5965 Pin, C. and Carme, F. 1987. A Sm-Nd isotopic study of 500 Ma old oceanic crust in the  
22 Variscan belt of Western Europe: the Chamrousse ophiolite complex, Western Alps  
23 (France). *Contributions to Mineralogy and Petrology*, 96, 406-413.  
24 5966  
25  
26 5967
- 27 5968 Pin, C. and Paquette, J.L. 1998. A mantle-derived bimodal suite in the Hercynian Belt: Nd  
28 isotope and trace element evidence for a subduction-related rift origin of the Late  
29 Devonian Brévenne metavolcanics, Massif Central (France). *Contributions to  
30 Mineralogy and Petrology*, 129, 222-238.  
31 5969  
32  
33 5970
- 34 5971 Pin, C. and Paquette, J.L. 2002. Le magmatisme basique calcoalcalin d'âge dévono-dinantien  
35 du nord du Massif Central, témoin d'une marge active hercynienne: arguments  
36 géochimiques et isotopiques Sr/Nd. *Geodinamica Acta*, 15,63-77.  
37 5972  
38  
39 5973
- 40 5974 Pin, C. and Rodríguez, J. 2009. Comment on "Rheic Ocean ophiolitic remnants in southern  
41 Iberia questioned by SHRIMP U-Pb zircon ages on the Beja-Acebuches amphibolites"  
42 by A. Azor et al. *Tectonics*, 28. <https://doi.org/10.1029/2009TC002495>.  
43 5975  
44  
45 5976
- 46 5977 Pin, C. and Vielzeuf, D. 1988. Les granulites de haute-pression de l'Europe moyenne témoins  
47 d'une subduction éo-hercynienne. Implications sur l'origine des groupes leptyno-  
48 amphiboliques. *Bulletin de la Société Géologique de France*, 8 (4), 13-20.  
49 5978  
50  
51 5979
- 52 5980 Pin, C., Dupuy, C. and Peterlongo, J.M. 1982. Répartition des terres rares dans les roches  
53 volcaniques basiques dévono-dinantiennes du Nord-Est du Massif central. *Bulletin de  
54 la Société Géologique de France*, 7, 669-676.  
55 5981  
56  
57 5982  
58  
59 5983  
60  
61  
62  
63  
64  
65

- 5984 Pin, C., Paquette, J.L., Santos Zalduegui, J.F. and Gil Ibarra, J.I. 2002. Early Devonian  
1 supra-subduction zone ophiolite related to incipient collisional processes in the  
2 5985 Western Variscan Belt: The Sierra de Careón unit, Ordenes Complex, Galicia. In:  
3 5986 Martínez Catalán, J.R., Hatcher Jr., R.D., Arenas, R. and Díaz García, F. (Eds.),  
4 5987 Variscan-Appalachian Dynamics: The Building of the Late Paleozoic Basement,  
5 5988 Geological Society of America Special Paper, 364, 57-71.  
6 5989
- 10  
11 5990 Pin, C., Paquette, J.L., Ábalos, B., Santos, F.J. and Gil Ibarra, J.I. 2006. Composite origin  
12 of an early Variscan transported suture: Ophiolitic units of the Morais Nappe Complex  
13 5991 (north Portugal). *Tectonics*, 25, 1-19, TC5001.  
14 5992 <https://doi.org/10.1029/2006TC001971>.  
15 5993  
16 5994
- 17 5995 Pin, C., Fonseca, P.E., Paquette, J.L., Castro, P. and Matte, P. 2008. The ca. 350 Ma Beja  
18 5996 Igneous Complex: A record of transcurrent slab break-off in the Southern Iberia  
19 5997 Variscan Belt? *Tectonophysics*, 461, 356-377.  
20 5998 <https://doi.org/10.1016/j.tecto.2008.06.001>.  
21 5999
- 22 6000 Piqué, A. 1988. The Variscan belt of Morocco. *Trabajos de Geología, Universidad de Oviedo*,  
23 6001 17, 145-153. ISSN 0474-9588.  
24 6002
- 25 6003 Piqué, A. 1989. Variscan terranes in Morocco. In: Dallmeyer, R.D. (Ed.): *Terranes in the*  
26 6004 *Circum-Atlantic Paleozoic Orogens*. Geological Society of America Special Paper,  
27 6005 230, 115-129.  
28 6006
- 29 6007 Piqué, A. 2001. *Geology of Northwest Africa*. Beiträge zur regionalen geologie der Erde, 29,  
30 6008 310 pp. Gebrüder Borntraeger, Berlin.  
31 6009
- 32 6010 Piqué, A. and Michard, A. 1989. Moroccan Hercynides, a synopsis. The Palaeozoic  
33 6011 sedimentary and tectonic evolution at the northern margin of West Africa. *American*  
34 6012 *Journal of Sciences*, 289, 286–330.  
35 6013
- 36 6014 Pitra, P., Burg, J.P. and Giraud, M. 1999. Late Variscan strike-slip tectonics between the  
37 6015 Teplá-Barrandian and Moldanubian terranes (Czech Bohemian Massif):  
38 6016 petrostructural evidence. *Journal of the Geological Society, London*, 156, 1003-1020.  
39 6017
- 40 6018 Pitra, P., Ballèvre, M. and Ruffet, G. 2010. Inverted metamorphic field gradient towards a  
41 6019 Variscan suture zone (Champtoceaux Complex, Armorican Massif, France). *Journal of*  
42 6020 *Metamorphic Geology*, 28, 183-208.  
43 6021  
44 6022  
45 6023  
46 6024  
47 6025  
48 6026  
49 6027  
50 6028  
51 6029  
52 6030  
53 6031  
54 6032  
55 6033  
56 6034  
57 6035  
58 6036  
59 6037  
60 6038  
61 6039  
62 6040  
63 6041  
64 6042  
65 6043



- 6014 Ploquin, A. and Stussi, J.M. 1994. Felsic plutonism and volcanism in the Massif Central. In:  
1  
26015 Keppie, J.D. (Ed.), Pre-Mesozoic Geology in France and related areas. Germany,  
3  
46016 Springer-Verlag, Berlin,363-378.
- 5  
66017 Pouclet, A., Ouazzani, H. and Fekkak, A. 2008. The Cambrian volcano-sedimentary  
7  
86018 formations of the westernmost High Atlas (Morocco): their place in the geodynamic  
9  
106019 evolution of the West African Palaeo-Gondwana northern margin. Geological Society,  
11  
126020 London, Special Publications, 297, 303-327.
- 13  
146021 Pouclet, A., Álvaro, J.J., Bardintzeff, J.M., Gil Imaz, A., Monceret, E. and Vizcaïno, D. 2017.  
15  
166022 Cambrian-early Ordovician volcanism across the South Armorican and Occitan  
17  
186023 domains of the Variscan Belt in France: Continental break-up and rifting of the  
19  
206024 northern Gondwana margin. *Geoscience Frontiers*, 8, 25-64.  
216025 <https://doi.org/10.1016/j.gsf.2016.03.002>.
- 22  
236026 Poujol, M., Pitra, P., Van Den Driessche, J., Tartèse, R., Ruffet, G., Paquette, J.L. and Poilvet,  
24  
256027 J.C. 2017. Two-stage partial melting during the Variscan extensional tectonics  
26  
276028 (Montagne Noire, France). *International Journal of Earth Sciences*, 106, 477-500.  
28  
296029 <https://doi.org/10.1007/s00531-016-1369-1>.
- 30  
316030 Puga, E., Díaz de Federico, A., Nieto, J.M., Martín-Algarra, A., González-Lodeiro, F.,  
32  
336031 Estévez, A. and Jabaloy, A. 2004. Complejo Nevadofilábride. Sucesiones litológicas y  
34  
356032 petrología. In: Vera, J.A. (Ed.), *Geología de España*, SGE-IGME, Cap. 4, Madrid,  
36  
376033 424-427.
- 38  
396034 Quesada, C. 1991. Geological constrains on the Paleozoic tectonic evolution of  
40  
416035 tectonostratigraphic terranes in the Iberian Massif. *Tectonophysics*, 185, 225-245.
- 42  
436036 Quesada, C., Fonseca, P.E., Munhá, J., Oliveira, J.T. and Ribeiro, A. 1994. The Beja-  
44  
456037 Acebuches ophiolite (Southern Iberia Variscan fold belt): Geological characterization  
46  
476038 and geodynamic significance. *Boletín Geológico y Minero*, 105, 3-49.
- 48  
496039 Quesada, C., and Oliveira, J.T (Eds.). 2019. *The Geology of Iberia: A geodynamic approach*,  
50  
516040 Volume 2: The Variscan Cycle. *Regional Geology Reviews*, Simancas, J.F. (Coord.),  
52  
536041 Springer, 544 pp.
- 54  
556042 Rabu, D., Brun, J.P. and Chantraine, J. 1994. Structure and metamorphism, The Cadomian  
56  
576043 Orogeny in the Armorican Massif. In: Keppie, J.D. (Ed.), *Pre-Mesozoic Geology in*  
58  
596044 *France and related areas*. Springer-Verlag, Berlin, 96-110.

- 6045 Racek, M., Lexa, O., Schulmann, K., Corsini, M., Štípská, P. and Maierová P. 2017. Re-  
1  
26046 evaluation of polyphase kinematic and  $^{40}\text{Ar}/^{39}\text{Ar}$  cooling history of Moldanubian hot  
3  
46047 nappe at the eastern margin of the Bohemian Massif. *International Journal of Earth*  
5  
66048 *Sciences*, 106, 397-420. <https://doi.org/10.1007/s00531-016-1410-4>.
- 7  
86049 Ramsay, J.G. and Huber, M.I. 1983. *The techniques of modern Structural Geology*. Volume  
9  
106050 1: Strain Analysis. Academic Press, London, 308 pp.
- 11  
126051 Rey, P., Burg, J.P. and Casey, M. 1997. The Scandinavian Caledonides and their relationship  
13  
146052 to the Variscan Belt. In: Burg, J.P. and Ford, M. (Eds.), *Orogeny Through Time*.  
15  
166053 Geological Society, London, Special Publication 121, 179-200.
- 17  
186054 Ribeiro, A. 1974. Contribution a l'étude tectonique de Trás-os-Montes Oriental. *Memória dos*  
19  
206055 *Serviços Geológicos de Portugal*, 24 (Nova Série), 179 pp., 8 fold maps.
- 21  
226056 Ribeiro, M.L. 1991. Contribuição para o conhecimento estratigráfico e petrológico da região a  
23  
246057 SW de Macedo de Cavaleiros (Trás-os-Montes Oriental). *Memórias dos Serviços*  
25  
266058 *Geológicos de Portugal*, 30, 106 pp.
- 27  
286059 Ribeiro, A., Quesada C. and Dallmeyer, R.D. 1990. Part VIII: Evolution of the Iberian  
29  
306060 Massif. In: Dallmeyer, R.D. and Martínez-García (Eds.), *Pre-Mesozoic Geology of*  
31  
326061 *Iberia*, 399-409, Springer-Verlag, New York.
- 33  
346062 Ries, A.C. and Shackleton, R.M. 1971. Catazonal complexes of northwest Spain and north  
35  
366063 Portugal remnants of a Hercynian thrust plate. *Nature Phys. Sci.* 234, 65-69.
- 37  
386064 Robardet, M. 1981. Late Ordovician tillites in Iberian Peninsula. In: Hamberg, M.J. and  
39  
406065 Harland, W.B. (Eds.) *Earth's pre-Pleistocene glacial record*. Cambridge University  
41  
426066 Press, 585-589.
- 43  
446067 Robardet, M. 2002. Alternative approach to the Variscan Belt of southwestern Europe:  
45  
466068 Preorogenic paleobiogeographical constraints. In: Martínez Catalán, J.R., Hatcher Jr.,  
47  
486069 R.D., Arenas, R. and Díaz García, F. (Eds.), *Variscan-Appalachian Dynamics: The*  
49  
506070 *Building of the Late Paleozoic Basement*, Geological Society of America, Special  
51  
526071 Paper, 364, 1-15.
- 53  
546072 Robardet, M. 2003. The Armorica 'microplate': fact or fiction? Critical review of the concept  
55  
566073 and contradictory paleobiogeographical data. *Palaeogeography, Palaeoclimatology,*  
57  
586074 *Palaeoecology*, 195, 125-148.

- 6075 Robardet, M. and Gutiérrez Marco, J.C. 1990. Ossa-Morena Zone. Stratigraphy. Passive  
1  
26076 Margin Phase (Ordovician-Silurian-Devonian). In: Dallmeyer, R.D. and Martínez  
3  
46077 García, E. (Eds.), Pre-Mesozoic Geology of Iberia. Springer-Verlag, Berlin, 267-272.
- 5  
66078 Robardet, M., Paris, F. and Racheboeuf, P.R. 1990. Paleogeographic evolution of  
7  
86079 southwestern Europe during Early Paleozoic times. In: McKerrow, W.S. and Scotese,  
9  
96080 C.R. (Eds.), Paleozoic palaeogeography and biogeography. Geological Society,  
10  
116081 London, Memoir 12, 411-419.
- 12  
13  
146082 Robardet, M., Bonjour, J.L., Paris, F., Morzadec, P. and Racheboeuf, P.R. 1994. Ordovician,  
15  
166083 Silurian, and Devonian of the Medio-North-Armorican Domain. In: Keppie, J.D.  
17  
186084 (Ed.), Pre-Mesozoic Geology in France and related areas. Springer-Verlag, Berlin,  
19  
196085 142-151.
- 20  
216086 Robert-Charrue, C. and Burkhard, M. 2008. Inversion tectonics, interference pattern and  
22  
236087 extensional fault-related folding in the Eastern Anti-Atlas, Morocco. Swiss Journal of  
24  
256088 Geosciences, 101, 397-408.
- 26  
276089 Rodriguez, B., Chew, D.M., Jorge, R.C.G.S., Fernandes, P., Veiga-Pires, C. and Oliveira, J.T.  
28  
296090 2015. Detrital zircon geochronology of the Carboniferous Baixo Alentejo Flysch  
30  
316091 Group (South Portugal); constraints on the provenance and geodynamic evolution of  
32  
336092 the South Portuguese Zone. Journal of the Geological Society, London, 172, 294-308.
- 34  
356093 Rodríguez Aller, J. 2005. Recristalización y deformación de litologías supracorticales  
36  
376094 sometidas a metamorfismo de alta presión (Complejo de Malpica-Tuy, NO del Macizo  
38  
396095 Ibérico). Laboratorio Xeolóxico de Laxe, Instituto Universitario de Xeoloxía, A  
40  
416096 Coruña, Spain, Serie Nova Terra, 29, 572 pp.
- 42  
436097 Rodríguez, J., Cosca, M.A., Gil Ibarguchi, J.I. and Dallmeyer, R.D. 2003. Strain partitioning  
44  
456098 and preservation of  $^{40}\text{Ar}/^{39}\text{Ar}$  ages during Variscan exhumation of a subducted crust  
46  
476099 (Malpica-Tui complex, NW Spain). Lithos, 70, 111-139.
- 48  
496100 Rodríguez-Cañero, R., Jabaloy-Sánchez, A., Navas-Parejo, P. and Martín-Algarra, A. 2018.  
50  
516101 Linking Palaeozoic palaeogeography of the 1 Betic Cordillera to the Variscan Iberian  
52  
536102 Massif: new insight through the first conodonts of the Nevado-Filábride Complex.  
54  
556103 International Journal of Earth Sciences, 107, 1791-1806.  
56  
576104 <https://doi.org/10.1007/s00531-017-1572-8>.

- 6105 Rolet, J., Le Gall, B., Darboux, J.R., Thonon, P. and Gravelle, M. 1986. L'évolution  
1 géodynamique dévono-carbonifère de l'extrémité occidentale de la chaîne hercynienne  
2 6106 d'Europe sur le transect Armorique-Cornwall. Bulletin de la Société Géologique de  
3 6107 France, 8, II (1), 43-54.  
4  
5 6108  
6  
7 6109 Rolet, J., Gresselin, F., Jegouzo, P., Ledru, P. and Wyns, R. 1994. Intracontinental Hercynian  
8 6110 events in the Armorican Massif, The Variscan Orogeny in the Armorican Massif,  
9 6111 Structure and Metamorphism. In: Keppie, J.D. (Ed.), Pre-Mesozoic Geology in France  
10 and related areas. Springer-Verlag, Berlin, 195-219.  
11 6112  
12  
13 6113 Rolin, P., Marquer, D., Colchen, M., Cartannaz, C., Cocherie, A., Thiery, V., Quenardel, J.M.  
14 6114 and Rossi, P. 2009. Famenco-Carboniferous (370-320 Ma) strike slip tectonics  
15 6115 monitored by syn-kinematic plutons in the French Variscan belt (Massif Armoricain  
16 and French Massif Central). Bulletin de la Société Géologique de France, 180 (3),  
17 6116 231-246.  
18  
19 6117  
20  
21 6118 Rosa, D.R.N., Finch, A.A., Andersen, T. and Inverno, C.M.C. 2009. U-Pb geochronology and  
22 6119 Hf isotope ratios of magmatic zircons from the Iberian Pyrite Belt. Mineralogy and  
23 6120 Petrology, 95, 47-69.  
24  
25 6121 Rosenbaum, G., Lister, G.S. and Duboz, C. 2002. Reconstruction of the tectonic evolution of  
26 6122 the western Mediterranean since the Oligocene. Journal of the Virtual Explorer, 8,  
27 6123 107-130.  
28  
29 6124 Rossetti, F., Theye, T., Lucci, F., Bouybaouene, M. L., Dini, A., Gerdes, A., Phillips, D. and  
30 6125 Cozzupoli, D. 2010. Timing and modes of granite magmatism in the core of the  
31 6126 Alboran Domain, Rif chain, northern Morocco: Implications for the Alpine evolution  
32 6127 of the western Mediterranean. Tectonics, 29, TC2017.  
33  
34 6128 Rossi, P., Oggiano, G. and Cocherie, A. 2009. A restored section of the "southern Variscan  
35 6129 realm" across the Corsica-Sardinia microcontinent. Comptes Rendus Geoscience, 341,  
36 6130 224-238. <https://doi.org/10.1016/j.crte.2008.12.005>.  
37  
38 6131 Rötzler, K. and Plessen, B. 2010. The Erzgebirge: a pile of ultrahigh- to low-pressure nappes  
39 6132 of Early Palaeozoic rocks and their Cadomian basement. In: Linnemann, U. and  
40 6133 Romer, R.L. (Eds.), Pre-Mesozoic Geology of Saxo-Thuringia – From the Cadomian  
41 6134 Active Margin to the Variscan Orogen. Stuttgart, 253-270.  
42  
43  
44  
45  
46  
47  
48  
49  
50  
51  
52  
53  
54  
55  
56  
57  
58  
59  
60  
61  
62  
63  
64  
65

- 6135 Rötzler, J. and Romer, R.L. 2010. The Saxon Granulite Massif: a key area for the geodynamic  
1 evolution of Variscan central Europe. In: Linnemann, U. and Romer, R.L. (Eds.), Pre-  
2 6136 Mesozoic Geology of Saxo-Thuringia – From the Cadomian Active Margin to the  
3 6137 Variscan Orogen. Stuttgart, 233-252.  
4  
5 6138  
6
- 7 6139 Rötzler, J., Carswell, D.A., Gerstenberger, H. and Haase, G. 1999. Transitional blueschist-  
8 epidote amphibolite facies metamorphism in the Frankenberg massif, Germany, and  
9 6140 geotectonic implications. *Journal of Metamorphic Geology*, 16 (1), 109-125.  
10 6141  
11  
12
- 13 6142 Rubatto, D., Ferrando, S., Compagnoni, R. and Lombardo, B. 2010. Carboniferous high-  
14 pressure metamorphism of Ordovician protolith in the Argentera Massif (Italy),  
15 6143 Southern European Variscan Belt. *Lithos*, 116, 65-76.  
16 6144  
17  
18
- 19 6145 Rubio Ordóñez, A., Valverde-Vaquero, P., Corretgé, L.G., Cuesta-Fernández, A., Gallastegui,  
20 6146 G., Fernández-González, M. and Gerdes, A. 2012. An Early Ordovician tonalitic–  
21 granodioritic belt along the Schistose-Greywacke Domain of the Central Iberian Zone  
22 6147 (Iberian Massif, Variscan Belt). *Geological Magazine, Rapid Communication*, 1-13.  
23 6148 <https://doi.org/10.1017/S0016756811001129>.  
24  
25  
26  
27 6149  
28
- 29 6150 Rubio Pascual, F.J., Arenas, R., Martínez Catalán, J.R., Rodríguez Fernández, L.R. and  
30 6151 Wijbrans, J. 2013a. Thickening and Exhumation of the Variscan roots in the Iberian  
31 Central System: Tectonothermal processes and  $^{40}\text{Ar}/^{39}\text{Ar}$  ages. *Tectonophysics*, 587,  
32 6152 207-221. <https://doi.org/10.1016/j.tecto.2012.10.005>.  
33 6153  
34  
35  
36
- 37 6154 Rubio Pascual, F.J., Matas, J. and Martín Parra, L.M. 2013b. High-pressure metamorphism in  
38 the Early Variscan subduction complex of the SW Iberian Massif. *Tectonophysics*,  
39 6155 592, 187-199. <https://doi.org/10.1016/j.tecto.2013.02.022>.  
40 6156  
41  
42
- 43 6157 Rubio Pascual, F.J., López-Carmona, A. and Arenas, R. 2016. Thickening vs. Extensión in  
44 the Variscan belt: P-T modelling in the Central Iberian Autochthon. *Tectonophysics*,  
45 6158 681, 144-158. <https://doi.org/10.1016/j.tecto.2016.02.033>.  
46 6159  
47  
48
- 49 6160 Ruiz-Cruz, M.D. and Sanz de Galdeano, C. 2013. Coesite and diamond inclusions, exsolution  
50 microstructures and chemical patterns in ultrahigh pressure garnet from Ceuta  
51 6161 (Northern Rif, Spain). *Lithos*, 177, 184-206.  
52 6162  
53  
54
- 55 6163 Ruiz Cruz, M.D. and Sanz de Galdeano, C. 2014. Garnet variety and zircon ages in UHP  
56 meta-sedimentary rocks from the Jubrique zone (Alpujarride Complex, Betic  
57 6164  
58  
59  
60  
61  
62  
63  
64  
65

- 6165 Cordillera, Spain): evidence for a pre-Alpine emplacement of the Ronda peridotite,  
1  
2 6166 International Geology Review, 56, 845-868.  
3
- 4 6167 Salman, K. and Montero, P. 1999. Geochronological, geochemical and petrological studies in  
5  
6 6168 two areas of the Ossa-Morena Zone: the Monesterio Complex and Calera de León  
7  
8 6169 granite. XV Reunión de Geología del Oeste Peninsular. International Meeting on  
9  
10 6170 Cadomian Orogens. Journal of Conference Abstracts 4/3: 1020, Badajoz, España.
- 11  
12 6171 Sánchez-García, T., Quesada, C., Bellido, F., Dunning, G. and González del Tánago, J. 2008.  
13  
14 6172 Two-step magma flooding of the upper crust during rifting: the Early Paleozoic of the  
15  
16 6173 Ossa-Morena Zone (SW Iberia). Tectonophysics, 461, 72-90.
- 17  
18 6174 Sánchez-García, T., Bellido, F., Pereira, M.F., Chichorro, M., Quesada C., Pin, C. and Silva,  
19  
20 6175 J.B. 2010. Rift related volcanism predating the birth of the Rheic Ocean (Ossa-Morena  
21  
22 6176 Zone, SW Iberia). Gondwana Research, 17, 392-407.
- 23  
24 6177 Sánchez-García, T., Pereira, M.F., Bellido, F., Chichorro, M., Silva, J.B., Valverde-Vaquero,  
25  
26 6178 P., Pin, C. and Solá, A.R. 2014. Early Cambrian granitoids of North Gondwana  
27  
28 6179 margin in the transition from a convergent setting to intra-continental rifting (Ossa-  
29  
30 6180 Morena Zone, SW Iberia). International Journal of Earth Sciences, 103, 1203-1218.  
31  
32 6181 <https://doi.org/10.1007/s00531-013-0939-8>.
- 33  
34 6182 Sánchez Martínez, S., Arenas, R., Díaz García, F., Martínez Catalán, J.R., Gómez-Barreiro, J.  
35  
36 6183 and Pearce, J.A. 2007a. Careón Ophiolite, NW Spain: Suprasubduction zone setting  
37  
38 6184 for the youngest Rheic Ocean floor. Geology, 35, 53-56.  
39  
40 6185 <https://doi.org/10.1130/G23024A.1>.
- 41  
42 6186 Sánchez Martínez, S., Arenas, R., Andonaegui, P., Martínez Catalán, J.R. and Pearce, J.A.  
43  
44 6187 2007b. Geochemistry of two associated ophiolites from the Cabo Ortegal complex  
45  
46 6188 (Variscan belt of northwest Spain). In: Hatcher Jr., R.D., Carlson, M.P., McBride, J.H.  
47  
48 6189 and Martínez Catalán, J.R. (Eds.), 4-D framework of continental crust. Geological  
49  
50 6190 Society of America, Memoir 200, 445-467. [https://doi.org/10.1130/2007.1200\(23\)](https://doi.org/10.1130/2007.1200(23)).
- 51  
52 6191 Sánchez Martínez, S., Arenas, R., Gerdes, A., Castiñeiras, P., Potrel, A. and Fernández-  
53  
54 6192 Suárez, J. 2011. Isotope geochemistry and revised geochronology of the Purrido  
55  
56 6193 Ophiolite (Cabo Ortegal Complex, NW Iberian Massif): Devonian magmatism with  
57  
58 6194 mixed sources and involved Mesoproterozoic basement. Journal of the Geological  
59  
60 6195 Society, London, 168 (3), 733-750.  
61  
62  
63  
64  
65

- 6196 Sánchez-Navas, A., García-Casco, A. and Martín-Algarra, A. 2014. Pre-Alpine discordant  
1  
2 6197 granitic dikes in the metamorphic core of the Betic Cordillera: tectonic implications.  
3  
4 6198 Terra Nova, 26, 477-486.
- 5  
6 6199 Santallier, D., Briand, B., Ménot, R.P. and Piboule, M. 1988. Les complexes leptyno-  
7  
8 6200 amphiboliques (C.L.A.): revue critique et suggestions pour un meilleur emploi de ce  
9  
10 6201 terme. Bulletin de la Société Géologique de France, 8 (4), 3-12.
- 11  
12 6202 Santallier, D., Lardeaux, J.M., Marchand, J. and Marignac, Ch. 1994. Metamorphism, The  
13  
14 6203 Massif Central. In: Keppie, J.D. (Ed.), Pre-Mesozoic Geology in France and related  
15  
16 6204 areas. Springer-Verlag, Berlin, 324-340.
- 17  
18 6205 Santamaría-López, Á. and Sanz de Galdeano, C. 2018. SHRIMP U-Pb detrital zircon dating  
19  
20 6206 to check subdivisions in metamorphic complexes: a case of study in the Nevado-  
21  
22 6207 Filábride complex (Betic Cordillera, Spain). International Journal of Earth Sciences,  
23  
24 6208 107, 2539-2552.
- 25  
26 6209 Santos, J.F., Soares de Andrade, A. and Munhá, J.M. 1990. Magmatismo orogénico Varisco  
27  
28 6210 no limite meridional da Zona de Ossa-Morena. Comunicações dos Serviços  
29  
30 6211 Geológicos de Portugal. 76, 91-124.
- 31  
32 6212 Santos, J.F., Schärer, U., Gil Ibarra, J.I. and Girardeau, J. 2002. Genesis of pyroxenite-rich  
33  
34 6213 peridotite at Cabo Ortegal (NW Spain): geochemical and Pb-Sr-Nd isotope data.  
35  
36 6214 Journal of Petrology, 43, 17-43.
- 37  
38 6215 Santos Zalduegui, J.F., Schärer, U. and Gil Ibarra, J.I. 1995. Isotope constraints on the age  
39  
40 6216 and origin of magmatism and metamorphism in the Malpica-Tuy allochthon, Galicia,  
41  
42 6217 NW-Spain. Chemical Geology, 121, 91-103.
- 43  
44 6218 Santos Zalduegui, J.F., Schärer, U., Gil Ibarra, J.I. and Girardeau, J. 1996. Origin and  
45  
46 6219 evolution of the Paleozoic Cabo Ortegal ultramafic-mafic complex (NW Spain): U-Pb,  
47  
48 6220 Rb-Sr and Pb-Pb isotope data. Chemical Geology, 129, 281-304.
- 49  
50 6221 Sanz-López, J. and Blanco Ferrera, S. 2012. Lower Bashkirian conodonts from the Iraty  
51  
52 6222 Formation in the Alduides-Quinto Real Massif (Pyrenees, Spain). Geobios, 45, 397-  
53  
54 6223 411.
- 55  
56 6224 Sanz-López, J. and Blanco Ferrera, S. 2013. Early evolution of Declinognathodus close to the  
57  
58 6225 Mid-Carboniferous Boundary interval in the Barcaliente type section (Spain).  
59  
60 6226 Palaeontology, 56 (5), 927-946.

- 6227 Schäfer, H.J. 1990. Geochronological investigations in the Ossa-Morena Zone, SW Spain.  
1  
26228 Ph.D. Thesis, Univ. Zurich. Diss. ETH 9246, 153 pp.  
3
- 46229 Schäfer, H.J., Gebauer, D., Nägler, T.F. and Eguiluz, L. 1993a. Conventional and ion-  
5  
66230 microprobe U-Pb dating of detrital zircons of the Tentudía Group (Serie Negra, SW  
7  
86231 Spain): implications for zircon systematics, stratigraphy, tectonics and the  
9  
96232 Precambrian/Cambrian boundary. *Contributions to Mineralogy and Petrology*, 113:  
10  
116233 289-299.  
12
- 13  
146234 Schäfer, H.J., Gebauer, D., Gil Ibarguchi, J.I. and Peucat, J.J. 1993b. Ion-microprobe U-Pb  
15  
166235 zircon dating on the HP/HT Cabo Ortegal Complex (Galicia, NW Spain): preliminary  
176236 results. *Terra Abstracts*, 5, 4, 22.  
18
- 19  
206237 Scherer, E.E., Mezger, K. and Münker, C. 2002. Lu-Hf ages of high-pressure metamorphism  
21  
226238 in the Variscan fold belt of southern Germany. *Geochimica et Cosmochimica Acta*,  
236239 66, A677.  
24
- 25  
266240 Schermerhorn, L.J.G. and Kotsch, S. 1984. First occurrence of lawsonite in Portugal and  
27  
286241 tectonic implications. *Comunicações dos Serviços Geológicos de Portugal*, 70, 23-29.  
29
- 306242 Schmädicke, E. 1994. Die Eklogite des Erzgebirges. *Freiberger Forschungshefte*, C456, 1-  
31  
326243 338.  
33
- 346244 Schmädicke, E., Mezger, K., Cosca, M.A. and Okrusch, M. 1995. Variscan Sm-Nd and Ar-Ar  
35  
366245 ages of eclogite facies rocks from the Erzgebirge, Bohemian Massif. *Journal of*  
37  
386246 *Metamorphic Geology*, 13 (5), 537-552. [https://doi.org/10.1111/j.1525-  
396247 1314.1995.tb00241.x](https://doi.org/10.1111/j.1525-1314.1995.tb00241.x).  
40
- 41  
426248 Schneider, J.L., Hassenforder, B. and Paicheler, J.C. 1990. Une ou plusieurs 'Ligne des  
43  
446249 Klippes' dans les Vosges du Sud (France)? Nouvelles données sur la nature des  
45  
466250 'klippes' et leur signification dans la dynamique varisque. *Comptes Rendus de*  
476251 *l'Académie des Sciences, Paris*, 311, 1221-1226.  
48
- 49  
506252 Schneider, J., Corsini, M., Reverso-Peila, A. and Lardeaux, J.M. 2014. Thermal and  
51  
526253 mechanical evolution of an orogenic wedge during Variscan collision: an example in  
53  
546254 the Maures-Tanneron Massif (SE France). In: Schulmann, K., Martínez Catalán, J.R.,  
556255 Lardeaux, J.M., Janousek, V. and Oggiano, G. (Eds.), *The Variscan Orogeny: Extent,*  
56  
576256 *Timescale and the Formation of the European Crust*. Geological Society, London,  
58  
596257 *Special Publication 405*, 313-331. <https://doi.org/10.1144/SP405.4>.  
60  
61  
62  
63  
64  
65



- 6258 Schott, J.J. 1981. The north pyrenean fault as a limit of the Iberian plate. Paleomagnetic  
1 evidence. *Terra Cognita*, 1, 75.  
2
- 46260 Schulmann, K., Ledru, P., Autran, A., Melka, R., Lardeaux, J.M., Urban, M. and Lobkowicz,  
5 M. 1991. Evolution of nappes in the eastern margin of the Bohemian Massif—a  
6 kinematic interpretation. *Geologische Rundschau*, 80 (1),73-92.  
7
- 106263 Schulmann, K., Melka, R., Lobkowicz, M., Ledru, P., Lardeaux, J.M. and Autran, A. 1994.  
11 Contrasting styles of deformation during progressive nappe stacking at the  
12 southeastern margin of the Bohemian Massif (Thaya Dome). *Journal of Structural  
13 Geology*, 16 (3), 355-370.  
14
- 186267 Schulmann, K. and Gayer, R. 2000. A model of an obliquely developed continental  
19 accretionary wedge: NE Bohemian Massif. *Journal of the Geological Society, London*,  
20 156, 401-416.  
21
- 246270 Schulmann, K., Schaltegger, U., Ježek, J., Thompson, A.B. and Edel, J. B. 2002. Rapid burial  
25 and exhumation during orogeny: thickening and synconvergent exhumation of  
26 thermally weakened and thinned crust (Variscan orogen in Western Europe).  
27 *American Journal of Science*, 302, 856-879.  
28
- 326274 Schulmann, K., Kröner, A., Hegner, E., Wendt, I., Konopásek, J., Lexa, O. and Štípská, P.  
33 2005. Chronological constraints on the pre-orogenic history, burial and exhumation of  
34 deep-seated rocks along the eastern margin of the Variscan orogen, Bohemian Massif,  
35 Czech Republic. *American Journal of Science*, 305, 407-448.  
36
- 406278 Schulmann, K., Lexa, O., Štípská, P., Racek, M., Tajcmanová, L., Konopásek, J., Edel, J.B.,  
41 Peschler, A. and Lehmann, J. 2008. Vertical extrusion and horizontal channel flow of  
42 orogenic lower crust: key exhumation mechanisms in large hot orogens? *Journal of  
43 Metamorphic Geology*, 26, 273-297. [https://doi.org/10.1111/j.1525-  
44 1314.2007.00755.x](https://doi.org/10.1111/j.1525-1314.2007.00755.x).  
45
- 496283 Schulmann, K., Konopásek, K., Janousek, V., Lexa, O., Lardeaux, J.-M., Edel, J.-B., Štípská,  
50 P. and Ulrich, S. 2009. An Andean type Palaeozoic convergence in the Bohemian  
51 Massif. *Comptes Rendus Geoscience*, 341, 266-286.  
52 <https://doi.org/10.1016/j.crte.2008.12.006>.  
53
- 576287 Schulmann, K., Martínez Catalán, J.R., Lardeaux, J.-M., Janousek, V. and Oggiano, G. (Eds.).  
58 2014a. *The Variscan Orogeny: Extent, timescale and the formation of the European*  
59

- 6289 crust. Geological Society, London, Special Publication 405, 406 pp. ISBN: 978-1-  
1  
26290 86239-658-6.
- 3  
46291 Schulmann, K., Lexa, O., Janousek, V., Lardeaux, J.-M. and Edel, J.-B. 2014b. Anatomy of a  
5  
66292 diffuse cryptic suture: An example from the Bohemian Massif, European Variscides.  
7  
86293 *Geology*, 42 (4), 275-278. <https://doi.org/10.1130/G35290.1>.
- 9  
106294 Schulz, B., Krenn, E., Finger, F., Brätz, H. and Klemd, R. 2007. Cadomian and Variscan  
11  
126295 metamorphic events in the Léon Domain (Armorican Massif, France): P-T data and  
13  
146296 EMP monazite dating. In: Linnemann, U., Nance, R.D., Kraft, P. and Zulauf, G.  
15  
166297 (Eds.), *The evolution of the Rheic Ocean: From Avalonian-Cadomian active margin to*  
176298 *Alleghenian-Variscan collision*. Geological Society of America Special Paper, 423,  
18  
196299 267-285. [https://doi.org/10.1130/2007.2423\(12\)](https://doi.org/10.1130/2007.2423(12)).
- 20  
216300 Serrano Pinto, M., Casquet, C., Ibarrola, E., Corretgé, L.G. and Portugal Ferreira, M. 1987.  
22  
236301 Síntese geocronológica dos granitoides do Maciço Hespérico. In: Bea, F., Carnicero,  
24  
256302 A., Gonzalo, J.C., López Plaza, M. and Rodríguez Alonso, M.D. (Eds.), *Geología de*  
26  
276303 *los granitoides y rocas asociadas del Macizo Hespérico*. Rueda. Madrid. 69-86.
- 28  
296304 Seston, R., Winchester, J.A., Piasecki, M.A.J., Crowley, Q.G. and Floyd, P.A. 2000. A  
30  
316305 structural model for the western-central Sudetes: a deformed stack of Variscan thrust  
32  
336306 sheets. *Journal of the Geological Society, London*, 157, 1155-1167.
- 34  
356307 Siddans, A.W.B. 1972. Slaty cleavage – A review of research since 1815. *Earth-Science*  
36  
376308 *Reviews*, 8, 205-232.
- 38  
396309 Silva, J.B., Oliveira, J.T. and Ribeiro, A. 1990. South Portuguese Zone. Structural outline. In:  
40  
416310 Dallmeyer, R.D. and Martínez García, E. (Eds.), *Pre-Mesozoic Geology of Iberia*.  
42  
436311 Springer-Verlag. Berlin. 348-362.
- 44  
456312 Simancas, F. 2004. Evolución de la Zona Sudportuguesa y su contacto con la Zona de Ossa-  
46  
476313 Morena. In: Vera, J.A. (Ed.), *Geología de España, SGE-IGME*, Madrid, 215-217.
- 48  
49  
506314 Simancas, F., Martínez Poyatos, D., Expósito, I., Azor, A. and González Lodeiro, F. 2001.  
51  
526315 The structure of a major suture zone in the SW Iberian Massif: the Ossa-  
53  
546316 Morena/Central Iberian contact. *Tectonophysics*, 332, 295-308.
- 55  
566317 Simancas, F., González Lodeiro, F., Expósito Ramos, I., Azor, A., and Martínez Poyatos, D.  
57  
586318 2002. Opposite subduction polarities connected by transform faults in the Iberian  
59  
606319 Massif and western European Variscides. In: Martínez Catalán, J.R., Hatcher Jr., R.D.,  
61  
62  
63  
64  
65

- 6320 Arenas, R. and Díaz García, F. (Eds.), *Variscan-Appalachian Dynamics: The Building*  
1  
2 6321 *of the Late Paleozoic Basement*, Geological Society of America Special Paper 364,  
3 6322 253-262.
- 4  
5  
6 6323 Simancas, F., Carbonell, R., González Lodeiro, F., Pérez-Estaún, A., Juhlin, C., Ayarza, P.,  
7  
8 6324 Kashubin, A., Azor, A., Martínez Poyatos, D., Almodóvar, G.R., Pascual, E., Sáez, R.  
9  
10 6325 and Expósito, I. 2003. Crustal structure of the transpressional Variscan orogen of SW  
11 6326 Iberia: SW Iberia deep seismic reflection profile (IBERSEIS). *Tectonics*, 22 (6),  
12  
13 6327 TC1062, 1-19. <https://doi.org/10.1029/2002TC001479>.  
14
- 15 6328 Simancas, J.F., Tahiri, A., Azor, A., González Lodeiro, F., Martínez Poyatos, D. and El Hadi,  
16  
17 6329 H. 2005. The tectonic frame of the Variscan-Alleghanian orogen in Southern Europe  
18  
19 6330 and Northern Africa. *Tectonophysics*, 398, 181-198.  
20  
21 6331 <https://doi.org/10.1016/j.tecto.2005.02.006>.  
22
- 23 6332 Simancas, J.F., Carbonell, R., González-Lodeiro, F., Pérez-Estaún, A., Juhlin, C., Ayarza, P.,  
24  
25 6333 Kashubin, A., Azor, A., Martínez Poyatos, D., Sáez, R., Almodóvar, G.R., Pascual, E.,  
26  
27 6334 Flecha, I. and Marti, D. 2006. Transpressional tectonics and mantle plume dynamics:  
28  
29 6335 the Variscides of Southwestern Iberia. Geological Society, London, Memoir 32, 345-  
30  
31 6336 354.
- 32  
33 6337 Simancas, J.F., Azor, A., Martínez Poyatos, D., Tahiri, A., El Hadi, H., González-Lodeiro, F.,  
34  
35 6338 Pérez-Estaún, A. and Carbonell, R. 2009. Tectonic relationships of Southwest Iberia  
36  
37 6339 with the allochthons of Northwest Iberia and the Moroccan Variscides. *Comptes*  
38  
39 6340 *Rendus Geoscience*, 341, 103-113. <https://doi.org/10.1016/j.crte.2008.11.003>.
- 40  
41 6341 Simancas, J.F., Ayarza, P., Azor, A., Carbonell, R., Martínez Poyatos, D., Pérez-Estaún, A.  
42  
43 6342 and González Lodeiro, F. 2013. A seismic geotraverse across the Iberian Variscides:  
44  
45 6343 Orogenic shortening, collisional magmatism, and orocline development. *Tectonics*, 32,  
46  
47 6344 417-432. <https://doi.org/10.1002/tect.20035>.
- 48  
49 6345 Sintubin, M., Debacker, T.N. and Van Baelen, H. 2009. Early Palaeozoic orogenic events  
50  
51 6346 north of the Rheic suture (Brabant, Ardenne): A review. *Comptes Rendus Geoscience*,  
52  
53 6347 341, 156-173. <https://doi.org/10.1016/j.crte.2008.11.012>.
- 54  
55 6348 Skácel, J. 1989. Crossing of the Lugian boundary fault with Nýznerov dislocation belt  
56  
57 6349 between Vápenná and Javorník in Silesia. *Acta Universitatis Palackianae*  
58 6350 *Olomucensis*, 95, 31-45.
- 59  
60  
61  
62  
63  
64  
65

- 6351 Skrzypek, E., Tabaud, A.S., Edel, J.B., Schulmann, K., Cocherie, A., Guerrot, C. And Rossi,  
1  
2 6352 P. 2012. The significance of Late Devonian ophiolites in the Variscan orogen: a record  
3  
4 6353 from the Vosges Klippen Belt. *International Journal of Earth Sciences*, 101 (4), 951-  
5  
6 6354 972.
- 7  
8 6355 Skrzypek, E., Schulmann, K., Tabaud, A. S. and Edel, J.B. 2014. Palaeozoic evolution of the  
9  
10 6356 Variscan Vosges Mountains. In: Schulmann, K., Martínez Catalán, J.R., Lardeaux, J.M.,  
11  
12 6357 Janoušek, V. and Oggiano, G. (Eds.), *The Variscan Orogeny: Extent, Timescale and the*  
13  
14 6358 *Formation of the European Crust*. Geological Society, London, Special Publications  
15  
16 6359 405, 45-75. <http://dx.doi.org/10.1144/SP405.8>.
- 17  
18 6360 Smith, A.J. and Curry, D. 1975. The structure and geological evolution of the English  
19  
20 6361 Channel. *Philosophical Transactions of the Royal Society, London, A*. 279, 3-30.
- 21  
22 6362 Soejono, I., Žáčková, E., Janoušek, K., Machek, M. and Košler, J. 2010. Vestige of an Early  
23  
24 6363 Cambrian incipient oceanic crust incorporated in the Variscan orogen: Letovice  
25  
26 6364 Complex, Bohemian Massif. *Journal of the Geological Society, London*, 167, 1113-  
27  
28 6365 1130.
- 29  
30 6366 Solá, A.R., Pereira, M.F., Williams, I.S., Ribeiro, M.L., Neiva, A.M.R., Montero, P., Bea, F.  
31  
32 6367 and Zinger, T. 2008. New insights from U-Pb zircon dating of Early Ordovician  
33  
34 6368 magmatism on the northern Gondwana margin: The Urra Formation (SW Iberian  
35  
36 6369 Massif, Portugal). *Tectonophysics*, 461, 114-129.
- 37  
38 6370 Solá, A.R., Williams, I.S., Neiva, A.M.R. and Ribeiro M.L. 2009. U-Th-Pb SHRIMP ages  
39  
40 6371 and oxygen isotope composition of zircon from two contrasting late Variscan  
41  
42 6372 granitoids, Nisa-Albuquerque batholith, SW Iberian Massif: Petrologic and regional  
43  
44 6373 implications. *Lithos*, 111(3-4), 156-167. <https://doi.org/10.1016/j.lithos.2009.03.045>.
- 45  
46 6374 Soulaïmani, A., Ouanaimi, H., Saddiqi, O., Baidder, L. and Michard, A. 2018. The Anti-Atlas  
47  
48 6375 Pan-African Belt (Morocco): Overview and pending questions. *Comptes Rendus*  
49  
50 6376 *Geoscience*, 350 279-288.
- 51  
52 6377 Spahić, D. and Gaudenyi, T. 2019. Primordial geodynamics of Southern Carpathian-Balkan  
53  
54 6378 basements (Serbo-Macedonian Mass): Avalonian vs. Cadomian arc segments.  
55  
56 6379 *Proceedings of the Geologists' Association*, 130, 142-156.  
57 6380 <https://doi.org/10.1016/j.pgeola.2018.10.006>.

- 6381 Stampfli, G.M. and Borel, G.D. 2002. A plate tectonic model for the Paleozoic and Mesozoic  
1  
26382 constrained by dynamic plate boundaries and restored synthetic oceanic isochrons.  
3  
46383 Earth and Planetary Science Letters, 196, 17-33.  
5
- 6384 Stampfli, G.M., von Raumer, J.F. and Borel, G.D. 2002. Paleozoic evolution of pre-Variscan  
7  
86385 terranes: From Gondwana to the Variscan collision. In: Martínez Catalán, J.R.,  
9  
106386 Hatcher Jr., R.D., Arenas, R. and Díaz García, F. (Eds.), Variscan-Appalachian  
11  
126387 Dynamics: The Building of the Late Paleozoic Basement. Geological Society of  
13  
146388 America Special Paper, 364, 263-280.
- 156389 Stampfli, G.M. and Kozur H.W. 2006. Europe from the Variscan to the Alpine cycles. In:  
16  
176390 Gee, D.G. and Stephenson, R.A. (Eds.), European Lithosphere Dynamics. Geological  
18  
196391 Society, London, Memoir 32, 57-82. [https://doi.org/0435-4052/06/\\$15.00](https://doi.org/0435-4052/06/$15.00).
- 216392 Stampfli, G.M., Hochard, C., Vérard, C., Wilhem, C. and von Raumer, J. 2013. The formation  
22  
236393 of Pangea. Tectonophysics, 593, 1-19. <https://doi.org/10.1016/j.tecto.2013.02.037>.
- 256394 Stephan, T., Kroner, U. and Romer, R.L. 2019. The pre-orogenic detrital zircon record of the  
26  
276395 Peri-Gondwanan crust. Geological Magazine, 156 (2), 281-307.  
28  
296396 <https://doi.org/10.1017/S0016756818000031>.
- 316397 Stille, H. 1924. Grundfragen der Vergleichenden. Tectonik. Gebrueder Borntragen. Berlin,  
32  
336398 443 pp.
- 356399 Stille, H. 1928. Zur Einfuehrung in die Phasen der paläozoischen Gebirgsbildung. Zeitschrift  
36  
376400 der Deutschen Geologischen Gesellschaft (Zeitsch der Deutsch. Geol. Gesellsch.), 80  
38  
396401 (1), 1-24.
- 416402 Štípská, P. and Schulmann, K. 1995. Inverted metamorphic zonation in a basement-derived  
42  
436403 nappe sequence, eastern margin of the Bohemian Massif. Geological Journal, 30 (3-4),  
44  
456404 385-413.
- 476405 Štípská, P., Schulmann, K., Thompson, A.B., Ježek, J. and Kröner, A. 2001. Thermo-  
48  
496406 mechanical role of a Cambro-Ordovician paleorift during the Variscan collision: the  
50  
516407 NE margin of the Bohemian Massif. Tectonophysics, 332, 239-253.
- 536408 Štípská, P., Schulmann, K. and Kröner, A. 2004. Vertical extrusion and middle crustal  
54  
556409 spreading of omphacite granulite: A model of synconvergent exhumation (Bohemian  
56  
576410 Massif, Czech Republic). Journal of Metamorphic Geology, 22 (3), 179-198.  
58

- 6411 Štípská, P., Pitra, P. and Powell, R. 2006. Separate or shared metamorphic histories of  
1  
2 6412 eclogites and surrounding rocks? An example from the Bohemian Massif. *Journal of*  
3  
4 6413 *Metamorphic Geology*, 24, 219-817.
- 5  
6 6414 Štípská, P., Chopin, F., Skrzypek, E., Schulmann, K., Pitra, P., Lexa, O., Martelat, E.,  
7  
8 6415 Bollinger, C. and Žáčková, E. 2012. The juxtaposition of eclogite and mid-crustal  
9  
10 6416 rocks in the Orlica-Šniežnik Dome, Bohemian Massif. *Journal of Metamorphic*  
11  
12 6417 *Geology*, 30 (2), 213-234. <https://doi.org/10.1111/j.1525-1314.2011.00964.x>.
- 13  
14 6418 Štípská, P., Hacker, B.R., Racek, M., Holder, R., Kylander-Clark, A.R.C., Schulmann, K. and  
15  
16 6419 Hasalová, P. 2015. Prograde and retrograde monazite ages in barrovian-type  
17  
18 6420 metamorphism (Thaya window, Bohemian massif). *Journal of Petrology*, 56 (5), 1007-  
19  
20 6421 1035. <https://doi.org/10.1093/petrology/egv026>.
- 21  
22 6422 Štípská, P., Powell, R., Hacker, B.R., Holder, R. and Kylander-Clark, A.R.C. 2016.  
23  
24 6423 Uncoupled U/Pb and REE response in zircon during the transformation of eclogite to  
25  
26 6424 mafic and intermediate granulite (Blanský les, Bohemian Massif). *Journal of*  
27  
28 6425 *Metamorphic Geology*, 34, 551-572.
- 29  
30 6426 Štípská, P., Hasalová, P., Powell, R., Závada, P., Schulmann, K., Racek, M., Aguilar, C. and  
31  
32 6427 Chopin, F. 2019. The effect of melt infiltration on metagranitic rocks: the Šniežnik  
33  
34 6428 Dome, Bohemian Massif. *Journal of Petrology*, 60, 591-618.
- 35  
36 6429 Štípská, P., Schulmann, K., Racek, M., Lardeaux, J.M., Hacker, B.R., Kylander-Clark,  
37  
38 6430 A.R.C., Holder, R. and Košuličová, M. 2020. Finite pattern of Barrovian metamorphic  
39  
40 6431 zones: interplay between thermal reequilibration and post-peak deformation during  
41  
42 6432 continental collision—insights from the Svatka dome (Bohemian Massif).  
43  
44 6433 *International Journal of Earth Sciences*, 109, 1161-1187.
- 45  
46 6434 Subias, I., Villas, E. and Álvaro, J.J. 2015. Hirnantian (Late Ordovician)  $\delta^{13}\text{C}$  HICE excursion  
47  
48 6435 in a North Gondwanan (NE Spain) periglacial setting and its relationships to  
49  
50 6436 glacioeustatic fluctuations. *Chemie der Erde*, 75, 335-343.
- 51  
52 6437 Suess, E. 1885-1909. *Das Antlitz der Erde*. Vol. I-III (1885, 1888, 1909), 780, 508, 790 pp.  
53  
54 6438 Tempisky, Wien.
- 55  
56 6439 Suess, E. 1888. *Das Antlitz der Erde*. Vol. II, 508 pp. Tempisky, Wien.
- 57  
58 6440 Suess, F.E. 1912. Suess, F.E. 1912. *Die Moravischen Fenster und ihre Beziehungen zum*  
59  
60 6441 *Grundgebirge des hohen Gesenkes*. *Denkschrift der Kaiserlichen Akademie der*

- 6442           Wissenschaften in Wien, Mathematisch-Naturwissenschaftliche Klasse (Math.-nat.  
1  
26443           Kl.), 88, 541-631.  
3
- 46444       Suess, F.E. 1926. Intrusionstektonik und Wandertektonik im variszischen Grundgebirge.  
5  
66445           Gebrüder Borntraeger, Berlin, 268 pp.  
7
- 86446       Tabaud, A.S., Whitechurch, H., Rossi, P., Schulmann, K., Guerrot, C. and Cocherie, A. 2014.  
9  
106447           Devonian–Permian magmatic pulses in the northern Vosges Mountains (NE France):  
11  
126448           result of continuous subduction of the Rhenohercynian Ocean and Avalonian passive  
13  
146449           margin. Geological Society, London, Special Publications, 405, 197-223.  
15
- 166450       Tabaud, A.S., Janoušek, V., Skrzypek, E., Schulmann, K., Rossi, P., Whitechurch, H.,  
17  
186451           Guerrot, C. and Paquette, J.L. 2015. Chronology, petrogenesis and heat sources for  
19  
206452           successive Carboniferous magmatic events in the southern–central Variscan Vosges  
21  
226453           Mts. (NE France). Journal of the Geological Society, London, 172, 87-102  
236454           <https://doi.org/10.1144/jgs2013-123>.  
24
- 256455       Tabaud, A.S., Štípská, P., Mazur, S., Schulmann, K., Míková, J., Wong, J. and Sun, M. 2021.  
26  
276456           Evolution of a Cambro-Ordovician active margin in northern Gondwana: Geochemical  
28  
296457           and zircon geochronological evidence from the Góry Sowie metasedimentary rocks,  
30  
316458           Poland. Gondwana Research, 90, 1-26. <https://doi.org/10.1016/j.gr.2020.10.011>.  
32
- 336459       Tahiri, A., Montero, P., El Hadi, H., Martínez Poyatos, D., Azor, A., Bea, F., Simancas, J.F.  
34  
356460           and González Lodeiro, F. 2010. Geochronological data on the Rabat-Tiflet granitoids:  
36  
376461           their bearing on the tectonics of the Moroccan Variscides. Journal of African Earth  
38  
396462           Sciences, 57, 1-13.  
40
- 416463       Talavera, C., Montero, P. and Bea, F. 2008. Precise single-zircon Pb-Pb dating reveals that  
42  
436464           Aljucén (Mérida) is the oldest plutonic body of the Central Iberian Zone. Geo-Temas,  
44  
456465           10, 249-252.  
46
- 476466       Talavera, C., Montero, P., Bea, F., González Lodeiro, F. and Whitehouse, M. 2013. U-Pb  
48  
496467           Zircon geochronology of the Cambro-Ordovician metagranites and metavolcanic rocks  
50  
516468           of central and NW Iberia. International Journal of Earth Sciences, 102, 1-23.  
52  
536469           <https://doi.org/10.1007/s00531-012-0788-x>.  
54
- 556470       Tamain, G. 1971. El Alcudiense y la orogénesis Cadomiense en el sur de la Meseta Ibérica  
56  
576471           (España). Primer Centenario de la Real Sociedad Española de Historia Natural, 438-  
58  
596472           464.  
60  
61  
62  
63  
64  
65

- 6473 Teixeira, C. 1955. Notas sobre Geologia de Portugal: O Complexo xisto-grauváquico ante-  
1  
26474 ordoviciano. Empresa Literaria Fluminense, Lisboa, 50 pp.  
3
- 46475 Thiéblemont, D., Cabanis, B., Wyns, R. and Treuil, M. 1987a. Etude géochimique (majeurs et  
5  
66476 traces) de la formation amphibolitique de Saint-Martin-des-Noyers (complexe  
7  
86477 cristallophyllien des Essarts, Vendée). Mise en évidence d'un paléo-arc insulaire dans  
9  
106478 la partie interne de l'orogénèse varisque. Bulletin de la Société Géologique de France,  
116479 1987, 7 (2), 371-378.  
12
- 13  
146480 Thiéblemont, D., Cabanis, B. and Le Métour, J. 1987b. Etude géochimique d'un magmatisme  
156481 de distension intracontinentale: la série bimodale ordovico-silurienne du Choletais  
166482 (Massif vendéen). Géologie de la France, 1987 (1), 65-76.  
17  
18
- 19  
206483 Thiéblemont, D., Triboulet, C. and Godard, G. 1988. Mineralogy, petrology and P-T-t paths  
216484 of Ca-Na amphibole assemblages, Saint-Martin-des-Noyers formation, Vendée,  
226485 France. Journal of Metamorphic Geology, 6, 697-715.  
23  
24
- 25  
266486 Thiéblemont, D., Guerrot, C., Le Métour, J. and Jézéquel, P. 2001. Le complexe de Cholet-  
276487 Thouars: un ensemble volcano-plutonique cambrien moyen au sein du bloc  
286488 précambrien des Mauges. Géologie de la France, 2001 (1-2), 7-17.  
29  
30
- 31  
326489 Timmermann, H., Štědrá, V., Gerdes, A., Noble, S.R., Parrish, R.R. and Dörr, W. 2004. The  
336490 problem of dating high-pressure metamorphism: a U-Pb isotope and geochemical  
346491 study on eclogites and related rocks of the Mariánské Lázně Complex, Czech  
356492 Republic. Journal of Petrology, 45, 1311-1338.  
36  
37  
38
- 39  
406493 Timmermann, H., Dörr, W., Krenn, E., Finger, F. and Zulauf, G. 2006. Conventional and in  
416494 situ geochronology of the Teplá Crystalline Unit, Bohemian Massif: implications for  
426495 the processes involving monazite formation. International Journal of Earth Sciences,  
436496 95, 629-647.  
44  
45  
46
- 476497 Tollmann, A. 1982. Großräumiger variszischer Deckenbau im Moldanubikum und neue  
486498 Gedanken zum Variszikum Europas. Geotektonische Forschungen, 64, 1-91.  
49  
50
- 51  
526499 Tomek, F., Vacek, F., Žák, J., Petronis, M.S., Verner, K. and Foucher, M.S. 2019.  
536500 Polykinematic foreland basins initiated during orthogonal convergence and terminated  
546501 by orogen-oblique strike-slip faulting: An example from the northeastern Variscan  
556502 belt. Tectonophysics, 766, 379-397. [https://doi.org/ 10.1016/j.tecto.2019.05.023](https://doi.org/10.1016/j.tecto.2019.05.023).  
56  
57  
58  
59  
60  
61  
62  
63  
64  
65



- 6503 Toto, E.A., Kaabouden, F., Zouhri, L., Belarbi, M., Benammi M., Hafid, M. and Boutib, L.  
1  
2 6504 2008. Geological evolution and structural style of the Palaeozoic Tafilalt sub-basin,  
3  
4 6505 eastern Anti-Atlas (Morocco, North Africa). *Geological Journal*, 43, 59-73.
- 5  
6 6506 Trap, P., Roger, F., Cenki-Tok, B. and Paquette, J.L. 2017. Timing and duration of partial  
7  
8 6507 melting and magmatism in the Variscan Montagne Noire gneiss dome (French Massif  
9  
10 6508 Central). *International Journal of Earth Sciences*, 106, 453-476.  
11 6509 <https://doi.org/10.1007/s00531-016-1417-x>.
- 12  
13  
14 6510 Trautmann, F., Becq-Giraudin, J.F. et Carn, A. 1994. Notice explicative de la carte  
15  
16 6511 géologique de France au 1:50000, feuille Janzé (353). BRGM, Orléans, 78 pp.
- 17  
18 6512 Triboulet, C. 1974. Les glaucophanites et roches associées de l'Île de Groix (Morbihan,  
19  
20 6513 France): étude minéralogique et pétrogénétique. *Contributions to Mineralogy and  
21  
22 6514 Petrology*, 45, 65-90.
- 23  
24 6515 Truyols, J., Arbizu, M.A., García Alcalde, J.L., García-López, S., Méndez Bedia, I., Soto, F.  
25  
26 6516 and Truyols Massoni, M. 1990. The Asturian-Leonese Domain (Cantabrian Zone). In:  
27  
28 6517 Dallmeyer R.D. and Martínez García E. (Eds.), *Pre-Mesozoic Geology of Iberia*.  
29  
30 6518 Springer-Verlag. Berlín, Ch. 2, Stratigraphy, 10-19.
- 31  
32 6519 Turniak, K., Mazur, S. and Wysoczanski, R. 2000. SHRIMP zircon geochronology and  
33  
34 6520 geochemistry of the Orlica-Śnieżnik gneisses (Variscan belt of Central Europe) and  
35  
36 6521 their tectonic implications. *Geodinamica Acta*, 13, 1-20.
- 37  
38 6522 Vacek, F. and Žák, J. 2017. A lifetime of the Variscan orogenic plateau from uplift to collapse  
39  
40 6523 as recorded by the Prague Basin, Bohemian Massif. *Geological Magazine*, 156 (3),  
41  
42 6524 485-509.
- 43  
44 6525 Valín, M.L., Garcia-López, S., Brime, C., Bastida, F. and Aller, J. 2016. Tectonothermal  
45  
46 6526 evolution in the core of an arcuate fold and thrust belt: the south-eastern sector of the  
47  
48 6527 Cantabrian Zone (Variscan belt, north-western Spain). *Solid Earth*, 7, 1003-1022.  
49  
50 6528 <https://doi.org/0.5194/se-7-1003-2016>.
- 51  
52 6529 Valle Aguado, B., Azevedo, M.R., Schaltegger, U., Martínez Catalán, J.R. and Nolan, J.  
53  
54 6530 2005. U-Pb zircon and monazite geochronology of Variscan magmatism related to  
55  
56 6531 syn-convergence extension in Central Northern Portugal. *Lithos*, 82 (1-2), 169-184.
- 57  
58 6532 Valle Aguado, B., Azevedo, M.R., Nolan, J., Medina, J., Costa, M.M., Corfu, F. and Martínez  
59  
60 6533 Catalán, J.R. 2017. Granite emplacement at the termination of a major Variscan

- 6534 transcurrent shear zone: The late collisional Viseu batholith. *Journal of Structural*  
1  
2 6535 *Geology*, 98, 15-37. <https://doi.org/10.1016/j.jsg.2017.04.002>.  
3
- 4 6536 Valverde Vaquero, P. and Fernández, F.J. 1996. Edad de enfriamiento U/Pb en rutilos del  
5  
6 6537 Gneis de Chímparra (Cabo Ortegal, NO de España). *Geogaceta*, 20, 475-478.  
7
- 8 6538 Valverde-Vaquero, P., Cuesta Fernández, A., Gallastegui, G., Suárez, O., Corretgé, L.G. and  
9  
10 6539 Dunning G.R. 1999. U-Pb dating of late-Variscan magmatism in the Cantabrian Zone  
11  
12 6540 (northern Spain). EUG 10, European Union of Geosciences, Strasbourg, France,  
13  
14 6541 *Journal of Conference Abstracts*, 4 (1), 101.  
15
- 16 6542 Valverde-Vaquero, P. and Dunning, G.R. 2000. New U-Pb ages for Early Ordovician  
17  
18 6543 magmatism in Central Spain. *Journal of the Geological Society*, London, 157, 15-26.  
19  
20 6544 <https://doi.org/10.1144/jgs.157.1.15>.  
21
- 22 6545 Valverde-Vaquero, P., Marcos, A., Farias, P. and Gallastegui, G. 2005. U-Pb dating of  
23  
24 6546 Ordovician felsic volcanism in the Schistose Domain of the Galicia-Trás-os-Montes  
25  
26 6547 Zone near Cabo Ortegal (NW Spain). *Geológica Acta*, 3 (1), 27-37.  
27  
28 6548 <https://doi.org/10.1344/105.000001412>.  
29
- 30 6549 Valverde-Vaquero, P., Díez Balda, M.A., Díez Montes, A., Dörr, W., Escuder Viruete, J.,  
31  
32 6550 González Clavijo, E., Maluski, H., Rodríguez-Fernández, L.R., Rubio, F. and Villar,  
33  
34 6551 P. 2007a. The "hot orogen": two separate variscan low-pressure metamorphic events in  
35  
36 6552 the Central Iberian Zone. In: Faure, M., Lardeaux, J.-M., Ledru, P., Peschler, A. and  
37  
38 6553 Schulmann, K. (Eds.), *Mechanics of Variscan Orogeny: a modern view on orogenic*  
39  
40 6554 *research. Géologie de la France*, 2007 (2), 168. Société Géologique de France and  
41  
42 6555 Bureau de Recherches Géologiques et Minières.
- 43 6556 Valverde-Vaquero, P., Farias, P., Marcos, A. and Gallastegui, G. 2007b. U-Pb dating of  
44  
45 6557 Siluro-Ordovician volcanism in the Verín Synform (Ourense; Schistose Domain,  
46  
47 6558 Galicia-Trás-os-Montes Zone). *Geogaceta*, 41, 247-250.  
48
- 49 6559 Van Calsteren, P.W.C., Boelrijk, N.A.I.M., Hebeda, E.H., Priem, H.N.A., Tex, E. Den,  
50  
51 6560 Verdurmen, E.A.T.H. and Verschure, R.H. 1979. Isotopic dating of older elements  
52  
53 6561 (including the Cabo Ortegal mafic-ultramafic complex) in the Hercynian Orogen of  
54  
55 6562 NW Spain: manifestations of a presumed Early Paleozoic Mantle-plume. *Chemical*  
56  
57 6563 *Geology*, 24, 35-56.  
58  
59  
60  
61  
62  
63  
64  
65

- 6564 Vanderhaeghe, O., Laurent, O., Gardien, V., Moyen, J.F., Gévelin, A., Chelle-Michou, C.,  
1 6565 Couzinié, S., Villaros, A. and Bellanger, M. 2020. Flow of partially molten crust  
2 controlling construction, growth and collapse of the Variscan orogenic belt: the  
3 6566 geologic record of the French Massif Central. *Bulletin de la Société Géologique de*  
4 France, 191 (25), 1-56. <https://doi.org/10.1051/bsgf/2020013>.  
5 6567  
6 76568  
7  
8  
9 6569 Van der Voo, R. 1969. Paleomagnetic evidence for the rotation of the Iberian Peninsula.  
10 *Tectonophysics*, 7, 5-56.  
11 6570  
12  
13 6571 Van der Voo, R. and Baessenkool, A. 1973. Permian paleomagnetic results from the western  
14 Pyrenees delineating the plate boundary between the Iberian Peninsula and stable  
15 6572 Europe. *Journal of Geophysical Research*, 78 (23), 5118-5127.  
16  
17 6573  
18  
19 6574 Velde, B. 1972. The origin of some granulite facies rocks from the Baie d’Audierne,  
20 Finistère. *Bulletin de la Société Géologique et Minéralogique de Bretagne*, (C) IV, 91-  
21 6575 95.  
22  
23 6576  
24  
25 6577 Venera, Z., Schulmann, K. and Kröner, A. 2000. Intrusion within a transtensional tectonic  
26 domain: the Čistá granodiorite (Bohemian Massif)—structure and rheological  
27 6578 modelling. *Journal of Structural Geology*, 22, 1437-1454.  
28  
29 6579  
30  
31 6580 Vera, J.A. (Ed.). 2004. *Geología de España*. Sociedad Geológica de España-Instituto  
32 Geológico y Minero de España, Madrid, 884 pp.  
33 6581  
34  
35 6582 Verneuil, E. de, and Barrande, J. 1855. Description des fossiles trouvés dans les terrains  
36 Silurien et Dévonien d’Almadén, d’une partie de la Sierra Morena et des Montagnes  
37 6583 de Tolède. *Bulletin de la Société Géologique de France*, (II) 12, 964-1025.  
38  
39 6584  
40  
41 6585 Vidal, M., Dabard, M.P., Gourvenec, R., Le Hérissé, A., Loi, A., Paris, F., Plusquellec, Y.  
42 and Racheboeuf, P.R. 2011. Le Paléozoïque de la presqu’île de Crozon, Massif  
43 6586 Armoricaïn (France). *Géologie de la France*, 1, 3-45. [https://hal-insu.archives-](https://hal-insu.archives-ouvertes.fr/insu-00664523)  
44 6587 [ouvertes.fr/insu-00664523](https://hal-insu.archives-ouvertes.fr/insu-00664523).  
45  
46 6588  
47  
48  
49 6589 Villaseca, C., Ruiz-Martínez, V.C. and Pérez-Soba, C. 2017. Magnetic susceptibility of  
50 Variscan granite-types of the Spanish Central System and the redox state of magma.  
51 6590 *Geologica Acta*, 15 (4), 379-394. <https://doi.org/10.1344/GeologicaActa2017.15.4.8>.  
52  
53 6591  
54  
55 6592 Villeneuve, M. 2005. Paleozoic basins in West Africa and the Mauritanide thrust belt. *Journal*  
56 of African Earth Sciences, 43, 166-195.  
57 6593  
58  
59  
60  
61  
62  
63  
64  
65

- 6594 Villeneuve, M., Gärtner, A., Youbi, N., El Archi, A., Vernhet, E., Rjimati, E.C., Linnemann,  
1 6595 U., Bellon, H., Gerdes, A., Guillou, O., Corsini, M. and Paquette, J.L. 2015. The  
2 6596 southern and central parts of the “Souttoufide” belt, Northwest Africa. *Journal of*  
3 6597 *African Earth Sciences*, 112, 451-470.  
4 6598 <http://dx.doi.org/10.1016/j.jafrearsci.2015.04.016>.
- 9 6599 Vogel, D.E. 1967. Petrology of an eclogite -and pyrigarnite- bearing polymetamorphic rock  
10 6600 Complex at Cabo Ortegal, NW Spain. *Leidse Geologische Mededelingen*, 40, 121-  
11 6601 213.
- 15 6602 von Raumer, J.F. and Neubauer, F. 1993. Late Precambrian and Paleozoic evolution of the  
16 6603 Alpine basement - An overview. In: von Raumer, J.F. and Neubauer, F. (Eds.), *Pre-*  
17 6604 *Mesozoic geology in the Alps*. Springer, Berlin, 625-639.
- 21 6605 von Raumer, J.F. and Stampfli, G.M. 2008. The birth of the Rheic Ocean – Early Palaeozoic  
22 6606 subsidence patterns and subsequent tectonic plate scenarios. *Tectonophysics*, 461, 9-  
23 6607 20. <https://doi.org/10.1016/j.tecto.2008.04.012>.
- 27 6608 von Raumer, J.F., Ménot, R.P., Abrecht, J. and Biino, G. 1993. The Pre-Alpine evolution of  
28 6609 the External Massifs. In: von Raumer, J.F. and Neubauer, F. (Eds.), *Pre-Mesozoic*  
29 6610 *geology in the Alps*. Springer, Berlin, 221-240.
- 33 6611 von Raumer, J.F., Finger, F., Veselá, P. and Stampfli, G.M. 2014. Durbachites-Vaugnerites –  
34 6612 a geodynamic marker in the central European Variscan orogen. *Terra Nova*, 26 (2),  
35 6613 85-95. <https://doi.org/10.1111/ter.12071>.
- 39 6614 Wegener, A. 1929. *Die Entstehung der Kontinente und Ozeane*. Vieweg, Braunschweig.
- 42 6615 Weil, A.B. 2006. Kinematics of orocline tightening in the core of an arc: Paleomagnetic  
43 6616 analysis of the Ponga Unit, Cantabrian Arc, northern Spain. *Tectonics*, 25, 1-23,  
44 6617 TC3012. <https://doi.org/10.1029/2005TC001861>.
- 48 6618 Weil, A., Gutiérrez-Alonso, G. and Conan, J. 2010. New time constraints on lithospheric-  
49 6619 scale oroclinal bending of the Ibero-Armorican Arc: a palaeomagnetic study of earliest  
50 6620 Permian rocks from Iberia. *Journal of the Geological Society, London*, 167, 127-143.  
51 6621 <https://doi.org/10.1144/0016-76492009-002>.
- 55 6622 Weil, A.B., Gutiérrez-Alonso, G. and Wicks, D. 2012. Investigating the kinematics of local  
56 6623 thrust sheet rotation in the limb of an orocline: a paleomagnetic and structural analysis

- 6624 of the Esla tectonic unit, Cantabrian-Asturian Arc, NW Iberia. *International Journal of*  
1  
26625 *Earth Sciences*, 102 (1), 43-60. <https://doi.org/10.1007/s00531-012-0790-3>.
- 3  
46626 Wendt, J. 1985. Disintegration of the continental margin of northwestern Gondwana: Late  
5  
66627 Devonian of the eastern Anti-Atlas (Morocco). *Geology*, 13, 815-818.
- 7  
86628 Wendt, J., Kaufmann, B. and Belka, Z. 2001. An exhumed Palaeozoic underwater scenery:  
9  
106629 the Visean mud mounds of the eastern Anti-Atlas (Morocco). *Sedimentary Geology*,  
11  
126630 145, 215-233.
- 13  
146631 Will, T.M. and Schmädicke, E. 2001. A first report of retrogressed eclogites in the Odenwald  
15  
166632 Crystalline Complex: evidence for high-pressure metamorphism in the Mid-German  
17  
186633 Crystalline Rise, Germany. *Lithos*, 59, 109-125.
- 19  
206634 Will, T.M. and Schmädicke, E. 2003. Isobaric cooling and anti-clockwise PT paths in the  
21  
226635 Variscan Odenwald Crystalline Complex. *Journal of Metamorphic Geology*, 21, 469-  
23  
246636 480.
- 25  
266637 Will, T.M., Schulz, B. and Schmädicke, E. 2017. The timing of metamorphism in the  
27  
286638 Odenwald-Spessart basement, Mid-German Crystalline Zone. *International Journal of*  
29  
306639 *Earth Sciences*, 106, 1631-1649. <https://doi.org/10.1007/s00531-016-1375-3>.
- 31  
326640 Winchester, J.A., Floyd, P.A., Chocyk, M., Horbowy, K. and Kozdroj, W. 1995.  
33  
346641 Geochemistry and tectonic environment of Ordovician meta-igneous rocks in the  
35  
366642 Rudawy Janowickie Complex, SW Poland. *Journal of the Geological Society, London*,  
37  
386643 152 (1), 105-115.
- 39  
406644 Wood, D.S. 1974. Current views of the development of slaty cleavage. *Annual Review of*  
41  
426645 *Earth and Planetary Sciences*, 2, 369-401.
- 43  
446646 Woodcock, N.H., Soper, N.J. and Strachan, R.A. 2007. A Rheic cause for the Acadian  
45  
466647 deformation in Europe. *Journal of the Geological Society, London*, 164, 1023-1036.
- 47  
486648 Wyns, R., Lardeux, H. and Weyant, M., 1989. Présence de Dévonien dans le Groupe de  
49  
506649 Réaumur (synclinal de Chantonnay, Vendée). Conséquence sur l'évolution  
51  
526650 géodynamique de la Vendée. *Comptes Rendus de l'Académie des Sciences, Paris, II-*  
53  
546651 308, 855-860.
- 55  
566652 Young, T.P. 1990. Ordovician sedimentary facies and faunas of Southwest Europe:  
57  
586653 palaeogeographic and tectonic implications. In: McKerrow, W.S. and Scotese, C.R.

- 6654 (Eds.), *Palaeozoic Palaeogeography and Biogeography*. Geological Society, London,  
1  
2 6655 Memoir 12, 421-430.  
3
- 4 6656 Žáčová, E. Konopásek, J., Jeřábek, P., Finger, F. and Košler, J. 2010. Early carboniferous  
5  
6 6657 blueschist-facies metamorphism in metapelites of the West Sudetes (Northern  
7  
8 6658 Saxothuringian Domain, Bohemian Massif). *Journal of Metamorphic Geology*, 28,  
9  
10 6659 361-379.
- 11  
12 6660 Žák, J., Holub, F.V. and Verner, K. 2005. Tectonic evolution of a continental magmatic arc  
13  
14 6661 from transpression in the upper crust to exhumation of mid-crustal orogenic root  
15  
16 6662 recorded by episodically emplaced plutons: the Central Bohemian Plutonic Complex  
17 6663 (Bohemian Massif). *International Journal of Earth Sciences*, 94, 385-400.  
18
- 19  
20 6664 Žák, J., Verner, K., Sláma, J., Kachlík, V. and Chlupáčová, M. 2013 Multistage magma  
21  
22 6665 emplacement and progressive strain accumulation in the shallow-level Krkonoše–  
23 6666 Jizera plutonic complex, Bohemian Massif. *Tectonics*, 32, 1493-1512.  
24
- 25  
26 6667 Žák, J., Verner, K., Janoušek, V., Holub, F.V., Kachlík, V., Finger, F., Hajná, J., Tomek, F.,  
27  
28 6668 Vondrovic, L. and Trubač, J. 2014. A plate-kinematic model for the assembly of the  
29  
30 6669 Bohemian Massif constrained by structural relationships around granitoid  
31  
32 6670 plutons. In: Schulmann, K., Martínez Catalán, J.R., Lardeaux, J.M., Janousek, V. and  
33 6671 Oggiano, G. (Eds.), *The Variscan Orogeny: Extent, Timescale and the Formation of*  
34  
35 6672 *the European Crust*. Geological Society, London, Special Publication 405, 169-196.  
36  
37 6673 <https://doi.org/10.1144/SP405.9>.  
38
- 39 6674 Závada, P., Schulmann, K., Racek, M., Hasalová, P., Jeřábek, P., Weinberg, R.F., Štípská, P.  
40  
41 6675 and Alice Roberts, A. 2018. Role of strain localization and melt flow on exhumation  
42  
43 6676 of deeply subducted continental crust. *Lithosphere*, 10 (2), 217-238.  
44  
45 6677 <https://doi.org/10.1130/L666.1>.  
46
- 47 6678 Závada, P., Štípská, P., Hasalová, P., Racek, M., Jeřábek, P., Schulmann, K., Kylander-  
48  
49 6679 Clarke, A. and Holder, R. 2021. Monazite geochronology in melt-percolated UHP  
50  
51 6680 meta-granitoids: An example from the Erzgebirge continental subduction wedge,  
52  
53 6681 Bohemian Massif. *Chemical Geology*, 559. 119919.  
54
- 55 6682 Zeck, H.P. and Williams, I.S. 2001. Hercynian metamorphism in nappe core complexes of the  
56  
57 6683 Alpine Betic-Rif Belt, Western Mediterranean – a SHRIMP zircon study. *Journal of*  
58  
59 6684 *Petrology*, 42, 1373-1385.  
60  
61  
62  
63  
64  
65

- 6685 Zeck, H.P. and Whitehouse, M.J. 2002. Repeated age resetting in zircons from Hercynian-  
 1 6686 Alpine polymetamorphic schists (Betic-Rif tectonic belt, S Spain) – a U-Th-Pb ion  
 2 6687 microprobe study. *Chemical Geology*, 182, 275-292.  
 3  
 4  
 5  
 6 6688 Zeck, H.P., Whitehouse, M.J. and Ugidos, J.M. 2007a. 496±3 Ma zircon ion microprobe age  
 7 6689 for pre-Hercynian granite, Central Iberian Zone, NE Portugal (earlier claimed 618±9  
 8 6690 Ma). *Geological Magazine*, 144 (1), 21-31.  
 9 6691 <https://doi.org/10.1017/S0016756806002718>.  
 10  
 11  
 12  
 13 6692 Zeck, H.P., Wingate, M.T.D. and Pooley, G. 2007b. Ion microprobe U–Pb zircon  
 14 6693 geochronology of a late tectonic granitic-gabbroic rock complex within the Hercynian  
 15 6694 Iberian belt. *Geological Magazine*, 144, 157-177.  
 16  
 17  
 18  
 19 6695 Zeh, A. and Gerdes, A. 2010. Baltica- and Gondwana-derived sediments in the Mid-German  
 20 6696 Crystalline Rise (Central Europe): Implications for the closure of the Rheic ocean.  
 21 6697 *Gondwana Research*, 17, 254-263. <https://doi.org/10.1016/j.gr.2009.08.004>.  
 22  
 23  
 24  
 25 6698 Zeh, A. and Will, T. 2010. The Mid-German Crystalline Zone. In: Linnemann, U. and Romer,  
 26 6699 R.L. (Eds.), *Pre-Mesozoic Geology of Saxo-Thuringia - From the Cadomian Active  
 27 6700 Margin to the Variscan Orogen*. Stuttgart, 195-220.  
 28  
 29  
 30  
 31 6701 Zehnder, A.T. and Allmendinger, R.W. 2000. Velocity field for the trishear model. *Journal of  
 32 6702 Structural Geology*, 22 (8), 1009-1014.  
 33  
 34  
 35  
 36 6703 Zulauf, G., Bues, C., Dörr, W. and Vejnar, Z. 2002. 10 km Minimum throw along the West  
 37 6704 Bohemian shear zone: Evidence for dramatic crustal thickening and high topography  
 38 6705 in the Bohemian Massif (European Variscides). *International Journal of Earth  
 39 6706 Sciences*, 91, 850-864. <https://doi.org/10.1007/s00531-001-0250-y>.  
 40  
 41  
 42  
 43  
 44  
 45

## Figure captions

- 46 6708  
 47  
 48  
 49 6709  
 50  
 51 6710 **Fig. 1.** Sketch of the Variscan belt in an early Permian reconstruction that postdates ductile  
 52 6711 and brittle transcurrence. **Zones (Z):** CZ, Cantabrian; CIZ, Central Iberian (OVD, Obejo-  
 53 6712 Valsequillo Domain); GTMZ, Galicia-Trás-os-Montes; MSZ, Moravo-Silesian; MZ,  
 54 6713 Moldanubian; OMZ, Ossa-Morena; RHZ, Rhenohercynian; SPZ, South Portuguese; STZ,  
 55 6714 Saxo-Thuringian; TBZ, Teplá-Barrandian; WALZ, West Asturian-Leonese. Armorican  
 56 6715 Domains (AD): CAD, Central; NAD, North; SAD, South; MM: Moroccan Meseta (AA, Anti-  
 57  
 58  
 59  
 60  
 61  
 62  
 63  
 64  
 65

6716 Atlas; CB, Coastal Block; EM, Eastern Meseta; SB, Sehoul Block; WM, Western Meseta).  
 1  
 26717 **Shear zones (SZ), faults (F) and fault zones (FZ):** BBSZ, Baden-Baden; BCSZ, Badajoz-  
 3  
 46718 Córdoba; BrF: Bray; EFZ, Elbe; JPSZ, Juzbado-Penalva; LLSZ, Lalaye-Lubine; MMFZ,  
 56719 Middle Meseta; MT, Moldanubian Thrust; NASZ, North Armorican; NEF, Nort-sur-Erdre;  
 6  
 76720 NPF, North Pyrenean; PASZ, Posada-Asinara; PTSZ, Porto-Tomar; SAF, South Atlas; SASZ,  
 8  
 96721 South Armorican (N and S, northern and southern branches); SHF, Sillon Houiller; SIF, South  
 10  
 116722 Iberia; SISZ, Southern Iberian; SMF, South Meseta; TTZ, Teisseyre-Tornquist Zone; VF,  
 12  
 136723 Variscan Front; WMSZ, Western Meseta. **Arcs (A):** BA, Bohemian; CIA, Central Iberian;  
 14  
 156724 EMA, Eastern Meseta; IAA, Ibero-Armorican; MCA, Massif Central. **Other:** BAU, Beja-  
 166725 Acebuches Unit; BM, Basque Massifs; Bu, Buçaco; Co, Corsica; Cr, Crozon. FMC, French  
 17  
 186726 Massif Central; LC, Lizard Complex; MTM, Maures-Tanneron Massif; MGCH, Mid-German  
 19  
 206727 Crystalline High; MN, Montagne Noire; Sa, Sardinia; SWM, Schwarzwald Massif; VM,  
 21  
 226728 Vosges Massif.

23  
 246729  
 25  
 266730 **Fig. 2. (a)** Geological map of the Iberian Peninsula showing the Variscan massifs and the  
 27  
 286731 zones of the Iberian Massif, continued into the Pyrenees, Iberian Chain and Catalonia Coast  
 29  
 306732 Ranges. Based on the Geological map of Spain and Portugal to scale 1:1000 000 (IGME-  
 31  
 326733 LNEG, 2015) and in Martínez Catalán (2012). The most important structures are shown,  
 33  
 346734 including early and late folds, thrust faults, and the main ductile strike-slip shear zones. **(b)**  
 35  
 366735 Detail of the geology of the Galicia allochthonous complexes showing the distribution of the  
 37  
 386736 three Allochthons and the Parautochthon. **(c)** Detail of the geology of the Portuguese  
 396737 allochthonous complexes. **Zones (Z):** CZ, Cantabrian; CIZ, Central Iberian; GTMZ, Galicia-  
 40  
 416738 Trás-os-Montes; OMZ, Ossa-Morena; SPZ, South Portuguese; WALZ, West Asturian-  
 42  
 436739 Leonese. **Domains of the CIZ (D):** DRF, of Recumbent Folds; DUF, of Upright Folds; OSD,  
 44  
 456740 Ollo de Sapo; OVD, Obejo-Valsequillo; SGD, Schist-Greywacke. **Allochthonous**  
 46  
 476741 **complexes:** B, Bragança; CO, Cabo Ortegal; M, Morais; MT, Malpica-Tui; O, Órdenes.  
 48  
 496742 **Other units:** BAU, Beja-Acebuches; CU, Central Unit; EAMB, Évora-Aracena Metamorphic  
 506743 Belt; NSSB, Northern Sierra de Sevilla Batholith; PL, Pulo do Lobo Unit. **Shear zones (SZ)**  
 51  
 526744 **and faults (F):** BCSZ, Badajoz-Córdoba; JPSZ, Juzbado-Penalva; NPF, North Pyrenean;  
 53  
 546745 PTSZ, Porto-Tomar; SISZ, Southern Iberian. **Arcs (A):** CIA, Central Iberian; IAA, Ibero-  
 55  
 566746 Armorican. **Pyrenees:** AZ, Axial Zone; NM, Northern Massifs; Basque Massifs: CV, Cinco  
 57  
 586747 Villas; QR, Quinto Real; UB, Ursuya-Baygura. **Balearic Islands:** Ma, Majorca; Me,



Menorca; Ib, Ibiza. **Allochthonous groups:** LA, Lower Allochthon; MA, Middle Allochthon; PA, Parautochthon; UA, Upper Allochthon (IP, Intermediate-P; HP-HT, High-P/High-T).

**Fig. 3.** Cross sections representative of the structure of the Iberian Massif including the Variscan sutures. **(a)** Northwest Iberian section A-A', modified from Martínez Catalán et al. (2014). **(b)** Central Iberian section B-B', based on Martínez Poyatos et al. (2012). **(c)** Southwest Iberian section C-C', based on Simancas et al. (2003) and partly on Rubio Pascual et al. (2013b). The sections are built from field geology and partly using deep seismic reflection profiles. For section A-A', these are ESCIN-1 (Pérez-Estaún et al., 1994, 1995), ESCIN-3.2 (Álvarez-Marrón, 1995, 1996) and ESCIN-3.3 (Martínez Catalán et al., 1995; Ayarza et al., 1998). The two latter were acquired offshore, while section A-A' derives from onshore geology. In the parts of section A-A' roughly corresponding to these two profiles, (GTMZ, CIZ and WALZ), the seismic reflections have been placed approximately. Section B-B' roughly follows the seismic line ALCUDIA (Martínez Poyatos et al., 2012). Section C-C' follows the seismic line IBERSEIS (Simancas et al., 2003). Whrench faults are continued at depth avoiding to cross low-dipping reflections. Colors corresponding to zones or groups are superposed to frames or grey shades indicating lithologies or units. **Zones (Z):** CZ, Cantabrian; CIZ, Central Iberian; GTMZ, Galicia-Trás-os-Montes; OMZ, Ossa-Morena; SPZ, South Portuguese; WALZ, West Asturian-Leonese. **Domains of the CIZ (D):** DRF, of Recumbent Folds; DUF, of Upright Folds; OSD, Ollo de Sapo; OVD, Obejo-Valsequillo; SGD, Schist-Greywacke. **Other units:** BAU, Beja-Acebuches; EAMB, Évora-Aracena Metamorphic Belt; IRB, Iberian Reflective Body. **Other:** Upper Allochthon: IP, Intermediate-P; HP-HT, High-P/High-T. See Figure 2 for location of the sections.

**Fig. 4.** Geological map of the French and related Variscan Massifs. Based on the Geological map of France to scale 1:1 000 000 (BRGM, 1996), and in Faure et al. (2009), Ballèvre et al. (2014), and Lardeaux et al. (2014). **Zones (Z):** MZ, Moldanubian; RHZ, Rhenohercynian; STZ, Saxothuringian; WALZ, West Asturian-Leonese; **Armorican Domains (AD):** CAD, Central; NAD, North; SAD, South. **Shear zones (SZ) and faults (F):** BBSZ, Baden-Baden; BrF: Bray; GCF, Granville-Cancalle; LLSZ, Lalaye-Lubine; NASZ, North Armorican; NEF, Nort-sur-Erdre; NPF, North Pyrenean; SASZ, South Armorican (N and S, northern and southern branches); SHF, Sillon Houiller. **Arms (A):** MCA, Massif Central. **Pyrenees:** AZ,

6780 Axial zone; NM, Northern massifs; Basque Massifs: CV, Cinco Villas; QR, Quinto Real; UB,  
 1  
 2 6781 Ursuya-Baygura. **Other:** Au, Audierne Bay Complex; BC, Bois-de-Cené Unit; Bv, Brévenne  
 3  
 4 6782 Unit; Cé, Cévennes; Ch, Champtoceaux Complex; ChO, Chamrousse Ophiolite; ChS,  
 5  
 6 6783 Chantonay Syncline; Co, Corsica; EmA, External Massifs of the Alps (AaM, Aar; ArM,  
 7  
 8 6784 Argentera; BeM, Belledonne; MBM, Mont Blanc); Es, Essarts Unit; GN, Giessen Nappe; IG,  
 9  
 10 6785 Ile-de-Groix; LC, Lizard Complex; LiO, Limousin ophiolite; Ln, Léon; Ly, Lyonnais; MTM,  
 11  
 12 6786 Maures-Tanneron Massif; MGCH, Mid-German Crystalline High; MN, Montagne Noire; Mo,  
 13  
 14 6787 Morvan Arc; Ms, Mauges Unit; Nj, Najac Massif; Od, Odenwald Massif; Ru, Ruhla Massif;  
 15  
 16 6788 SG, St. Georges-sur-Loire Unit; Sp, Spessart Massif; SWM, Schwarzwald Massif; TA, Tuffs  
 17  
 18 6789 Anthracifères; TP, Thiviers-Payzac Unit; VD, Velay Dome; VM, Vosges Massif.

19 6790  
 20  
 21 6791 **Fig. 5.** Cross sections representative of the structure of the French Variscan massifs. **(a)**  
 22  
 23 6792 Armorican section A-A'', including the Mid-Variscan suture in the southern part. **(b)** Western  
 24  
 25 6793 Massif Central section B-B'. **(c)** Eastern Massif Central section C-C''. The sections are built  
 26  
 27 6794 from field geology, based on the Geological map of France to scale 1:1 000 000 (BRGM,  
 28  
 29 6795 1996), and on geological sections by Ledru et al. (1994b), Faure et al. (2009), Ballèvre et al.  
 30  
 31 6796 (2014), and Lardeaux et al. (2014). Section A-A'' follows the trace of seismic reflection  
 32  
 33 6797 profiles ARMOR 2 South and 2 North (Bitri et al., 2003, 2010), AR2, AR1 and SWAT 10  
 34  
 35 6798 (Bitri et al., 2001), whose interpretations have been included. For the Central Armorican  
 36  
 37 6800 Domain, reflections from the Brittany Wide Angle Reflection Profile (BWARF; Matte and  
 38  
 39 6801 Hirn, 1988) separated c. 100 km to the east, have been projected into the section. Whrench  
 40  
 41 6802 faults are continued at depth avoiding to cross low-dipping reflections. Colors corresponding  
 42  
 43 6803 to zones or groups are superposed to frames or grey shades indicating lithologies or units.  
 44  
 45 6804 **Armorican Domains (AD):** CAD, Central; NAD, North; SAD, South. **Shear zones (SZ)** and  
 46  
 47 6805 **faults (F):** CF, Combrailles; GCF, Granville-Cancalle; NASZ, North Armorican; NEF, Nort-  
 48  
 49 6806 sur-Erdre; OF, Ouzilly; SASZ, South Armorican (N and S, northern and southern branches);  
 50  
 51 6807 SLF, South Limousin. **Other:** FMC, French Massif Central; MN, Montagne Noire. Upper  
 52  
 53 6808 Allochthon: IP, Intermediate-P; HP-HT, High-P/High-T. See Figure 4 for location of the  
 54  
 55 6809 sections.

56  
 57 6810 **Fig. 6.** Geological map of the Bohemian Massif. Based on the Geological maps of Germany  
 58  
 59 6811 to scale 1:1 000 000 (BGR, 1993), and the Czech Republic to scale 1:500 000 (Czech  
 60  
 61  
 62  
 63  
 64  
 65

Geological Survey, 2007), and in Mazur and Aleksandrowski (2001), Franke and  
 Żelaźniewicz (2000, 2002), Schulmann et al. (2009, 2014), Zeh and Will (2010), Mazur et al.  
 (2015) and Martínez Catalán et al. (2019). **Zones (Z):** MZ, Moldanubian; MSZ, Moravo-  
 Silesian; NPhZ, Northern Phyllite; RHZ, Rhenohercynian; SPhZ, Southern Phyllite; STZ,  
 Saxothuringian; TBZ, Teplá-Barrandian. **Shear zones (SZ), faults (F) and fault zones (FZ):**  
 DF, Danube; EFZ, Elbe; FF, Franconian; ISF, Intra-Sudetic; MT, Moldanubian Thrust; OFZ,  
 Odra; PF, Pfahl; SBF, Sudetic Boundary. **Arcs (A):** BA, Bohemian. **Massifs and units:** BL,  
 Blanský les; Dr, Drosendorf; EB, Erzgebirge; EV, Erbenhof-Vohenstrauß; F, Frankenberg;  
 Gf, Gföhl; GS, Góry Sowie; HM, Harz Mountains; Ka, Kaczawa Complex; KH, Kutna Hora;  
 Kr, Krkonoše; LB, Lausitz Block; Mü, Münchberg; ML, Mariánské Lázně; NMe, Nové  
 Město; OS, Orlica-Šniežnik Dome; PS, Praha Syncline; SG, Saxonian Granulitebirge; SK,  
 South Krkonoše; SM, Staré Město; W, Wildenfels. **Other:** CBPC, Central Bohemian Plutonic  
 Complex; ISB, Intra-Sudetic Basin; MGCH, Mid-German Crystalline High; Ru, Ruhla; SBB,  
 South Bohemian Batholith; Sv, Svatka window; Th, Thaya window.

**Fig. 7.** Representative sections across the Bohemian Massif showing the crustal structure. **(a)**  
 Northern section A-A", based on Krawczyk et al. (2000), Schulmann and Gayer (2000),  
 Chopin et al. (2012) and Tomek et al. (2019). **(b)** Southern section B-B", based on Franke  
 (2000), Schulmann et al. (2005) and Guy et al. (2011). The sections are partly based on deep  
 seismic reflection profiles GRANU 9501 and 9502 (DEKORP, 1999; Krawczyk et al., 2000),  
 and 9HR (Chlupáčová and Švancara, 1994). The seismic profiles are more or less close to, but  
 do not coincide with the geological sections, and the reflections have been projected  
 approximately on them. Colors corresponding to zones or groups are superposed to frames or  
 grey shades indicating lithologies or units. **Zones (Z):** MZ, Moldanubian; MSZ, Moravo-  
 Silesian; NPhZ, Northern Phyllite; RHZ, Rhenohercynian; STZ, Saxothuringian; TBZ, Teplá-  
 Barrandian. See Figure 6 for location of the sections.

**Fig. 8.** Geological map of Variscan Morocco. Based on the Geological map of Europe and  
 Adjacent Areas to scale 1:5 000 000 (BGR, 2005), Michard et al. (2010a) and Ouanaimi et al.  
 (2016). **Zones (Z):** AA, Anti-Atlas; CB, Coastal Block; EM, Eastern Meseta; SB, Schoul  
 Block; WM, Western Meseta. **Shear zones (SZ), faults (F) and fault zones (FZ):** MMFZ,  
 Middle Meseta; RTFZ, Rabat-Tiflet; SAF, South Atlas; SMF, South Meseta; WMSZ,

6844 Western Meseta. **Arcs (A):** EMA, Eastern Meseta. **Other:** NZ, Nappe Zone; SMFr, South  
1  
2 6845 Meseta Front.

3  
4 6846  
5  
6 6847 **Fig. 9.** Correlation of zones, groups and units and of early Variscan and Variscan orogenic  
7  
8 6848 magmatism along the Variscan Belt. Only the main massifs are included, while small ones  
9  
10 6849 can generally be assimilated to nearby large ones. Colors and abbreviations are the same used  
11  
12 6850 in maps and sections.

13  
14 6851  
15  
16 6852 **Fig. 10.** Timing of early Variscan and Variscan events of the large massifs. The time interval  
17  
18 6853 spans 425-275 Ma. Small massifs are assumed to have similar evolutions as the massifs to  
19  
20 6854 which they are related in the text, and many of them are included in the figure. Bar colors and  
21  
22 6855 abbreviations are the same used in the maps, sections and text. The events related to  
23  
24 6856 subduction of the Rheic and Rhenohercynian oceans are given separated from those  
25  
26 6857 considered related with the building of the Mid-Variscan accretionary complex forming the  
27  
28 6858 Allochthon, their emplacement on the northern Gondwana Autochthon and the subsequent  
29  
30 6859 evolution of the ensemble.

31  
32 6860  
33  
34 6861 **Fig. 11.** Partial retrodeformation of brittle and ductile late orogenic deformation of the  
35  
36 6862 Variscan Belt. The start point is the late Carboniferous reconstruction shown in Figure 1.  
37  
38 6863 Black continuous lines represent faults not restored yet, while dashed lines represent faults  
39  
40 6864 whose translation was removed in the last step. **(a)** After removing displacement of the main  
41  
42 6865 late Variscan NW-SE faults (SIZ, NPF, BrF and EFZ). **(b)** The IAA has been partially  
43  
44 6866 unfolded. **(c)** Displacement of a large dextral shear zone equivalent to the PTSZ, NEF, LLSZ  
45  
46 6867 and BBSZ has been partially removed, and the IAA is shown at an incipient stage, as well as  
47  
48 6868 the BA. **(d)** Sinistral motion of the BCSZ and SISZ has been removed. **(e)** Early dextral  
49  
50 6869 motion along the NASZ and SASZ has been removed. **(f)** Internal deformation associated to  
51  
52 6870 ductile dextral megashear has been restored in the Allochthon, the CAD, EM, WM and the  
53  
54 6871 Mediterranean province, while the little deformed CB and NAD are tentatively placed to the  
55  
56 6872 south. Ductile restoration is indicated by homogeneous, sinistral simple shear with a shear  
57  
58 6873 angle of  $56.3^\circ$ , equivalent to a shear value  $\gamma = 1.5$ . **Zones (Z):** CZ, Cantabrian; CIZ, Central  
59  
60 6874 Iberian (OVD, Obejo-Valsequillo Domain); GTMZ, Galicia-Trás-os-Montes; MSZ, Moravo-  
61  
62 6875 Silesian; MZ, Moldanubian; OMZ, Ossa-Morena; RHZ, Rhenohercynian; SPZ, South

6876 Portuguese; STZ, Saxothuringian; TBZ, Teplá-Barrandian; WALZ, West Asturian-Leonese.  
 1  
 2 6877 Armorican Domains (AD): CAD, Central; NAD, North; SAD, South; MM: Moroccan Meseta  
 3  
 4 6878 (AA, Anti-Atlas; CB, Coastal Block; EM, Eastern Meseta; WM, Western Meseta). **Shear**  
 5 6879 **zones (SZ), faults (F) and fault zones (FZ):** BBSZ, Baden-Baden; BCSZ, Badajoz-Córdoba;  
 6  
 7 6880 BrF: Bray; EFZ, Elbe; LLSZ, Lalaye-Lubine; NEF, Nort-sur-Erdre; NPF, North Pyrenean;  
 8  
 9 6881 PTSZ, Porto-Tomar; SIF, South Iberia; SISZ, Southern Iberian; SMF, South Meseta. **Arcs**  
 10  
 11 6882 **(A):** BA, Bohemian; CIA, Central Iberian; EMA, Eastern Meseta; IAA, Ibero-Armorican;  
 12  
 13 6883 MCA, Massif Central. **Other:** Bu, Buçaco; Cr, Crozon.

14  
 15 6884  
 16  
 17 6885 **Fig. 12.** Evolution of the Variscan Belt in the context of Paleozoic plate dynamics. The main  
 18  
 19 6886 continental masses and the elements forming the Variscan Belt are shown in orthographic  
 20  
 21 6887 projection for different ages. Northern and eastern territories (Siberia, China, Indonesia) are  
 22  
 23 6888 omitted. For the late Cambrian and Lower Ordovician, a projection centered in the South Pole  
 24  
 25 6889 has been used. The geographic grid is drawn every 15°, with a thicker line for the Equator,  
 26  
 27 6890 and is fixed for the 500-470 and 400-290 Ma intervals. This figure was built using animations  
 28  
 29 6891 500.A97 and 470.A97 of GMap2015, the reconstruction geometries of Matthews et al. (2016)  
 30  
 31 6892 for GPlates, and the partial retrodeformation carried out in this work (Fig. 11). Blue lines  
 32  
 33 6893 indicate the location of sections in Figure 13 (dotted parts not shown). Note that the Mid-  
 34  
 35 6894 Variscan Allochthon represents the future Upper Allochthon until 400 Ma. Between 390 and  
 36  
 37 6895 360 Ma it progressively incorporated the Middle and Lower Allochthons and by 340 Ma also  
 38  
 39 6896 the Parautochthon.

40 6897  
 41  
 42 6898 **Fig. 13.** Proposed plate dynamics of the Variscan Belt depicted using cross-sections, the  
 43  
 44 6899 location of which is indicated by continuous blue lines in Figure 12. The sections vary for  
 45  
 46 6900 each time frame. They are located to cut across the Mid-Variscan Allochthon except at 370  
 47  
 48 6901 Ma, designed to highlight the role of the Silurian-Devonian arc. The late Variscan evolution  
 49  
 50 6902 related with transcurrent dextral shearing is not shown. In this figure, the three allochthons  
 51  
 52 6903 and the Parautochthon are depicted with the colors used in previous figures (maps, sections  
 53  
 54 6904 and correlations) to shown their progressive incorporation to the accretionary wedge and its  
 55  
 56 6905 thrusting onto the Autochthon during Variscan collision.

57 6906  
 58  
 59  
 60  
 61  
 62  
 63  
 64  
 65

**Fig. 14.** Late evolution of the Variscan Belt shown in three steps in relation with the relative position of Laurussia and Gondwana using the reconstruction of Matthews et al. (2016). The geographic grid is drawn every 15°, with a thicker line for the Equator. The Variscan Belt became progressively squeezed between the two mayor plates, as shown by the angle formed by two reference red lines. This angle decreases between 340 and 290 Ma imposing an internal deformation in the triangular area in between, comparable to the trishear kinematic model (Erslev, 1991). The dashed line at 340 Ma approximately represents the position of the parallel continuous line 20 Ma later if only translation had occurred. The curved dashed line at 290 Ma represents a realistic trace of the continuous straight line drawn in Laurussia at 340 Ma. Legend as in Figure 12.

6918

1  
2  
3  
4  
5  
6  
7  
8  
9  
10  
11  
12  
13  
14  
15  
16  
17  
18  
19  
20  
21  
22  
23  
24  
25  
26  
27  
28  
29  
30  
31  
32  
33  
34  
35  
36  
37  
38  
39  
40  
41  
42  
43  
44  
45  
46  
47  
48  
49  
50  
51  
52  
53  
54  
55  
56  
57  
58  
59  
60  
61  
62  
63  
64  
65

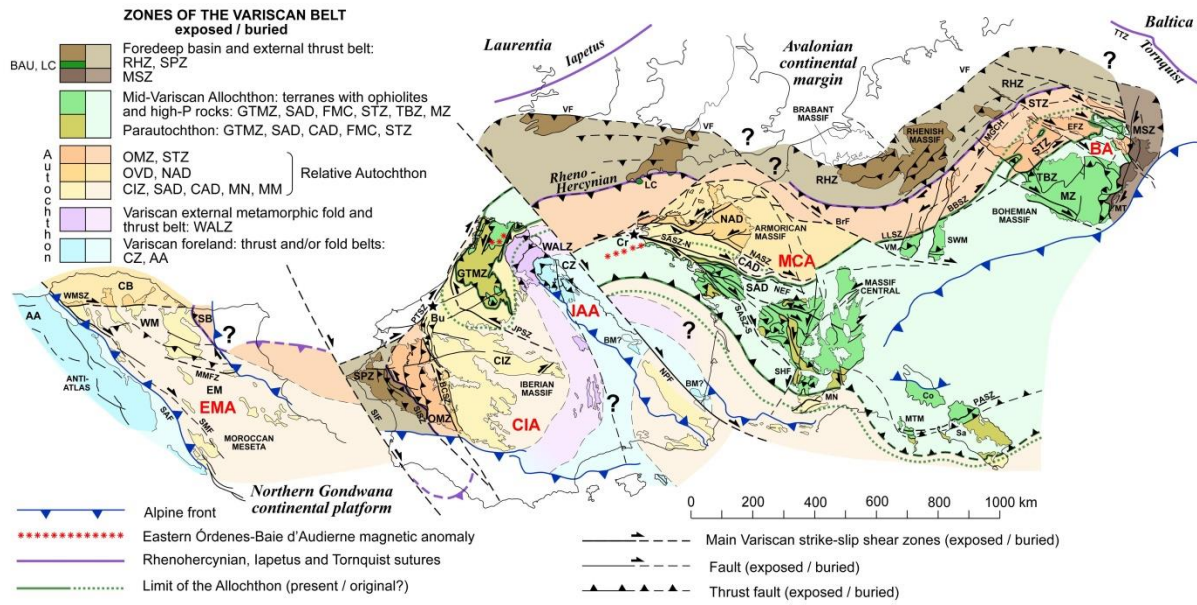


Fig. 1

6919

6920





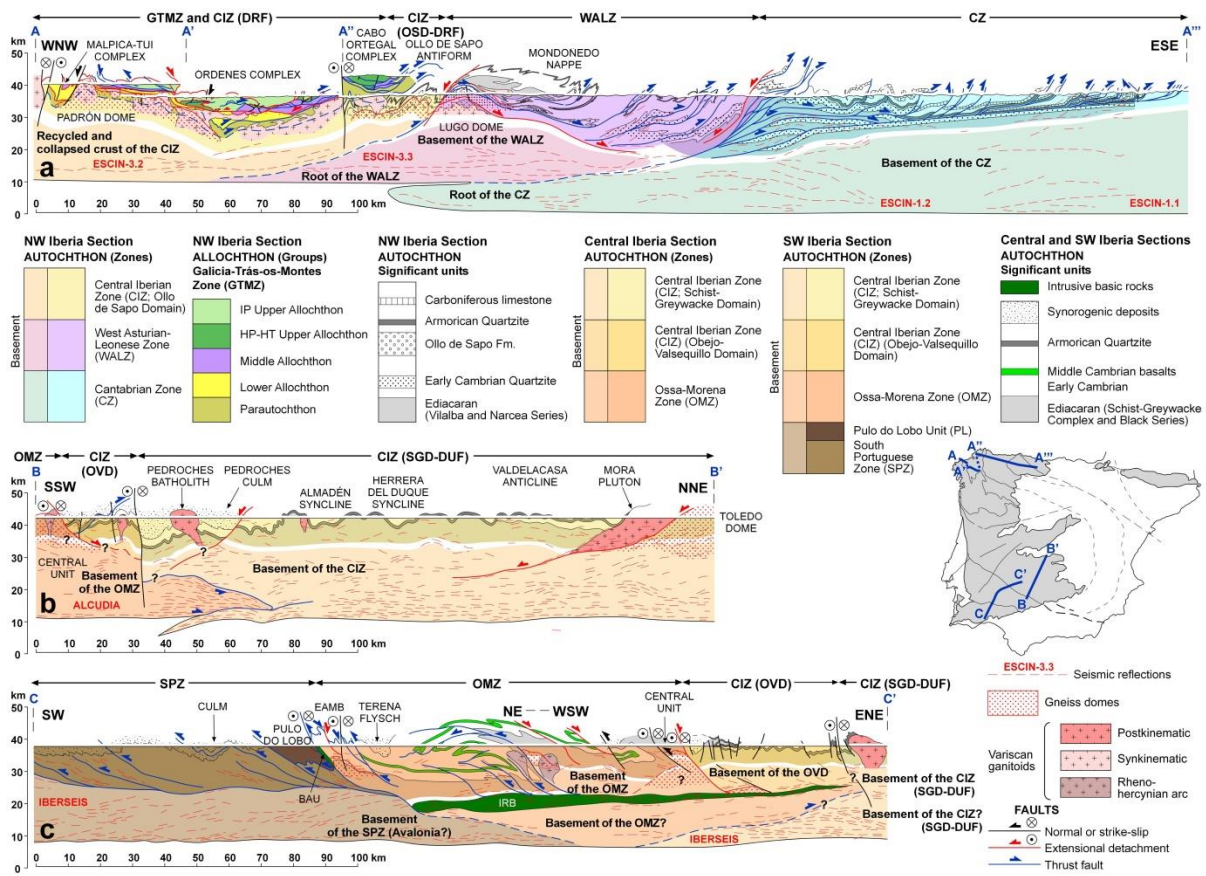
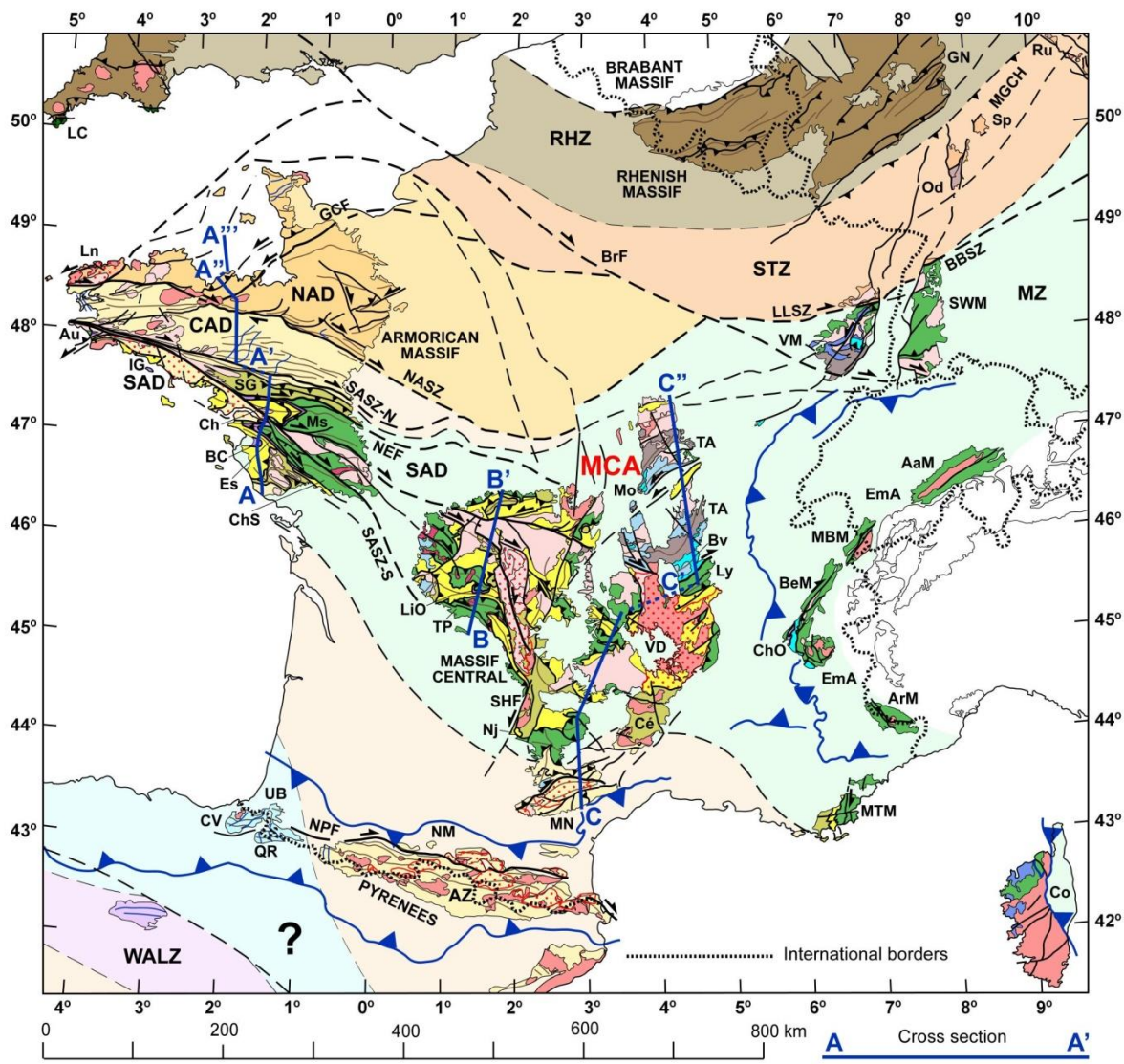


Fig. 3

6923

6924



Early folds     
  Thrust fault     
  Main strike-slip shear zones  
 Late folds     
  Other faults     
 Alpine fronts

**ZONES OF THE FRENCH AND RELATED MASSIFS (exposed / buried)**

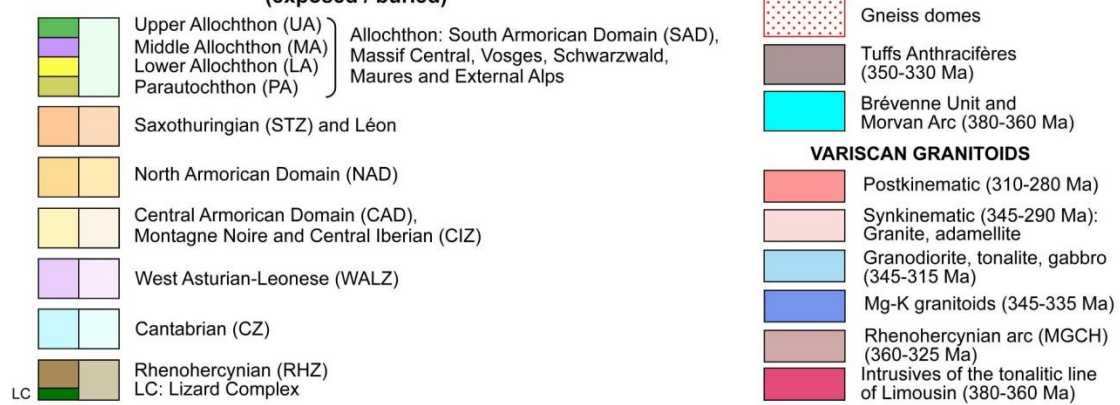


Fig. 4

6925

6926

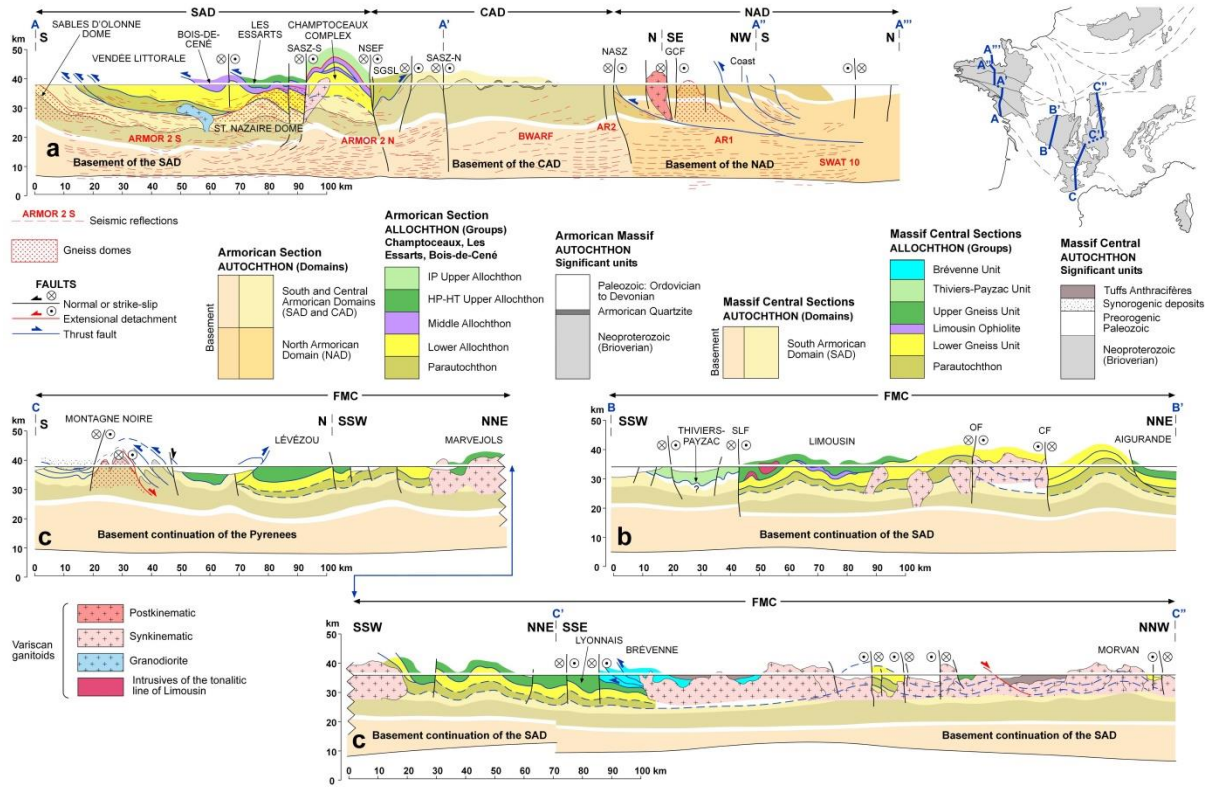


Fig. 5

6927

6928



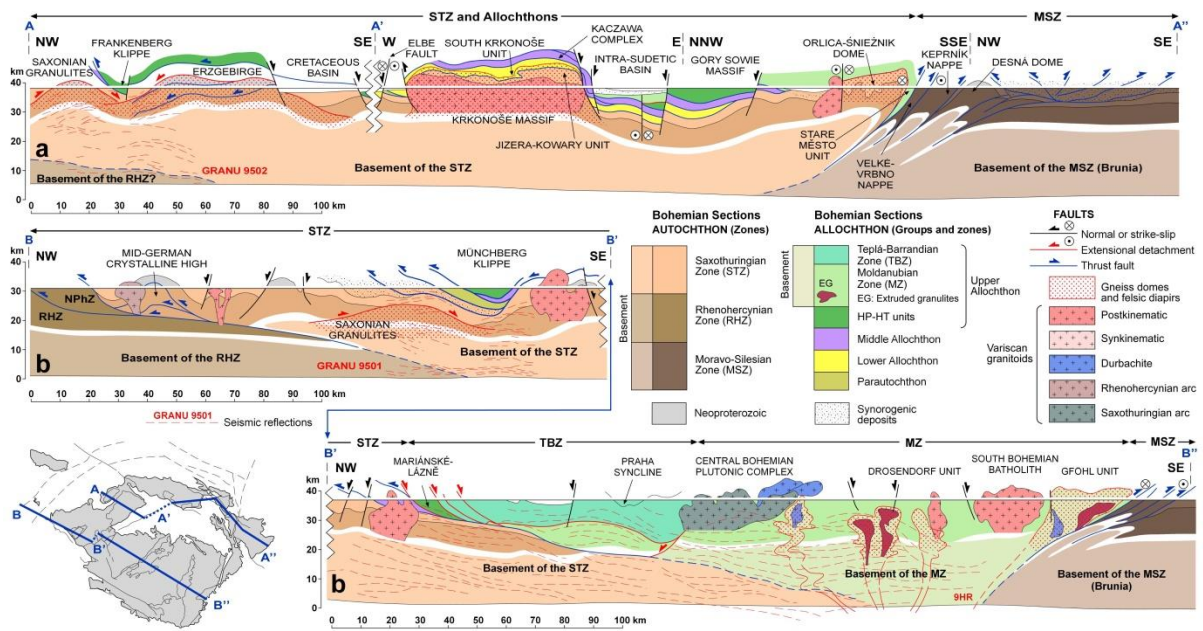


Fig. 7

6931

6932

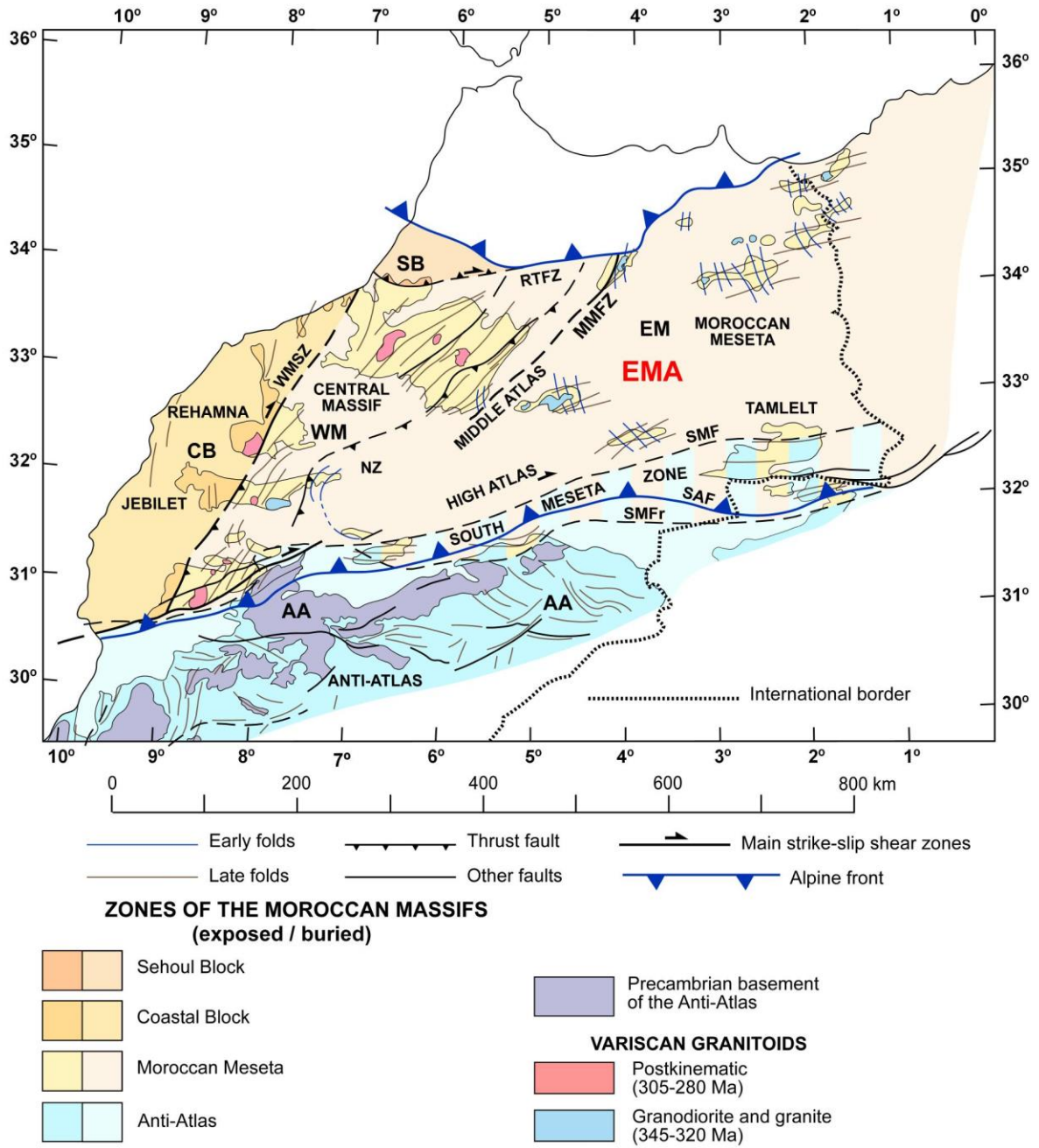


Fig. 8

6933

6934

Northern Morocco	Iberian Massif	Armorican Massif	French Massif Central	Bohemian Massif
	Galicía-Trás-os-Montes Zone IP Upper Allochthon	South Armorican Domain IP Upper Allochthon	Upper Gneiss Unit IP and LP metasediments	Teplá-Barrandian Zone Moldanubian Zone
	Galicía-Trás-os-Montes Zone HP-HT Upper Allochthon	South Armorican Domain HP-HT Upper Allochthon	Upper Gneiss Unit Leptyno-Amphibolitic Complex	Teplá-Barrandian Zone HP-HT Units Saxothuringian Zone Allochthonous HP-HT Units
	Galicía-Trás-os-Montes Zone Lower Devonian Middle Allochthon	South Armorican Domain Lower Devonian Middle Allochthon	Middle Allochthon Limousin Ophiolite	Saxothuringian Zone Prasinite Units Sudetic Silurian-Devonian Ophiolitic U.
	Galicía-Trás-os-Montes Zone Cambro-Ordovician Middle Allochthon	South Armorican Domain Cambro-Ordovician Middle Allochthon	Middle Allochthon Leptyno-Amphibolitic Complex	Saxothuringian Zone Sudetic Cambro-Ordovician Oceanic U.
	Galicía-Trás-os-Montes Zone Lower Allochthon	South Armorican Domain Lower Allochthon	Lower Gneiss Unit	Saxothuringian Zone Sudetic Lower Allochthon
	Galicía-Trás-os-Montes Zone Parautochthon	South Armorican D. Vendée littorale Central Armorican Domain St. Georges-sur-Loire Unit	Parautochthon	Saxothuringian Zone Münchenberg Parautochthon
Anti-Atlas	Cantabrian Zone			
Moroccan Meseta Eastern and Western Mesetas	West Asturian-Leonese Zone Central Iberian Zone	South Armor. Domain Autochthon Central Armorican Domain	Montagne Noire	
Coastal Block	Obejo-Valsequillo Domain	North Armorican Domain		
	Central Unit	Pays de Léon		Saxothuringian Zone Autochthon
Sehoul Block	Ossa-Morena Zone			
	South Portuguese Zone			Rhenohercynian Zone Moravo-Silesian Zone?

VARISCAN OROGENIC MAGMATISM	Northern Morocco	Iberian Massif	Armorican Massif	French Massif Central	Bohemian Massif
Postkinematic granitoids: heat input and melts partly derived from thinned mantle lithosphere	305-280 Ma WM, CB	310-285 Ma WALZ, CIZ, OMZ, GTMZ	310-285 Ma NAD, CAD, SAD	310-280 Ma FMC	310-300 Ma MZ
Synkinematic granitoids: related with crustal thickening, LP-HT metamorphism and extension Pink: peraluminous, S-type Blue: metaluminous, I-type	345-320 Ma EM, WM	322-305 Ma WALZ, CIZ, GTMZ	340-290 Ma NAD, CAD, SAD	345-310 Ma FMC, VM	335-310 Ma STZ, TBZ, MZ
	335-320 Ma EM, WM	347-320 Ma WALZ, CIZ, GTMZ		345-315 Ma N of FMC, VM	
Mg-K rich magmatism: partial melting of subducted lower crust or enriched subcontinental upper mantle		~340 Ma GTMZ		345-332 Ma VM	345-335 Ma MZ
Rhenohercynian arc: tholeiitic and calc-alkaline subduction of Rhenohercynian oceanic lithosphere		355-335 Ma OMZ, SPZ		350-330 Ma FMC, VM	370-325 Ma MGCH
Saxothuringian Arc: Subduction of Saxothuringian/ Mid-Variscan oceanic lithosphere			375-370 Ma SAD	380-360 Ma NW of FMC	380-360 Ma NE of FMC
Silurian-Devonian arc: Subduction of the Rheic Ocean	~370 Ma SB	~400 Ma SPZ	~390 Ma NAD		425-390 Ma MGCH

Fig. 9

6935

6936

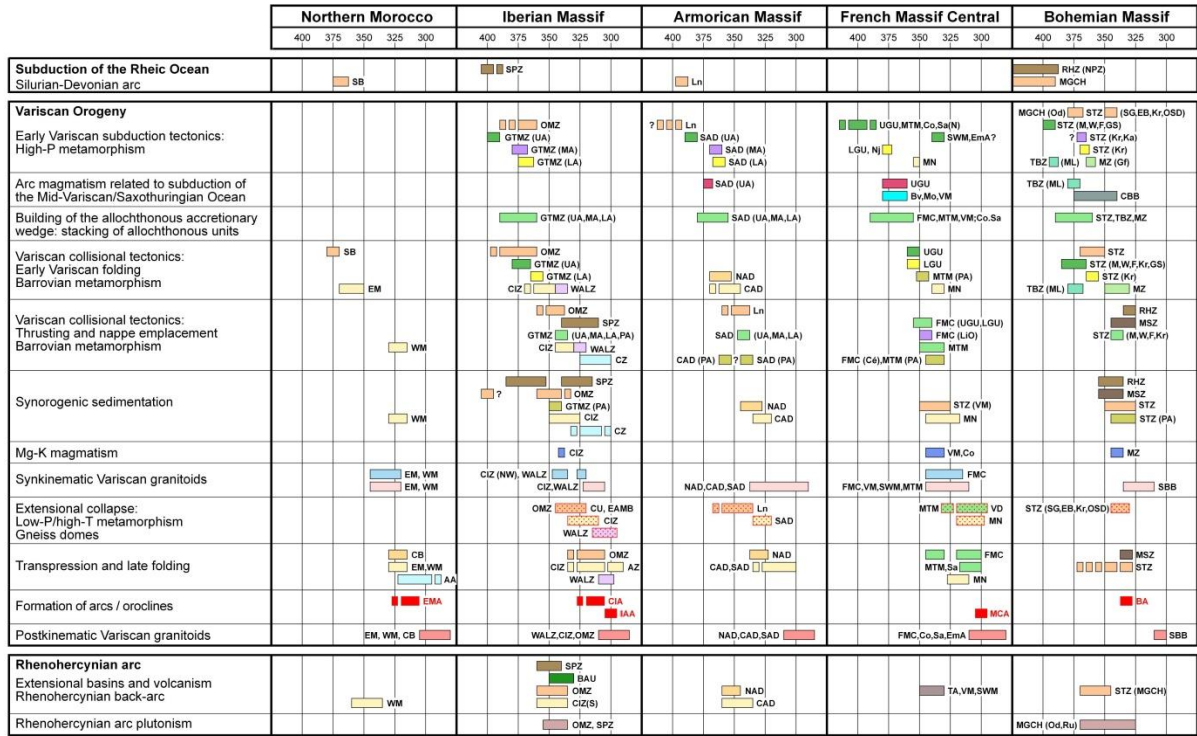


Fig. 10

6937

6938



1  
2  
3  
4  
5  
6  
7  
8  
9  
10  
11  
12  
13  
14  
15  
16  
17  
18  
19  
20  
21  
22  
23  
24  
25  
26  
27  
28  
29  
30  
31  
32  
33  
34  
35  
36  
37  
38  
39  
40  
41  
42  
43  
44  
45  
46  
47  
48  
49  
50  
51  
52  
53  
54  
55  
56  
57  
58  
59  
60  
61  
62  
63  
64  
65

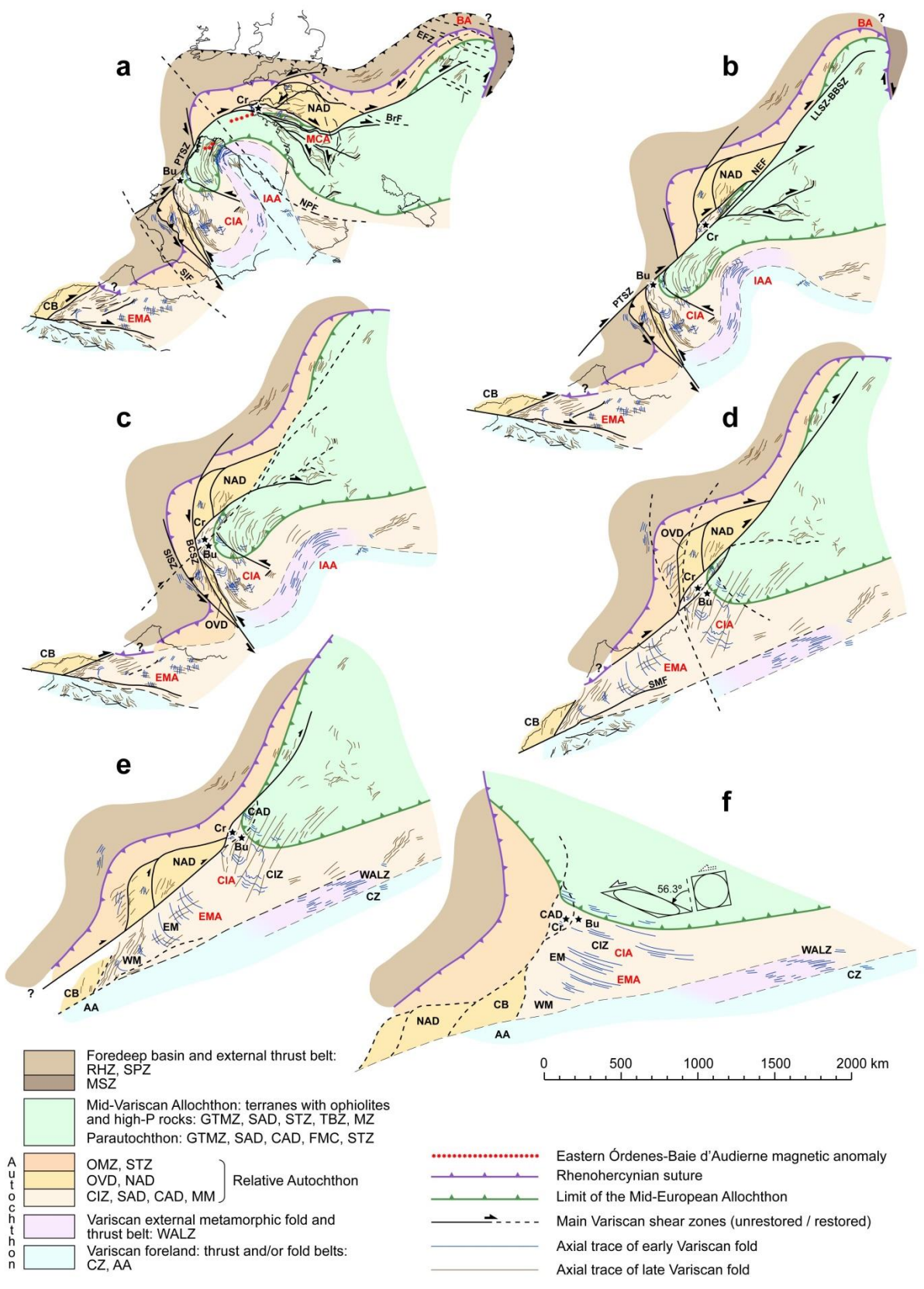


Fig. 11

6939

6940

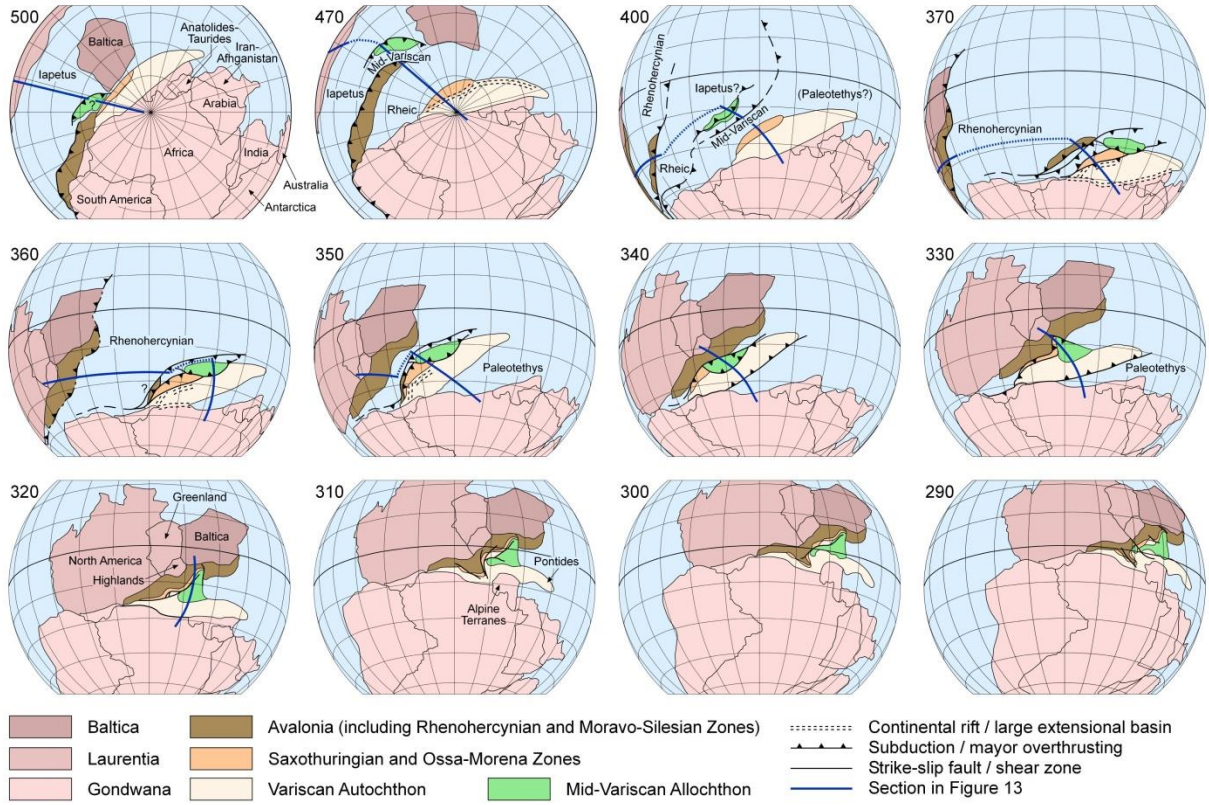


Fig. 12

1  
2  
3  
4  
5  
6  
7  
8  
9  
10  
11  
12  
13  
14  
15  
16  
17  
18  
19  
20  
21  
22  
23  
24  
25  
26  
27  
28  
29  
30  
31  
32  
33  
34  
35  
36  
37  
38  
39  
40  
41  
42  
43  
44  
45  
46  
47  
48  
49  
50  
51  
52  
53  
54  
55  
56  
57  
58  
59  
60  
61  
62  
63  
64  
65

6941  
6942

1  
2  
3  
4  
5  
6  
7  
8  
9  
10  
11  
12  
13  
14  
15  
16  
17  
18  
19  
20  
21  
22  
23  
24  
25  
26  
27  
28  
29  
30  
31  
32  
33  
34  
35  
36  
37  
38  
39  
40  
41  
42  
43  
44  
45  
46  
47  
48  
49  
50  
51  
52  
53  
54  
55  
56  
57  
58  
59  
60  
61  
62  
63  
64  
65

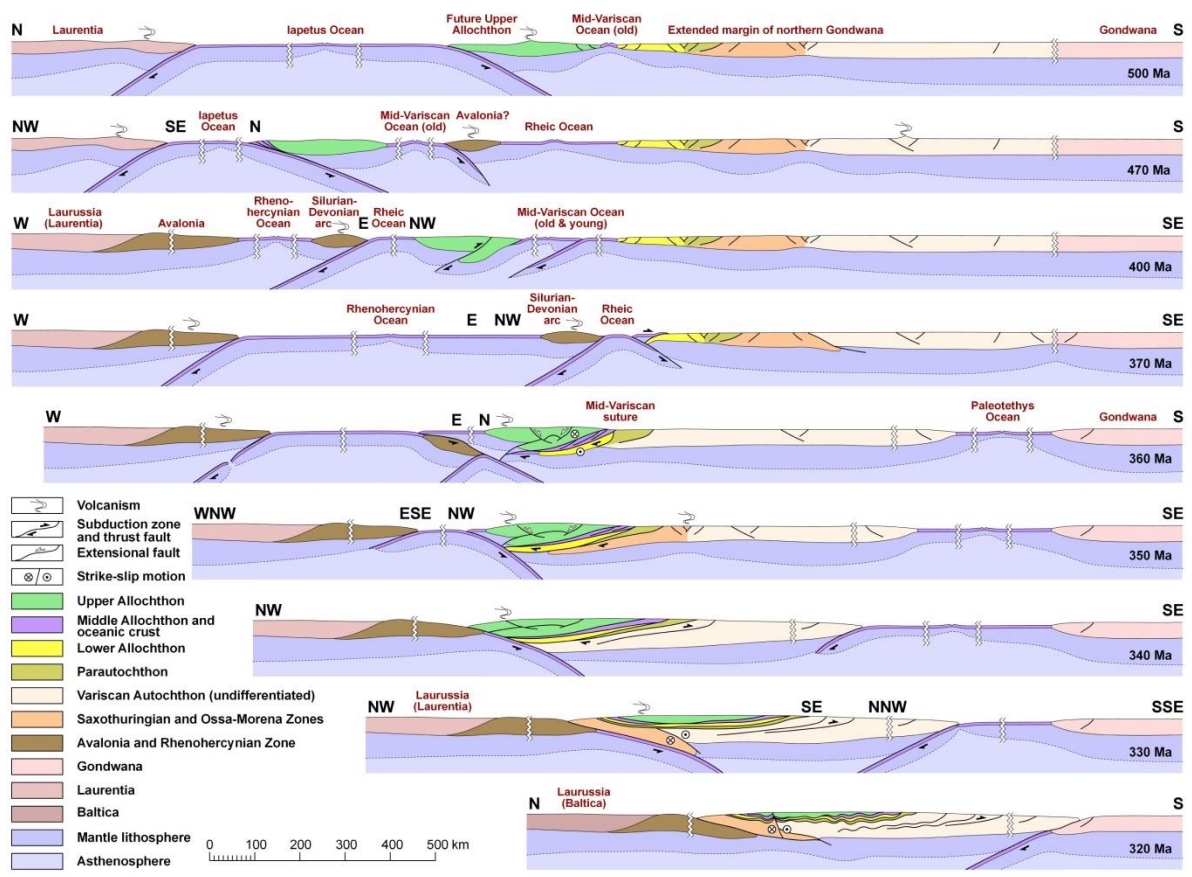


Fig. 13

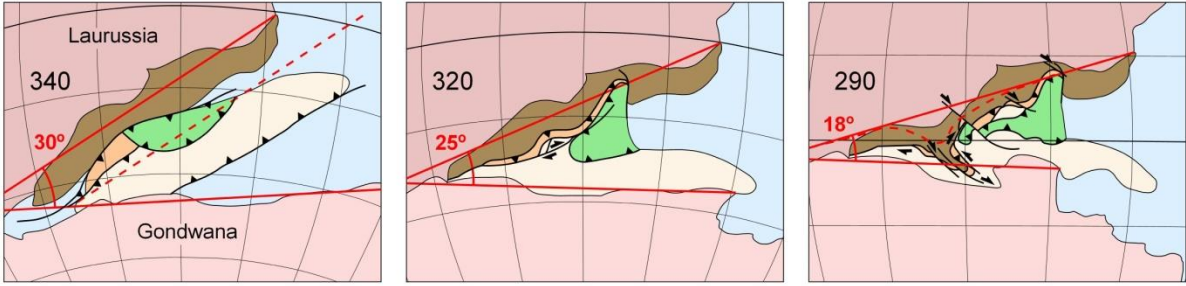


Fig. 14

1  
2  
3  
4  
5  
6  
7  
8  
9  
10  
11 6945  
12  
13 6946  
14  
15 6947  
16  
17  
18  
19  
20  
21  
22  
23  
24  
25  
26  
27  
28  
29  
30  
31  
32  
33  
34  
35  
36  
37  
38  
39  
40  
41  
42  
43  
44  
45  
46  
47  
48  
49  
50  
51  
52  
53  
54  
55  
56  
57  
58  
59  
60  
61  
62  
63  
64  
65

## Abbreviations

The list includes in alphabetical order the abbreviations used in the text and figures.

15				
16				
17				
18				
19				
20				
21				
22				
23	AA	Anti-Atlas (Morocco)	EB	Erzgebirge Massif (Bohemian Massif)
24	AaM	Aar Massif (Alps)	EFZ	Elbe Fault Zone (Bohemian Massif)
25	AMM	Argentera Massif (Alps)	EM	Eastern Meseta (Morocco)
26	Au	Audierne Bay Complex (Armorican Massif)	Ema	External Massifs of the Alps
27	AZ	Axial Zone (Pyrenees)	EMA	Eastern Meseta Arc (Morocco)
28	B	Bragança (NW Iberia allochthonous complex)	Es	Essarts Unit (Armorican Massif)
29	BA	Bohemian Arc	EV	Erbendorf-Vohenstrauß Unit (Bohemian Massif)
30	BAU	Beja-Acebuches Unit (Iberian Massif)	F	Frankenberg Klippe (Bohemian Massif)
31	BBSZ	Baden-Baden Shear Zone (Schwarzwald Massif)	FF	Franconian Fault (Bohemian Massif)
32	BC	Bois-de-Cené Unit (Armorican Massif)	FMC	French Massif Central
33	BCSZ	Badajoz-Córdoba Shear Zone (Iberian Massif)	GCF	Granville-Cancalle Fault (Armorican Massif)
34	BeM	Belleme Massif (Alps)	Gf	Gföhl Unit (Bohemian Massif)
35	BL	Blansky les Unit (Bohemian Massif)	GN	Griessen Nappe (Rhenish Massif)
36	BM	Basque Massifs	GS	Göry Sowte Massif (Bohemian Massif)
37	BtF	Bray Fault	GTMZ	Galicia-Trás-os-Montes Zone (Iberian Massif)
38	Bu	Buçaco (Portugal)	HM	Harz Mountains (Germany)
39	Bv	Brévenne Unit (French Massif Central)	HP-HT	High-P/High-T Upper Allochthon (European massifs)
40	CAD	Central Armorican Domain	IAA	Ibero-Armorican Arc
41	CB	Coastal Block (Morocco)	Ib	Ibiza (Balearic Islands)
42	CBPC	Central Bohemian Plutonic Complex	IG	Ile-de-Groix (Armorican Massif)
43	Cé	Cévennes (French Massif Central)	IP	Intermediate-P Upper Allochthon (European massifs)
44	CF	Combrailles Fault (French Massif Central)	IRB	Iberian Reflective Body
45	Ch	Champtoceaux Complex (Armorican Massif)	ISB	Intra-Sudetic Basin (Bohemian Massif)
46	ChO	Chamrousse Ophiolite (Alps)	ISF	Intra-Sudetic Fault (Bohemian Massif)
47	CHS	Chantonnay Syncline (Armorican Massif)	JPSZ	Juzbado-Penalva Shear Zone (Iberian Massif)
48	CIA	Central Iberian Arc	Ka	Kaczawa Complex (Bohemian Massif)
49	CIZ	Central Iberian Zone	KH	Kuthna Hora Unit (Bohemian Massif)
50	Co	Corsica	Kr	Krkonoše Massif (Bohemian Massif)
51	CO	Cabo Ortegal (NW Iberia allochthonous complex)	LA	Lower Allochthon (European massifs)
52	Cr	Crozon (Armorican Massif)	LB	Lausitz Block (Bohemian Massif)
53	CU	Central Unit (Iberian Massif)	LC	Lizard Complex (England)
54	CV	Cinco Villas (Basque Massif, Pyrenees)	LiO	Limousin ophiolite (French Massif Central)
55	CZ	Cantabrian Zone (Iberian Massif)	LLSZ	Lalaye-Lubine Shear Zone (Vosges Massif)
56	DF	Danube Fault (Bohemian Massif)	Ln	Léon (Armorican Massif)
57	Dr	Drosendorf Unit (Bohemian Massif)	Ly	Lyonnais (French Massif Central)
58	DRF	Domain of Recumbent Folds (Iberian Massif)	M	Morais (NW Iberia allochthonous complex)
59	DUF	Domain of Upright Folds (Iberian Massif)	Ma	Majorca (Balearic Islands)
60	EAMB	Évora-Aracena Metamorphic Belt (Iberian Massif)	MA	Middle Allochthon (European massifs)
61				
62				
63				
64				
65				

15				
16				
17				
18	MBM	Mont Blanc Massif (Alps)	RHZ	Rhenoherynian Zone
19	MCA	Massif Central Arc	RTFZ	Rabat-Tiflet Fault Zone (Morocco)
20	Me	Menorca (Balearic Islands)	Ru	Ruhla Massif (Germany)
21	MECS	Maures-Estérel-Corsica-Sardinia block	Sa	Sardinia
22	MGCH	Mid-German Crystalline High	SAD	South Armorican Domain
23	ML	Mariánské Lázně Unit (Bohemian Massif)	SAF	South Atlas Fault (Morocco)
24	MM	Moroccan Meseta	SASZ-N	South Armorican Shear Zone, Northern branch
25	MMFZ	Middle Meseta Fault Zone (Morocco)	SASZ-S	South Armorican Shear Zone, Southern branch
26	MN	Montagne Noire (French Massif Central)	SB	Sehoul Block (Morocco)
27	Mo	Morvan Arc (French Massif Central)	SBB	South Bohemian Batholith
28	Ms	Mauges Unit (Armorican Massif)	SBF	Sudetic Boundary Fault (Bohemian Massif)
29	MSZ	Moravo-Silesian Zone (Bohemian Massif)	SG	St. Georges-sur-Loire Unit (Armorican Massif)
30	MT	Moldanubian Thrust (Bohemian Massif)	SGD	Schist-Greywacke Domain (Iberian Massif)
31	MTM	Maures-Tanneron Massif (Southern France)	SGr	Saxonian Granulitebirge (Bohemian Massif)
32	MTu	Malpica-Tui (NW Iberia allochthonous complex)	SHF	Sillon Houiller (French Massif Central)
33	Mü	Münchberg Klippe (Bohemian Massif)	SIF	South Iberia Fault
34	MZ	Moldanubian Zone (Bohemian Massif)	SISZ	Southern Iberian Shear Zone
35	NAD	North Armorican Domain	SK	South Křkonosé Unit (Bohemian Massif)
36	NASZ	North Armorican Shear Zone	SLF	South Limousin Fault (French Massif Central)
37	NEF	Nort-sur-Erdre Fault (Armorican Massif)	SM	Staré Město Unit (Bohemian Massif)
38	Nj	Najac Massif (French Massif Central)	SME	South Meseta Fault (Morocco)
39	NM	Northern Massifs (Pyrenees)	SMEFr	South Meseta Front (Morocco)
40	NMe	Nové Město Unit (Bohemian Massif)	Sp	Spessart Massif (Germany)
41	NPF	North Pyrenean Fault	SPhZ	Southern Phyllite Zone (Germany)
42	NPhZ	Northern Phyllite Zone (Germany)	SPZ	South Portuguese Zone
43	NSSB	Northern Sierra de Sevilla Batholith (Iberian Massif)	STZ	Saxothuringian Zone
44	NZ	Nappe Zone (Morocco)	Sv	Svatka window (Bohemian Massif)
45	O	Ordnes (NW Iberia allochthonous complex)	SWM	Schwarzwalde Massif (Germany)
46	Od	Odenwald Massif (Germany)	TA	Tufts Anthracifères (French Massif Central)
47	OF	Ouzilly Fault (French Massif Central)	TBZ	Teplá-Barrandian Zone (Bohemian Massif)
48	OFZ	Odra Fault Zone (Bohemian Massif)	Th	Thaya window (Bohemian Massif)
49	OMZ	Ossa-Morena Zone (Iberian Massif)	TP	Thiviers-Payzac Unit (French Massif Central)
50	OS	Orlica-Šnieżnik Dome (Bohemian Massif)	TTZ	Teisseyre-Tornquist Zone (Baltica)
51	OSD	Olló de Sapo Domain (Iberian Massif)	UA	Upper Allochthon (European massifs)
52	OVD	Obejo-Valsequillo Domain (Iberian Massif)	UB	Ursuya-Baygura (Basque Massif, Pyrenees)
53	PA	Parautochthon (NW Iberian Massif)	VD	Velay Dome (French Massif Central)
54	PASZ	Posada-Asinara Shear Zone (Sardinia)	VF	Variscan Front
55	PF	Pfahl Fault (Bohemian Massif)	VM	Vosges Massif (France)
56	PL	Pulo do Lobo Unit (Iberian Massif)	W	Wildentfels Klippe (Bohemian Massif)
57	PS	Praha Syncline (Bohemian Massif)	WALZ	West Asturian-Leonese Zone (Iberian Massif)
58	PTSZ	Porto-Tomar Shear Zone (Iberian Massif)	WM	Western Meseta (Morocco)
59	QR	Quinto Real (Basque Massif, Pyrenees)	WMSZ	Western Meseta Shear Zone (Morocco)
60				
61				
62				
63				
64				
65				